Accumulation of Sulphur-Containing Dietary Bioactives and the Impact on the Transcriptional Signature of the Prostate

Tracey Laura Livingstone BSc (Hons), MBBS, MRCS.

Quadram Institute Bioscience

A thesis for the degree of Doctor of Medicine to the

University of East Anglia 2022

Abstract

Epidemiological evidence suggests that the consumption of sulphur-containing plant bioactives derived from cruciferous and alliaceous vegetables reduce the risk of prostate cancer incidence and progression.

The anti-cancer properties of cruciferous vegetables are largely attributed to the glucosinolate degradation product sulforaphane, which has a multi-modal effect on cancer pathways. Sulforaphane and its metabolites are documented to accumulate within the urine of patients consuming a high glucoraphanin diet but have not been shown to accumulate within the human prostate gland. Alliaceous vegetables also accumulate bioactive organosulphur compounds, namely the S-alk(en)yl-L-cysteine sulfoxides and γ-glutamyl S-allyl-L cysteines, which (along with their organosulphur metabolites) are attributed to a reduction in prostate cancer risk. Despite cell, animal and epidemiological evidence, there are currently no human intervention studies analysing the effect of alliaceous vegetables on prostate cancer.

39 men scheduled for transperineal prostate biopsies completed a randomised, 2^2 factorial design, double-blinded intervention study. Patients received high-dose dietary supplementation with myrosinase-activated glucoraphanin, alliin, and/or placebo, for at least 28 days prior to their procedure.

Free Sulforaphane was detected at significantly higher levels in the prostate of all patients consuming a glucoraphanin intervention ($p < 0.0001$). The sulforaphane metabolite sulforaphane-N-acetylcysteine was detected at significantly higher concentrations in the peripheral zone of patients consuming glucoraphanin supplementation ($p = 0.0281$) compared to a non-glucoraphanin intervention. S-allyl-L-cysteine was detected to significantly higher levels in the transition zone of patients consuming an Alliin intervention. Transcriptional analysis of the prostate demonstrated that the peripheral and transition zones possess unique transcriptional signatures, which may explain the differing propensity of the peripheral zone towards cancer. Both dietary compounds are capable of altering the transcriptional pathways associated with prostate cancer.

This is the first evidence for the accumulation of sulforaphane and alliin metabolites within the human prostate, whereby they subsequently influence a variety of oncogenic pathways to reduce prostate cancer risk.

Contents

List of Figures

Chapter Three

Chapter Four

Chapter Five

List of Tables

Chapter Two

Chapter Three

Chapter Four

Chapter Five

Abbreviations

ABCA1	ATP-binding cassette transporter isoforms A1
ABCG1	ATP-binding cassette transporter isoforms G1
ACC1	Acetyl-CoA carboxylase 1
ACLY	Acetyl CoA by ATP citrate lyase
ACN	Acetonitrile
ADT	Androgen deprivation treatment
AKT/PKB	Protein kinase B
ALMA	Allylmercapturic acid
AMACR	α-methylacyl-CoA racemase
AMS	Allyl methyl sulfide
AMSO	Allyl methyl sulfoxide
AMSO$_2$	Allyl methyl sulfone
AR	Androgen receptor
ARE	Androgen response elements
ASAP	Atypical small acinar proliferation
ASPN	Asporin
ATF3	Activating transcription factor 3
ATP	Adenosine triphosphate
BAUS	British Association of Urological Surgeons
BBSRC	Biotechnology and Biological Sciences Research Council
BCG	Bacillus Calmette–Guerin
BFI	Biomarkers of food intake
BH	Benjamini-Hochberg
BM	Bone metastatic
BMI	Body mass index
BMP5	Bone morphogenetic protein
BPH	Benign prostatic hyperplasia
BSE	Broccoli seed extract
BWA	Burrows-Wheeler aligner
CA	Cancer

cAMP	Cyclic adenosine monophosphate
CBP	cAMP response element-binding protein
CD-	Cluster of differentiation-
CDKN1A	Cyclin Dependent Kinase Inhibitor 1A
CI	Confidence interval
CK-	Cytokeratin-
CMA	Carboxymethoxylamine
COX	Cyclooxygenase
CPT1A	Carnitine palmitoyltransferase 1A
CRF	Clinical research facility
CST	Cystatin
CTL	Cytotoxic T-lymphocyte
CTLA	Cytotoxic T lymphocyte-associated antigen
CVD	Cardiovascular disease
CVFFQ	Arizona Cruciferous Vegetable Food Frequency Questionnaire
CXCR4	Chemokine receptor type 4
DADS	Diallyl disulfide
DAS	Diallyl sulfide
DATS	Diallyl trisulfide
DGE	Differential gene expression
DHEA	Dehydroepiandrosterone
DHT	5α-dihydrotestosterone
DMSO	Dimethyl sulfoxide
DNA	Deoxyribonucleic acid
DRE	Digital rectal examination
E2F	E2 factor
EAAC1	Aspartate transporter
EAU	European Assoiation of Urology
ECG	Epicatechin-3-gallate
EGCG	Epigallocatechin-3-gallate
EGF	Epidermal growth factor
EMT	Epithelial mesenchymal transition
ERK	Extracellular signal-regulated protein kinases

ES	Electrospray
ESI	Electrospray Ionisation
FA	Fatty acid
FASN	Fatty acid synthase
FDR	False discovery rate
FFQ	Food frequency questionnaire
FGF	Fibroblast growth factor
FGFR	Fibroblast growth factor receptor
FKHRL1	Forkhead transcription factors
FM	Ferragina-Manzini
FOX-	Forkhead box-
FSP1	Fibroblast-specific protein 1
G2M	G2-M DNA damage checkpoint
GFN	Glucoraphanin
GREM2	Gremlin 2, DAN Family BMP Antagonist
GSEA	Gene set enrichment analysis
GSL	Glucosinolates
GST	Glutathione S-transferase
GSTM1	Glutathione S-transferase Mu 1
HAT	Histone acetyltransferase
HCA	Heterocyclic amines
HDAC-	Histone deacetylase-
HGPIN	High-grade prostatic intraepithelial neoplasia
HIV	Human immunodeficiency virus
HLH	Helix-loop-helix
HO1	Heme oxygenase 1
HOXD13	Homeobox D13
HPC	High performance computing
HPLC	High performance liquid chromatography
HPMC	Hydroxypropylmethylcellulose
HRA	Health Research Authority
HRGC	Human Research Governance Committee
HSD11B1	Hydroxysteroid 11-Beta Dehydrogenase 1

IAD	Intermittent androgen deprivation
IFN	Interferon
IGF	Insulin-like growth factor
IL-	Interleukin-
IQR	Interquartile range
ITC	Isothiocyanates
JAK	Janus kinase
keap	Kelch-like ECH-associated protein
KRAS	V-Ki-Ras2 Kirsten Rat Sarcoma 2 Viral Oncogene Homolog
LCMS	Liquid chromatography-mass spectrometry
LDL	Low-density lipoproteins
LFC	Log fold change
lncRNA	Long non-coding RNA
LXR	Liver X receptor
mAAT	Mitochondrial aspartate aminotransferase
MCC	Microcrystalline cellulose powder
MDM2	Mouse double minute 2 homolog
MDSC	Myeloid-derived suppressor cells
MEK	Mitogen-activated protein kinase kinase
MFAP5	Microfibrillar-associated protein 5
MHC	Major histocompatibility complex
MMP	Matrix metalloproteinases
MMTSI	S-methyl methanethiosulfinate
MMTSO	S-methyl methanethiolsulfonate
mpMRI	Multiparametric magnetic resonance imaging
MRM	Multiple-reaction monitoring
MTA1	Metastasis-associated protein 1
MTORC1	mammalian target of rapamycin complex 1
MYC,	Myelocytomatosis
MYH3	Myosin heavy chain 3
NAC-SAC	N-acetyl-S-allyl-L-cysteine
NADPH	Nicotinamide adenine dinucleotide phosphate
NBI	Norwich Bioscience Institute

NELL	Neural epidermal growth factor-like
NES	Normalised enrichment score
NFKB	Nuclear factor-kappa B
NHS	National Health Service
NICE	National Institute of Clinical Excellence
NNUH	Norfolk and Norwich University Hospital
NOV	Nephroblastoma Overexpressed
NQO1	NADPH:quinone oxidoreductase
NRES	National Research Ethics Service
NRF2	Nuclear factor erythroid 2-related factor 2
OCMHA	O-(carboxymethyl)hydroxylamine hemihydrochloride
ORF	Open reading frame
OSC	Organosulphur compound
P13K	Phosphatidylinositol 3-kinase
PBS	Phosphate buffered solution
PCa	Prostate cancer
PCF	Prostate Cancer Foundation
PCR	Polymerase chain reaction
PDH	Pyruvate dehydrogenase
PET	Positron emission topography
PIN	Prostatic intraepithelial neoplasia
PKB	Protein kinase B
PKC	Protein kinase C
PKHD1	Polycystic kidney and hepatic disease 1 gene
PSA	Prostate specific antigen
PTEN	Phosphatase and tensin homolog
PTGS1	Prostaglandin-Endoperoxide Synthase 1
PVR	Poliovirus receptor
PZ	Peripheral zone
QC	Qianliening capsules
QC	Quality control
QI	Quadram Institute
QIB	Quadram Institite Biosciences

RCT	Randomised control trial
REC	Research Ethics Committee
RNA	Ribonucleic acid
ROS	Reactive oxygen species
RRHO	Rank–rank hypergeometric overlap
S100A4	S100 Calcium Binding Protein A4
SAC	S-allyl-L cysteine
γSAC	γ-glutamyl S-allyl-L cysteine
SACSO	S-alk(en)yl-L-cysteine sulfoxide
SCMCSO	S-carboxymethyl-L-cysteine sulfoxide
SFN	Sulforaphane
SFRP	Secreted frizzled-related protein
SLIT1	Slit guidance ligand 1
SMCSO	S-methyl-L-cysteine sulfoxide
SOD	Superoxide dismutase
SPON1	Spondin 1
SRE	Sterol regulatory elements
SREBP	Sterol regulatory element-binding protein-2
STAT5	Signal transducer and activator of transcription 5
SYNPO	Synaptopodin
TAC	Total antioxidant capacity
TAM	Tumour associated macrophage
TAN	Tumour associated neutrophil
TCA (cycle)	Tricarboxylic acid cycle
TCA	Trichloroacetic acid
TGF	Transforming growth factor
THC	T-helper cells
TIGIT	T cell immunoreceptor with immunoglobulin and immunoreceptor tyrosine-based inhibitory motif domain
TNF	Tumour necrosis factor
TNM	Tumour, nodes, metastasis
TPB	Transperineal prostate biopsy
TRAIL	TNF-Related Apoptosis Inducing Ligand

TRAMP	Transgenic adenocarcinoma of the mouse prostate
TRUS	Trans rectal ultrasound
TZ	Transition zone
UNC5B	Unc-5 Netrin Receptor B
UPLC	Ultra performance liquid chromatography
USP	United States Pharmacopeia
UV	Ultraviolet
VEGF	Vascular endothelial growth factor
VEGFR2	Vascular endothelial growth factor receptor 2
VST	Variance stabilising transformation
WHO	World Health Organisation
WNT	Wingless-related integration site
ZIP1	Zinc transporter
ZNF-	Zinc finger protein-

Acknowledgements

I would like to thank my supervisors, Dr Maria Traka and Professor Richard Mithen, for providing me with the opportunity, enthusiasm and provisions to undertake this period of research, and to Dr Paul Kroon for his guidance and support throughout this research post.

Very special thanks go to Dr Shikha Saha who operated the LCMS/MS and analysed the prostate extractions, and Dr Perla Rey who undertook the bioinformatics analysis. Without their knowledge, time and support, this work would never have been possible. I would also like to thank Dr Antonietta Melchini for teaching me how to design and implement a human intervention study, Ms Wendy Hollands for her support with getting the study going, and Dr George Sava for teaching me to critically analyse my data. Thanks also extend to Prof. Ball for undertaking the histological analysis of prostate samples, and to Federico Bernuzzi for assisting with the genotyping analysis.

To Mr Mills, for his support and guidance, both with this research and my clinical career progression, I am eternally grateful.

To my colleagues and friends, especially Gemma Beasy, Federico Bernuzzi and Lee Kellingray, for always being there to offer support, answer my continuous questions, keep my head up, and helping with this research in any way they could, thank you.

A very special thanks go to my family for always supporting my career decisions and encouraging me to pursue my dreams.

Finally, my thanks extend to all the patients who contributed to my study and made this research possible.

Chapter One

General Introduction

1.1 The Prostate Gland Anatomy

The prostate gland is a walnut sized compound tubular-alveolar gland located at the base of the urinary bladder, anterior to the rectum. Approximately two-thirds of the prostate is glandular in structure with the remaining fibromuscular (1).

Anatomically, the prostate is divided into three major zones according to McNeal (2); the peripheral, transition and central zones. The peripheral zone (PZ) is the largest anatomical zone of the prostate, comprising approximately 65% of normal prostate volume, and is located posteriorly. The ducts of the glands from the peripheral zone empty vertically into the prostatic urethra, permitting urinary reflux. This factor may explain the high incidence of acute and chronic inflammation in this compartment and also possibly be linked to the high incidence (70-80%) of prostate cancer (PCa) within this zone (3). The posterior position of the peripheral zone means that it is easily palpable on digital rectal examination (DRE) (4). The transition zone (TZ) is located centrally, surrounding the urethra and comprises approximately 5-10% of normal prostate volume. Glands of the transition zone most typically undergo nodular growth, or benign prostatic hyperplasia (BPH), hence causing obstructive urinary symptoms as the urethra descends from the bladder. The central zone of the prostate comprises approximately 25% of normal prostate volume and surrounds the ejaculatory ducts running from seminal vesicles to the prostatic urethra. The oblique angle of the ducts emptying into the prostatic urethra make this zone relatively immune from urinary reflux.

The fibromuscular stroma (sometimes described as a fourth zone) is situated anteriorly within the gland, and merges with the tissue of the urogenital diaphragm. During prostatic embryogenesis, the prostate gland buds around the urethra and interacts with the horseshoe-like muscle precursor of the smooth and striated muscle which forms the internal and external urethral sphincter (5).

The primary function of the prostate is to secrete proteolytic enzymes to enable liquefication of semen and promote a nutrient-rich alkaline environment for the survival of sperm (6). Prostate-specific antigen (PSA) is a protease that liquefies semen by breaking down high molecular weight proteins and facilitates free motility of sperm. PSA is also detectable in serum and is used as a common laboratory test to aid PCa diagnosis. Proteolytic enzymes leave the prostate immediately prior to ejaculation, via prostatic ducts opening into the prostatic urethra on each side of the seminal colliculus (verumontanum)(7, 8).

1.2 Prostate Cancer Incidence

PCa has become the most common form of non-cutaneous (internal) cancer in men, accounting for 26% of all new visceral cancer cases in men in the UK, with over 47,000 new diagnoses every year (9). The aetiology of PCa is unclear for the majority of patients, but recognised risk factors include race, family history, and age; indeed, more than a third (35%) of new cases occur in men aged 75 and over (10-13).

The highest age-standardised incidences of PCa worldwide are seen in Westernised countries, including Australia, New Zealand, Europe and the Americas, compared to the lowest in South Central Asia (14, 15). This geographical variation in incidence cannot be explained by known risk factors such as age, race and family history (1), and implicates environmental factors, including diet (15-17). For example, the incidence of PCa in Asian countries is low compared to the West, however, this incidence rapidly increases (20-fold increased risk) in Asian immigrants to the United States that have adopted a western diet, reducing intakes of soy, tea, fish, fruits, and vegetables and increasing their intake of red meat and fat-rich food (1). Indeed, the recent rise in incidence and mortality of PCa in Eastern countries (although this may in part reflect rising capacity for diagnosis as opposed to true incidence), could partly be explained by the transition to a more westernised lifestyle (15). In addition, a study conducted in Western Australia has reported that the incidence of aggressive PCa is 80% higher in those consuming a western diet in comparison to those consuming a high vegetable or 'health conscious' diet (18). The difference in PCa rates thus implicates dietary, lifestyle, and environmental factors with the development and progression of PCa (15, 17, 19).

1.3 Diagnosis and Staging of Prostate Cancer

Routinely screening of all men to quantify serum PSA is controversial. As a result, there is no screening programme for PCa in the UK, although the European Association of Urology (EAU) has more recently moved to support the use of PSA as a screening tool by the use of a baseline PSA taken at the age of 45 to formulate "individual screening intervals" (20). However, PSA can be elevated for numerous reasons, including infection of the prostate or elsewhere in the urinary tract, benign prostatic hyperplasia (BPH), ejaculation, and instrumentation such as urethral catheterisation or DRE (1). Additionally, a significant proportion of men with PCa will have a PSA reading within the 'normal range' (21); 23.9% of men enrolled in the 'prevention trial' were diagnosed with PCa with a PSA value of 2.1 - 3.0 ng/ml, and 26.9% of patients with a PSA of 3.1 - 4.0 ng/ml (22).

Following results from the PROMIS (23) and PRECISION (24) studies, EAU and NICE guidelines have been updated to involve the use of multiparametric magnetic resonance imaging (mpMRI) of the prostate as part of PCa diagnosis for patients with clinically suspected localised disease (25, 26). Following the formalisation of mpMRI reporting, the Prostate Imaging Reporting and Data System (PI-RADS) is used to provide a likelihood score of PCa, and enable the urologist to target potentially malignant areas during biopsy based upon the imaging findings. The PROMIS study concluded that upfront mpMRI prevented approximately one quarter of unnecessary biopsies, reducing the number of clinically insignificant cancers diagnosed and improving the diagnosis of clinically significant PCa (23). In addition, following publication of the PRECISE study, mpMRI has also become a tool for accurate monitoring of progression of PCa in men on a program of active surveillance, whereby the index size lesion is assessed at baseline and each subsequent MRI to determine the 'true' change over time (27).

A formal diagnosis of PCa is therefore made following a prostate biopsy in patients with an elevated PSA or clinically suspicious prostate on DRE, and/or (depending upon local trust policy) suspicious findings on mpMRI. Traditionally, biopsies of the prostate are taken via the rectal route using transrectal ultrasound (TRUS) guided approach, however, due to the risk of post-procedure sepsis and the inability to biopsy all zones of the prostate thoroughly, the transperineal approach is now widely adopted.

A transperineal prostate biopsy (TPB) is currently performed under general or spinal (and more recently local) anaesthetic with appropriate prophylactic antibiotic cover. The patient is positioned supine in the lithotomy position (i.e. flat on their back with their legs in stirrups). Following appropriate preparation to ensure a sterile field, an ultrasound probe is inserted into the rectum to allow direct visualisation of the prostate, and for more direct targeting of specific areas of the prostate as dictated by a pre-procedure MRI scan. In the case of a template prostate biopsy, a specially designed grid is then attached to the probe and placed directly against the perineal skin. The grid has multiple holes to allow the passage of the biopsy needle and are spaced at 5mm intervals to enable systemic sampling of all prostatic zones; sampling of the anterior prostate is improved using this technique. During TPB, an average of 25 tissue cores of prostate are taken, whilst taking care to avoid the urethra. The amount of tissue cores taken will vary dependent upon the volume of the prostate gland (as measured by the ultrasound probe) (28).
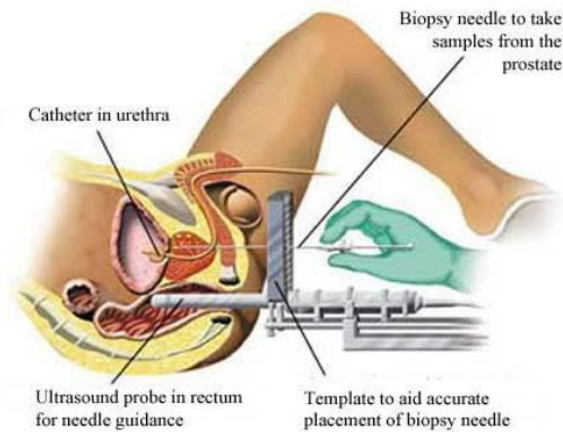
Figure 1.1 Transperineal template prostate biopsy procedure. Taken from the British Association of Urological Surgeons patient information sheet (28).

The Gleason system (described by Donald Gleason in the 1960's) was until recently, used to grade cancers of the prostate, whereby microscopically the cancer is graded from 1-5 according to its gland-forming differentiation at relatively low magnification. Given that 85% of PCas are multi-focal, the two most dominant grades were added together to give a sum score from 2-10. 75% of cancers diagnosed were graded 5, 6, or 7, and were considered moderately differentiated; 10% were graded 2 to 4 and were considered well differentiated; and 15% were considered poorly differentiated with a Gleason score of 8 to 10. A higher Gleason score corresponded to progressive loss of differentiation and therefore reliably a worse prognosis (29). The Gleason score has more recently been modified, given that patterns 1-2 are considered normal and hence the minimum sum for a PCa is 6 (Gleason 3+3). The revised system now implemented by the World Health Organisation (WHO), simplifies Gleason scores into a 'Grade Group' system, which reclassifies cancers into groups 1 to 5 according to prognostic risk and modified Gleason score (see figure 1.2) (30-32). The grade group, PSA and stage of the cancer (using the TNM classification system (33)) correlates with aggressiveness and hence prognosis, and is therefore used to determine the most appropriate patient management.

Figure 1.2 Histological appearance, Gleason pattern, score and corresponding Grade Group as described by Chen and Zhou, 2016 (32).

1.4 The Unique Metabolic and Transcriptional Profile of Prostate Cancer

Normal mammalian cells completely oxidise glucose and fats by relying on the synthesis and oxidation of citrate in the TCA cycle, producing ATP which is used as a major energy source (34). However, it is well documented that the prostate has a unique metabolism. The main function of the human prostate gland is to accumulate and secrete (rather than oxidise) large concentrations of citrate; the PZ citrate concentration is estimated to be 13,000 nmol/g, compared to 4,000 nmol/g in the CZ, and 8,000 nmol/g in 'mixed prostate tissue' (35). Importantly, the distinction between prostatic epithelial cells has demonstrated that the secretory function is largely associated with the glandular (secretory) epithelial cells of the PZ. The unique process of citrate production (at the expense of oxidation) is achieved by the ability of the prostatic acinar epithelial cells to accumulate large concentrations of zinc. The citrate becomes an end product of metabolism and is either excreted into prostatic fluid from the cytosol and used as an energy source for sperm (36), or converted back to acetyl CoA by ATP citrate lyase (ACLY) for lipid and cholesterol synthesis (35). High concentrations of zinc aid this latter process by inhibiting mitochondrial (m)-aconitase (37), the enzyme which catalyses the oxidation of citrate within the TCA cycle, and hence the TCA cycle is aborted prior to citrate oxidation. The lack of citrate oxidation is bioenergetically costly; citrate

oxidation via the TCA cycle would otherwise provide a significant amount of ATP, and hence these highly specialised cells adopt alternative metabolic pathways to afford their survival and function; they are highly glycolytic, replace TCA cycle intermediates with aspartate and glutamine, and utilise more fatty acids via beta oxidation.

PCa, like other cancers, modify their intermediary metabolism via the Warburg effect (38), in order to meet the energy demands of the highly proliferating cells. PCa cells however, do not rely heavily on glucose – a factor which limits the clinical value of positron emission topography (PET) (39, 40) – but rather reverse the excretion of citrate, and utilise more fatty acids via β-oxidation to produce acetyl CoA which subsequently feeds into the TCA cycle to produce ATP. Loss of zinc accumulation and downstream aconitase inhibition by cancerous cells redirects citrate back into the TCA cycle, producing more ATP in order to meet rising energy demands. As a result, ACLY, cholesterol, and fatty acids are commonly upregulated in PCa (41), whereas citrate and zinc have consistently been shown to decrease (a "hallmark" characteristic of PCa) (42, 43). The concentration of citrate has been shown to reduce to 500 nmol/g in PCa malignant tissue itself, and 1-2,000 nmol/g in PCa 'mixed tissue' (35). The upregulation of fatty acid synthase (FASN) to facilitate the increased *de novo* FA synthesis, is a common marker of PCa and often referred to as an oncogene. Fatty acids form the building blocks for cell growth and proliferation but are also able to be utilised as an energy source via beta oxidation. The process of utilising more long chain fatty acids via β-oxidation, relies upon the enzyme α-methylacyl-CoA racemase (AMACR), which is a highly sensitive marker for immunohistochemistry staining due to its overexpression in PCa (44).

The regulation of zinc accumulation in the epithelial acini and hence the production of citrate in the prostate, is under hormonal control via testosterone and prolactin (45-47). The hormonal control of zinc and citrate is achieved via their positive regulation of the gene expression of four important transporter enzymes involved in a complex metabolic sequence; ZIP1 zinc transporter; aspartate transporter (EAAC1); mitochondrial aspartate aminotransferase (mAAT); and pyruvate dehydrogenase E1a (PDH). Importantly, testosterone's hormonal regulation of zinc and citrate production is achieved by the presence of androgen response elements (ARE) located in the promoter regions of metabolic genes. Testosterone conversion to dihydrotestosterone (DHT), followed by its binding to the androgen receptor, results in activation of the ARE and increased gene expression (48). This provides a rapid androgen pathway for the regulation of the metabolic genes in the prostate cells. In comparison, prolactin regulation of metabolic genes occurs via an alternate signalling pathway from the cytokine effects of prolactin. The cytokine effects of prolactin in prostate cells are mediated predominantly through prolactin-receptor activation and initiation of a tyrosine kinase-associated signalling pathway (the phospholipase-diacylglycerol pathway). This

subsequently causes the activation of protein kinase C ε (PKCε) and thus increased transcription of metabolic effector genes.

Normal prostatic epithelial cells also have an abnormally high cholesterol content, which is detectable in both the cells and prostatic secretions, and appear to synthesise cholesterol at a higher rate than the liver (49). However, the level of cholesterol synthesis is not stable in the prostate, and can in fact double during progression to PCa (49, 50). Multiple factors are involved in the regulation of cholesterol levels in the cell; namely uptake, synthesis and efflux. Briefly, exogenous cholesterol can be taken-up by the cell as low-density lipoproteins (LDL) via LDL receptor mediated endocytosis. Alternatively, cholesterol can be directly synthesised by the cell via the mevalonate pathway, in which Acetyl CoA is used as a precursor to the formation of cholesterol (51, 52). The efflux of cholesterol from the cell occurs via the ATP-binding cassette transporter isoforms A1 (ABCA1) and G1 (ABCG1) (53, 54). Importantly however, cholesterol homeostasis is regulated at the transcriptional level, mainly via two master transcription factors, the sterol regulatory element-binding protein-2 (SREBP-2), which promotes cholesterol accumulation, and the liver X receptor (LXR) which reduces cholesterol accumulation (55, 56). Briefly, SREBP-2 is one of 3 SREBP isoforms which belong to the zipper family of transcription factors. It exists as a precursor in the endoplasmic reticulum bound to an activating protein (Scap). When cholesterol concentrations are low, SREBP is transported to the golgi membrane by Scap and cleaved by site-1 and -2 proteases, releasing the 'mature' transcription factor. SREBP migrates to the nucleus where it binds sterol regulatory elements (SREs) of target genes, resulting in an upregulation of genes involved in cholesterol synthesis and uptake (57, 58). This process is feedback-regulated by cholesterol concentrations. LXR however, the two isoforms of which (LXRα and LXRβ) both exist in human prostate tissue (59), reduce cholesterol accumulation (stimulated by high cholesterol levels) via the upregulation of genes involved in cholesterol efflux from the cell, and the ubiquitination of the LDL receptor (60, 61). Importantly, in addition to cholesterol, these mechanisms also exist (via differing isoforms) to modulate fatty acid synthesis (62). Recent evidence suggests that cholesterol homeostasis also pathways appear to be perturbed in PCa, which may in part explain the increasing concentrations of cellular cholesterol in PCa.

1.5 Immune Regulation and Evasion in Prostate Cancer

Several cancers including PCa are able to escape immune responses via multiple immune evasion mechanisms such as the development of a tumour-immunosuppressive microenvironment,

inhibition of antigen presentation and defective T cell responses (63, 64). Interestingly, there is evidence which suggests that PCas undergo Epithelial Immune Cell-like Transition through expressing molecules conventionally associated with immune cells such as immune transcription factors, that result in the suppression of anti-cancer immune activity (65).

Forming the main component of the tumour microenvironment are tumour-associated immune cells such as T regulatory cells (Tregs), tumour-associated macrophages (TAMs), tumour-associated neutrophils (TANs) and myeloid-derived suppressor cells (MDSCs). Many studies have indicated that these cells contribute towards the initiation and progression of PCa via direct interactions with the PCa cells or indirectly via cytokine secretion (66).

Normally, effector T cells are divided into Th1 and Th2 subgroups, however, Tregs expressing a CD4$^+$ and the more recently documented FOXP3$^+$ phenotype are able to regulate immune tolerance of the tumour microenvironment (67). A retrospective study found that PCa tumour infiltrating lymphocytes (TIL) expressing FOXP3$^+$ were negatively associated with overall survival of PCa patients (68). A further study has demonstrated that the penetration of CD4$^+$ FOXP3$^+$ Tregs into prostate tissue has a positive association with Gleason scores and T stage of tumour progression, as well as a fourfold increase in PCa risk in men expressing epithelial CD4$^+$ Tregs in normal prostate tissue (69). These findings suggest that the immune responses are initiated even prior to tumour development. Tregs also mediate immunosuppressive effects such as interacting with CD80/CD86 on antigen-presenting cells via the surface cytotoxic T lymphocyte-associated antigen 4 (CTLA-4), inhibiting the function of antigen-presenting cells which leads to inhibition of the anti-cancer functions of effector and cytotoxic T cells (70, 71).

Tumour-associated macrophages (TAMs) have also been shown to exert tumour promoting effects. According to their different pathways of activation, they can be divided into classical activation (M1 type) macrophages and alternative activation (M2 type) macrophages. In the tumour microenvironment, M2-type macrophages are more abundant than M1-type macrophages; M1-type macrophages promote inflammation, where M2-type macrophages promote tissue repair (72). The presence of TAMs has been associated with biochemical recurrence in PCa patients following radical prostatectomy; and in particularly M2-type macrophages are significantly associated with tumour extension and invasion (73). The mechanism by which TAMs modulate and promote tumourigenesis is not fully understood, however the upregulation of Nephroblastoma Overexpressed (NOV/CCN3) in PCa cells has been shown to induce the expression of CD204 by M2 type TAMs, which in turn activates NF-kB pathway and the secretion of VEGF, promoting tumour angiogenesis (74).

Tumour-associated neutrophils (TANs) – neutrophils that have been able to intrude into the tumour microenvironment – appear to have a complex role in tumourigenesis. TANs become tumour-promoting via the cytokine TGF-β, but in the presence of vast amounts of TGF-β, TANs appear to become tumour-inhibiting (75). TANs are known to play a vital role in the early stages of tumourigenesis whereby they activate angiogenesis; indeed neutrophils releasing MMP-9 appear to promote angiogenesis and vascular and lymphatic invasion in aggressive PCa (76). Recently however, neutrophils have been shown to mediate bone-metastatic PCa (BM-PCa), given the ability of PCa cells to stimulate the recruitment of neutrophils (the most abundant immune cell present in bone marrow); neutrophils appear to infiltrate regions of prostate tumour in bone where they induce apoptosis of PCa cells (77). This process is largely mediated via inhibition of STAT5, a transcription factor known to promote PCa progression (78). However, during tumour progression, PCa cells appear to evade neutrophil-mediated cytotoxicity, enabling the progression of BM-PCa (77).

Myeloid-derived suppressor cells (MDSCs) are immature myeloid cells, such as immature macrophages and dendritic cells. Studies have shown that the presence of MDSCs in the tumour microenvironment promote the proliferation and metastasis of cancer cells via immunosuppressive effects (79). Multinuclear MDSCs have been shown to induce immunosuppression and stimulate the development of PCa through the CD40-CD40L pathway and interactions with mast cells. This interaction has demonstrated the increased expression of MDSC-related genes to be associated with poor prognoses in PCa patients (80) Additionally, MDSC in the tumour microenvironment appears to upregulate the expression of IL-10 and downregulate the expression of IL-6 and MHC II in macrophages, thus promoting metastasis (81). The infiltration of MDSCs in the tumour microenvironment has been demonstrated to be linked with PI3K/PTEN/AKT pathway in PCa mouse models (82), however whether there is involvement of MDSCs and PTEN loss in PCa patients remains unknown. Phosphatidylserine-targeted therapy however, has been shown to inhibit differentiation of MDSCs, encourage the conversion of TAMs into M1 type thus inhibiting PCa growth (83), indicating a role of MDSCs in PCa progression.

Immune cells present in the prostate tumour microenvironment play a key role in the progression and development of PCa. Investigating the immune regulation of PCa further could identify potential key genes and/or mechanisms which facilitate the progression of PCa. This could give rise to more effective immunotherapy treatments for PCa in the future (84, 85).

Section 1.5 and 1.6 are taken from the published review article "Plant Bioactives and the Prevention of Prostate Cancer – Evidence from Human Studies", Livingstone et. al. 2019 (86) – with permission from Nutrients, and co-authors.

1.5 Diet and Prostate Cancer

Many epidemiological and case-control studies suggest that dietary factors such as animal fat, dairy products and red meat increase the risk of PCa, whereas the intake of fruit and vegetables are protective (87-89). A Mediterranean diet with high intake of fish, legumes and olive oil has also been linked with a reduced PCa risk (89, 90), and bioactive compounds such as sulphur metabolites found in cruciferous and alliaceous vegetables, epigallocatechin gallate in green tea, lycopene in tomato, curcumin in turmeric and polyphenols present in pomegranate and red wine have all received interest as possible protective agents in the diet (91-95). A double-blinded placebo-controlled randomised trial has shown that patients with localised PCa on active surveillance, who consumed a whole food supplement containing a combination of broccoli powder, turmeric powder, pomegranate whole fruit powder and green tea extract for 6 months, had a significantly lower median PSA rise (14.7% 95% CI 3.4 – 36.7%) when compared to a placebo control (78.5% 95% CI 48.1 – 115.5%) (P = 0.0008) (96), with PSA being one of the few biomarkers associated with risk of PCa. This study highlights the potential inverse association of multiple plant bioactives within the diet on inflammatory processes or PCa progression, although the role that each compound individually may contribute, is unclear.

The occurrence of cancer in the prostate is often associated with the development of what appear to be several apparently independent cancer foci. Studies have also shown that histologically 'healthy' prostate tissue in ageing glands comprise multiple mutations that are associated with carcinogenesis, which may facilitate the emergence and proliferation of cancerous clones (97). Diet and in particular, plant bioactives, may be able to directly or indirectly modify the cellular environment of the prostate and inhibit the emergence of new cancer clones, as well as preventing the proliferation of existing clones (98).

1.5.1 Sulphur-containing Bioactives from Cruciferous and Alliaceous Vegetables and Prostate cancer

1.5.1.1 Glucoraphanin and Sulforaphane from Cruciferous Vegetables

Cruciferous vegetables, including broccoli, Brussels sprouts and cauliflower, accumulate sulphur-containing glycosides known as glucosinolates (GSLs), which contribute to the organoleptic properties of these vegetables. GSLs do not exhibit biological effects themselves but are enzymatically hydrolysed either by the plant enzyme myrosinase, or bacterial myrosinases present in the gut microbiota, to give rise to breakdown derivates including indoles, thiocyanates and isothiocyanates (25).

The strongest evidence with regards to a reduction in PCa incidence and progression is for the 4-methylsulphinylbutyl glucosinolate, glucoraphanin (GFN), the most abundant glucosinolate found in broccoli. GFN is converted to the isothiocyanate sulforaphane (SFN) by the plant enzyme myrosinase, or in the gut by bacteria with microbial thioglucosidase activity (figure 1.3) (26).

Briefly, when GFN has been hydrolysed into SFN, it is passively absorbed into the enterocyte of the small or large intestine where it is conjugated (either passively or via the activity of glutathione-S-transferases (GSTs)) with glutathione, for transportation into the systemic circulation. The conjugate is then either metabolised via the mercapturic acid pathway to produce thiol conjugates which are excreted in the urine, or dissociates or is cleaved by GST, to become free SFN (25).
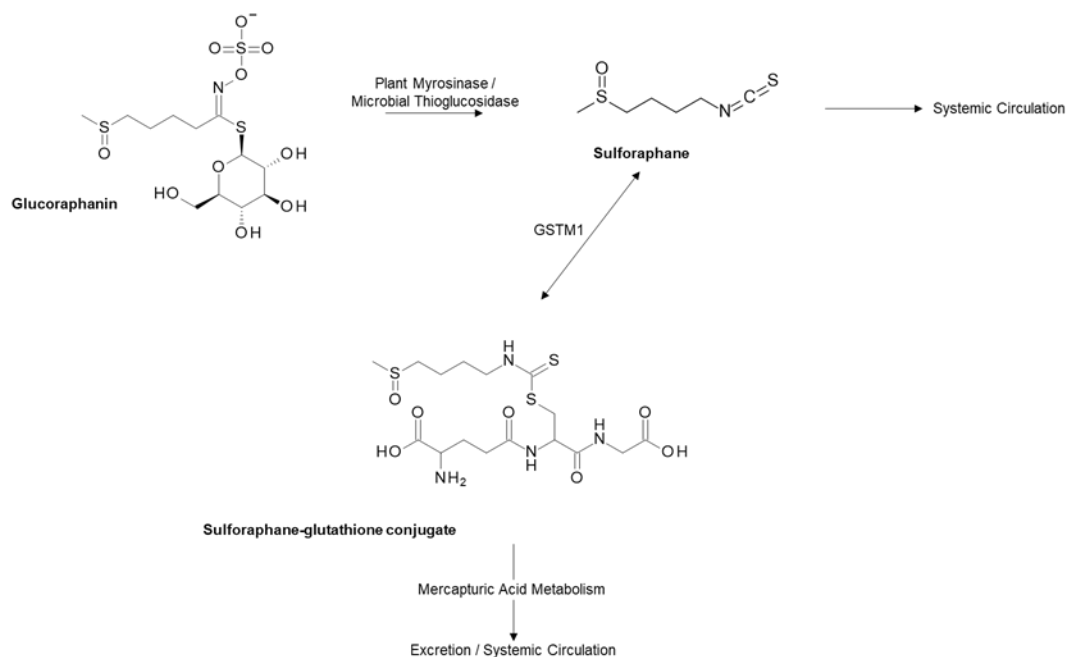
Figure 1.3 Metabolism of Glucoraphanin. Sulforaphane is absorbed readily into the enterocyte and conjugated with glutathione via the GSTM1 enzyme. Sulforaphane is then either metabolised and excreted in the urine via the mercapturic acid pathway or cleaved from glutathione into free sulforaphane (99).

SFN has been shown to provide multi-modal influences on a wide variety of metabolic and cell-signalling pathways involved in cancer; including the induction of antioxidant pathways, induction of apoptosis on cancer cells, inhibition of inflammation and angiogenesis, and detoxification of carcinogens (100). The most widely researched molecular target of SFN in relation to the induction of an antioxidant response, is that of nuclear factor erythroid 2-related factor 2 (Nrf-2) (101). Nrf-2, a transcription factor and regulator of nuclear factor-kappa B (NF-κB), is bound in the cytosol as a complex with Kelch-like ECH-associated protein (Keap1), which negatively regulates its transactivation potential. When reactive oxygen species are present (and indeed in the presence of SFN), the Nrf-2:Keap1 complex dissociates which ena*b*les the translocation of Nrf-2 to the nucleus whereby it can exhibit its effects and induce detoxification genes (102). Through this mechanism SFN has been shown to regulate phase I and II detoxification enzymes, nicotinamide adenine dinucleotide phosphate (NADPH) regeneration, and antioxidant defence (103). SFN may also be able to directly bind and inhibit NF-κB (known to be elevated in cancer) and subsequently reduce tumour cell proliferation (104, 105).

Research suggests that SFN also play a significant role with regards to the metabolic regulation of the prostate, thus leading to decreased PCa incidence and progression (106, 107) . Previously, SFN has been shown to inhibit the occurrence of prostatic intraepithelial neoplasia in transgenic

adenocarcinoma of the mouse prostate (TRAMP) mice through increased cytotoxicity of natural killer cells (106). However, more recently the treatment of LNCaP and castration-resistant (22Rv1) human PCa cells with SFN has shown to downregulate fatty acid (FA) metabolism proteins, including those involved in FA synthesis (acetyl-CoA carboxylase 1; ACC1 and fatty acid synthase; FASN) and FA uptake for β-oxidation (carnitine palmitoyltransferase 1A; CPT1A). Furthermore, SFN-treated TRAMP mice demonstrate a significant reduction in plasma and prostatic adenocarcinoma levels of free FAs, suggesting that the reduction in PCa progression by SFN is linked with reduced FA metabolism (107).

Alterations in the acetylation patterns on histones are a characteristic feature in PCa progression (108). SFN has been shown to interfere with a key androgen receptor (AR) chaperone, Hsp90, by inhibition of histone deacetylases (HDAC) enzymes, which remove acetyl groups from histones inhibiting HDAC activity within cancer cell lines (109). SFN has been shown to directly attenuate the AR pathways present in LNCaP PCa cell line via the inhibition of HDAC6 activity (110). In addition, SFN has been shown to inhibit epigenetic regulators including HDAC3 in PC3 PCa cell lines and decrease protein expression in the TRAMP model (111). SFN metabolites (sulforaphane-cysteine; SFN-Cys and sulforaphane-N-acetyl-cysteine; SFN-NAC) have been shown to induce the phosphorylation of extracellular signal-regulated protein kinases 1 and 2 (ERK1/2) leading to microtubule disruption and apoptosis in DU145 and PC3 human PCa cell lines (112).

Consistent with cell and animal models, epidemiological studies have demonstrated a link between the intake of cruciferous vegetables (in particular the active compound SFN) and a reduction in the incidence or progression of PCa (113-117) . A large data set meta-analysis including 6 population-based case-control studies and 7 cohort studies showed a significantly decreased PCa risk overall for cruciferous vegetable intake (RR = 0.90; 95% CI 0.85-0.96) as well as in the subgroup of case-control studies (RR = 0.79; 95% CI 0.69-0.89) (113). In addition, a prospective study involving patients with extra-prostatic disease, documented a 59% reduced risk of PCa progression for highest vs. lowest intake of cruciferous vegetables (HR: 0.41, 95% CI 0.22 - 0.76 P = 0.003) (118). There are however, few human intervention studies which support these findings.

In one such randomised control trial (RCT) involving 98 patients scheduled for a prostate biopsy as part of their routine clinical care (who had not previously received any PCa-related treatment procedures), patients consumed either myrosinase-treated broccoli seed extract (BSE) capsules, containing 100μmol of SFN twice daily, or a matched placebo control, for 4-6 weeks prior to their biopsy procedure (119). This study demonstrated a significant accumulation of total SFN and individual SFN metabolites in both the urine and plasma when compared to the placebo control. In addition to these findings, gene expression analysis of 55 prostate biopsy samples (taken from tissue away from areas of known PCa or prostatic intraepithelial neoplasia ((PIN)) identified three

significantly differentially expressed genes in the supplementation arm when compared to placebo. Despite this however, a difference in levels of other PCa epigenetic biomarkers was not demonstrated.

A further human intervention trial undertaken in Norfolk (UK) has demonstrated that the several hundred changes in gene expression and potentially oncogenic pathways (which are consistent with increased risk of carcinogenesis in normal prostate tissue) are suppressed in a dose-dependent manner by ingesting broccoli soups with increasing concentrations of GFN (98). This 3-arm parallel randomised double-blinded interventional study was conducted over a 12-month period, involving 49 participants on 'active surveillance' for PCa. Participants received a weekly 300 mL portion of soup made from either a standard broccoli (control) or from 1 of 2 experimental broccoli genotypes with enhanced concentrations of GFN for a period of 12-months, prior to a template-guided transperineal prostate biopsy (TPB). The broccoli genotypes used included a commercially available control broccoli, a commercial variety (Beneforté™) delivering 3-times the GFN level to that of the control (120), and a non-commercial variety, delivering 7-times that of the control. These results provide a mechanistic explanation of how consumption of the cruciferous vegetable broccoli may lead to a reduction in the risk of PCa progression.

1.5.1.2 Organosulphur compounds from Alliaceous Vegetables

Alliaceous vegetables, including garlic, onions, leeks, and shallots, are rich in a variety of bioactive compounds, such as flavonols, oligosaccharides, selenium, arginine and organosulphur compounds (OSCs), the latter being of most interest with regards to health benefits, especially in relation to cancer. The OSCs within Allium vegetables are responsible for the characteristic odour and flavour and comprise approximately 1% dry weight of garlic and 0.5% dry weight of onions. Two classes of OSC are found within whole garlic; S-alk(en)yl-L-cysteine sulfoxides (SACSO) and γ-glutamyl S-allyl-L cysteines. Alliin (S-allylcysteine sulfoxide) is the major SACSO found in garlic and isoalliin (trans-(+)-S-(propen-1-yl)-L-cysteine sulfoxide) is the predominant SACSO in onions (38-40). When garlic is cut, chopped, or crushed, the disruption of the cell membranes causes the transformation of SACSO to sulfenic acid intermediates by the enzyme alliinase, which are released from the vacuoles of the plant as part of its defense system. These intermediates are highly reactive and rapidly produce thiosulfinate compounds via condensation reactions (figure 2). Allicin (thio-2-propene-1-sulfinic acid S-allyl ester) is the major garlic thiosulfinate, and due to its unstable nature, is rapidly broken down to further compounds such as ajoene, vinyldithiins, and sulfides including diallyl sulfide (DAS), diallyl

disulfide (DADS), and diallyl trisulfide (DATS) (121). γ-glutamyl S-allyl-L cysteines on the other hand, is absorbed intact and hydrolysed to the water-soluble compounds S-allyl-L-cysteine (SAC) and trans-S-1-propenyl-L-cysteine (121, 122) and metabolised to further OSCs.
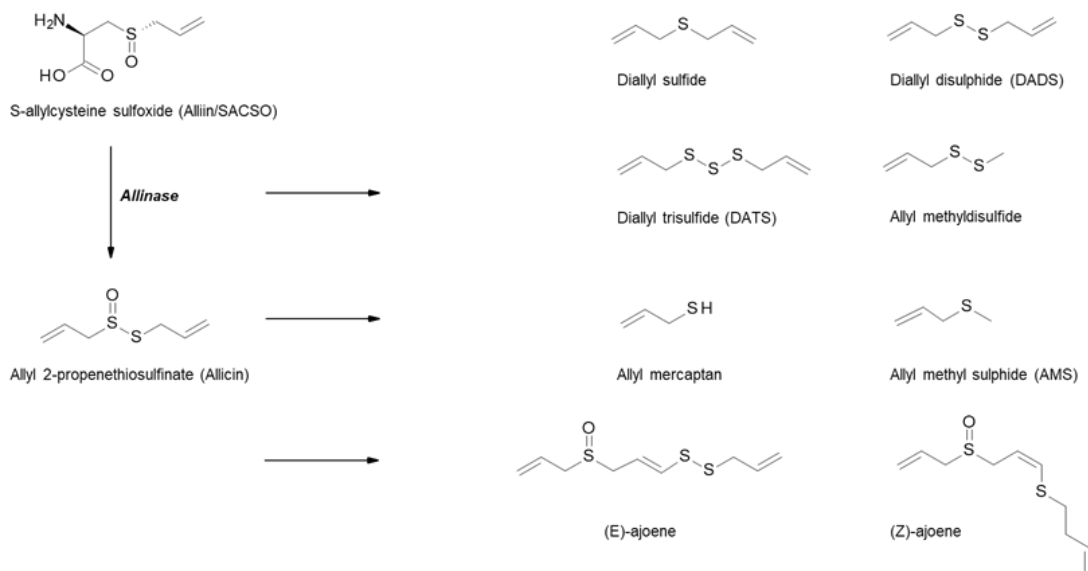
Figure 1.4 Metabolism of Organosulphur Compounds in Garlic. Schematic outlining the breakdown of SACSO (alliin) initially by alliinase, to thiosulfinates, and further compounds including sulfides (112, 113, 121).

Multiple cell and animal models have suggested a protective role of alliaceous vegetables on cancer risk, with several reported mechanisms, each targeting most of the cancer hallmarks defined by Hanahan and Weinberg (123), such as caspase-dependent and independent apoptosis induction, detoxification of carcinogens and cell cycle arrest (124-126). Some components of alliaceous vegetables are reported to block the metabolism of hydrocarbons and nitrosamines and modulate phase I and II enzymes and DNA repair (127). In addition, a further study has shown that S-allylmercaptocysteine can modulate the expression of androgen-responsive biomarkers and hence alter the androgenic action in prostatic cells (128).

Large data set epidemiological studies have supported this suggested negative correlation between the intake of alliaceous vegetables and the incidence of PCa (129, 130). Results from a large Shanghai-based case-control study showed that men ingesting more than 10 g/day of allium vegetables had a reduced risk of PCa compared with those who consumed less than 2.2 g/day (OR = 0.51, 95% CI = 0.34 –0.76, p 0.001), with the effect most pronounced for garlic and scallions, and for the risk of developing localised PCa (129). Research has shown that garlic consumption in the Shanghai population is significantly higher than found in British population studies (46% of Shanghai

males consume at least 6g/approx. 2 cloves of garlic a week compared to 15% of British males), compared to a higher consumption of onions in western populations (131). A further systematic literature review of 9 studies across 4 continents (including China, the Netherlands, Italy and USA) reported a significantly decreased risk of PCa with increasing intake of alliums overall (OR=0.80, 95% CI 0.70-0.92), and in particular for garlic (OR=0.77 95% CI 0.64-0.91), but not for onions (130). Despite this evidence, there are currently no published human intervention studies analysing the effect of alliaceous vegetables on PCa.

1.5.1.3 S-methyl-L-cysteine sulfoxide (SMCSO) from Cruciferous and Alliaceous Vegetables

In addition to glucosinolates, cruciferous vegetables including broccoli contain other sulphur-containing metabolites such as S-methyl-L-cysteine sulfoxide (SMCSO; methiin). SMCSO is found in higher concentrations (dry weight of 1 – 4 %) in comparison to glucosinolate concentration (0.1 – 0.6 %) (50). SMCSO is metabolised by plant or microbial based specific cysteine conjugate β lyases, and thus generating the biologically relevant volatile sulphur compounds S-methyl methanethiosulfinate (MMTSI) and S-methyl methanethiolsulfonate (MMTSO) *(132)*. MMTSO is produced through disproportionation of MMTSI (pathway shown in figure 3). The full mechanism for SMCSO metabolism is yet to be fully elucidated, but gut microbiota appears to play a significant role (51).
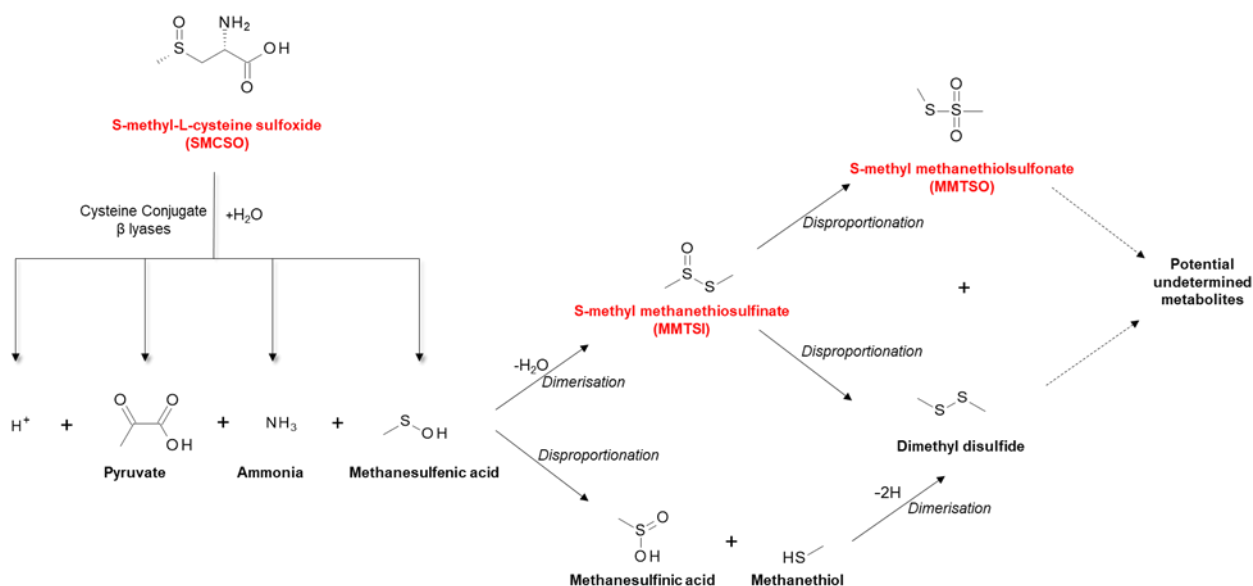
Figure 1.5 SMCSO metabolism. Schematic outlining the breakdown of SMCSO initially by specific cysteine conjugate β lyases leading to secondary bioactive products through dimerization and disproportionation

reactions. Highlighted in red are the sulphur-containing metabolites with potential, undetermined biological

activity (133)

In vitro studies on the effect of SMCSO and its breakdown products MMTSI and MMTSO on human PCa cells lines are well documented (132), but there have been limited human clinical interventional studies investigating this relationship. To date, there have been two reports of the pathway of SMCSO metabolism and excretion in humans. Following fourteen days of administration of radiolabelled SMCSO and S-carboxymethyl-L-cysteine sulfoxide (SCMCSO) to four healthy males, the radiolabelled compounds had completely degraded to sulfate, with urine being the major pathway of excretion (96% in 14 days) (134). More recently, SMCSO has been shown to accumulate within the prostate and peri-prostatic tissue of men consuming a high GFN broccoli soup three times a week for four weeks prior to a TPB. SMCSO was also detected within urine, and its levels were correlated with that in prostate tissue (133). There are no known routes by which mammals can synthesise SMCSO, which makes a dietary origin most likely.

Along with the S-alk(en)yl cysteine sulfoxides, SMCSO is also known to accumulate within alliaceous vegetables such as garlic. As described above, SMCSO has been shown to accumulate within the prostate and urinary system (133). This compound is structurally very similar to SACSO, which supports the theory that SACSO and its metabolites may accumulate within the prostate or urinary system when consumed at high concentrations and may therefore be responsible for beneficial health effects. The role of SMCSO in PCa prevention is yet to be elucidated but is an area of great interest.

1.5.1.4 The Role of Glutathione S-Transferase Mu 1 Genotype and Sulphur-Containing Dietary Bioactives

Polymorphisms in glutathione S-transferases (GSTs) have long been associated with PCa susceptibility, particularly when analysing the risk differences amongst racial groups (135, 136), but also have a role in the metabolism of both cruciferous and alliaceous vegetables. GSTs belong to a family of phase II detoxification enzymes; They catalyse the conjugation of glutathione (the first step in the mercapturic acid pathways) and are involved in both the inactivation of carcinogens and the removal of oxidative compounds which may ultimately lead to DNA damage (137). There are 8 classes of GSTs, but glutathione S-transferase Mu 1 (GSTM1), regulated by Nrf-2, is the most extensively studied GST with regards to PCa risk (138). For example, the metabolism and glutathione

conjugation of SFN has been linked to GSTM1 genotype (139), and bioavailability studies have demonstrated that SFN and its biologically-active thiol conjugates are more rapidly cleared from the systemic circulation in GSTM1 null individuals (140-142). Additionally, epidemiological studies have demonstrated that the presence of a functioning GSTM1 allele confers a greater benefit from cruciferous vegetable consumption with regards to PCa risk, compared to null individuals (136). Alliaceous vegetables also demonstrate the ability to induce GST enzymes in both rats and humans (143-146).

1.5.2 Carotenoids and Prostate cancer

1.5.2.1 Lycopene from Tomatoes

Lycopene is the most abundant carotenoid found in tomatoes, and accounts for >85% of all dietary sources (147). It is a 40-carbon atom, acyclic open chain hydrocarbon containing 11 conjugated and 2 non-conjugated double bonds, assigned in linear array building a chromatophore (figure 4). These double bonds allow for potential extensive isomerisation, which could theoretically result in 1056 *cis-trans* configurations (148). Despite this, there are only a few isomers found in nature, the most prevalent being the all-*trans*-isomer (the all-*trans* and 5-*cis* isomers being the most thermodynamically stable configurations). Isomerisation from *trans*-isomer to various other forms can occur secondary to heat, light, chemical reactions or secondary to *in vivo* mechanisms (149, 150).
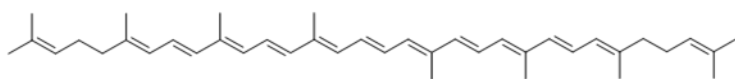
Figure 1.6 Chemical structure of Lycopene

The lycopene concentration in fresh fruit varies greatly; up to 15mg of lycopene has been found per 100g of deep-red tomato varieties, compared with only 0.5mg per 100g of yellow tomatoes (150, 151). Processed tomato-based foods have been shown to contain higher levels of lycopene than fresh raw tomatoes, with tomato sauces containing >17mg/100g and tomato paste containing >55mg/100g (152). The colour of the lycopene is directly related to its isomeric form, with all-*trans*

isomers being deep red, compared with tetra-*cis*-lycopenes which are more orange in appearance (153).

Lycopene is passively absorbed in the small intestinal mucosa via integration into dietary lipid micelles, along with other lipids and bile acids. Micelles are transported from the enterocyte to the liver in the form of chylomicrons in lymphatic fluid, prior to transportation in the plasma to target organs via low density and very low-density lipoproteins (figure 5). Absorption of lycopene ranges between 10-30% and is dependent upon many factors, including age, smoking, alcohol consumption, and dietary composition (154, 155). Importantly, the lipid soluble nature of lycopene means that its bioavailability is vastly increased by consuming it with fat (156). Lycopene appears to distribute unevenly across organs, perhaps due to differing metabolic/oxidation rates or lipoprotein receptor numbers (157, 158), however, lycopene preferentially accumulates to maximal concentrations in the testes, adrenal glands, liver and prostate (154, 158).
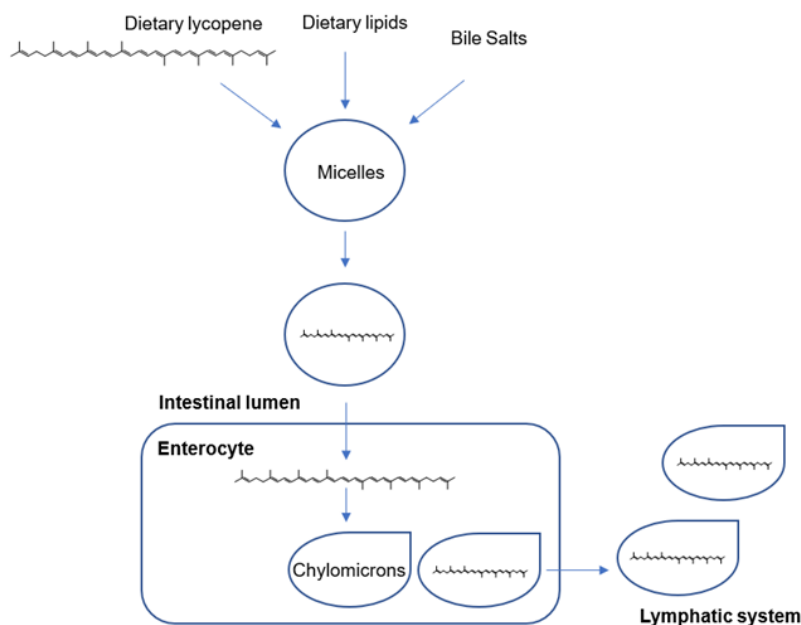
Figure 1.7 Digestion and absorption of lycopene in the small intestine. Lycopene is absorbed into the enterocyte in lipid micelles and transported in the lymph in chylomicrons to the liver prior to transportation in plasma to target organs (153).

The multiple conjugated double bonds are believed to be responsible for Lycopene's various protective (anti-oxidant) effects. Its active singlet oxygen (free radical) quencher is believed to assist DNA repair and may react with oxygen free radicals by transfer of the unpaired electron, leaving the

carotenoid in an excited triplet state. Indeed, lycopene has been shown to exhibit a singlet quenching ability twice as powerful as beta-carotene and tenfold greater than alpha-tocopherol (Vitamin E) (159).

Considerable *in vivo* work has demonstrated a potential antiproliferative effect of lycopene on PCa cells, with mechanisms linked to cell cycle arrest and apoptosis postulated. Lycopene has been shown to exert antiproliferative effects via its ability to induce G2/M-phase cell cycle arrest and apoptotic cell death on LNCaP cells, especially in unsynchronised cells (160). These findings have been reproduced by further studies (161). Similarly, treatment of androgen-independent PCa DU145 cells with lycopene has shown to induce G0/G1 phase cell cycle arrest and induction of apoptosis in a dose dependent manner (apoptosis rate increased by 42.4% in cells treated with 32µmol/l lycopene compared with controls) (162). Features of induction of apoptosis such as reduced mitochondrial potential, release of mitochondrial cytochrome c and annexin V binding, have been shown to upregulate when LNCaP cells are treated with increasing concentrations of lycopene (163). A recently published systematic review of cell and animal studies also suggests that lycopenes have the ability to interact with the androgen axis, downregulating androgen metabolism and signalling in PCa (164).

Most of the data linking the association between lycopenes and PCa originate from epidemiological or prospective studies. The literature surrounding the association with lycopene and PCa is mixed and remains controversial, particularly with reference to aggressive and/or advanced PCa. A systematic review and meta-analysis of 42 case-control studies (43,851 PCa cases) published up to 2016 showed that dietary intake (RR=0.88, 95% CI: 0.78–0.98, P=0.017) and circulating concentrations (RR=0.88, 95% CI: 0.79–0.98, P=0.019) of lycopene were associated with reduced (localised) PCa risk (165). This association was also shown to be dose-dependent; for every additional 2mg of lycopene, the risk of PCa decreased by 1% (P=0.026), and PCa risk decreased by 3.5 to 3.6% for each additional 10 µg dL^{-1} of circulating lycopene. This association however, was not shown to be protective against the incidence of advanced PCa. Similarly, a systematic review and dose-response meta-analysis of dietary intake of lycopenes in relation to PCa risk also showed a dose-dependent associated reduced risk of PCa incidence (RR for dietary lycopene intake: 0.86, 95%CI: 0.75–0.98; RR for blood lycopene levels: 0.81, 95% CI: 0.69–0.96), with no protection to the risk of advanced PCa (166). Dose-response analysis demonstrated a reduced risk of PCa by 3% per 1mg/day (95% CI: 0.94–0.99) increment of dietary lycopene intake.

A further case-control study of 408 controls in a Vietnamese population, showed that higher intakes of total carotenoids were significantly associated with a reduced risk of a diagnosis of PCa. Of all carotenoid intake, lycopene exhibited the most significant results, conferring an adjusted OR of 0.46

(95% CI: 0.27, 0.77) of PCa risk when comparing the highest versus lowest tertile of lycopene intake (167). These inverse associations were dose-responsive and independent of other confounding factors commonly associated with PCa, including age, family history of PCa, and body mass index.

In contrast to the above studies, pooled analysis of 15 studies failed to show any association between the intake of 7 major carotenoids and overall risk of PCa. However, high lycopene intake was shown to be inversely associated with risk of advanced stage PCa and aggressive disease (OR 0.65 95% CI: 0.46, 0.91; P =0.032) (168).

As is true for all nutrients, estimation of dietary lycopene intake through the use of questionnaires often creates bias (169). Further bias is introduced via bioavailable lycopene measurement error. A review of 11 studies comparing dietary lycopene intake with circulating levels document an average correlation of 0.2 (170). However, in one prospective study, participants consuming a high tomato sauce intake were found to have the highest published correlation of dietary and circulating lycopene (r = 0.46), indicating that consumption of tomato sauce captures most of the bioavailable lycopene in diet (170). In this study, lycopene intake was associated with reduced risk of PCa (RR=0.84 CI=0.73-0.96 P=0.03) for high versus low quintiles, with the greatest risk reduction attributed to high tomato sauce intake (RR 0.77 95% CI = 0.66 – 0.90 P<0.001 for >2 servings/week vs. <1 serving/month) especially for extra-prostatic cancers (RR = 0.65 95% CI = 0.42 – 0.99). In addition to highly concentrated sources of carotenoids found in tomato sauces, the thermal processing involved in the cooking of tomato sauces acts to increase the bioavailability of lycopene; heat causes the binding matrices to disrupt and an oily base improves take up into micelles and subsequent absorption in the intestine (170).

These findings are supported by the results of a clinical study in which 32 patients with biopsy confirmed PCa were randomised into either a treatment arm (consuming 30mg lycopene/day in the form of a tomato sauce) or a control arm, for 3 weeks prior to prostatectomy. Intervention with a tomato sauce resulted in an increased abundance of apoptotic cells (from 0.84 +/- 0.13% to 2.76 +/- 0.58% P = 0.0003) and degree of apoptotic cell death (from 0.84 +/- 0.13% to 1.17 +/- 0.19% p = 0.028) in resected tumour areas when compared to the non-intervention controls (171).

However, results from the post-hoc analysis of the 'Procomb trial' in which patients were followed up for two years following dietary intervention, (and underwent a prostate biopsy when there was either a clinical suspicion of PCa or PSA rise to >4ng/ml), did not provide any evidence for lycopene supplementation in protection from PCa incidence. Supplementation in this trial also included selenium. Larger human studies are required to elucidate the potential anti-PCa effects of lycopene (172).

1.5.3 Polyphenols and Prostate cancer

1.5.3.1 Resveratrol from Wine

Resveratrol (tran-3,5,4-trihydroxystilbene) is a stilbenoid polyphenol belonging to the phytoestrogens. Two isomeric forms of resveratrol exist; the trans- isomer is the most stable and biologically active form, whereas the cis- isomer is formed following the breakdown of the trans-form secondary to the action of UV light or high pH conditions during fermentation (figure 6). Both isomeric forms of resveratrol can be found in variable concentrations in grapes, as well as several fruits including tomatoes, raspberries, blueberries and mulberries. The highest concentration of resveratrol is found in the skin of black and red grapes (50-100 µg/g), and thus, red wine, and to a lesser degree in white and rosé wines. Commercially available wines have been shown to contain a concentration of resveratrol in the range of 0.1 – 14.3 mg/L (173, 174), with the Pinot Noir grape varieties containing the highest concentrations of trans- 3,5,4'trihydroxystilbene (175). Resveratrol is also found in cocoa and chocolate to a lesser degree (1.85 ± 0.43 µg/g and 0.35 ± 0.08 µg/g respectively). (173, 174, 176)

Following ingestion, resveratrol is passively absorbed via transepithelial diffusion into the small intestine where it undergoes immediate and extensive intestinal and hepatic metabolism (via conjugation with glucuronic acid). Oral absorption of resveratrol is documented as being as high as 75%. Following metabolism, the major metabolites occurring in plasma and urine are sulfates and glucuronides (via deconjugation enzymes such as B-glucuronidase), reduced conjugates of which can accumulate to varying concentrations in tissue. Although concentrations of 5g resveratrol daily are considered to be safe, evidence suggests that a daily intake of 0.5-1g can elicit pharmacological action in the GI tract (177), with mild to moderate gastrointestinal symptoms occurring at doses of 2.5-5g (173, 178), and other mild side effects such as headaches occurring at higher doses (179).
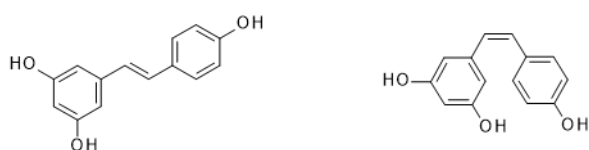
Figure 1.8 Isometric forms of resveratrol -trans (left) and -cis (right).

Resveratrol appears to have a significant multi-modal anti-tumoural activity on PCa cells, via increasing apoptosis, cell cycle arrest and downregulation of signal transduction pathways. Resveratrol has been shown to have proapoptotic effects on multiple PCa cell lines including LNCaP, DU–145, and PC–3; and in the athymic xenograft LNCaP and TRAMP mouse models (173). In addition, resveratrol increases the proapoptotic potential of TNF-Related Apoptosis Inducing Ligand (TRAIL) by activating the FOXO family of forkhead transcription factors (such as FKHRL1) and its target genes (180). TRAIL, a cytokine which incurs a low toxicity to non-malignant cells, has been shown to induce apoptosis in 60% of multiple PCa cell lines. The metastatic potential of PCa cells is also altered under the influence of resveratrol, via the reduction in expression of vascular endothelial growth factor (VEGF) and VEGF receptor 2 (VEGFR2), including the matrix metalloproteinases (MMPs) (180). In addition, both resveratrol and its analogues have been shown to regulate to action of metastasis-associated protein 1 (MTA1) and microRNA (181). Furthermore, resveratrol has demonstrated a direct and potent inhibitory effect (even at low concentrations) on DU145 PCa cells, as measured by the reduction of reactive oxygen species (ROS) production (182).

Resveratrol has also been shown to down-regulate AR expression in TRAMP mouse models (183), and alter the AR and chemokine receptor type 4 (CXCR4) pathways required for tumour progression and metastasis (184). CXCR4, a chemokine receptor which is upregulated in cancer metastasis, is significantly inhibited by resveratrol (both alone and in combination with bicalutamide), in addition to a reduction in the downstream genes associated with cell cycle progression. Importantly, resveratrol also appears to act on androgen-independent cells. In the presence of resveratrol, mediators of survival pathways such as phosphoinositide 3-kinase (PI3K) have been shown to decrease, leading to a reduction in the phosphorylation of downstream targets such as protein kinase B (PKB/Akt) (185).

Much of the clinical data supporting this relationship is derived from epidemiological studies. Alcohol intake has previously been associated with a significant dose-response increase in risk of PCa incidence and progression (186), but type of alcohol consumption was not analysed. A recent meta-analysis of 17 studies (non-randomised observational or case-control studies) including over 600,000 subjects reported that 'moderate' wine consumption did not increase the risk of PCa (0.98 95% CI 0.92–1.05, p=0.57) (187). The definition of 'moderate' consumption differs across all included studies, although the maximum intake for all studies was one glass of wine per day. However, multi-variant analysis produced varied and antagonistic results depending upon wine type; the overall risk of PCa incidence increased with moderate intake of white wine (RR 1.26 95% CI 1.10-1.43 p=0.001), whereas moderate red wine consumption demonstrated a protective role, with a risk reduction of 12% (RR 0.88 95% CI 0.78-0.999 p=0.047). However, exclusion of one large prospective study with a

16-year follow-up demonstrated no significant association between wine type and risk of PCa (188). Epidemiological studies involving alcohol, however, are often prone to significant reporter bias. Additionally, it remains difficult to separate the potential beneficial effects of resveratrol from the known and detrimental effects of ethanol (186).

A randomised placebo-controlled clinical study undertaken in middle-aged men with metabolic syndrome has shown that high dose dietary supplementation of resveratrol for 4 months (1,000mg/day) resulted in significantly lower serum levels of androgen precursors than a control. Androstenedione, dehydroepiandrosterone (DHEA) and dehydroepiandrosterone sulfate were all shown to be lowered by up to 50% (24% p=0.052, 41% p=<0.01 and 50% p<0.001 respectively), although no effect on PSA, prostate size, testosterone or dihydrotestosterone levels was seen (189). Future human studies are required to elucidate the clinical effect of resveratrol on PCa.

1.5.3.2 Catechins from Green Tea

A variety of teas are produced from the leaves of *Camellia sinensis*, including green, black and oolong. The production of green tea differs to that of black tea and oolong in that it is made by steaming the fresh leaves, thus preventing the oxidation of the polyphenol compounds (190). Green tea contains polyphenols known as catechins which include epicatechin (EC), epigallocatechin (EGC), epicatechin-3-gallate (ECG) and the most abundant epigallocatechin-3-gallate (EGCG), shown in figure 7. Green tea catechins, specifically EGCG, have been heavily studied at an *in vitro* and epidemiological level giving a vital insight into its effect on PCa incidence and progression.

EGCG has been shown to be one of the most potent modulators of the molecular pathways involved in prostatic carcinogenesis (191, 192). Preclinical i*n vitro* work on PCa cell lines exposed to EGCG have shown promising results. LNCaP PCa cells treated with $0 - 80$ μM EGCG resulted in suppression of cell proliferation (both dependent and independent of androgens) as well as a reduction in levels of PSA (193). Treatment with $0 - 50$ μM EGCG has been shown to prevent the proliferation of PC3 PCa cell lines with an IC_{50} value of 39 μM, via the activation of extracellular signal-regulated kinase (ERK 1/2), independently of mitogen-activated protein kinase kinase (MEK) signalling (194). Additionally, encapsulation of EGCG with polysaccharide nanoparticles induced apoptosis and reduced the cell viability of DU145 PCa cell lines more than free EGCG (195), suggesting a potential method for delivery that preserves the bioavailability of plant bioactives for chemoprevention.
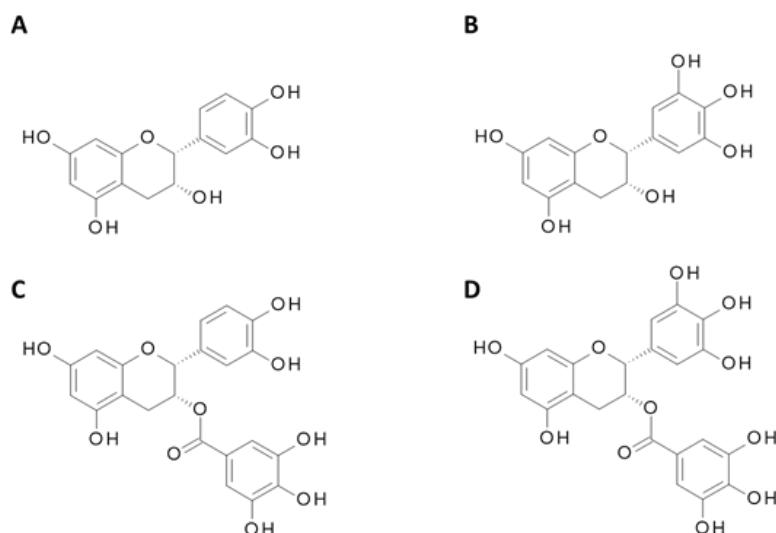
Figure 1.9 Chemical structure of major green tea catechins. A – Epicatechin (EC), B – Epigallocatechin (EGC) C – Epicatechin 3-gallate (ECG) D – Epigallocatechin-3-gallate (EGCG).

EGCG influences other anti-cancer mechanisms through cell cycle arrest and apoptosis, including protein kinase C pathways, inflammatory pathways such as NF-$_K$B cyclooxygenase-2 (COX-2), and the targeting of insulin-like growth factor (IGF) (196).

Meta-analyses of epidemiological studies have, however, reported conflicting results. Three meta-analyses have all demonstrated no significant inverse association between green tea intake and risk of PCa (RR 0.75 95% CI 0.53–1.07 (197), RR = 0.79, 95% CI 0.43–1.14 (198) and RR = 0.73, 95% CI 0.52–1.02) (199). However, following sensitivity analysis the most recent of these studies demonstrated significant heterogeneity caused by one individual study in which a Chinese population were consuming large amounts of green tea for >40 years (197, 200). Novel data excluding this study, demonstrated that consumption of green tea catechins may reduce the risk of PCa by 4.5% (P = 0.08) for each 1cup/day of green tea.

In the first placebo-controlled clinical trial undertaken analysing the effect of green tea on PCa incidence, 60 patients with high-grade prostatic intraepithelial neoplasia (HGPIN) were randomised into either a placebo group or intervention, receiving 600mg of green tea catechins per day. Over a 12-month follow up period, the incidence of progression to PCa (as diagnosed by prostate biopsies) was significantly reduced in the treatment arm (RR 0.38 P = 0.02) (201). These findings however, are contradicted by more recent studies, which demonstrate no reduction in risk of PCa in men with baseline HGPIN or atypical small acinar proliferation (ASAP) (202). However, one RCT in which 93 patients with confirmed PCa consumed 6 cups of green tea, black tea or water (placebo) daily prior to prostatectomy, demonstrated a significant uptake of green tea polyphenols in prostatic tissue, as

well as significantly reduced levels of prostatic NF-κB in the green tea arm. In addition, participants consuming green tea also exhibited a systemic antioxidant effect (as measured by urinary 8-hydroxydeoxy-guanosine [80HdG]) (203).

Further human studies are required to investigate the effects of green tea on PCa incidence and progression, either alone or in combination with other treatment modalities.

1.5.3.3 Curcumin from Turmeric

Curcumin is a polyphenolic compound and secondary metabolite isolated from the rhizome of the plant *Curcuma longa* (commonly known as turmeric), an herbaceous perennial plant of the ginger family (figure 8). Curcumin has long been associated with health benefits, having been used for centuries in traditional Indian medicine for a variety of conditions (204). Following ingestion, curcumin undergoes metabolic O-conjugation to curcumin glucuronide and curcumin sulfate, and bioreduction to additional metabolites including terahydrocurcumin, hexahydrocurcumin, octahydrocurcumin and hexahydrocurcumin. Reduced curcumin is also subjected to glucuronidation into curcumin glucuronide, dihydro-curcumin-glucuronide, tetrahydrocurcumin-glucuronide, and curcumin sulfate (205, 206). The majority of curcumin is metabolised in the liver and intestine, although small amounts remain detectable in blood, and a variety of organs including the heart, lung, brain and kidney (206). However, due to its poor absorption, extensive and rapid phase II metabolism, and rapid elimination, curcumin has a poor bioavailability. Several methods have been adopted to improve curcumin bioavailability, for example by blocking these metabolic pathways. The known bioavailability enhancer piperine (the active component of black pepper) can increase curcumin bioavailability by 2000% by creating a curcumin complex, and ultimately inhibiting hepatic and intestinal glucuronidation (207).
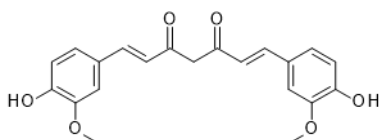
Figure 1.10 Chemical structure of Curcumin

Like many dietary bioactives, the effect of curcumin on PCa cells is multi-modal. Curcumin has been proven *in vitro* to inhibit the growth of PCa cells by increasing apoptosis, suppressing NF-κB

activation, downregulating the expression of B-cell lymphoma 2 (Bcl-2) and B cell lymphoma extra-large (Bcl-xL), and leading to an activation of caspase-3 and -8. Studies have confirmed the inhibition of PC3 cell viability in a dose-dependent manner, associated with a significant downregulation of mRNA and protein expression of inhibitor of DNA binding 1 (Id1) (208). Daily intraperitoneal injections of curcumin in PC-3 xenograft mouse models support these findings with a significant reduction in tumour growth within a one-month period. Inhibitor of DNA binding proteins belong to a subgroup of helix-loop-helix (HLH) transcription factors, and are vital regulators of cell differentiation, and hence metastatic progression of cancers. Although Id1 is the most significantly researched, Id4 ectopic expression in DU145 PCa cells has also been shown to upregulate apoptosis, expression of p53, and halt cell proliferation secondary to S-phase arrest (209). In addition, curcumin also appears to exhibit anti-carcinogenic effects via the activation of the Nrf-2 pathway (210). Derivates of curcumin have been shown to enhance levels of Nrf-2 and phase II detoxifying genes through epigenetic regulation in TRAMP C1 PCa cells (211).

The increasing activity of the AR, along with upregulation of AR-related co-factors, such as cAMP response element-binding protein (CBP) and coactivator protein p300, are salient features of aggressive and hormone-resistant PCas. Curcumin has been shown to interact with these factors in LNCaP and PC-3 cell lines, by inhibiting the expression of the AR (212), as well as suppressing occupancy at sites of AR function (213), thus reducing tumour growth and delaying the onset of hormone-resistant disease .

Multiple clinical trials have been undertaken to support these findings. Most of the trials, however, have described the use of curcumin as an adjunctive treatment, either to radiotherapy, hormonal or chemotherapeutic interventions. A recently published RCT was undertaken on patients managed with intermittent androgen deprivation (IAD) for the treatment of biochemical recurrence of PCa following localised treatment or metastatic disease at diagnosis. Patients received curcuminoid powder in capsule form at a total dose of 1440mg/day for 6 months, commencing at the time of androgen deprivation treatment (ADT) withdrawal. Although there was no significant difference in the overall 'off-treatment' duration of IAD, curcumin treatment resulted in a significantly lower PSA progression in comparison to the control group (10.3% vs 30.2%, P = 0.0259) (214).

Due to the antioxidant, radiosensitising and radioprotective properties of curcumin, interest in the adjuvant treatment of curcumin with radiotherapy is gaining increasing interest. In a further RCT analysing oxidation status, patients received either adjuvant treatment of 3g/day curcumin or placebo during external-beam radiotherapy (up to 74 Gy). Although plasma total antioxidant capacity (TAC) was seen to increase in all patients, this was significantly higher in the curcumin arm (P < 0.001), as was a reduction in the activity of superoxide dismutase (SOD) (P = 0.026). PSA

however, was shown to be reduced (to < 0.2ng/ml) in all patients, with no significant difference between treatment arms (215).

1.5.3.4 Ellagitannins from Pomegranate

Both the seeds and juice of the pomegranate fruit (from the tree *Punica granatum*) have been heavily researched with regards to their bioactive compounds, which are deemed to be anti-microbial, anti-inflammatory and anti-cancerous (216). Pomegranate contains various beneficial components including high levels of vitamin C and polyphenols such as ellagitannins (217). Ellagitannins, including punicalagin, are broken down following exposure to the intestinal pH and/or gut microbiota to ellagic acid, which is further metabolised by the gut microbiota to various urolithins, including the most biologically relevant, urolithin A (figure 9).

Punicalagin has been shown to increase growth inhibition and apoptosis in two human PCa cell lines (PC3 and LNCaP), suggesting a potential anticancer activity of the bioactives within pomegranate (218). Urolithin A has been shown to repress three PCa cell lines with differing p53 genotypes (LNCaP (p53+/+), 22RV1(p53-/+) and PC3 (p53-/-), including an induction of apoptosis (219). Tumour protein p53 is negatively regulated by the E3 ubiquitin-protein ligase MDM2 (mouse double minute 2 homolog) (220). Urolithin A treatment led to the increased p53 protein expression in 22RV1 and PC3 cells which subsequently resulted in the inhibition of MDM2-mediated p53 polyubiquitination (219), indicating that the presence of urolithin A possesses anti-cancer properties via influencing the p53-MDM2 pathway. Pomegranate peel extract (221) and pomegranate leaves extract (222) have also been shown to upregulate apoptosis, reduce tumour cell proliferation and reduce the metastatic potential of TRAMP-C1, DU145 and PC3 PCa cells.
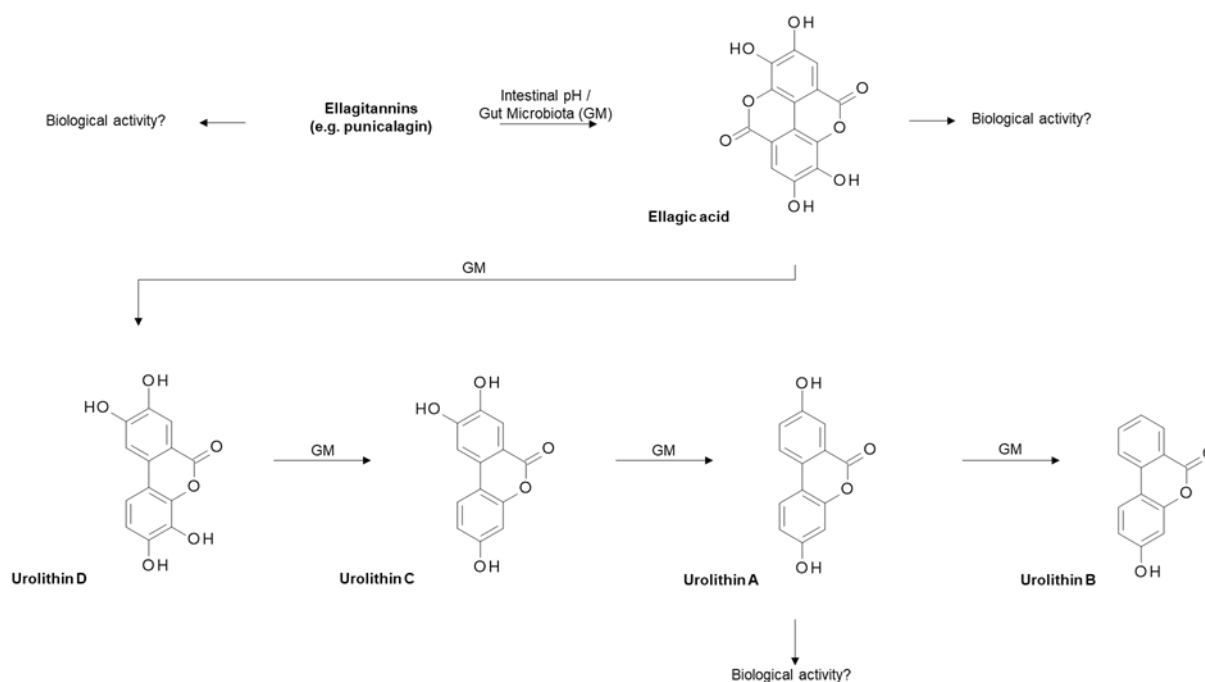
Figure 1.11 Metabolism of ellagitannin within pomegranate. Briefly, ellagitannins such as punicalagin, are metabolised by intestinal pH and/or gut microbiota (GM) to give ellagic acid, which is further broken down by gut microbiota to give various urolithins, of biological relevance urolithin A (223).

In addition, pomegranate extract has been shown to exhibit an inhibitory effect on the NF-κB inflammatory pathway, thus enabling the extract to demonstrate its pro-apoptotic effect (224). Increased NF-κB activity has been shown to be an important predictor of the biochemical recurrence of PCa and hence the transition from androgen-dependence to independence following local therapy (224-226). LAPC4 xenograft tumours (which exhibit a wild-type androgen receptor and features of hormone-dependent growth and metastasis (227)) treated with pomegranate, demonstrate delayed regrowth following castration with a reduction in the increased levels of NF-κB activity (227, 228). Pomegranate extract has also been shown to be effective in treating androgen-independent PCa in mouse C4-2 xenografts with skeletal metastasis, both alone and in combination with docetaxel treatment (229). In addition, the metabolites luteolin, ellagic acid and punicic acid have demonstrated PCa cell growth inhibition and reduced metastasis and angiogenesis in murine studies (230).

Much of the clinical research on pomegranate has focussed on its effects on cardiovascular disease (CVD) (231), however, there has been limited and controversial clinical evidence analysing the influence of pomegranate fruit/juice on PCa. The first clinical trial of pomegranate juice in PCa patients was conducted in 2006 whereby 48 PCa patients consumed pomegranate juice daily for up to 33 months (232). This phase II study demonstrated that those who drank pomegranate juice had a

statistically significant elongation in PSA doubling time. These results were reproduced by a further clinical trial (n = 104) which demonstrated that the consumption of either 1g or 3g pomegranate extract for up to 18 months resulted in an increase in PSA doubling time (from 11.9 months at baseline to 18.5 months after treatment P < 0.001) (233). However, in contrast, a short term placebo-controlled trial (n = 102) concluded that daily pomegranate intake has no impact of levels of PSA in patients with advanced PCa at one month (234). A further intervention study (n = 70) demonstrated that pomegranate supplementation daily for up to four weeks prior to radical prostatectomy resulted in urolithin A accumulation in prostate tissue (P = 0.031), but had no effect on prostatic oxidative stress, cell proliferation, tumour progression or PSA levels (235).

Whilst there is some evidence of pomegranate reducing PCa growth through murine studies and short-term intervention studies, the long-term impact of pomegranate consumption is not fully understood. Current clinical trials are ongoing and include: 'Pomegranate Juice in Treating Patients with Recurrent PCa, ClinicalTrials.gov Identifier: NCT00060086' (data pending) which will contribute to our understanding of how these bioactives influence PCa progression. This study, in which up to 40 patients who have undergone radical prostatectomy or radiotherapy for PCa will consume oral pomegranate juice daily for 18 months, aims to determine whether pomegranate juice consumption can decrease or slow the rate of rising PSA levels.

1.6 Exposure of Dietary Bioactives to the Prostate and the Concept of Urinary Reflux

From the evidence discussed, it is clear that certain dietary bioactives may be associated with either a reduction in the risk, and/or the progression of PCa. Studies in cell and animal model systems provide an insight into a variety of mechanisms by which these bioactives may exert their effect. However, despite well-documented associations, a clear understanding of the degree and mechanism of prostatic exposure to these dietary bioactives or their human or microbial metabolites, is lacking. Exposure of the prostate is conventionally considered to be via the systemic circulation, within which these dietary bioactives would be of a low concentration compared to those used in *in vitro* studies, and extensively metabolised through phase 2 metabolism, (including sulphation, glucuronidation and methylation), that is likely to reduce their biological activity (141, 236). It is possible, however, (as discussed in section 1.1) that the prostate may be exposed to a higher concentration of these compounds via urinary reflux (237).

Evidence of the reflux of urine into the prostatic ducts was first published in 1982, when, following intra-vesical instillation of carbon microspheres, 70% of prostate tissue removed by transurethral resection was found to contain microspheres (238). Additionally, granuloma formation following intra-vesical instillation of Bacillus Calmette–Guerin (BCG) used in the treatment of high-grade non-muscle-invasive bladder cancer occurs within the prostate as well as the primarily treated bladder (239, 240).

Due to its ductal anatomy, the peripheral zone is the most likely part of the prostate to be exposed to urinary components. The ducts draining the peripheral glands enter the urethra as a double lateral line along the whole of the distal urethral segment. The ducts are narrow but enter the urethra at a less obtuse angle than those from other zones, thus potentially making them more prone to the reflux of urine, perhaps with a contribution from turbulence (3). This anatomy makes the peripheral zone more susceptible to exposure from infectious agents (241, 242) and endogenous urinary metabolites and xenobiotics, either environmental or plant-derived bioactives, and their phase I/II metabolites, that may be present in the urine and have the potential to either enhance or reduce risk of PCa. The higher incidence of PCa (70%–80% of all PCas) within the peripheral zone compared to other zones may be a consequence of this exposure (1), in addition to an increased risk of PCa progression due to genomic alterations (243-245). It is therefore plausible that the prostate is exposed to plant-derived bioactive compounds present in urine, and in this way, may exert their potential beneficial effects via their anti-microbial, anti-inflammatory and immunomodulatory mechanisms, as described above.

There is also increasing evidence for a microbiological community associated with both the urinary tract and the prostate itself (246, 247). While certain members of this community, linked to both urinary tract and prostatic infections, may increase the risk of malignant changes (248-251), others (of particular relevance to the sulphur metabolites present in cruciferous and alliaceous vegetables) may metabolise plant-derived chemicals either from systemic exposure or from urinary reflux, to more biologically active forms (133, 252).

1.7 Dietary Supplements

Health claims pertaining to nutrition are highly regulated in order to inform as well as protect the public from false health declarations. In order to substantiate scientific findings, human intervention studies, although challenging, are therefore essential in supporting the role of plant-derived bioactives in preventing PCa (253, 254). Central to this is the careful consideration that needs to be

given to experimental design, selection of appropriate biomarkers of effect and/or clinical endpoints, as well as defining the appropriate interventions (254). For example, it may be difficult to extrapolate concentrations from those used *in vitro* to clinical dosages for use in human studies. Understanding of the bioavailability and pharmacokinetics of relevant phytochemicals is therefore essential to the effective design and outcome of human trials (122, 169, 255, 256). These factors will inevitably alter dependent upon practicalities such as their development and route of administration.

One option for determining the effects of individual plant-derived bioactives is to utilise genomic technologies and develop novel foods that will deliver increased bioactives whilst maintaining the relatively unchanged background composition of the plant (257). Such novel foods would not only differentiate between the effects mediated by individual bioactives compared to effects due to the ingestion of the whole plant, but also facilitate double-blinded intervention trials, the gold standard in clinical nutrition. One such example is the development of the high-GFN broccoli (120). However, the development of such novel foods requires significant investment of both time and effort to understand and manipulate plant biosynthetic pathways. Another option is to deliver isolated pure compounds via dietary supplementation. However, isolating pure compounds is sometimes challenging due to issues with stability, but also the potential to miss, in some cases, unknown compounds derived from the same plant of interest that may also exhibit bioactivity either additively or synergistically (169). Although isolating and utilising pure compounds can be challenging, delivering bioactive compounds in the form of supplements may in fact combat and bypass potential issues with the denaturing of enzymes susceptible in the preparation stage, as well as issues associated with first-pass metabolism (256, 258).

Historically, the discovery of 'micronutrients' (although at the time still in the form of foods) was advanced due to the scale of deficiency diseases prevalent in the population, e.g. citrus fruits and leafy green vegetables for the treatment of scurvy, and cod liver oil for the treatment of rickets. However, in terms of dietary association, the overwhelming cause of chronic diseases such as diabetes, cardiovascular disease, and indeed cancer, in the current population (although multi-factorial), is overconsumption.

Although the majority of required micronutrients can generally be obtained from a well-balanced diet, the use of dietary supplements has increased significantly over the past decade. Dietary supplements are often used by consumers who believe consumption will prevent them from becoming unwell and have hence often been labelled as the "worried well". Studies have shown that age, gender and educational level are significant factors determining the demographic of supplement consumers; 48% of people believe that consuming supplements are 'an easy way to stay

healthy' (259, 260). This increase in use comes despite public health guidelines which state that in general there is no role for supplement use in adults apart from in those who are unwell, and more recently, vitamin D supplementation in at risk groups of the population in the UK" (261).

In much the same way as vitamin D supplementation is now recommended for 'at risk groups', it may be possible to identify and isolate certain dietary bioactive compounds present in foods which can be utilised specifically in other 'at-risk' categories, or in patients known to have a specific condition, in order to prevent disease progression. As is the case for the large amount of consumers utilising cholesterol-lowering products such as butters and yoghurt drinks (259), patients with PCa who follow a programme of active surveillance whereby treatment is delayed until progression warrants the need for intervention, provide an ideal cohort for dietary intervention or supplementation with specific compounds to ascertain whether natural history may be altered.

1.8 Thesis Objectives

This thesis describes the specific impact of sulphur-containing compounds on the prostate, namely the effects of myrosinase-activated glucoraphanin, and garlic/alliin supplements.

The primary hypothesis is that consumption of these dietary compounds will result in an accumulation of their human or microbial metabolites in the urine and prostate, whereby they can exert transcriptional changes associated with PCa development and/or progression.

The study will also test the hypothesis that consumption of these supplements will lead to transcriptional changes in the prostate, and that these will be more pronounced within the peripheral zone than the transition zone.

The experimental approach includes:

- Analysis of commercially available dietary supplements for use in a human study
- Design and completion of a randomised, double-blinded, 2^2 factorial design dietary supplement study, involving patients awaiting a transperineal biopsy of the prostate for known or suspected PCa
- Analysing targeted metabolite accumulation in the urine and prostate tissue
- Analysing the spacial distribution of metabolite accumulation within the peripheral and transition zone of the prostate
- Analysing the transcriptional differences between the peripheral and transition zone from prostate biopsy samples in patients consuming placebo capsules

- Investigating the effects of dietary supplementation on transcriptional pathways associated with PCa development and/or progression.

Chapter Two

A Pre-Biopsy Window-of-Opportunity Study to Measure the Accumulation of Dietary Bioactives in Human Prostate Following Alliin and Glucoraphanin Dietary Supplementation

2.1 Introduction

As discussed in chapter one, both cruciferous and alliaceous vegetables accumulate sulphur-containing bioactive compounds, which are responsible for their characteristic flavour. Degradation of these compounds leads to the production of highly reactive sulphur-containing intermediates (isothiocyanates and organosulphur compounds respectively) and their metabolites, which are thought to be responsible for the anti-cancer properties associated with these vegetables. Although the bioavailability of these compounds within the plasma and urine are well documented, there is currently no compelling evidence from human studies that the effects of these compounds are due to their circulating concentrations existing in the systemic circulation, or indeed due to more local effects on the tissue of interest. In addition, whether these compounds are capable of accumulating within the prostate tissue (where they may elicit their effects) is currently unknown.

A recent intervention study failed to demonstrate accumulation of SFN in the prostate of patients consuming a GFN-rich broccoli soup (133). In this study, eighteen men were randomised to consume either a GFN-rich broccoli soup 3 times per week for a minimum of 4 weeks, or to continue their normal diet. The GFN-rich soup was manufactured from a genetically modified broccoli cultivar heterozygous for Myb28^{villosa} (255). Myb 28 is a well-studied transcription factor, which can modulate the expression of genes involved in glucosinolate synthesis and hence has a role in the expression of GFN levels in *Brassicas*. Introgression of the allele from Brassica *villosa* results in the increased expression of Myb28 mRNA and hence contains a higher concentration of glucosinolates (262). In this case, the Myb28^{villosa} soup contained 280 ± 8.8 µmoles of GFN. This soup intervention was prepared using frozen broccoli, a process which denatures the myrosinase enzyme present in the plant, and additional myrosinase enzyme was not added to the soup preparation. Therefore, there is likely a reduced conversion of GFN to SFN following consumption, reducing the concentration of free SFN which the prostate could subsequently become exposed to. This is supported by the fact that only 2-15% of ingested glucoraphanin was excreted in the urine of the participants as SFN and its thiol conjugates, consistent with other studies in which GFN is consumed with inactivated myrosinase (the bioavailability of GFN and SFN are discussed in greater detail in chapter 3).

In addition to glucosinolates, cruciferous vegetables including broccoli, contain other sulphur-containing metabolites such as S-methyl-L-cysteine sulfoxide (SMCSO; methiin), and to much higher concentrations. SMCSO is also present in alliaceous vegetables such as garlic. The SAP study

inadvertently demonstrated an accumulation of SMCSO in the prostate and peri-prostatic adipose tissue of all participants consuming GFN-enriched broccoli soups, and to significantly greater levels in the supplementation arm than the non-supplementation arm (p=0.005). The level of accumulation in the prostate was also shown to correlate with the concentrations detected in the urine. The soup intervention contained 1513 ± 36.8 µmoles of SMCSO (133). However, SMCSO is known to have a very different pharmacokinetic behaviour to that of SFN; nearly all SMCSO is absorbed, and excreted over a much longer time frame (days rather than hours) (263), which may therefore allow for more sustained exposure to the prostate gland. However, this study was not primarily designed to test metabolite accumulation, and hence the time between the final portion of soup being consumed and the biopsy procedure was not standardised amongst the study participants.

2.1.1 Levels of Bioactive Compounds in Normal Diets Compared to Dietary Supplements

The abundance of literature which describes the link between cruciferous and alliaceous vegetables and PCa risk is derived from epidemiological studies. It is vital to recognise that this poses issues with validity and standardisation given the variable nature of consumption in different populations. For example, studies suggest that cruciferous and alliaceous vegetable intake is highly variable amongst individuals, and low in the westernised population compared to the east. The EPIC study which analysed vegetable intake in a variety of European populations, estimates that the consumption of cruciferous vegetables is 0.4 servings/day in the UK, similar to that of the USA population, which is approx. 0.2 servings/day (264). Importantly however, the type of crucifer ingested varies between countries (cabbage and brussels sprouts are the most consistently consumed crucifers in the UK, compared to broccoli and cauliflower in the US), and for gender (females consume more cruciferous vegetables than males). Interestingly, the UK population is most likely to consume these vegetables following cooking compared to other European countries, which will likely influence the concentration of dietary bioactive compounds consumed due to the action of cooking on the myrosinase enzymes. Regarding alliaceous vegetables, the EPIC study demonstrated that garlic and onion intake is low in the UK, only higher than Greek and Spanish populations, compared to Scandinavian countries such as Denmark and Sweden in which consumption is highest (264). Compared to Eastern countries however, this intake is vastly different; research has also shown that garlic consumption in the Shanghai population is significantly higher than elsewhere, with 46% of Shanghai males consuming at least 6g (approx. two cloves) of garlic per week compared to <15% of British males (86, 131). The highly variable nature of cruciferous and alliaceous vegetable intake,

makes the interpretation of epidemiological studies difficult, especially when assessing habitual intake.

As discussed in chapter one, there are multiple ways in which increased levels of dietary bioactive compounds can be delivered, including the development of novel foods (262), or the isolation of pure compounds via dietary supplementation, for analysis of effect in human studies. By giving isolated bioactive compounds in the form of dietary supplements rather than food, it is possible to deliver a known concentration of the pure compound(s) of interest, whilst eliminating potential issues with preparation and cooking.

2.1.1.1 Glucoraphanin Supplements

GFN is present in all parts of the broccoli plant, although the concentration is greatest in the florets and the seeds. Studies however, have demonstrated the significant variation in concentration of GFN in different samples; for example, the analysis of 31 fresh uncooked broccoli heads from a variety of supermarkets found the mean concentration of GFN was 0.38 µmol per gram fresh weight, but with a range of < 0.005 to 1.13 µmol/gram. Other studies analysing the GFN concentration of 75 different genotypes of field-grown hybrid broccoli was 0.88 and 1.10 µmol per gram fresh weight.

Given the amount of GFN and hence SFN required to elicit clinical effects as seen in previous studies, the amount of broccoli that would need to be ingested (although perhaps achievable), is not habitual for the population. As such, dietary supplementation of these isolated compounds would enable a much higher intake and be more pragmatic for day to day consumption. Intake of cruciferous vegetables and dietary SFN are considered safe and have not been associated with any serious adverse side effects (265).

Multiple clinical trials have utilised broccoli-based preparations, with varying concentrations. For example, one review of GFN-based supplements utilised doses ranging from 25-800 µmol per person per day (median 190 µmol), and SFN-based supplements ranging from 9.9 to 847 µmol per person per day (median 100 µmol) (266). The higher doses of GFN used reflect the recognised limited conversion of GFN to SFN in the absence of myrosinase. This has been overcome in some studies by utilising preparations which contain activated myrosinase, such as Broccomax, and in addition, avoids the increased risks of adverse-effects such as a burning sensation in the throat and dyspepsia following SFN supplementation over 100 µmol (267).

In breast cancer studies, participants consumed 2x Broccomax capsules 3x/day, giving a total daily dose of GFN was 224mg GFN for 8 weeks (268). This dose was determined based upon the amount administered in a pilot study and other trials achieving a significant increase in blood and urine ITC levels within one month, with no reported adverse effects (265, 268, 269). Broccomax was therefore highlighted as a possible intervention for a GFN dietary supplement in a new human study.

2.1.1.2 Garlic / Alliin Supplements

Fresh garlic cloves contain approximately 2-6mg/g of γ-glutamyl-S-allyl-L-cysteine (0.2%-0.6% of fresh weight) and 6-14 mg/g of alliin (0.6%-1.4% of fresh weight) (270). In much the same way as myrosinases present in cruciferous vegetables, the enzyme alliinase can also be inactivated by heat, reducing the bioavailable concentration of bioactive compounds (271-273). Data demonstrating a link between the organosulphur compounds in garlic and its potential clinical effects (270, 274), suggest that the consumption of concentrations of garlic required to produce clinical effects would not be achievable in a normal diet, or indeed tolerated. Supplementation of these isolated compounds may provide an ideal alternative for use in human studies (122).

Multiple types of garlic supplementation exist, including powdered (dehydrated) preparations, 'aged-garlic' (garlic fluid) extracts, and garlic oils. All preparations vary with regards to principal organosulphur compounds contained, their bioavailability, and the level of allicin-derived compounds delivered (122, 270). Garlic powder tablets are deemed to be the most appropriate intervention type for human studies investigating PCa, as they contain the major OSCs of garlic associated with a reduction in the risk and/or progression of disease; cysteine sulfoxides (Alliin) and γ-Glutamyl-L-cysteine peptides (275); concentrations of which must meet USP standards (276). Powdered garlic is produced from garlic cloves dried at a low temperature (thus preventing alliinase inactivation) which are then pulverised and made into tablets. In the same way as heating, the low pH of the stomach can inactivate alliinase, and garlic powder supplements are usually therefore enteric-coated. Although powdered garlic supplements do not contain allicin, manufacturers often provide a value for the "allicin yield", demonstrating the 'true' bioavailability of the supplement and maximum achievable yield under conditions mimicking the stomach and intestine (276-278).

Kwai garlic tablets have previously been used in multiple published human trials at varying doses; in a recent paper comparing allicin bioavailability and bioequivalence from garlic supplements and foods, Kwai was well tolerated at a dose of 3 tablets/day, and allicin bioavailability was high (80%),

validating it as representing raw garlic (122). Kwai supplements were therefore deemed potentially an ideal intervention for the Alliin treatment in a new human study.

The 'Norfolk ADaPt' trial was a standalone trial designed to explore whether a short-term intervention in the form of dietary supplements (rather than foodstuffs) containing the isolated bioactives of broccoli and garlic, will lead to an accumulation of these bioactives or their metabolites in prostate tissue. It was hypothesized that delivering higher levels of isolated dietary bioactives, will result in the accumulation of these compounds or their metabolites in prostate tissue, where they may then alter transcriptional pathways associated with prostate cancer. It is hoped that these findings may subsequently influence dietary choices in men on a program of active surveillance.

2.2. Aims

2.2.1 Dietary Supplement Analysis

- To quantify the levels of dietary bioactive compounds in the commercially available 'Broccomax' capsules, including GFN, SFN and SMCSO

- To quantify the levels of dietary bioactive compounds in the commercially available garlic supplement 'Kwai garlic', including SACSO (S(+)-allyl-L-cysteine sulfoxide), γ-glutamyl S-allyl-L cysteine, Allicin, and SMCSO.

2.2.2 The 'Norfolk ADaPt' Study Aims

The aims of the Norfolk ADaPt study, as specified in the original protocol, are detailed below. The primary role of this study was to determine whether bioactives from supplementation with Alliin and/or Glucoraphanin, accumulated within the prostate tissue itself, when compared with placebo controls. Additional outcome measures, including spatial accumulation throughout the prostatic zones and alterations in gene expression, aimed to further test the hypothesis that accumulation of

these bioactives may be capable of altering the transcriptional environment of the prostate, which may ultimately impact downstream biological pathways associated with PCa risk and/or progression. The impact of GSTM1 genotype on the metabolism and bioavailability of sulphur-containing dietary bioactives and PCa risk is well established (as discussed in chapter one), and hence all results were quantified by genotype. Results were also interpreted in the context of habitual cruciferous and allium vegetable intake as assessed by food frequency questionnaires.

2.2.2.1 Primary Aim

- To test whether, in men scheduled for transperineal prostate biopsy, dietary bioactive compounds from dietary supplements, or their human and microbial metabolites will accumulate in prostate tissue.

2.2.2.2 Secondary Aims

- To determine whether there is a differing spatial accumulation of dietary bioactive compounds or their human and microbial metabolites in the transition and peripheral zones of the prostate following an intervention with dietary supplementation.

- To estimate the level of dietary bioactive compounds or their human and microbial metabolites detectable in urine over a 24-hour period following initiation of dietary supplementation.

- To test whether dietary bioactive compounds or their human and microbial metabolites result in a difference in human gene expression using next generation RNA sequencing following an intervention with dietary supplementation.

- To assess whether the above endpoints are influenced by the glutathione S-transferase Mu 1 (GSTM1) genotype.

2.3 Materials and Methods

2.3.1 Quantification of Bioactive Compounds in Broccomax Capsules

BroccoMax® supplements are produced by Jarrow Formulas Los Angeles, CA. Broccomax is a standardised concentration of GFN extracted from Broccoli seeds, manufactured to preserve the myrosinase enzyme that metabolises GFN in the small intestine into SFN, and hence deliver higher amounts of SFN. Broccomax is documented to contain 30mg GFN and yield approximately 8mg of SFN per capsule. Broccomax has previously been used in multiple published human trials at doses ranging from 2 to 6 capsules daily with good compliance, tolerability and no adverse reactions (269) and was therefore potentially an ideal intervention for the GFN treatment in a new human study.

Broccomax capsules were purchased from Jarrow Formulas, Los Angeles, CA. Ten capsules were used for the quantification of bioactive compounds, one each from ten separate batches, to ensure there was no significant inter-batch variation.

2.3.1.1 Glucoraphanin Extraction from Capsules

Capsule glucosinolates were measured using a previously described method that converts glucosinolates to the equivalent desulfoglucosinolates (279).

To extract glucosinolates, ten capsules were emptied, individually mortar ground, and measured out to approximately 40-50 mg each. A 10 ml aliquot of 70°C 70% (v/v) aqueous methanol followed by 50 µl of internal standard, 16 mM sinigrin (Sigma). All samples were vortexed thoroughly and incubated in a water-bath preheated to 70°C for 30 min to inactivate plant myrosinase enzymes. During incubation, the samples were vortexed twice. After cooling, samples were centrifuged at 4000 xg for 10 min at 4°C. Three millilitres of liquid supernatant were collected from each sample, placed onto the ion exchange columns and left to drip through slowly, enabling the glucosinolates to absorb onto the column. Once the liquid had completely passed through, the column was washed twice with 0.5 ml Milli- Q® water and 0.5 ml 0.02 M sodium acetate (pH 5) in order to remove any interfering ionic matter. Collecting vials (Agilent) were subsequently placed under the needles and the glucosinolates were desulfated by the addition of 75 µl purified sulphatase (Sigma) to the column, which was left at room temperature overnight. The following day, the desulfated glucosinolates in the ion exchange column were eluted with 1.25 ml of Milli- Q® water. Once eluted, a cap (Agilent) was crimped on top of the collecting vial and samples were stored at -20°C until analysis.

2.3.1.2 Liquid chromatography-mass spectrometry (LC-MS) Detection and Quantification of Glucosinolates

Capsule glucosinolates were measured using a previously described method that converts glucosinolates to the equivalent desulfoglucosinolates (279).

A model 1100 High Performance Liquid Chromatography (HPLC) system (Agilent Technologies) including a binary pump, cooled autosampler, degasser, column oven and diode array detector, was used. Mobile phase A of Milli- Q® water with 0.1% formic acid and mobile phase B of LC-MS grade acetonitrile (Merck) with 0.1% formic acid were used. For analysis, the flow rate was set at 1 ml/min with a maximum pressure 300 bar and a gradient of an increasing proportion of acetonitrile from 5% to 100% over 25 minutes was applied, prior to re-equilibration to 5% B for 7 minutes. Samples were analysed using a Waters Spherisorb ODS2 (4.6 x 250 mm id, 5 μm particle size) column (Waters) equipped with a Waters Spherisorb guard column (Waters). The mass spectroscopy was run by positive ion mode with Electrospray source (ES[+]). Desulphoglucosinolate quantification was achieved, using absorbance at 229 nm, by comparison with the peak area ratio of the internal standard (sinigrin), and the relevant desulphoglucosinolate ultraviolet (UV) light relative response factor.

2.3.1.3 Hydrolysis of Glucosinolates

The hydrolysis products of glucoraphanin were measured according to Saha et al. (280).

Briefly, ten capsules were emptied, individually mortar ground, and measured out to approximately 40-50 mg into individual 100 ml volumetric flasks. All preparations were repeated with three independent measures. 100 ml of 1X phosphate buffered solution (PBS, GIBCO, 10X stock diluted 1:10 in Milli- Q® water) was added to each flask. The samples were sealed, vortexed and incubated for 2 hours at 37°C in a water bath. The samples were vortexed every 15 min to ensure optimal hydrolysis. After 2 hours incubation, samples were cooled at room temperature and 1 ml from each sample was transferred to a 2 ml screwtop tube and centrifuged at 13,000 rpm for 30 min at 4°C. The supernatant from each sample was transferred into HPLC vials and sulforaphane-D8 was added as an internal standard for quantification of hydrolysed products. A cap was crimped on top of each collecting vial, vortexed and stored at -20 °C until analysis.

2.3.1.4 Liquid chromatography-tandem mass spectrometry (LC-MS/MS) Detection of Isothiocyanates

A model Agilent 6490 Triple Quadrupole LC/MS system equipped with a binary pump, cooled autosampler, degasser, column oven and diode array detector, was used. A mobile phase A of 0.1% ammonium acetate (Sigma), adjusted to pH 4 with 0.1% acetic acid (Biosolve) in Milli- Q® water, and a mobile phase B of 0.1% acetic acid in LC-MS grade acetonitrile (Merck) were used. For analysis, the flow rate was set at 0.25 ml/min, with the column temperature and autosampler temperature maintained at 20°C and 4°C respectively. Samples were separated on a Phenomenex Luna 3u C18(2) 100A (100 x 2.1 mm) column, using a programmed gradient mobile phase, by multiple-reaction monitoring (MRM) mode. The injection volume was 2 µl per sample. Quantification was conducted through the identification of sulforaphane at a retention time of approx. 7.294, to generate a standard curve. Briefly, sulforaphane (S8044, LKT Laboratories) was dissolved in DMSO to give a 100 mM stock solution and further diluted in Milli- Q® water to generate a working concentration of 1 mM. The stock was diluted in both the relevant matrix and water from 0 mM to the highest concentration of 50 mM. Note: the dilution in water gave better calibration with internal standard. All standards were made prior to each run.

2.3.1.5 S-methyl cysteine sulphoxide (SMCSO) Extraction from Samples

SMCSO was extracted as previously described (281).

Ten capsules were emptied, individually mortar ground and measured out to approximately 40-50 mg each. A 5 ml aliquot of 1.1 mg/ml O-(carboxymethyl)hydroxylamine hemihydrochloride (OCMHA) was diluted in Milli- Q® water to inhibit allinase activity. All samples were vortexed thoroughly and placed on a horizontal shaker at 1000 rpm for 10 min at 4°C. All samples were then centrifuged at 15,000 rpm for 10 min at 4°C. If the supernatant appeared cloudy, a 1 ml aliquot of the supernatant was taken and centrifuged again at 4000 xg for 10 min at 4 °C. The clear liquid was diluted 1:10 in HPLC-H2O containing 0.1 % formic acid and placed into HPLC vials (Agilent), followed by 10 µg/ml Trideutromethyl 34S Cysteine Sulfoxide (SMCSO internal standard) in Milli- Q® water (synthesised by Dr. Paul Needs). A cap (Agilent) was crimped on top of each collecting vial, vortexed and stored at -20°C until analysis.

2.3.1.6 LC-MS/MS Detection of SMCSO

LC-MS/MS detection of SMCSO was undertaken as previously described (281).

A model Agilent 6490 Triple Quadrupole LC/MS system equipped with a binary pump, cooled autosampler, degasser, column oven and diode array detector, was used. A mobile phase A of 10 mM ammonium acetate (Sigma) and 0.05% hetaflurobutyric acid (Sigma) in Milli- Q® water, and a mobile phase B of 10 mM ammonium acetate (Sigma) and 0.05% hetaflurobutyric acid (Sigma) diluted in 10 % Milli- Q® water with the remaining volume made up with 100 % methanol were used. Initially, the flow rate was set at 0.1 ml/min to purge the binary pump. For analysis, the flow rate was 0.3 ml/min with the column temperature and autosampler temperature maintained at 20 °C and 4 °C respectively. Samples were analysed using Agilent SB-AQ 1.8 mM (100 x 2.1 mm) C18 column with an Agilent Zorbax guard column, using a programmed gradient mobile phase and ESI positive MRM. The injection volume was 2 μl per sample and the retention time of SMCSO was approx. 0.906. Quantification was performed using calibration standards. Briefly, SMCSO standard (Methiin, Abcam) was dissolved in Milli- Q® water to each give a 1 mg/ml stock. The stock was diluted in both the relevant matrix and water from 0 μg/ml to the highest concentration of 500 μg/ml. Note: the dilution in water gave better calibration with internal standard. All standards were made prior to each run.

2.3.2 Quantification of Bioactive Compounds in Garlic Capsules

Kwai Heartcare® supplements are produced by Klosterfrau Healthcare Group, Cologne, Germany. Kwai is derived from garlic cultivated in China and prepared using techniques to preserve the active allicin content. Kwai is standardised to contain 300mg concentrated dried garlic powder, to yield 1800μg allicin.

Kwai garlic tablets were purchased from a well-known health food store. Ten tablets were used for the quantification of bioactive compounds, one each from ten separate batches, to ensure there was no significant inter-batch variation.

2.3.2.1 Alliin (S(+)-allyl-L-cysteine sulfoxide) extraction from Kwai® garlic supplements using HPLC – UV

Alliin was analysed using ion pair HPLC-UV as previously described (282).

Eight tablets were mortar ground, measured out to approximately 500mg, and each extracted with 25ml of 20 mM CMA buffer (alliinase inhibitor). These samples were mixed, vortexed and sonicated for 15 mins. From each sample, 1ml was added to a small labelled screwtop tube and centrifuged at 15000 rpm for 10 mins at 4°c. Following centrifugation, 50 µl of the supernatant was added to each labelled HPLC vial.

Alliin was analysed using ion pair HPLC-UV (Luna C18 250mm X 4.6mm column). Solvent A consisted of 20mM sodium heptanesulfonate and 20mM sodium phosphate monobasic, pH adjusted to 2.1. Solvent B was Acetonitrile (ACN). The column was heated at 38 °c with a flow rate of 1.0 ml/min. The gradient was set from 0% B to 15% B in 5 min, then to 22% B by 15 mins and held until 17 min, then back to 0% B by 18 min and held to 24 min.

A calibration curve was formed using Alliin (+) standard purchased from Sigma-Aldrich, which was measured and diluted to 1 ml/ml stock. 2-fold dilutions were then undertaken.

2.3.2.2 γ-glutamyl S-allyl-L cysteine (γ-SAC), S-allyl-L cysteine (SAC) and Allicin extraction from Kwai® garlic supplements using LC-MS/MS

SAC, γ-SAC and Allicin were analysed using LC-MS/MS as previously described (283).

Eight tablets were individually mortar ground and measured out to approximately 20 mg each. 20 mg of garlic powder was dissolved into 1 ml 0.01 M HCl for 25 mins at 40 °c. The solution was centrifuged for 10 mins at 17000rpm at 4 °c and 50 µl of supernatant transferred into HPLC insert vials. After adding 5 µl of labelled ^{34}S-trideuteromethylcysteine sulfoxide (^{34}S-d3 SMCSO) as an internal standard, samples were vortex again and analysed using LC MS/MS.

All compounds were analysed using an Agilent 6490 triple-quad LC MS mass spectrometer (Agilent technologies) with Phenomenex Kinetex F5, (4.6 x 100mm, 2.6 µm) column. The system comprised a degasser, binary pump, column oven, cooled autosampler (4°C), diode array detector and 6490 mass spectrometer.

Separation was carried out using water + 0.1 % formic acid (mobile phase A) and 100 % methanol (mobile phase B). The gradient started at 2 % mobile phase B increasing over 15 min to 100 % mobile phase B, 15-20 min 100% B for column washing, and finally re-equilibrated to 2 % mobile phase B for 5 min. The column temperature was set 30 ˚C. The LC eluent flow was sprayed into the mass spectrometer interface without splitting. All ions were monitored using mass spectrometry in Multiple Reaction Monitoring mode (MRM) in positive polarity with electrospray ionization (ESI) source. The source parameters were: gas temperature 200 ˚C with a gas flow of 16 l/minute, sheath gas temperature of 300 ˚C with a sheath gas flow of 11 l/minute, a nebuliser pressure of 50 psi and a capillary voltage of 3500 °C. The quantification was performed using a matrix match calibration curve. Identification was achieved based on retention time and product ions.

2.3.3 Production of Placebo Capsules

Production of 20,000 placebo capsules was undertaken with the use of the Profiller 1100, enabling the fulfilment of 100 uncoated capsules at any given time. The use of the tampering equipment helps to ensure uniformity of material that is being encapsulated. Microcrystalline cellulose powder (MCC) was used to encapsulate size 0 hydroxypropylmethylcellulose (HPMC) capsules. MCC is a purified, partly depolymerised cellulose with shorter, crystalline polymer chains. It has a strong binding performance and is therefore commonly used as a filler and binder in drug formulations. The product is manufactured by controlled partial hydrolysis of high purity wood pulp, followed by purification and drying.

Empty capsules were placed onto the filler with Position I and II markings facing the front, ensuring the Cam Lever is set to 3 o' clock. Closed capsules were poured onto Orienter, and the tabs pressed down to lift the gate and pour off excess capsules. The front locating feet of the Orienter were placed into holes at position I on Caps Tray. The sliding portion of Orienter was pushed to the left 1-3 times to drop capsules into the filler, filling every section row, being careful to avoid incorrect orientation of capsules. This process was repeated with the front locating feet of Orienter placed into holes at position II on Caps Tray. The Locking Plate was held by handles and placed onto Caps Tray by inserting 4 Caps Tray posts into 4 larger holes in the Locking Plate, ensuring the ProFiller logo is the right side up. The locking plate was twisted clockwise to lock into place, prior to pulling the Cam Lever towards the post to secure the capsule bodies in the Filler. To separate capsule caps and bodies, the Locking Plate handles were pushed down on, whilst lifting the Caps Tray (the top metal piece). The Caps Tray was set aside with the Locking Place. To drop the capsule bodies into the Filler,

the Cam Lever was released. Whilst wearing a dust mask, MCC filler was poured onto the filler and spread evenly to fill all capsules, using the tamper to pack the powder where necessary. Following removal of the Powder Tray, the Caps Tray was placed with the Locking Plate onto the Filler, (ensuring the Profiller logo is the right side up). To lock the capsules back into place, the clear Locking Plate was pushed down with thumbs whilst pulling up the Lifting Plate. This was repeated prior to removing the Locking Plate by twisting it anti-clockwise.

The 100 capsules were then sieved with granulated sugar to remove any excess MCC from the capsule exterior. Capsules were then visually inspected to ensure quality, and any damaged capsules were disposed of. This process was repeated 200 times to produce 20,000 capsules.

2.3.4 'Norfolk ADaPt' Study Design

Figure 2.1 below outlines the design of a randomised, double-blinded, 2^2 factorial design dietary supplement intervention study, delivering high-dose dietary supplement interventions to men in the pre-biopsy window prior to their transperineal prostate biopsy (TPB). 40 men were randomised to one of four study arms in which they were asked to consume a pre-determined combination of 4 capsules/tablets from either a garlic supplement, myrosinase-activated GFN supplement and/or placebo, once a day for a minimum of 4 weeks. Recruited participants completed a health questionnaire and 2 food frequency questionnaires prior to their procedure. On day one of the study following consumption of their first 4 capsules, participants collected all urine passes for 24 hours. On the final day of the study (the scheduled biopsy day) samples of whole blood, urine, and prostate tissue were collected. The TPB was performed as per their routine clinical care, with 8 additional tissue cores taken for research purposes. Follow-up care was continued by the urology consultants at the Norfolk and Norwich University Hospital (NNUH).

	Arm 1	Arm 2	Arm 3	Arm 4
Alliin (Kwai Heartcare® garlic)	✓✓	✓✓		
Sulforaphane (BroccoMax®)	✓✓		✓✓	
Placebo Capsule		✓✓	✓✓	✓✓✓✓
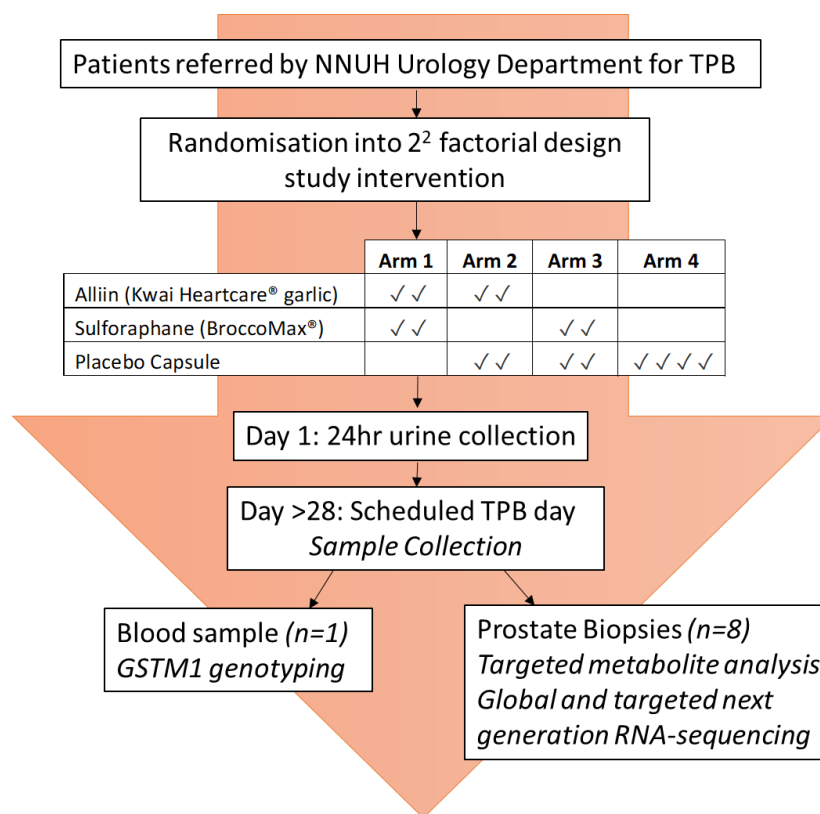
Figure 2. 1 Norfolk ADaPt Study Outline

2.3.4.1 Study Management

The Norfolk ADaPt study was funded by the Prostate Cancer Foundation (PCF, USA) and the Biotechnology and Biological Sciences Research Council (BBSRC, UK) and was carried out at the Quadram Institute Bioscience (QIB), in collaboration with the Urology and Histopathology departments at the NNUH. The named scientists were Professor Richard Mithen (chief investigator), me (primary investigator), and Mr Robert Mills (NHS investigator). Histopathological input was provided by Professor Richard Ball (NHS co-investigator). The protocol was approved by the Human Research Governance Committee (HRGC QIB 02/2019) at QIB in February 2019 for submission to the National Research Ethics Service (NRES). The East of England – Cambridge East Research Ethics Committee (REC) and the NHS Health Research Authority (HRA) gave full ethical approval in June 2019 and the trial was registered on a publicly-accessible database (ClinicalTrials.gov, NCT04046653). The Norfolk and Norwich University Hospital Research and Development department gave confirmation of capacity and capability in July 2019.

2.3.4.2 Sample Size and Power Calculation

There are no prior data on the likely level of accumulation of bioactives in the prostate, nor on its variability, or baseline level, given a usual diet. Also, there is no evidence on what levels are likely to be clinically relevant. Hence the sample size of 40 is based on pragmatic considerations.

Using a factorial design, with a sample size of 40 patients, there will be 20 participants per group for each primary comparison. This will enable an estimate of accumulation to be made with a standard error of $\sqrt{(2/20)} = 0.32$ standard deviations of the usual variation (i.e. the standard deviation of levels in un-supplemented people) between patients in each outcome. Initially, it was planned that one-sided t-tests would be used, whereby there would be 80% power to detect a difference of 0.80 or more standard deviations between groups. One-sided t-tests were chosen initially given the belief that there was little to no theoretical possibility of supplementation reducing the levels of compounds detectable. However, two-sided tests were utilised in the final analysis, given their stricter threshold for significance.

Although the power calculation plan refers only to t-tests, non-parametric tests were also used for much of the final analysis because the variability in the data didn't meet the assumptions for the t-test.

2.3.4.3 Study Population

Men aged 18-80, smokers and non-smokers with a body mass index (BMI) between 19.5-35kg/m^2 who were on the waiting list for TPB at the NNUH as part of their routine clinical care were targeted for enrolment. This included all men on the waiting list, whether they had a confirmed diagnosis of prostatic cancer on active surveillance or were under investigation for a suspected prostatic cancer. The inclusion and exclusion criteria are shown in table 2.1. If any participants enrolled on the study were offered a biopsy date within the 4-week intervention period, they were excluded from the study to ensure that there was no delay in their routine clinical care.

Table 2. 1 Inclusion and exclusion criteria for participation in the 'Norfolk ADaPt' Study

Basic Inclusion Criteria	Basic Exclusion Criteria
Males	Those regularly taking 5α-reductase inhibitors or testosterone replacement medicines
Aged 18-80 years	Those on warfarin treatment
BMI between 19.5-35kg/m²	Those diagnosed with diabetes
Smokers and non-smokers	Those diagnosed with or suspected to be high-risk for human immunodeficiency virus (HIV) and/or viral hepatitis
Scheduled for TPB as part of routine investigation or staging of prostate cancer	Those allergic to any of the ingredients included in the supplements
	Those taking additional dietary supplements or herbal remedies that could affect the study outcome
	Those that are unable to understand English or give informed consent
	Parallel participation in another research project that involves dietary intervention
	Any person related to or living with any member of the study team

2.3.4.4 Study Recruitment and Randomisation

Recruitment was undertaken by me, with close communication with Mr Mills (Urology Consultant) and the urology booking office at the NNUH. Eligible patients were identified primarily from the waiting list of patients awaiting a TPB, but also through out-patient clinic visits. Eligible patients were sent an information pack containing an invitation letter and a participant information sheet, and if patients expressed their interest either verbally or by returning their response sheet, they were contacted by telephone to discuss the study further. Participants who expressed continued interest were then invited to attend the Clinical Research Facility (CRF) at QI (following a consideration period of at least 24 hours). During the study talk, written consent was obtained – a written consent form for the study, and a tissue bank consent form for the Norwich Biorepository enabling the future

use of biological samples for research purposes. Following this, participants were randomised into one of four study arms and provided with 2 pots containing the study interventions. Figure 2.2 highlights the involvement of volunteers throughout the study.

Randomisation was performed by a third party with the use of an online randomisation generator (www.randomisation.com). The method of 'block randomisation' ensured that participants were evenly distributed between both study arms. Allocation sequence concealment was undertaken, and codes placed in an envelope for each participant, ensuring the study scientists were not aware of the treatment code the patient would receive until the time of distribution.

Identification of Potential Participants

➢ NHS Urology team to identify potential participants either directly from clinic or via TPB waiting lists (for patients on active surveillance)
➢ Potential participants to be sent an 'Information Pack', containing an invitation letter, Participant Information Sheet (PIS), response slip, and contact details of the study scientists.
➢ Potential participants who respond positively to the information pack by returning the response slip will be contacted at a mutually convenient time by one of the study scientists.

Information Exchange (telephone)

➢ The information exchange will enable the study scientist to discuss the study in more detail and answer any questions that potential participants may have.
➢ Following the conversation, potential participants will be given a 'consideration period' of at least 24 hours before being invited to the QI CRF.

Visit One to the Clinical Research Facility (CRF)

➢ Visit One to the CRF will enable a further discussion regarding the study, and the scientists will answer any further questions.
➢ Participants willing to take part in the study will be asked to complete 2 written consent forms (inclusion into the study, and the storage of samples in the NRP Biorepository).
➢ Participants will be asked to complete a brief health questionnaire with the help of the study scientist or CRF research nurse.
➢ Participants will be randomised into 1 of 4 study arms and provided with two pots of capsules (labelled A, B, C or D) and asked to consume two capsules from each pot once daily (at breakfast) for ≥4 weeks (until the date of their scheduled TPB) and a record sheet to record each time their capsules are consumed.
➢ Participants will be given a 24-hour urine sample collection pot and asked to collect all urine passes for the first 24 hours following the ingestion of the first 2 capsules. This urine collection will need to be returned to the study scientists on the day of completion (if participants are unable to return their sample to the CRF, then arrangement will be made for one the study scientists to collect it from them).

Study Intervention (consumption of capsules) >4 weeks

Combination 1	Combination 2	Combination 3	Combination 4
Consume 2 x Alliin and 2 x Glucoraphanin Dietary Supplements once a day	Consume 2 x Alliin Dietary Supplements and 2 x Placebo capsules once a day	Consume 2 x Glucoraphanin Dietary Supplements and 2 x Placebo capsules once a day	Consume 4 x Placebo capsules once a day

Visit Two at the NNUH (scheduled TPB day)

➢ Participants will be met by the Urologist and study scientists. They will be asked to return their empty capsule pots and consumption chart.
➢ Participants will be asked to complete two food frequency questionnaires (the validated Arizona cruciferous vegetable food frequency questionnaire, and a non-validated Allium food frequency questionnaire), with the assistance of the study scientist.
➢ The Urologist will discuss and complete the NNUH consent form for the procedure (as per routine clinical care), prior to sample collection:

Blood Sample (n=1)	Urine Sample (n=1)	Prostate Biopsies (n=8)

End of Study

➢ Ongoing clinical care to continue as per NNUH.
➢ Official end of the study will be the date when all samples have been collected and questionnaires from all participants have been returned.
➢ Biological specimens will be transferred at the NRP Biorepository after the end of the study for long term storage

Figure 2. 2 Study outline describing the involvement of volunteers in the study

2.3.4.5 Biopsy Day Procedure

On the final day of the study, participants underwent their scheduled TPB procedure. A standard NHS consent form was completed by the urologist undertaking their TPB procedure as per routine clinical practice.

As discussed in chapter 1, TPB is performed under general or spinal anaesthetic with antibiotic prophylaxis. A blood sample was taken at the same time as cannulation for anaesthetic, either by the anaesthetist or urologist, to prevent further venepuncture being required.

The patient was positioned supine in the lithotomy position (with legs in stirrups). The prostate was visualised via an ultrasound probe inserted into the rectum, and a template grid (with holes spaced at 5mm intervals) placed against the sterilised skin of the perineum. The prostate gland is then systematically sampled for clinical purposes. For the purpose of the ADaPt study, eight prostate biopsies were taken at the start of the procedure. They were specifically taken from areas not known or suspected to contain cancer. Four cores (two from each of the PZ and TZ) were placed directly into RNAlater solution for next-generation RNA sequencing, three (two from the PZ and one from the TZ) were immediately snap frozen for targeted metabolite analysis, and one placed directly into 80% methanol. Samples in methanol were incubated at room temperature for 24 hours. Tissue samples snap frozen were immediately placed on dry ice and transferred to the QIB laboratory for storage at -80°C. All biopsies were carried out by Mr Mills at the NNUH, to minimise variation in prostate sampling.

2.3.4.6 Histopathology

Biopsies taken for clinical (non-study purposes) were taken from areas suspicious for PCa as per routine clinical practice. Biopsies were fixed in formalin and then processed to paraffin wax blocks, using laboratory protocols, and 4um H&E stained sections were reported (including Gleason grading and attributing a Grade group) according the current good practice. The distribution of neoplastic lesions was delineated in the samples provided for assessment. The material for diagnostic purposes was reported to the clinical team in the standard electronic form. The tissue cores analysed for research purposes (which were taken from areas not suspected to contain cancer), were analysed by

a single consultant histopathologist, (Professor Richard Ball), to prevent inter-observer error, and were reported in the same fashion as above, but relayed to the research team anonymously.

2.3.4.7 Genotyping

DNA was extracted from whole blood samples using the QIAamp DNA minikit following the manufacturer's instructions (Qiagen Inc.). Both the DNA and 260:280 ratio was quantified on a Nanodrop™ spectrophotometer (ThermoFisher). Genotype was determined with 20ng genomic DNA in a StepOnePlus real-time PCR system (Applied Biosystems), with GSTM1 primer (ThermoFisher) and Taqman™ universal master mix II (Applied Biosystems). A 10-minute activation period was carried out at 95°C, followed by 40 PCR cycles at 92°C for 15 seconds and 60°C for 90 seconds. G/C Allelic discrimination of GSTM1 genotype was determined using StepOne™ v2.3 software (Applied Biosystems). GSMT1 positive individuals were determined as being either homo- or hetero-zygotes for alleles G and/or C, whereas GSTM1 null individuals were determined as having neither of the alleles.

2.3.4.8 Food Frequency Questionnaires

The 'Arizona Cruciferous Vegetable Food Frequency Questionnaire' (CVFFQ), developed by the University of Arizona was completed either prior to, or on the study day, to assess cruciferous vegetable intake (as well as other food stuffs known to be sources of isothiocyanates) during the period of the study. The CVFFQ has previously been shown to provide reproducible, valid estimates of cruciferous vegetable exposure and improved relationship between crucifer consumption and urinary dithiocarbamate, a biomarker of cruciferous vegetable exposure (284). Data were adjusted according to portion size and cooking method. Results are shown in g/day for cruciferous vegetables, and total glucosinolate intake (mg/day) according to data from the US Department of Agriculture (USDA) Nutrient Database (285).

A non-validated Allium FFQ was completed either prior to, or on the study day, to estimate the alliaceous vegetable intake during the period of the study. This FFQ was developed by the study team, in the absence of any validated Allium questionnaires, and is primarily designed to highlight any major outliers secondary to a very high alliaceous vegetable intake.

2.4 Results

2.4.1 Dietary Supplements

In order to quantify the exact concentration of dietary bioactive compounds present in commercially available dietary supplements for use in a human intervention study, targeted analysis was undertaken. The following results show the quantification of compounds detected in the two treatments that were subsequently used in the 'Norfolk ADaPt' study.

2.4.1.2 Quantification of Glucoraphanin and Sulforaphane from Broccomax supplements

The GFN and SFN content of Broccomax dietary supplements were analysed using the LC-MS/MS as previously described. The average weight of the contents of one Broccomax capsule was 530mg.

As shown in figure 2.3a, there was consistency in the yielded amounts of GFN in 10 Broccomax capsules each from differing batch numbers, with very minimal variability. Figure 2.3b shows the mean GFN content (per gram dried weight) to be 97.74µmol, i.e. 42.7mg/g dry weight SD 2.930 CV 2.998%.
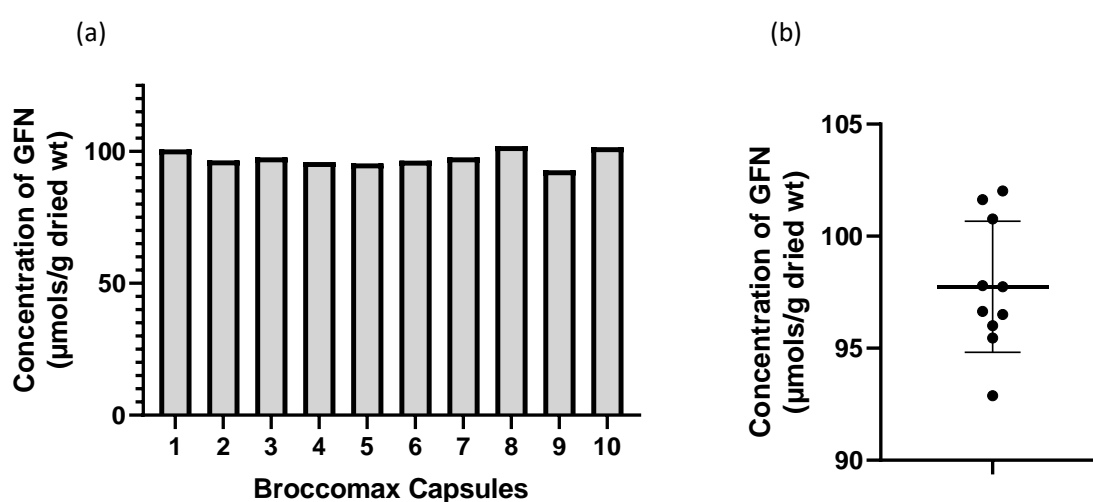
Figure 2. 3 a) GFN content of 10 Broccomax capsules from differing batches, and b) mean GFN content. Data shown as mean ± SD.

Figure 2.4a shows the amount of SFN extracted from 10 Broccomax capsules. The mean content of SFN (per gram dried weight) is 89.537µmol, i.e. 15.9mg/g dry weight SD 12.102 CV 13.51% (figure 2.4b). Given the average weight of the contents of one Broccomax capsule is 530mg, we can estimate that the contents of one capsule contains 103.46µmol (22.631mg) of GFN, yielding approximately 95.06µmol (8.472mg) SFN.
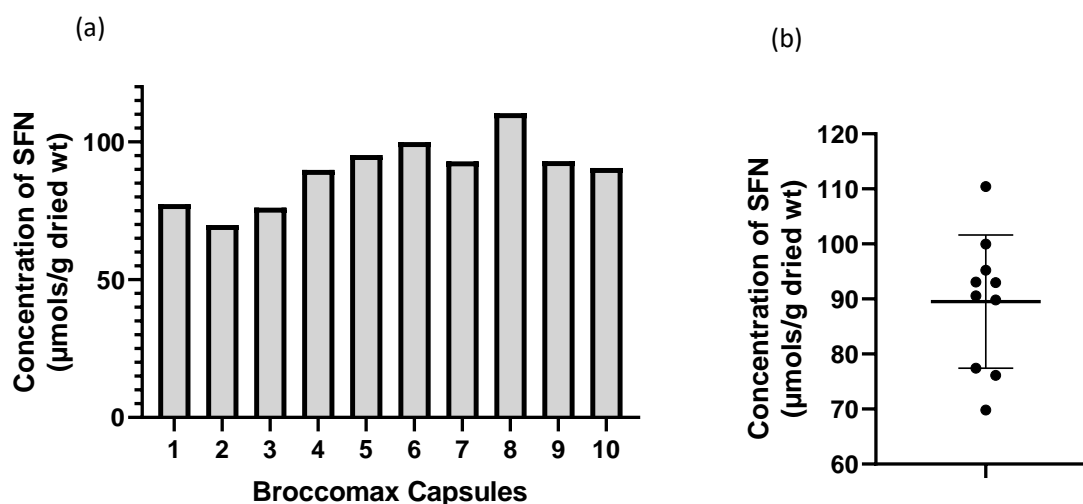
Figure 2. 4 a) SFN content of 10 Broccomax capsules from differing batches, and b) mean SFN content. Data shown as mean ± SD.

2.4.1.3 Quantification of SMCSO from Broccomax and Kwai Garlic Supplements

Given that SMCSO is present in both cruciferous and alliaceous vegetables, the content of SMCSO was quantified from both Broccomax and Kwai Garlic supplements. Both supplements contain very small concentrations of SMCSO compared to that of the soup used in the previous SAP study (133); the mean concentration of SMCSO detected was 2.15µmol and 6.61µmol in Broccomax and Kwai garlic capsules respectively (figure 2.5). The concentration of SMCSO in Kwai garlic was, however, significantly higher when compared to Broccomax.
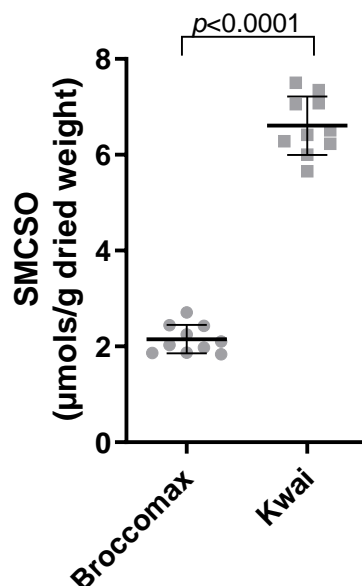
Figure 2. 5 Concentration of SMCSO in Broccomax and Kwai Garlic Supplements (μmols/g dried weight). Data shown as mean ± SD. Analysis using unpaired T test.

2.4.1.4 Quantification of Alliin, γ-SAC and SAC from Kwai Garlic Supplements

S-alk(en)yl-L-cysteine sulfoxide (SACSO/Alliin,) γ-glutamyl S-allyl-L cysteine (γ-SAC), S-allyl-L cysteine (SAC) and Allicin were all detected in Kwai garlic supplements. Table 2.2 shows the mean concentration of detected compounds and the corresponding concentration consumed in the treatment groups. The most abundant bioactive detected was Alliin (35.19μmol/g dry weight).

Table 2. 2 The mean concentration of garlic metabolites detected in Kwai garlic supplements demonstrated as umol/g dry weight and the concentration consumed if in a treatment group.

	Mean conc. (μmols/g dry weight.)	SD	CV (%)	Mean conc. per tablet (μmol)	Conc. consumed/day in Alliin-containing treatment groups (μmol)
SAC	1.75	±0.16	9.39	1.25	2.50
γ-SAC	19.34	±1.91	9.86	13.82	27.64
Allicin	21.41	±2.10	9.79	15.30	30.59
Alliin	35.19	±0.52	1.49	25.23	50.46
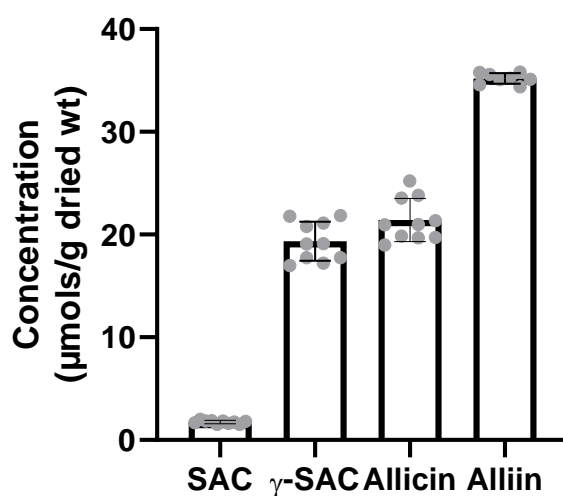
Figure 2. 6 Concentration of garlic metabolites in kwai garlic supplements, including S-alk(en)yl-L-cysteine sulfoxide (SACSO/Alliin,) γ-glutamyl S-allyl-L cysteine (γ-SAC), S-allyl-L cysteine (SAC) and Allicin. Data shown as mean ± SD.

2.4.2 The 'Norfolk ADaPt' Study

2.4.2.1 Recruitment

Based on recruitment from two previous studies (the SAP and ESCAPE studies) using similar study design, with a recruitment rate of 20%, a timeline for completion of recruitment was set for six months, with the final participant recruited by the end of January 2020. The first information packs were sent on 5th August 2019, and as demonstrated in figure 2.7 recruitment completed ahead of schedule; the final participant was recruited on the 11th December 2019, and the last biopsy was completed on the 11th January 2020.
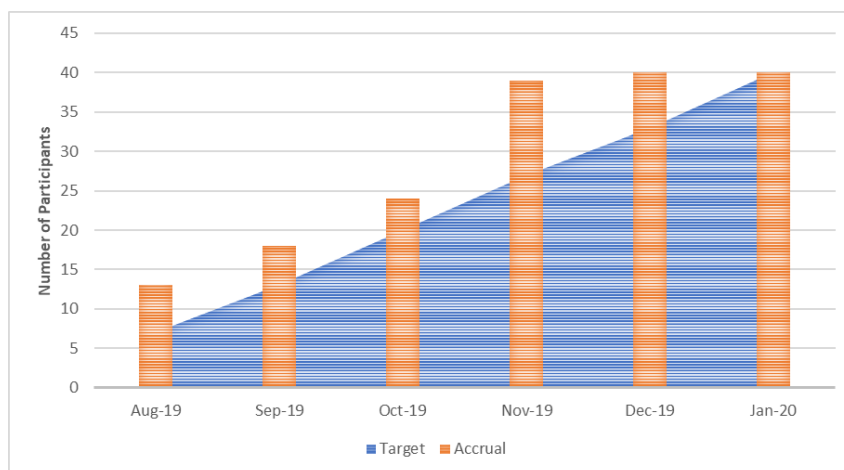
Figure 2. 7 Norfolk ADaPt study recruitment timeline.

During the recruitment period, 103 patients were identified as awaiting a TPB via the TPB waiting list provided by the Urology Waiting List Coordinators. These 103 patients were then pre-screened using clinical letters and previous discharge summaries available on the hospital administration system. 48 patients were deemed ineligible in this manner, and information packs were sent to the remaining 65. The positive response rate for those receiving information packs was high (80% of patients responded positively), and of these, 10 were deemed ineligible. 65% of patients contacted met the inclusion criteria and were recruited onto the study. Two participants dropped out during the study as they were offered an earlier biopsy date and were replaced. One participant had to be excluded two weeks prior to the final study biopsy date due to foreign travel and was not replaced. 39 participants therefore completed the study (10 participants consumed GFN/Placebo, 10 participants consumed Alliin/Placebo, 10 participants consumed GFN/Alliin, and 9 participants consumed placebo/placebo.
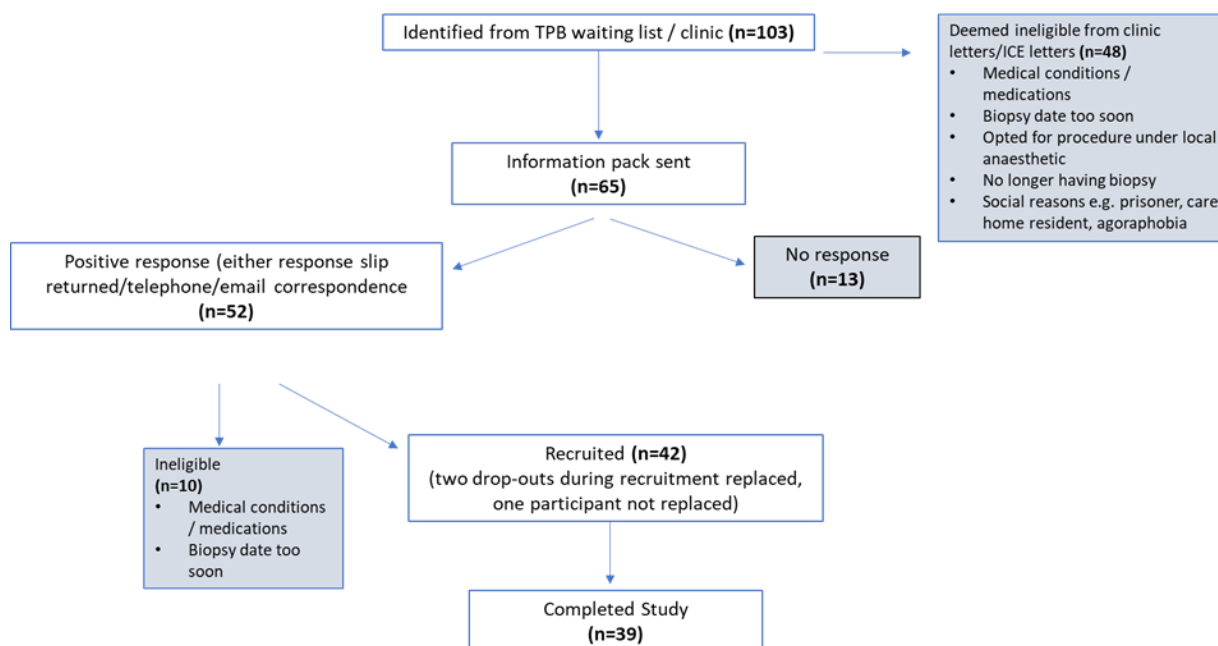
Figure 2. 8 Flow chart of the Norfolk ADaPt recruitment pathway

2.4.2.2 Participant Demographics

Block randomisation distributed participants equally into the four treatment groups, with no statistically significant difference in age or BMI (using one-way ANOVA and Tukey's multiple comparisons test with a single pooled variance). The mean BMI for men in all treatment groups fell into the overweight category.

Table 2. 3 Patient demographics across intervention type. Data shown as mean ± SD.

	GFN / Placebo	GFN / Alliin	Alliin / Placebo	Placebo / Placebo
Age (years)	67.40 ± 5.62	64.30 ± 8.15	63.50 ± 5.70	63.78 ± 5.29
BMI (kg/m^2)	26.46 ± 2.94	26.73 ± 2.89	25.99 ± 4.86	27.17 ± 5.00

2.4.2.3 Cruciferous Vegetable Intake

All volunteers who completed the Norfolk ADaPt study completed and returned the validated Arizona Cruciferous Vegetable Food Frequency Questionnaire (CVFFQ) on either the day of their biopsy procedure, or in the coming days preceding this. The questionnaire is designed to reflect habitual intake during the study period. Data analysis confirmed a wide inter-individual variation in cruciferous consumption, but no statistically significant difference was demonstrated in the consumption of cruciferous vegetables when stratified by intervention group, as highlighted in table 2.4 and figure 2.9.

Table 2. 4 CVFFQ data representing the daily intake of cruciferous vegetables stratified by intervention type. Data presented as mean ± SD.

	GFN/Placebo (n=10)	GFN/Alliin (n=10)	Alliin/Placebo (n=10)	Placebo/Placebo (n=9)
Cruciferous Vegetable Intake (servings/day)	1.06 ± 0.66	1.09 ± 0.55	0.98 ± 0.37	0.62 ± 0.53
Cruciferous Vegetable Intake (g/day)	67.17 ± 33.81	83.94 ± 39.35	61.06 ± 31.40	46.95 ± 46.67
Glucosinolate Intake (mg/day)	48.23 ± 31.78	71.23 ± 43.93	43.15 ± 23.40	40.36 ± 48.39

A)

B)

C)
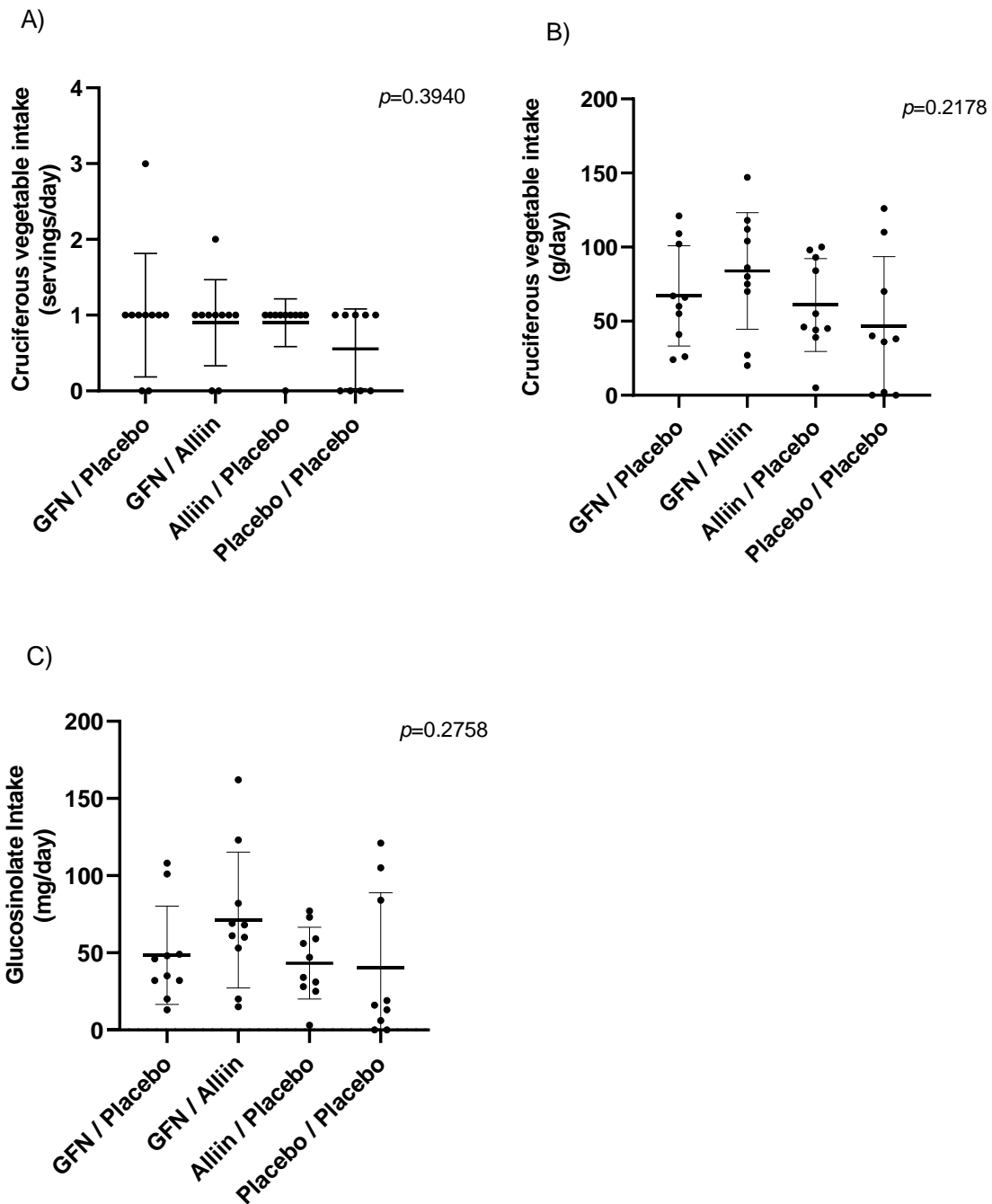
Figure 2. 9 Consumption of cruciferous vegetables. Data calculated from the Arizona CVFFQs. Data stratified by intervention type and shown as A) servings/day B) grams/day and C) glucosinolates (mg/d). Data shown as mean ± SD. No statistically significant difference is demonstrated in intake per graph between intervention types (analysis by one-way ANOVA).

2.4.2.4 Alliaceous Vegetable Intake

All volunteers who completed the Norfolk ADaPt study completed and returned the non-validated alliaceous vegetable intake questionnaire on either the day of their biopsy procedure, or in the coming days preceding this. As with the CVFFQ, this questionnaire is designed to reflect habitual intake during the study period. This questionnaire provided a qualitative indication of allium intake only, and was designed to ensure any outliers in results could be fully investigated. As such no quantitative data can be extrapolated. However, analysis of the allium FFQ demonstrated that in general, participants consumed low amounts of alliums during the study period (as part of their habitual diet). The most commonly consumed alliums were onion and garlic. Onions were most likely to be diced and garlic crushed prior to frying over medium or high heats. There was little to no inter-individual variability nor discernible variability between treatment groups.

2.4.2.5 Genotyping

GSTM1 genotyping was performed for all 39 participants who completed the study. Polymorphism of this gene occurs due to a C/G Transversion substitution at Exon 7 of the GSTM1 gene and has been associated/identified with two alleles: GSTM1 C and GSTM1 G. Figure 2.10 demonstrates the allelic expression of the participants. 54% of participants were GSTM1 positive; of these, the majority were homozygous positive carrying a C or G allele, whilst only 3 participants were heterozygous positive carrying one copy of the C allele and one copy of the G allele. The rest of the participants were GSTM1 null implying loss of the GSTM1 gene/protein. Figure 2.11 shows the proportion of GSTM1 positive (heterozygous and homozygous for C/G alleles) and null (no alleles expressed) per intervention group. No statistical significance was demonstrated between the distribution of positive and null GSTM1 genotype between intervention groups.
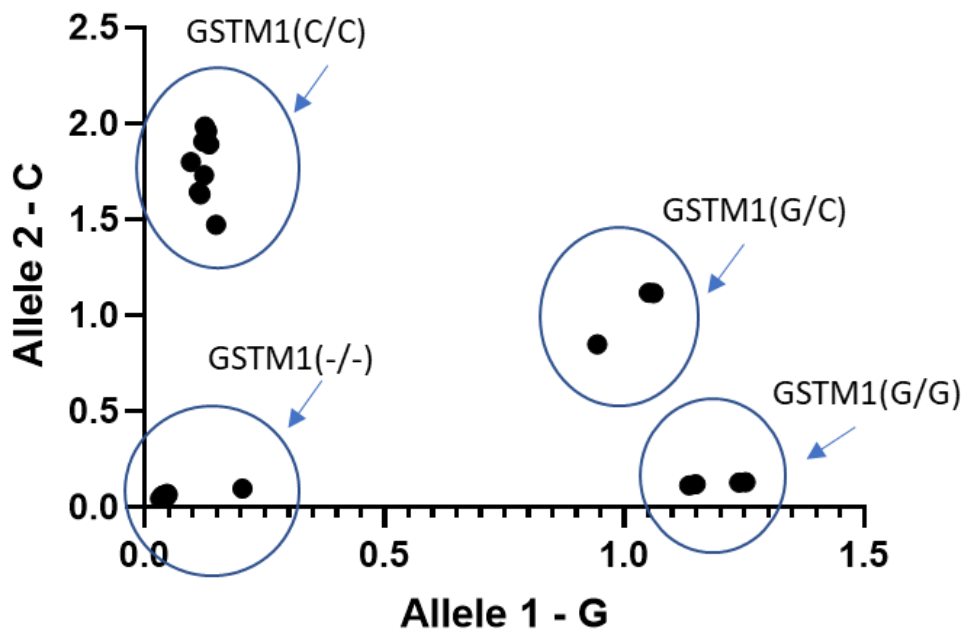
Figure 2. 10 Graph to show the distribution of allelic variation of GSTM1 genotype amongst the 39 'Norfolk-ADaPt' participants. Labelled are GSTM1(-/-), and GSTM1- 'positive' as demonstrated by homozygous GSTM1(C/C), GSTM1 (G/G), or heterozygous GSTM1(C/G) expression.
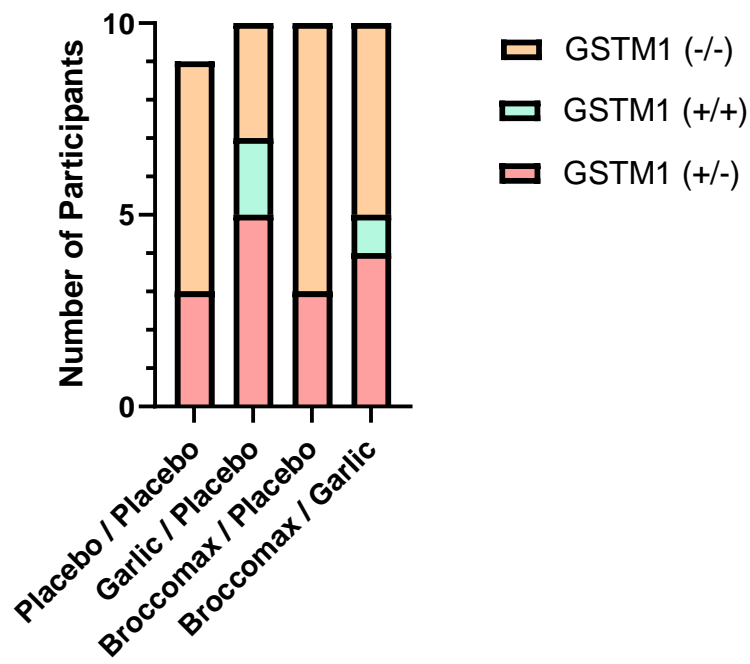
Figure 2. 11 Graph representing the number of participants who are GSTM1 positive (+/+) or (+/-) and GSTM1 (-/-) per intervention group (n=39).

2.4.2.6 Cancer Grade and Volume

Histological analysis undertaken on one tissue core, indicated that tumour was present in 14 of the 39 participants (25 participants had benign disease). The distribution amongst groups is demonstrated in Figure 2.12a.

In 3 of the 14 participants who had tumour present, there was insufficient tissue for a formal grading to be made (see figure 2.13).
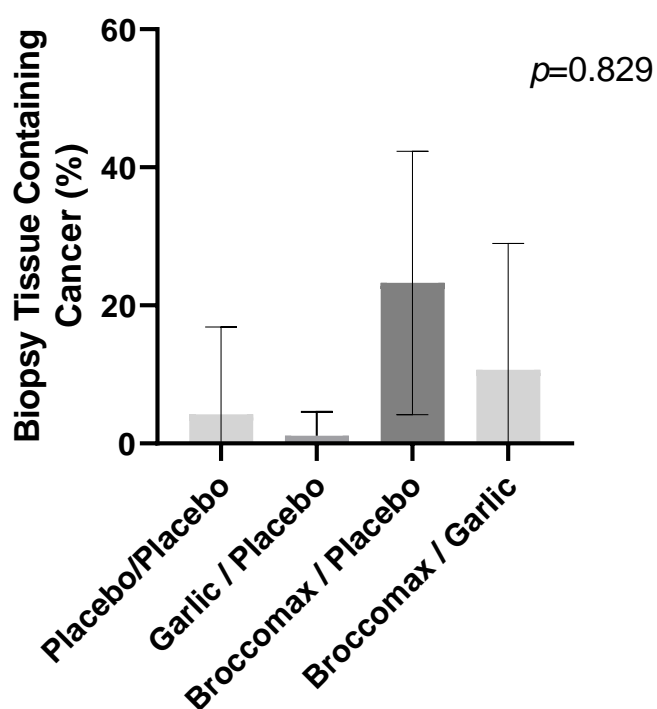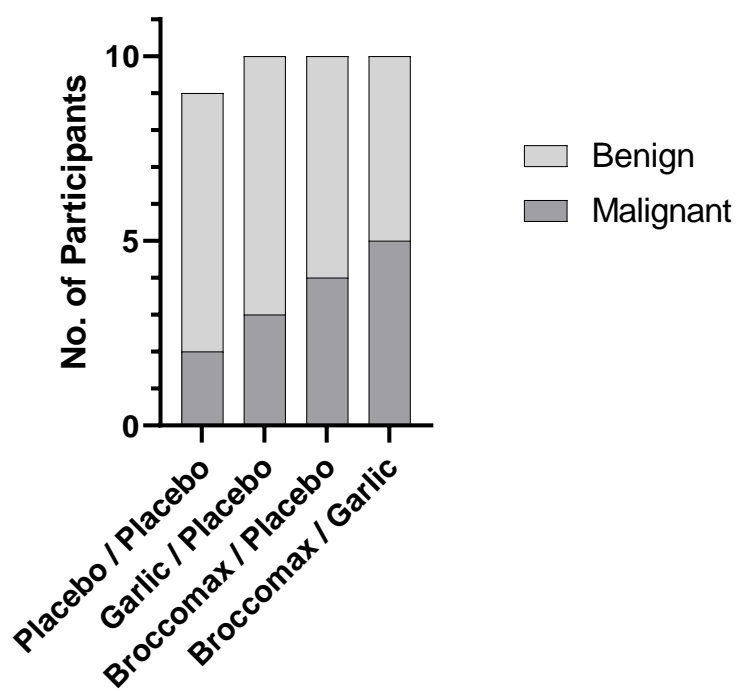
Figure 2. 12 Histological findings in all treatment groups. A) number of participants with benign vs. malignant cores per treatment group. B) percentage of total tissue received for histological analysis that contained cancer (data shown as mean ± SD, p=0.829 by mixed model ANOVA)
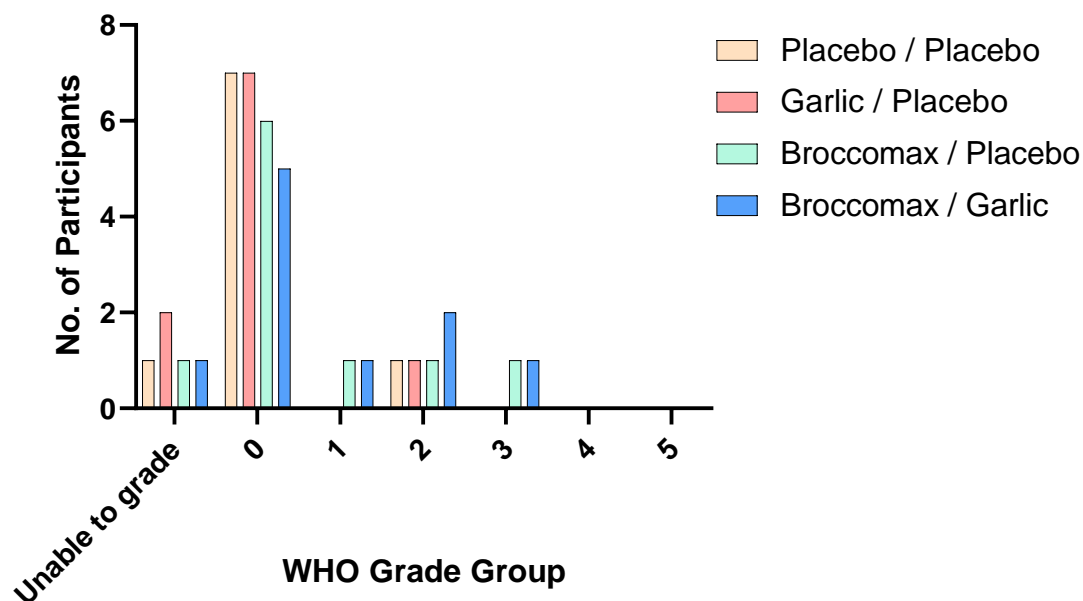
Figure 2. 13 Grade of cancer by WHO grade group and intervention group

2.5 Discussion

2.5.1 Dietary Supplements

The use of dietary supplements in human trials allows for isolated bioactive compounds of interest to be given in potentially higher concentrations than is reasonably achievable in a habitual diet.

Broccomax is a commercially available GFN supplement, which contains activated myrosinase enzyme to enable a greater SFN yield. The analysis of Broccomax capsules in this chapter demonstrates consistent amounts of GFN (97.74 µmol/g dry weight) and SFN (89.537 µmol/g dry weight) across multiple batches. The average weight of the contents of one Broccomax capsule is 530mg, and therefore we can estimate that the contents of one capsule contains 51.73 µmol of GFN, yielding approximately 47.53 µmol SFN. Participants consuming Broccomax treatment therefore consumed 103.46 µmol GFN once per day (from two capsules daily). This concentration was well tolerated with no side effects throughout the study. When compared to the SAP study, participants consumed one portion of the GFN-rich study soup three times *per week,* totaling 840 µmol of GFN (133). In the ADaPt study, the weekly consumption of GFN in the form of Broccomax was 724.22 µmol. However, unlike the GFN-rich soup (in which myrosinase would have been denatured in the

manufacturing process, and did not contain added myrosinase enzyme), Broccomax capsules contain activated myrosinase, which would enable a greater conversion of GFN to the active compound SFN.

Kwai is a commercially available enteric-coated garlic supplement. Analysis of Kwai supplements in this chapter demonstrates the presence of S-alk(en)yl-L-cysteine sulfoxide (SACSO/Alliin,) γ-glutamyl S-allyl-L cysteine (γ-SAC), S-allyl-L cysteine (SAC) and Allicin. The most abundant compound was Alliin, and from this analysis we can estimate that participants consuming Kwai consumed 50.46 μmol Alliin once per day. Given the estimated concentration of Alliin per clove of garlic ranges between 33.86-79.00 μmol (122, 270), one tablet provides approximately the median of this value, representing one garlic clove. Participants receiving the Kwai intervention therefore consumed the equivalent of approx. 2 garlic cloves per day (14 garlic cloves per week), which is unachievable for most as part of their habitual diet. This concentration was well tolerated with no significant adverse effects reported throughout the study.

2.5.2 The 'Norfolk ADaPt' Study

During the recruitment process, alterations to practice in the diagnostic and surveillance pathways for PCa at the NNUH added potential difficulties with recruitment into the ADaPt study. TPBs have traditionally been undertaken under general or spinal anaesthesia, which enables additional research biopsies to be obtained with no additional discomfort or documented risk to the patient. Ethical approval for the ADaPt study was therefore based upon samples being taken when the patient was under general or spinal anaesthesia. However, recently there has been a move towards local anaesthetic TPB (an option now being utilised by the NNUH), which reduces the time spent by the patient in the hospital, and significantly reduces costs associated with theatre capacity and staff requirements. All patients being offered a TPB were therefore initially given an opportunity by their clinician to have the procedure under LA, thus reducing the cohort available for inclusion into the ADaPt study. This alteration in clinical practice may impact on the ability to utilise prostate biopsy samples for research purposes in the future, due to the potential increase in discomfort associated with taking additional biopsies. Additionally, as a result of the PRECISION trial (286), the European Association of Urology and 2019 NICE Guidelines in Prostate Cancer now recommend performing an mp-MRI prior to prostate biopsy in biopsy-naive men (287). However, despite these factors, recruitment into the ADaPt study exceeded expectations and completed ahead of schedule.

Recruitment into dietary intervention studies can be difficult (288), which often reflects the populations unwillingness to make alterations to their lifestyle; however, the use of commercially available dietary supplements rather than foods (unlike previous dietary intervention studies at the QIB) may have helped to boost recruitment. Multiple participants recorded having little to no cruciferous or alliaceous consumption in their habitual diet, and claimed that they may not have been willing to participate had the intervention been a foodstuff rather than capsules.

Reviews have demonstrated drop-out rates of >20% in 18% of randomised controlled trials published in the top four medical journals (289, 290), highlighting a major issue in the completion of human intervention studies. However, during the ADaPt study, only two participants dropped out during the study as they were offered an earlier biopsy date and were immediately replaced into the same group. A further participant dropped out prior to the final biopsy date of the study and was not replaced. There were no reported complications from taking part in the study.

All groups in the study were homogenous for age, BMI, vegetable intake, GSTM1 genotype and histology.

2.6 Conclusion

The 'Norfolk ADaPt' study was a successful 'window-of-opportunity' study, recruiting 39 patients who completed the study. Utilising laboratory techniques, commercially available dietary supplements were tested to ensure the study interventions delivered the appropriate concentration of bioactive compounds derived from cruciferous and alliaceous vegetables, to maximise the opportunity of fulfilling the study outcomes.

Chapter Three

Accumulation of Dietary Bioactives in Men

Enrolled in The Norfolk-ADaPt Study

3.1 Introduction

In chapter two, the metabolites present in commercially available supplements for use in the 'Norfolk ADaPt' study were analysed. Whilst the bioavailability of some of these compounds have been reported, human studies have yet to demonstrate their ability to accumulate within the prostate itself, whereby they may exhibit their chemotherapeutic or other desirable effects.

This chapter investigates whether, in men scheduled for transperineal prostate biopsy, dietary supplements or their human and microbial metabolites will accumulate in the urine and prostate tissue (primary aims of the Norfolk ADaPt study), and whether there is differential accumulation in the transition and peripheral zone of the prostate.

3.1.1 Glucoraphanin and Sulforaphane

As discussed in chapter one, GFN is enzymatically hydrolysed either by the plant or gut bacterial myrosinases to give rise to the isothiocyanate SFN. SFN is passively absorbed into the small or large intestine and following conjugation is transported into the systemic circulation. This conjugate is then metabolised by the mercapturic acid pathway and excreted in the urine (99, 252, 291).

However, following ingestion, GFN hydrolysis and ITC absorption are influenced by many other factors; the length of time they are in the GI tract, the residual glucosinolate concentrations plant myrosinase activity, and the composition of the gut microflora (252, 292). Additionally, individuals may show different GFN metabolism because of polymorphisms in genes coding for glutathione-S-transferases (GST), which plays a key role in isothiocyanate conjugation with glutathione to different extents (120, 141).

The bioavailability and pharmacokinetic behaviour of SFN in plasma and urine is well documented. A recent study analysing the bioavailability of GFN and SFN from broccoli with different genotypes demonstrated that a broccoli variety with a high GFN content due to the Myb28 $^{V/V}$ genotype, when delivered as soup to humans, resulted in enhanced SFN levels both in the urine and plasma, compared to the similar variety with a low GFN content (255). In this study, participants were randomised into three groups, and consumed one of three soups containing different concentrations of GFN; Myb28$^{V/V}$ and Myb28$^{B/V}$ broccoli soups (containing 452 ± 10.6 μmols GFN per 300 mL portion and 280 ± 8.8 μmols GFN per 300 mL portion respectively), approximately five- and threefold greater GFN levels, compared to Myb28$^{B/B}$ broccoli soup containing 84 ± 2.8 μmols GFN per

300 mL. This study demonstrated that SFN and metabolites were detected in the urine of participants within 1h of consumption, with a T_{max} of 6-9 hours, irrespective of the concentration of GFN consumed. However, the cumulative amount of SFN and metabolites excreted in the urine was shown to be significantly higher following consumption of the soups with Myb28$^{V/V}$ and Myb28$^{B/V}$ than with Myb28$^{B/B}$. The total concentration of SFN and metabolites in urine after 24 hours ranged from 8.7 to 39.98 µmol in participants consuming the lowest and highest concentration GFN soups respectively. However, the urinary excretion of SFN as a percentage of GFN consumed varied between 2 and 15%, suggesting that an individual's ability to metabolise GFN varies, likely due to differences in individual gut microbiota. The most abundant urinary metabolite detected was sulforaphane-NAC, followed by Erucin-NAC, with consumption of all three types of soups, which is in keeping with previous evidence (293).

A similar study assessing the pharmacokinetics of SFN (where SFN thioglucosidases remained active following preparation, hence removing the need for gut myrosinase activity) has shown that the mean excretion of SFN metabolites in the urine of individuals ranges between 40-90% (294). This is supported by further evidence which confirmed that no participants excrete all SFN metabolites; in a study comparing ITC concentrations in urine following consumption of fresh vs. frozen broccoli soups, the mean excretion of SFN metabolites in the urine of participants consuming a fresh GFN-containing soup (with intact myrosinase) was 58.5%, with the highest yield being 79.6% (295). In general, evidence suggests that if GFN is consumed with intact myrosinase, between 30-80% of SFN is excreted in the urine, whereas significantly less is excreted where myrosinase is inactive (<10%). This, along with a later T_{max}, reflects that in the absence of activated myrosinase, absorption is colonic rather than via the upper GI tract (296).

Despite the well documented evidence that SFN and metabolites accumulate within the urine of participants consuming high dose GFN, human studies have yet to significantly demonstrate that these compounds are capable of accumulation within human prostate tissue. As discussed in chapter two, a human intervention study did not demonstrate that SFN or its metabolites were capable of accumulation within the prostate (263). More recently however, SFN has been detected in the prostate of 3 of 50 individuals consuming myrosinase-activated broccoli seed extract (BSE) supplementation as part of a double-blinded intervention study, in concentrations ranging from 23-62.3pmol/g (297). SFN has also been shown to accumulate within other epithelial enriched tissue such as human breast tissue, following single dose of BSE containing 200µl SFN (298).

Theoretically, urinary reflux provides a possible route by which urinary metabolites such as SFN could accumulate in prostate tissue, providing a mechanism for the epidemiological association between these compounds and the reduction in PCa risk.

3.1.2 Alliin Metabolites

As discussed in chapters one and two, garlic contains organosulphur compounds, the main two of which are the non-volatile S-ally-L-cysteine sulfoxides (Alliin) and γ-glutamyl-L-cysteine peptides. Upon preparation of garlic, the enzyme allinase catalyses the formation of sulfenic acids such as Allicin from Alliin. These sulfenic acids are highly unstable and react with each other to form thiosulfinates which then rapidly break down to form other allicin-derived organosulphur compounds. These compounds are more unstable and considered to be much less bioavailable than the water-soluble products of γ-glutamyl-L-cysteine peptides (122).

As a result, allicin derived products have previously been detected in human urine using highly sensitive gas chromatography-mass spectrometry/olfactometry (GC-MS/O) methods (299). In one such study, urine was collected from 12 volunteers at set time-points up to 26 hours following consumption of approximately 3 g raw garlic (1-2 garlic cloves). Three allicin metabolites were detected in the urine; allyl methyl sulfide (AMS), allyl methyl sulfoxide (AMSO) and allyl methyl sulfone ($AMSO_2$), confirming that garlic is heavily metabolised prior to urinary excretion. Time blank urine was also tested to confirm no products were present prior to consumption. The rates of urinary excretion of these highly volatile although hydrophilic metabolites, demonstrated significant inter-individual variability, with a plateau and even a second peak occurring in some participants, a surprising finding that has previously been demonstrated in rat plasma and urine (300). The peak concentration of these metabolites in human urine generally occurred between 1 and 4 hrs post consumption, although levels were still observed in some cases up to 20 hrs. It may be plausible that, as is the case for other compounds including volatile short-chain fatty acids (301), garlic metabolites are absorbed at a variety of anatomical locations following consumption, from the oral cavity to the large colon, with or without colonic microbiota interaction.

By comparison, γ-glutamyl-L-cysteine peptides are absorbed intact and hydrolysed to the water-soluble derivatives S-ally-L-cysteine (SAC) via its deglutamylation, and *trans*-S-1-propenyl-L-cysteine. SAC is further metabolised to N-acetyl-S-allyl-L-cysteine (NAC-SAC, otherwise known as allylmercapturic acid ALMA), via N-acetylation by the cysteine-S-conjugate N-acetyltransferase (302).

These compounds have been extensively demonstrated to accumulate in human plasma and urine, as well as the kidney and liver of SAC-fed animals, again using highly sensitive gas chromatography-mass spectrometry (GC-MS) methods. A systematic review of 27 papers confirmed that that NAC-SAC, allyl methyl sulfide (AMS), allyl methyl sulfoxide (AMSO) allyl methyl sulfone ($AMSO_2$) and S-allyl cysteine (SAC) levels in urine or plasma, were potential candidates for use as biomarkers of food intake (BFI), due to their specificity and defined dose-response kinetics post-consumption (303). This also makes these metabolites reliable markers of compliance in human studies analysing garlic consumption (304, 305). All analysis for urinary metabolites has previously used highly specific gas chromatography-mass spectrometry (GC-MS) (302, 306-310) or in the case of breath and plasma, high performance liquid chromatography mass spectrometry (HPLC-MS) (310).

Despite the well documented evidence that excreted urinary garlic metabolites are detectable in human urine using highly sensitive methods, and the vast epidemiological associations and *in vitro* evidence of its role in preventing PCa, whether these metabolites accumulate within human prostate tissue itself is not known.

In this chapter, urinary metabolite excretion, and prostate metabolite accumulation in participants who completed the Norfolk ADaPt study is analysed. This study was described in full in chapter 2.

3.2 Aims

3.2.1 Primary Aims

- To determine whether and estimate the extent to which Sulforaphane and or Alliin, and their metabolites, are detectable in 24-hour urine samples using LC-MS/MS

- To determine whether and estimate the extent to which Sulforaphane and or Alliin and their metabolites, are detectable in prostate tissue using LC-MS/MS

- To determine whether the above endpoints are influenced by GSTM1 genotype

3.2.2 Secondary Aims

- To determine whether Sulforaphane and or Alliin and their metabolites accumulate differently between the peripheral and transition zones of the prostate

- To determine whether there is a correlation between the concentration of detected metabolites in the prostate and those detected in the urine

- To determine whether there is any evidence to suggest that consuming the analysed compounds as a combination affects the accumulation of the individual metabolites in the prostate.

3.3 Methods

3.3.1 Sample Collection and Processing

As previously described in Chapter 2, ethical approval for the Norfolk ADaPt study was granted by the East of England – Cambridge East REC in May 2019. Written informed consent was obtained for study participation and tissue banking consent at the Norwich Biorepository.

3.3.1.1 Urine Samples

Following consumption of 4 capsules on day one of the ADaPt study, participants collected all urine passes for 24 hours in a 3L universal container containing 1g ascorbic acid. Following collection and mixing, the sample was weighed, and urine was divided into 1ml aliquots and frozen at -80°c until required for analysis.

3.3.1.2 Prostate Samples

Participants consumed their final supplements the morning prior to their scheduled biopsy. On the day of the biopsy procedure, additional NHS clinical consent was gained from the consultant surgeon. Biopsy cores of prostate were taken from both the peripheral and transition zone through the template grid during transperineal biopsy. Research samples were immediately snap frozen on dry ice. Following the procedure, samples were then transferred to the QIB and stored at -80°c until required for analysis. Prostate samples were analysed in 2 batches.

3.3.2 Isothiocyanates

ITC metabolite analysis in urine and prostate tissues samples were performed as previously described (133) with slight modification. The modifications were as follows: Acquity UPLC, HSS T3 1.8 um, 2.1 x 100 mm column was used instead of Phenomenex® Luna 3u C18 (2) 100A 100 x 2.1 mm column due to more efficiency for separation and sensitivity, and d8-sulforaphane was used as an internal standard. All other parameters and sample preparation were the same.

3.3.2.1 Urine

Aliquots of urine were thawed on ice, vortexed briefly and 100μl was transferred to a new Eppendorf tube. As previously described (133) a 10-fold dilution in 5% TCA was performed, the sample was vortexed again and then incubated on ice for 10 minutes to precipitate proteins. The sample was centrifuged at 14,000g for 10 minutes at 4°C and the supernatant transferred to an HPLC vial for analysis by LC-MS/MS.

3.3.2.2 Prostate

Individual snap-frozen prostate biopsy cores (1 from each of peripheral and transition zone per patient) were weighed on a Cubis® high-sensitivity balance (Sartorius) and transferred to screw-top tubes. As previously described (133) 200μl of cold Milli- Q® water and 300mg of autoclaved, acid-washed 710 to 1180μm glass beads (Sigma®) were added to each tube. The tissue was completely homogenised using a DNA FastPrep® (MP Biomedicals) at 4.0m/s for 3 cycles of 60 seconds each. The samples were then placed on a revolving shaker for 15 minutes at 4°C. The tubes were

centrifuged at 17,000g for 10 minutes at 4°C and 50µl of supernatant transferred to a new Eppendorf. 10µl of 50% trichloroacetic acid (TCA) was added to each sample to precipitate proteins. The centrifugation step was repeated and 50µl of supernatant transferred to HPLC insert vials for analysis by LC MS/MS.

3.3.3 Alliin and Metabolites

Urine and prostate samples were analysed for Alliin and the Alliin metabolites for which there are documented LC-MS/MS methods.

3.3.3.1 Urine

Aliquots of urine were thawed on ice and vortexed briefly. 10µl of urine and 90µl of 0.1 % formic acid containing water was added to a new Eppendorf tube. The sample was centrifuged at 17,000G for 10 minutes at 4° C. After centrifugation 50µl of supernatant was transferred to HPLC insert vials and 5µl of labelled ^{34}S-trideuteromethylcysteine sulfoxide (^{34}S-d3 SMCSO) as an internal standard was added. Samples were vortexed again and analysed by LC MS/MS.

3.3.3.2 Prostate

Individual snap-frozen prostate biopsy cores (1 from each of peripheral and transition zone per patient) were weighed on a high-sensitivity balance and transferred to screw-top tubes. 200µl of cold Milli-Q® water and 300mg of autoclaved, acid-washed 710 to 1180µm glass beads (Sigma) were added to each tube. The tissue was completely homogenised using a DNA Fast-Prep® (MP Biomedicals) at 4.0m/s for 3 cycles of 60 seconds each. The samples were then placed on a revolving shaker for 15 minutes at 4° C. The tubes were centrifuged at 17,000G for 10 minutes at 4° C and 50µl of supernatant transferred to a new Eppendorf. 10µl of 50% trichloroacetic acid (TCA) were added to each sample to precipitate proteins. The centrifugation step was repeated and 50µl of supernatant transferred to HPLC insert vials. After adding 5 µl of labelled ^{34}S-trideuteromethylcysteine sulfoxide (^{34}S-d3 SMCSO) as an internal standard, samples were vortex again and analysed by LC MS/MS.

All compounds were analysed using an Agilent 6490 triple-quad LC MS mass spectrometer (Agilent technologies) with Phenomenex Kinetex F5, (4.6 x 100mm, 2.6 µm) column. The system comprised a degasser, binary pump, column oven, cooled autosampler (4°C), diode array detector and 6490 mass spectrometer.

Separation was carried out using water + 0.1% formic acid (mobile phase A) and 100 % methanol (mobile phase B). The gradient started at 2% mobile phase B increasing over 15 min to 100% mobile phase B, 15-20 min 100% B for washing up column and finally re-equilibrated to 2% mobile phase B for 5 min. The column temperature was set 30 °C. The LC eluent flow was sprayed into the mass spectrometer interface without splitting. All ions were monitored using mass spectrometry in Multiple Reaction Monitoring mode (MRM) in positive polarity with electrospray ionization (ESI) source. The source parameters were: gas temperature 200 ˚C with a gas flow of 16 l/minute, a sheath gas temperature was 300˚C with a sheath gas flow of 11 l/minute. The nebuliser pressure was 50 psi and capillary voltage was 3500°C. The quantification was performed using a matrix match calibration curve. Identification was achieved based on retention time and product ions. Table 3.1 summarises the monitored ions and the optimised MS operating parameters of the analytes.

Table 3. 1 The monitored ions and the optimised MS operating parameters of the analytes.

Analyte	Retention time (mins)	Precursor ion (m/z)	Product ion (m/z)	Collision energy
L-alliin	*4.24*	*178.21*	*87.9*	*10*
L-alliin	*4,24*	*178.21*	*42.1*	*28*
Allicin	*8.34*	*163.11*	*72.9*	*14*
Allicin	*8.34*	*163.11*	*39*	*62*
S-allyl-L-cysteine	*3.6*	*162.23*	*41.1*	*30*
S-allyl-L-cysteine	*3.6*	*162.23*	*39*	*50*
γ-glutamyl-S-allyl-L-cysteine	*4.2*	*291.35*	*145.1*	*18*
γ-glutamyl-S-allyl-L-cysteine	*4.2*	*291.35*	*83.9*	*30*
N-acetyl-S-allyl-L-cysteine	*5.6*	*204.3*	*145*	*10*
N-acetyl-S-allyl-L-cysteine	*5.6*	*204.3*	*41*	*30*

SMCSO	*3.0*	*152.19*	*87.9*	*4*
SMCSO	*3.0*	*152.19*	*42.1*	*20*
^{34}S-d3 SMCSO	*3.0*	*157.05*	*87.9*	*4*
^{34}S-d3 SMCSO	*3.0*	*157.05*	*42.1*	*28*

3.4 Results – Primary Outcomes

3.4.1 Isothiocyanates

A total of 40 participants returned a 24-hour urine collection from day one of the Norfolk-ADaPt study, although only 39 completed the study in its entirety (as demonstrated in chapter two). Participants collected all urine passes following the consumption of 4 capsules on the morning of day one until up until the time of consuming the next day's capsules. Urine was analysed for urinary ITCs in two batches.

A total of 39 participants underwent TPB of the prostate on the final day of the ADaPt study. Biopsy cores were taken from both the peripheral and transition zone of the prostate.

3.4.1.1 Consumption of Broccomax Glucoraphanin capsules led to a significant accumulation of ITC's in the urine

Targeted LCMS/MS analysis of ITCs collected from the Norfolk-ADaPt study revealed significantly higher levels of total urinary ITCs in participants consuming a GFN-containing intervention (n=20) compared to non-GFN containing interventions (n=20) ($p<0.0001$). Figure 3.1 demonstrates that the mean concentration of excreted urinary ITCs in patients consuming a GFN-containing intervention was 58.15 µmol/L ± 19.31, compared to 1.96 µmol/L ± 3.63.
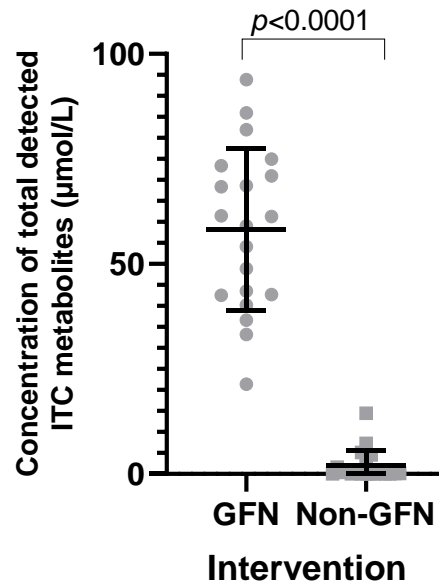
Figure 3. 1 Concentration of total sulforaphane and metabolites detected in urine samples of patients consuming glucoraphanin (n=20) vs. a non-glucoraphanin intervention (n=20). Samples were analysed for sulforaphane, and the sulforaphane metabolites including, sulforaphane-cysteine, sulforaphane-NAC, and erucin-NAC. Results are shown as mean ± SD. Analysis using a two-tailed unpaired T-test with Welch's correction.

The compounds detected in urine included free sulforaphane, and the sulforaphane metabolites including sulforaphane-cysteine, sulforaphane-NAC, and erucin-NAC. Figure 3.2 shows that SFN-NAC was the most abundant metabolite detected in urine of participants consuming a GFN-containing intervention, followed by E-NAC.
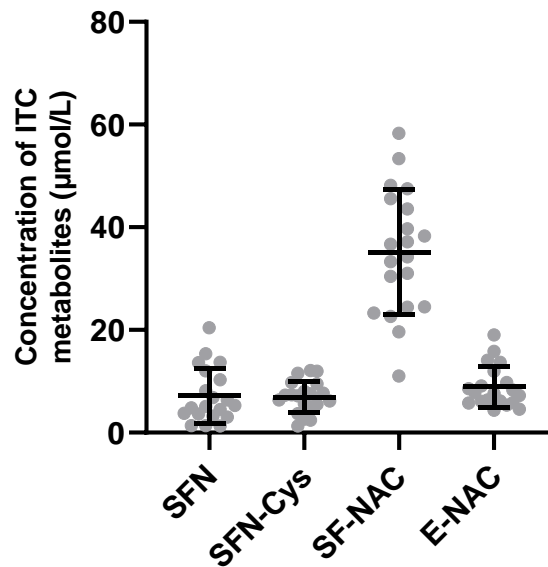
Figure 3. 2 Concentration of sulforaphane, and the sulforaphane metabolites detected in urine, including, sulforaphane-cysteine, sulforaphane-NAC, and erucin-NAC in patients consuming a glucoraphanin intervention (μmol) (n=20). Results are shown as mean ± SD.

Analysis of individual samples (demonstrated in figure 3.3) confirmed that although the total amount of urinary ITCs detected in urine differs amongst individuals (21.37-93.85 μmol/L) the proportion of individual metabolites remains roughly consistent.
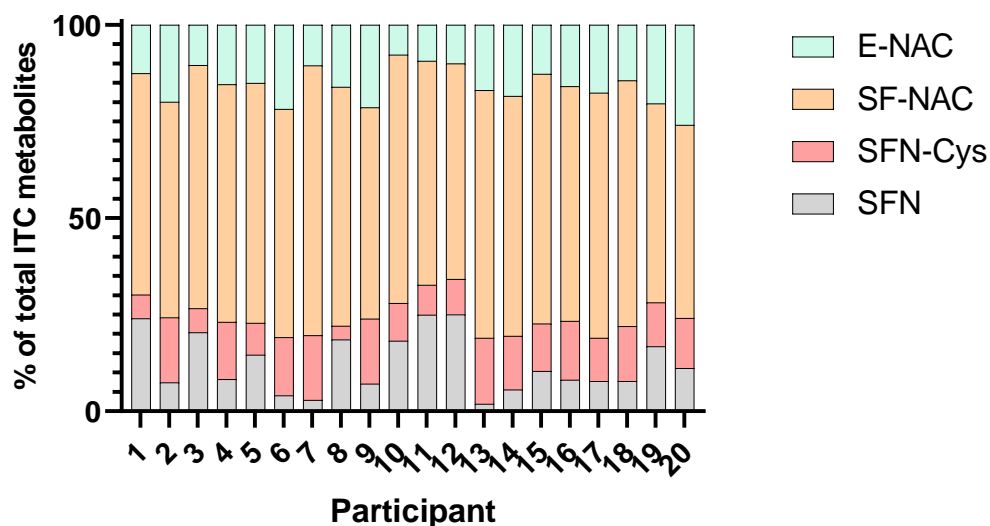
Figure 3. 3 Sulforaphane, and the sulforaphane metabolites detected in urine (including sulforaphane-cysteine ((SFN-Cys)), sulforaphane-NAC ((SFN-NAC)), and erucin-NAC ((E-NAC))), represented as a % of total excreted metabolites in each of the patients consuming a glucoraphanin-containing intervention (n=20).

Figure 3.4 demonstrates that the average excretion of ITC metabolites as a percentage of ingested GFN was 56% (range 21-91%, SD ± 18.66). This level of urinary excretion is in keeping with previous evidence that greater proportions of ITCs are detected in the urine of patients consuming GFN with intact or activated myrosinase enzyme.
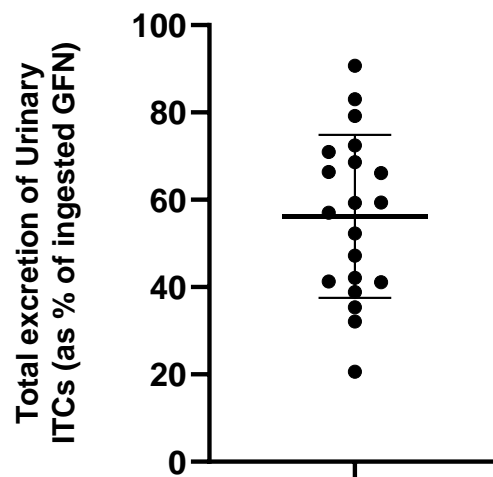
Figure 3. 4 Total excreted urinary isothiocyanates (ITCs) in participants consuming a glucoraphanin intervention (n=20), represented as a % of total glucoraphanin consumed. Metabolites include sulforaphane, and the sulforaphane metabolites including, sulforaphane-cysteine, sulforaphane-NAC, and erucin-NAC. Data shown as mean ± SD.

Figure 3.5 shows that SFN-NAC was the most abundant metabolite detected in urine of participants consuming a GFN-containing intervention, followed by E-NAC (60.19% and 15.59% respectively).
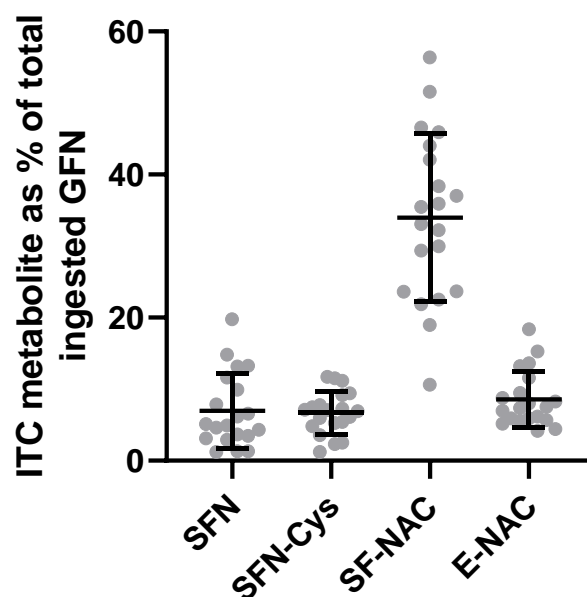
Figure 3. 5 Concentration of sulforaphane, and the sulforaphane metabolites detected in urine of patients consuming a glucoraphanin-containing intervention, represented as % of total ingested glucoraphanin. Sulforaphane metabolites include sulforaphane-cysteine, sulforaphane-NAC, and erucin-NAC in groups consuming a glucoraphanin intervention (n=20). Results shown as mean ± SD.

3.4.1.2 Consumption of Broccomax Glucoraphanin capsules led to a significant accumulation of SFN and SFN-NAC in Prostate Tissue

For the first time, targeted LCMS/MS analysis of ITCs collected from the Norfolk-ADaPt study detected SFN and SFN-NAC in the prostate. SFN-nitrile and E-NAC demonstrated small peaks in 3 samples but not to detectable levels for quantification. Other metabolites analysed but not detected included SFN-cysteine-glycine and SFN-glutathione.

The median concentration of total ITC metabolites detected in the prostate of patients consuming a GFN-intervention was 1.06 nmol/g (IQR 0.40 to 1.39), significantly higher in patients consuming a GFN-containing intervention (n=20) compared to a non-glucoraphanin intervention (n=19) (median 0.07 nmol/g IQR 0.00 to 0.90) (p=0.0023). Indeed, total ITC metabolites were detectable in all 20 patients consuming a GFN intervention compared to 10 consuming a non-GFN intervention.
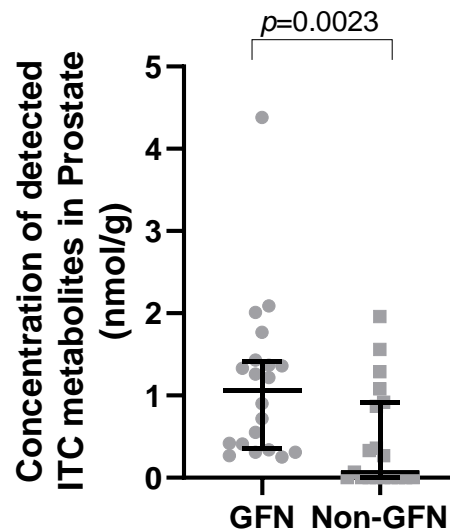
Figure 3. 6 Concentration of total isothiocyanates detected in prostate samples of participants consuming a glucoraphanin (n=20) vs. a non-glucoraphanin containing (n=19) intervention. Total metabolites include sulforaphane, and the sulforaphane metabolite sulforaphane-NAC. Results are shown as median ± IQR. P-value calculated using a Mann-Whitney test.

Individual metabolite concentrations detected in the prostate were then analysed, in order to determine whether the above accumulation was driven in particularly by SFN (figure 3.7) or SFN-NAC (figure 3.8).

SFN was detected in the prostate of all patients consuming a GFN-containing intervention, compared to only 5 participants consuming a non-GFN containing intervention. The median concentration of SFN detected in the prostate of patients consuming a GFN-containing intervention was 0.36 nmol/g (IQR 0.30 to 0.47), which was significantly higher compared to a non-GFN containing intervention (p=0.001).
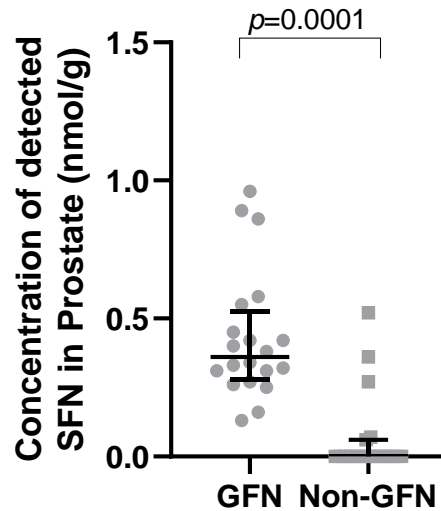
Figure 3. 7 Concentration of Sulforaphane detected in prostate samples of participants consuming a glucoraphanin (n=19) vs. a non-glucoraphanin intervention (n=19). Results are shown as median ± IQR. Analysis using Mann Whitney.

SFN-NAC was detected in the prostate of 14/20 participants consuming a GFN-containing intervention. The median concentration of SFN-NAC detected in the prostate of patients consuming a GFN-containing intervention was 0.57 nmol/g (IQR 0 to 0.98), the effect of which was not deemed statistically significantly higher compared to a non-GFN containing intervention (p=0.0876).
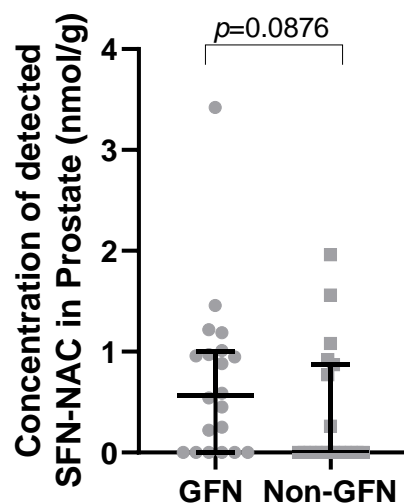
Figure 3. 8 Concentration of Sulforaphane-NAC detected in prostate samples of participants consuming a glucoraphanin (n=19) vs. a non-glucoraphanin containing intervention (n=20). Results are shown as median ± IQR. Analysis using Mann Whitney.

3.4.2 Alliin Metabolites

As previously discussed, all 40 participants returned at 24-hour urine sample on day one of supplement consumption. Urine was analysed for urinary Alliin and metabolites in two batches.

As above, a total of 39 participants underwent TPB of the prostate on the final day of the ADaPt study. Biopsy cores were taken from both the peripheral and transition zone of the prostate and analysed for Alliin and metabolites in 2 batches.

3.4.2.1 Consumption of Kwai Garlic Supplements led to an accumulation of garlic metabolites in the Urine

The metabolites detected in urine using targeted LCMS/MS analysis were Alliin, S-allyl-cysteine (SAC), and N-acetyl-S-allyl-cysteine (NAC-SAC). γ-glutamyl-S-ally-L-cysteine (γ-SAC) was detected in the urine of one participant only but was not quantifiable.

Total excreted Alliin and metabolites was higher among patients when supplemented with Alliin (median 0.0023 μmol/L IQR 0.002 – 0.004, p=0.0039). When individual compounds are considered, only NAC-SAC is significantly higher (p=0.0036) while SAC is not (p=0.422), and there is some evidence that Alliin concentration is also increased (p=0.0961) (Figure 3.9-3.12)
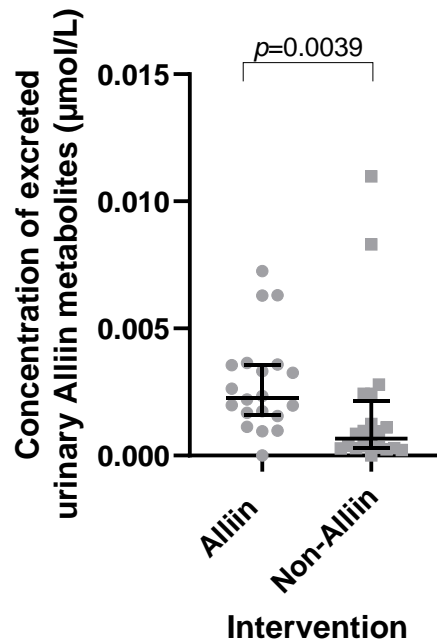
Figure 3. 9 Concentration of total Alliin metabolites detected in urine samples of participants consuming an Alliin-containing intervention (n=20) compared to a non-Alliin containing intervention (n=19). Metabolites include; Alliin, S-allyl-cysteine (SAC), and N-acetyl-S-allyl-cysteine (NAC-SAC). Results are shown as median ± interquartile range. Analysis using Mann-Whitney.
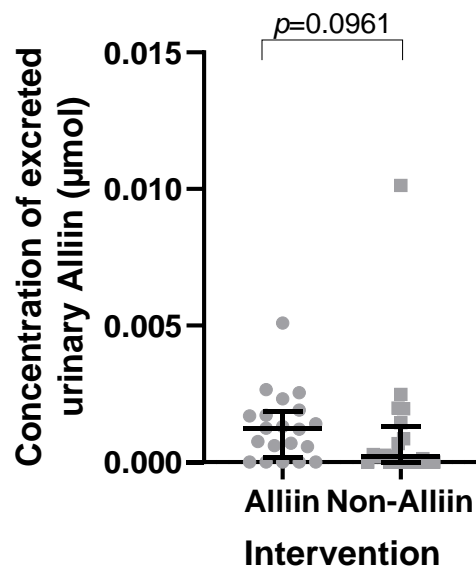
Figure 3. 10 Concentration of Alliin detected in urine samples of participants consuming an Alliin-containing intervention (n=20) compared to a non-Alliin containing intervention (n=19). Results are shown as median ± interquartile range. Analysis using Mann-Whitney.
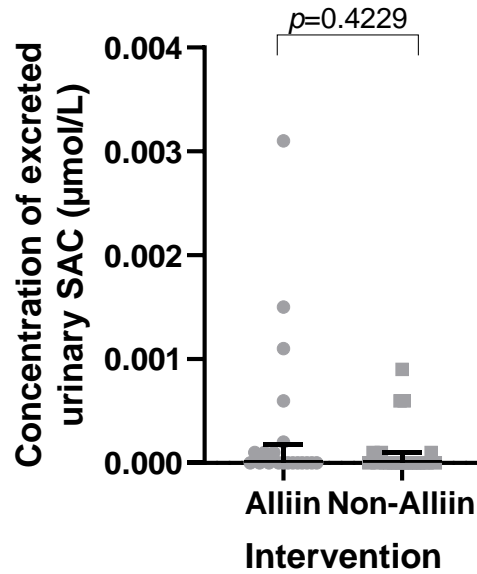
Figure 3. 11 Concentration of S-allyl-cysteine (SAC) detected in urine samples of participants consuming an Alliin-containing intervention (n=20) compared to a non-Alliin containing intervention (n=19). Results are shown as median ± interquartile range. Analysis using Mann-Whitney.
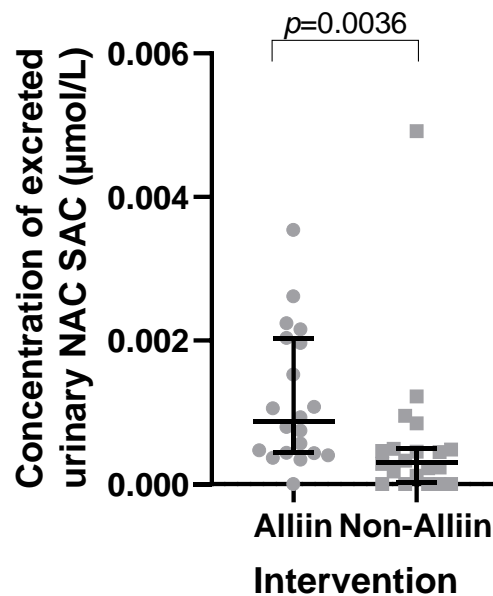
Figure 3. 12 Concentration of N-acetyl-S-allyl-cysteine (NAC-SAC) detected in urine samples of participants consuming an Alliin-containing intervention (n=20) compared to a non-Alliin containing intervention (n=19). Results are shown as median ± interquartile range. Analysis using Mann-Whitney.

3.4.2.2 Consumption of Kwai Garlic Supplements did not lead to an Accumulation of Alliin or Alliin-metabolites in the Total Prostate

Alliin, S-allyl-cysteine (SAC) and γ-glutamyl-S-ally-L-cysteine (γ-SAC) were detected in the prostate of men enrolled in the Norfolk ADaPt study using targeted LCMS/MS. γ-glutamyl-S-ally-L-cysteine (γ-SAC) was detected to a very small concentration in some patients. No other organosulphur compound metabolites from garlic were detected, including Allicin.

The median concentration of total Alliin metabolites detected in the prostate (combined PZ and TZ) of patients consuming an Alliin-containing intervention was 16.61 nmol/g (IQR 12.58 to 22.65) which was not statistically higher than in the non-Alliin containing group (p=0.5925).
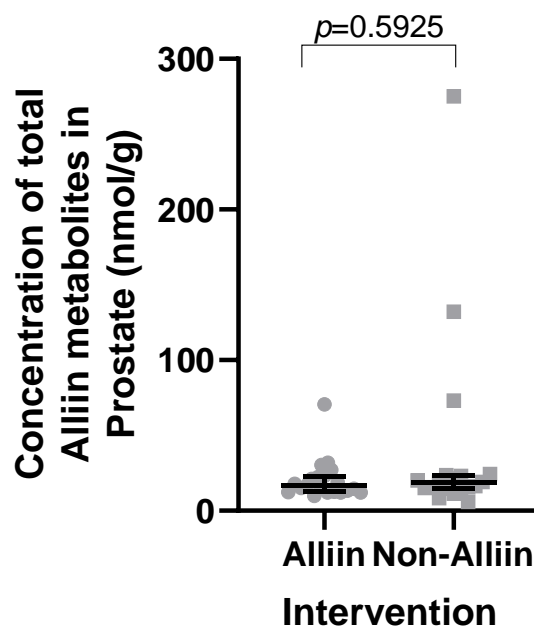
Figure 3. 13 Concentration of total Alliin metabolites detected in the Prostate of participants consuming an Alliin-containing intervention (n=20) compared to a non-Alliin containing intervention (n=19). Metabolites include; Alliin, S-allyl-cysteine (SAC) and γ-glutamyl-S-ally-L-cysteine (γ-SAC). Results are shown as median ± interquartile range. Analysis using Mann-Whitney.

The median concentration of Alliin detected in the prostate (PZ and TZ) of patients consuming an Alliin-containing intervention compared to a non-Alliin containing intervention is shown in figure 3.14. The median concentration of Alliin was 15.75 nmol/g (IQR 11.85 to 1.64) which was not statistically higher than in the non-Alliin containing group (p=0.4779).

Figures 3.14 and 3.15 demonstrate the concentration of the Alliin metabolites S-allyl-cysteine (SAC) and γ-glutamyl-S-ally-L-cysteine (γ-SAC) detected in prostate tissue in those consuming an Alliin-containing vs. non-Alliin containing intervention. No difference was demonstrated between the treatment and control groups for either metabolite (p=0.3922 and 0.5915 respectively).
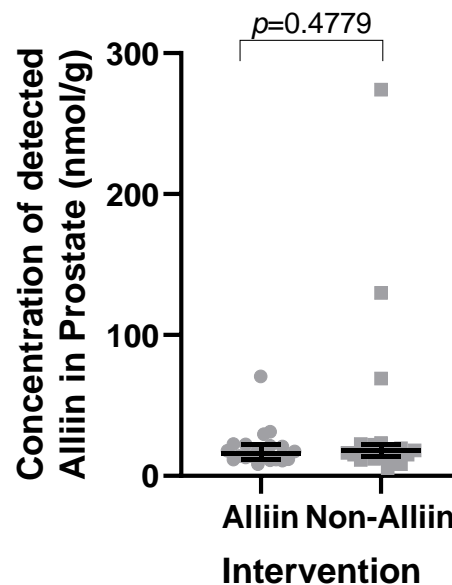
Figure 3. 14 Concentration of Alliin detected in the Prostate of participants consuming an Alliin-containing intervention (n=20) compared to a non-Alliin containing intervention (n=19). Results are shown as median ± interquartile range. Analysis using Mann-Whitney.
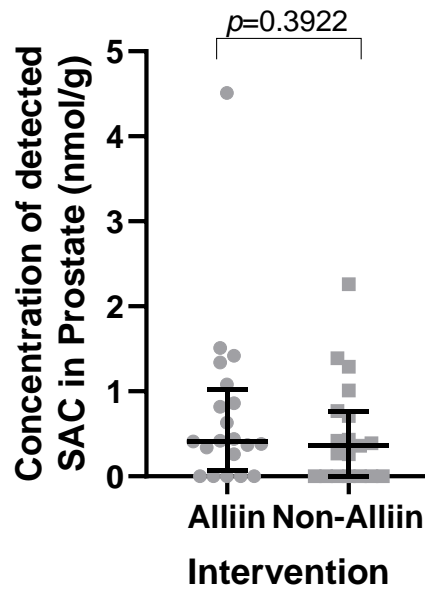
Figure 3. 15 Concentration of detected S-allyl-cysteine (SAC) in the Prostate of participants consuming an Alliin-containing intervention (n=20) compared to a non-Alliin containing intervention (n=19). Results are shown as median ± interquartile range. Analysis using Mann-Whitney.
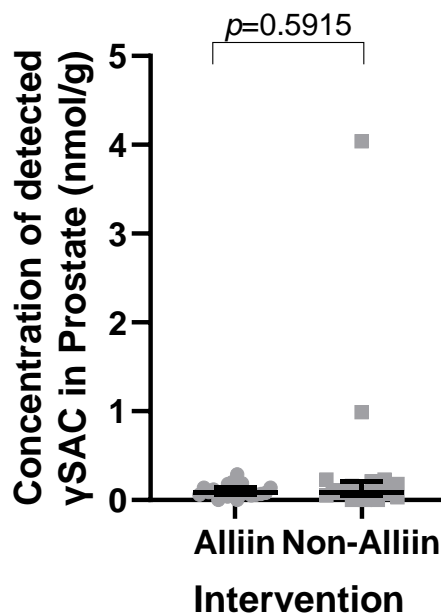
Figure 3. 16 Concentration of γ-glutamyl-S-ally-L-cysteine (γ-SAC) detected in the Prostate of participants consuming an Alliin-containing intervention (n=20) compared to a non-Alliin containing intervention (n=19). Results are shown as median ± interquartile range. Analysis using Mann-Whitney.

3.4.3 The Concentration of Urinary and Prostatic Metabolites were not affected by GSTM1 genotype

As previously discussed, evidence suggests that *GSTM1-* positive genotype provides a greater advantage from the anti-cancer properties of cruciferous vegetables, in particularly with regards to GFN and SFN derived from broccoli (139, 140, 311), as opposed to other crucifers such as Chinese cabbage (312). Although human studies reveal conflicting results, SFN metabolite concentrations detected in both plasma and urine have been shown to be higher in *GSTM1-* positive individuals consuming high-GFN and standard broccoli interventions (294), suggesting that SFN metabolism may play a significant role in the protective effect of *GSTM1-* positive individuals

To test whether there was any difference in the concentrations of urinary or prostate metabolites in patients enrolled in the Norfolk-ADaPt study according to genotype (figures 3.17 and 3.18), the previously reported metabolite data in this chapter was stratified according to the *GSTM1-* genotyping data (previously presented in chapter 2).

There is no significant evidence to statistically prove a difference in the concentration of excreted urinary ITC's in *GSTM1-* positive patients consuming a GFN-containing intervention, compared to GSTM1- null patients (p=0.8506) nor for the concentration of total ITC metabolites detected in the prostate (p=0.2962). However, given the median one group is almost twice what it is in the other, an effect may be present which this study is underpowered to detect. In addition, the same was observed for patients consuming Alliin-containing interventions (p=0.4269 and p=0.9692 for urinary and prostate metabolites respectively). However, this study may be underpowered to detect an effect in this outcome.
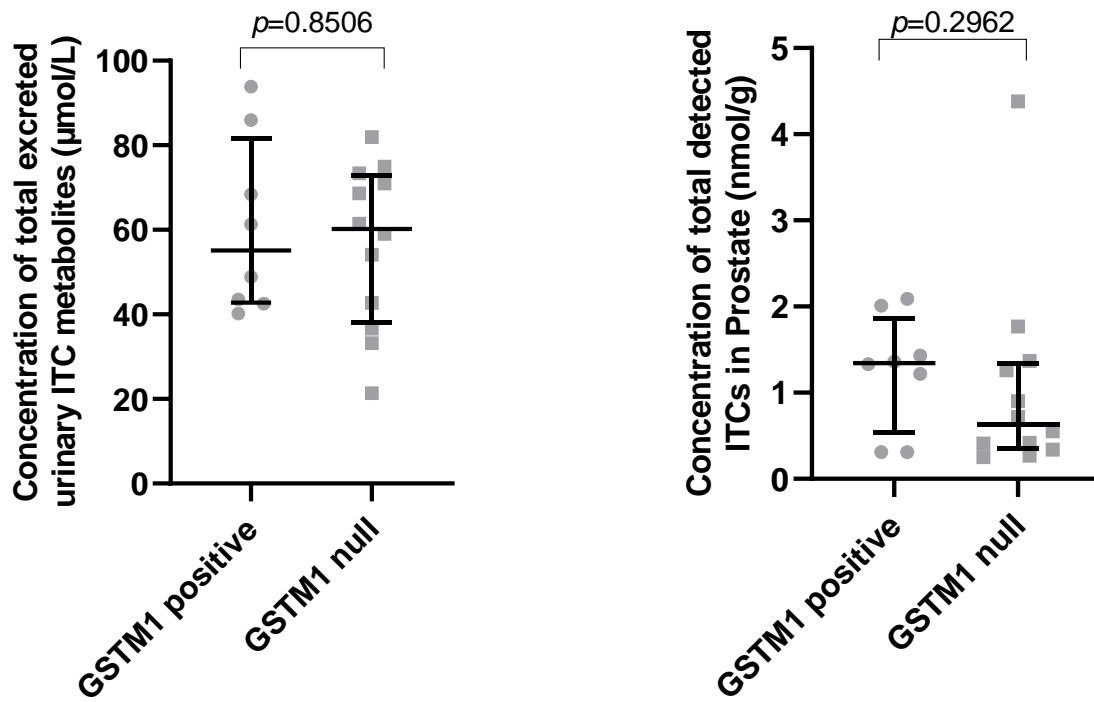
Figure 3. 17 Concentration of total excreted ITCs in A) urine and B) prostate, in participants consuming a glucoraphanin intervention (n=20) stratified according to GSTM1 genotype. Results are shown as median ± interquartile range. Analysis using Mann-Whitney.
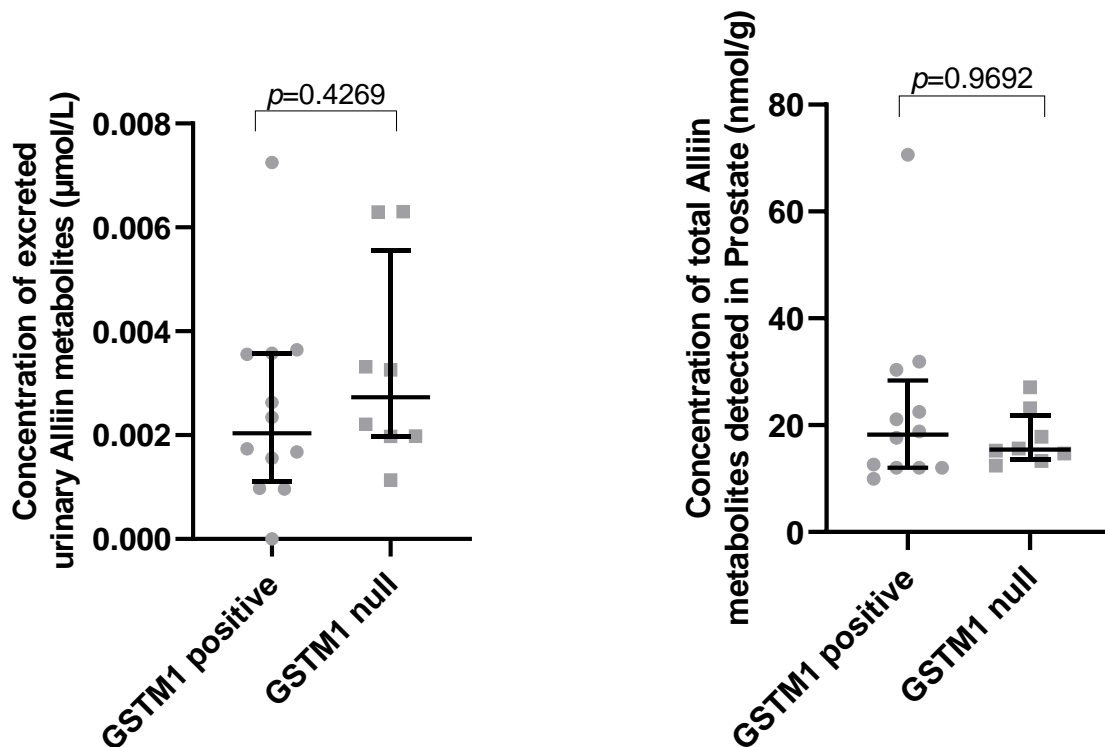
Figure 3. 18 Concentration of total excreted Alliin and metabolites in A) urine, and B) prostate in participants consuming an Alliin-containing intervention (n=20) stratified by GSTM1 genotype. Results are shown as median ± interquartile range. Analysis using Mann-Whitney.

3.5 Results – Secondary Supplementary Outcomes

3.5.1 Accumulation of ITC Metabolites by Prostatic Zone

Results of the primary outcomes demonstrated that SFN and metabolites were detected in the prostate of patients consuming a GFN-containing intervention. However, to determine whether these metabolites accumulate to different concentrations within the prostate, the samples from the peripheral and transition zone of the prostate were analysed separately. Given the extent of urinary excretion of these metabolites, and the theory of urinary reflux, it was hypothesised that SFN and its metabolites would accumulate to a greater extent in the PZ of the prostate. The concentrations of metabolite accumulation are summarised in table 3.2 (page 129).

3.5.1.1 Peripheral Zone

SFN and SFN-NAC were detected in the PZ of the prostate. Total median ITC metabolite concentration in the PZ of patients consuming a GFN intervention was 0.37 nmol/g (IQR 0.22 to 0.85), compared to those consuming a non-GFN containing intervention (median 0 nmol/g, IQR 0.00 to 0.44, mean 0.35 nmol/g) ($p=0.0104$).

In keeping with the hypothesis, all SFN and metabolites accumulated in the PZ of the prostate to a significantly higher concentration in the GFN-treatment group.

SFN was detected in the PZ all 20 patients consuming GFN capsules, compared to 5 in the control group. The median concentration of SFN was significantly higher in the treatment group consuming a GFN-containing intervention (0.18 nmol/g $p<0.0001$). SFN-NAC was detected in the PZ in 11 of 20 participants consuming GFN, with a median concentration of 0.20 nmol/g ($p=0.0281$).
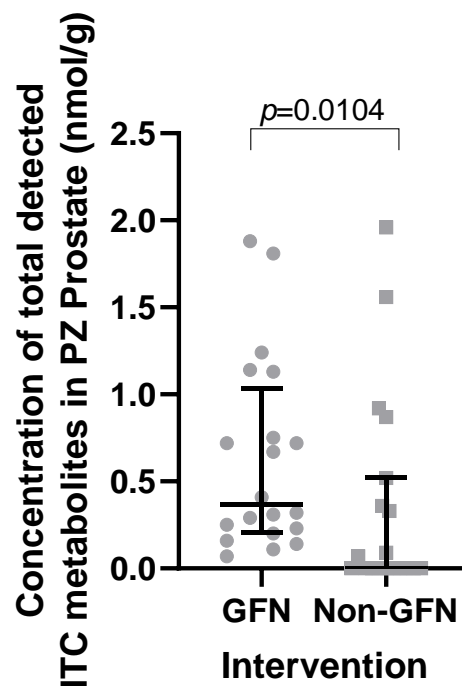
Figure 3. 19 Concentration of total ITC metabolites detected in the peripheral zone of the prostate in patients consuming a glucoraphanin-containing intervention (n=20) compared to a non-glucoraphanin intervention (n=19). Results are shown as median ± interquartile range. Analysis using Mann-Whitney.
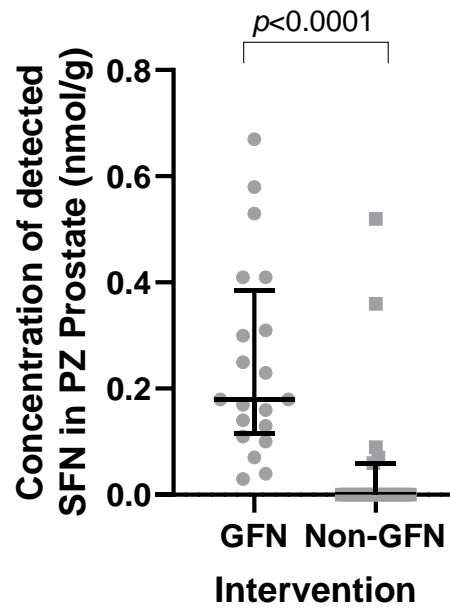
Figure 3. 20 Concentration of sulforaphane detected in the peripheral zone of the prostate in patients consuming a glucoraphanin-containing intervention (n=20) compared to a non-glucoraphanin intervention (n=19). Results are shown as median ± interquartile range. Analysis using Mann-Whitney.
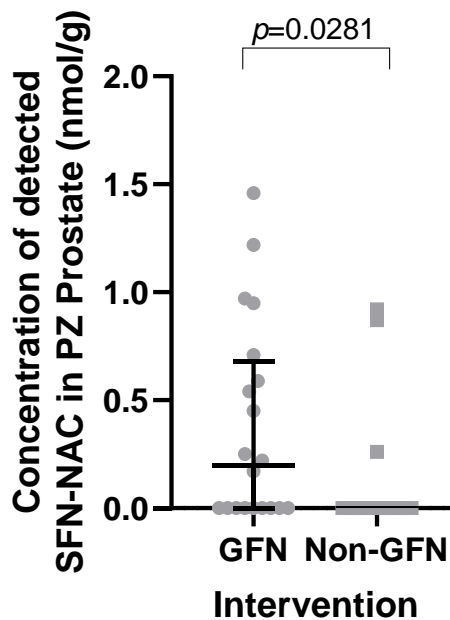
Figure 3. 21 Concentration of SFN-NAC detected in the peripheral zone of the prostate in patients consuming a glucoraphanin-containing intervention (n=20) compared to a non-glucoraphanin intervention (n=19). Results are shown as median ± interquartile range. Analysis using Mann-Whitney.

3.5.1.2 Transition Zone

SFN and SFN-NAC were detected in the transition zone of the prostate. Median total ITC concentration in the TZ of patients consuming a GFN intervention was 0.24 nmol/g (IQR 0.14 to 0.55), compared to those consuming a non-GFN containing intervention (median 0.00 nmol/g IQR 0.00 to 0.00, mean 0.11 nmol/g) ($p<0.0001$).

SFN was detected in the TZ in 18 of 20 patients consuming a GFN-intervention, compared to 1 in the control group. SFN was detected in the TZ to significantly higher concentrations in patients consuming GFN when compared to controls (median concentration 0.16 nmol/g IQR 0.13 to 0.23, $p<0.0001$). SFN-NAC was detected in the TZ in 7 of 20 participants, and was not deemed statistically significant compared to a non-GFN controls ($p=0.1105$).

Figure 3. 22 Concentration of total ITC metabolites detected in the transition zone of the prostate in patients consuming a glucoraphanin-containing intervention (n=20), compared to a non-glucoraphanin intervention (n=19). Results are shown as median ± interquartile range. Analysis using Mann-Whitney.

Figure 3. 23 Concentration of sulforaphane detected in the transition zone of the prostate in patients consuming a glucoraphanin-containing intervention (n=20) compared to a non-glucoraphanin containing intervention (n=19). Results are shown as median ± interquartile range. Analysis using Mann-Whitney.
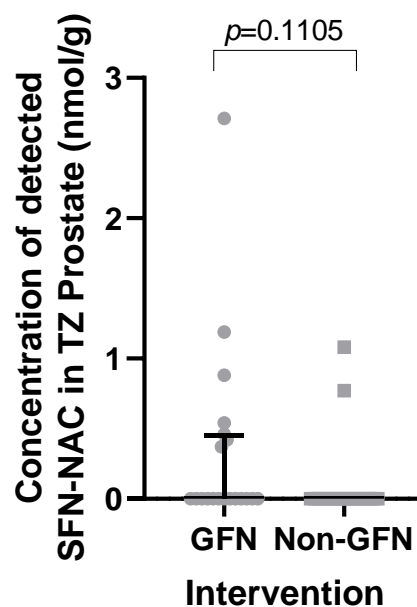
Figure 3. 24 Concentration of SFN-NAC detected in the transition zone of the prostate in patients consuming a glucoraphanin-containing intervention (n=20) compared to a non-glucoraphanin intervention (n=19). Results are shown as median ± interquartile range. Analysis using Mann-Whitney.

3.5.1.3 There is no evidence that the concentration of SFN accumulation is higher in the Peripheral Zone compared to the Transition Zone or that there is any correlation between zones

To ascertain whether the concentration of accumulated prostate metabolites differed between zones, paired analysis of prostate samples (from the PZ and TZ) of patients consuming a GFN-containing intervention were analysed (figures 3.25 and 3.26).

No significant difference was demonstrated between the concentration of total detected metabolites (SFN and SFN-NAC) found in the PZ compared to the TZ (p=0.526) nor was there a significant correlation demonstrated between the zones (r^2 = 0.0278), i.e. the concentration in one zone was not dependent upon the concentration in the other. This was also the case for the concentration of detected SFN only (p=0.1032, r^2 = 0.07872).
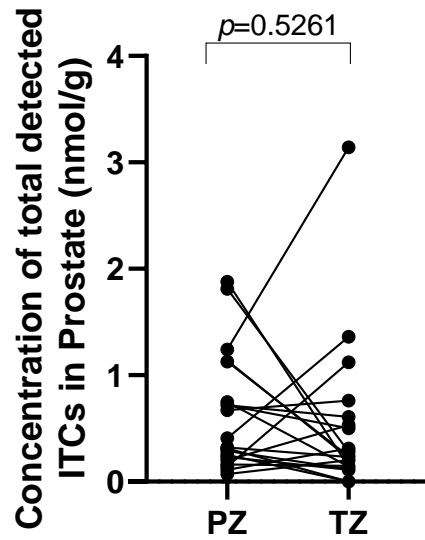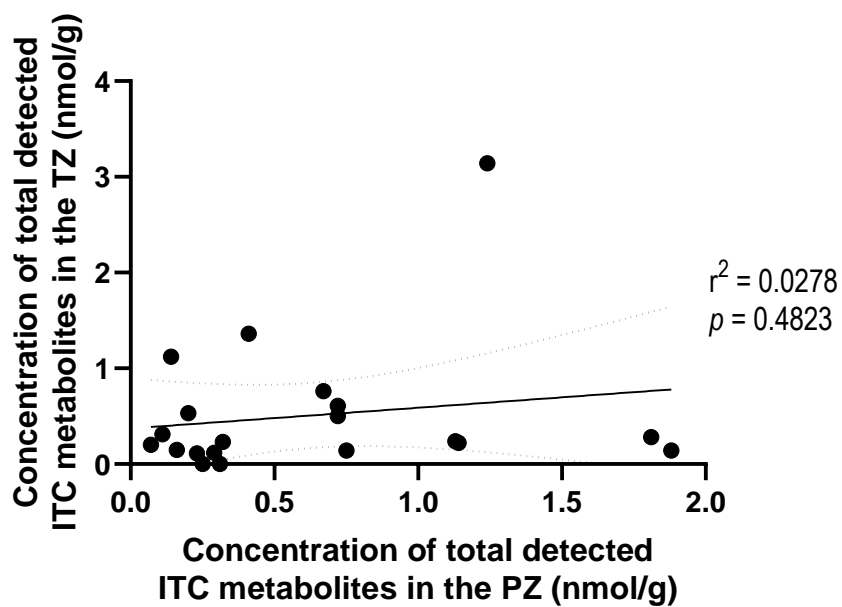
Figure 3. 25 A) Concentration of t*otal ITC metabolites (SFN + SFN-NAC) detected in the peripheral zone vs. the transition zone of the prostate (n=20) in patients consuming a GFN intervention. Results are shown as paired samples by line. Analysis using two-tailed paired T test B) Data presented as linear regression, r[2] = 0.0278.*

A)

B)
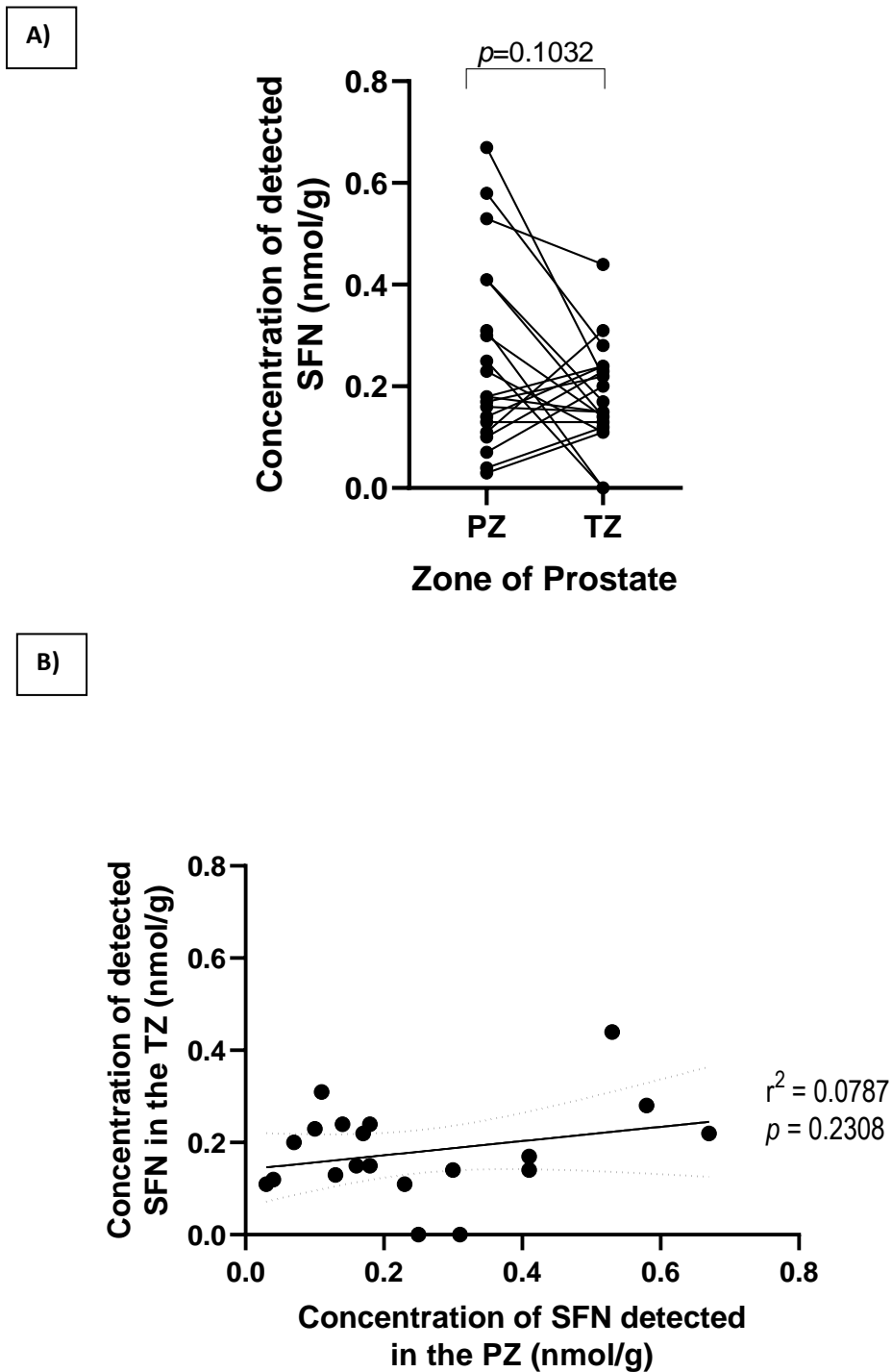
Figure 3. 26 A) *Concentration of SFN detected in the peripheral zone vs. the transition zone of the prostate in patients consuming a glucoraphanin intervention (n=20). Results shown as paired samples by line. Analysing using paired T test. B) Data presented as linear regression, r² = 0.0787.*

Table 3. 2 Summary table of the concentration of sulforaphane and metabolites detected in the peripheral and transition zones of the prostate, the total prostate (nmol/g), and urine (μmol/L) of participants consuming a GFN -containing intervention (n=20) vs. a non-GFN containing intervention (n=19). Metabolites include; Sulforaphane and N-acetyl-S-allyl-cysteine (SFN-NAC). Results are shown as mean ± standard deviation and median with IQR due to the variation in the normality of distribution of the data.

	GFN-Containing Intervention							
	PZ (nmol/g)		TZ (nmol/g)		Total Prostate (nmol/g)			Urine (µmol/L)
	SFN	SFN-NAC	SFN	SFN-NAC	SFN	SFN-NAC	Total Metabolites	Total Metabolites
Mean	0.25 ± 0.18	0.38 ± 0.47	0.18 ± 0.10	0.33 ± 0.66	0.43 ± 0.23	0.71 ± 0.80	1.14 ± 0.97	58.15 ± 19.31
Median	0.18	0.20	0.16	0.00	0.36	0.57	1.06	60.17
IQR	0.21	0.62	0.10	0.43	0.18	0.98	0.99	28.89
	Non GFN-Containing Intervention							
	PZ (nmol/g)		TZ (nmol/g)		Total Prostate (nmol/g)			Urine (µmol/L)
	SFN	SFN-NAC	SFN	SFN-NAC	SFN	SFN-NAC	Total Metabolites	Total Metabolites
Mean	0.06 ± 0.14	0.29 ± 0.59	0.01 ± 0.04	0.10 ± 0.30	0.07 ± 0.15	0.39 ± 0.62	0.46 ± 0.63	1.97 ± 3.63
Median	0.00	0.00	0.00	0.00	0.00	0.00	0.07	0.20
IQR	0.03	0.13	0.00	0.00	0.03	0.82	0.90	2.16

3.5.2 Accumulation of Alliin and Metabolites by Prostatic Zone

Results of the primary outcomes demonstrated that Alliin and metabolites (although detected in prostate) were not detected in the total prostate of patients consuming an Alliin-containing intervention to significantly higher concentrations of those consuming a non-Alliin containing intervention. However, to determine whether these metabolites accumulate to different concentrations within the prostate, the samples from the PZ and TZ of the prostate were analysed separately. The concentrations of metabolite accumulation are summarised in table 3.3 (page 140).

3.5.2.1 Peripheral Zone

Alliin and SAC were detected in the PZ of the prostate. γSAC was detected to a very small concentration (mean 0.10 nmol/g). Alliin was detected in all patients in the study, irrespective of intervention type.

The median concentration of total Alliin and metabolites in patients consuming an Alliin-containing intervention in the PZ was 8.09 nmol/g (IQR 6.05 to 14.49, mean 12.49 nmol/g), which was not significantly different to those in a non-Alliin intervention group (median 11.6 nmol/g, IQR 8.38 to 17.19, mean 33.39 nmol/g) (p=0.1494).

The median concentration of detected Alliin in patients consuming an Alliin-containing intervention in the PZ was 6.99 nmol/g (IQR 2.8 to 14.49, mean 12.13 nmol/g), which was not significantly different to those in a non-Alliin intervention group (median 11.6 nmol/g, IQR 8.28 to 16.34, mean 32.81 nmol/g) (p=0.3730). SAC was detected in the PZ in 8 of 20 patients consuming an Alliin-containing intervention, compared to 6 of 19 in the non-Alliin containing group. The concentration of detected SAC in patients consuming an Alliin-containing intervention in the PZ (median 0.00 nmol/g, IQR 0.00 to 0.59, mean 0.32 nmol/g) was not significantly different to those in a non-Alliin intervention group (median 0.00 nmol/g, IQR 0.00 to 0.58, mean 0.30 nmol/g) (p=0.8568).
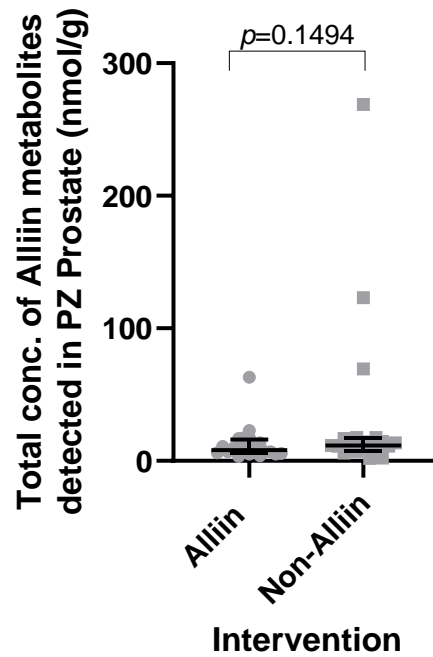
Figure 3. 27 Total concentration of all Alliin metabolites detected in the peripheral zone of the prostate (n=20,19) in patients consuming alliin compared to a non-alliin intervention. Metabolites include Alliin, S-allyl-cysteine (SAC) and γ-glutamyl-S-ally-L-cysteine (γ-SAC). Results are shown as median ± interquartile range. Analysis using Mann-Whitney.
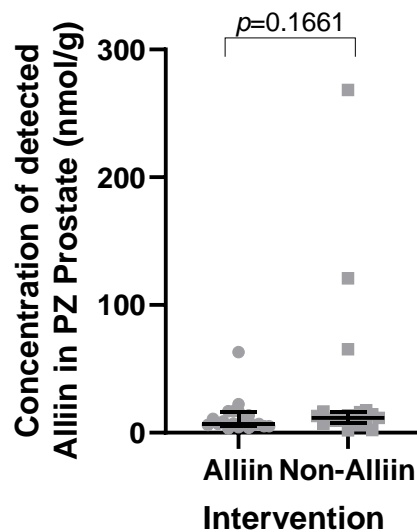
Figure 3. 28 Concentration of Alliin detected in the peripheral zone of the prostate (n=20,19) in patients consuming alliin compared to a non-alliin intervention Results are shown as median ± interquartile range. Analysis using Mann-Whitney.
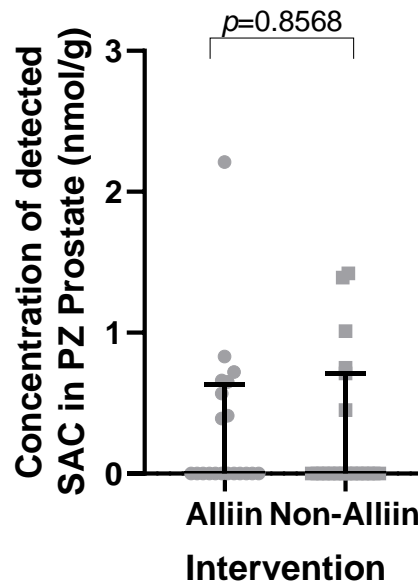
Figure 3. 29 Concentration of SAC detected in the peripheral zone of the prostate (n=20,19) in patients consuming alliin compared to a non-alliin intervention. Results are shown as median ± interquartile range. Analysis using Mann-Whitney.

3.5.2.2 Transition Zone

Alliin was detected in all prostate samples from the TZ of the prostate irrespective of treatment type.

The median concentration of total Alliin and metabolites in patients consuming an Alliin-containing intervention in the TZ was 7.05 nmol/g (IQR 5.54 to 9.51, mean 8.06 nmol/g), which was significantly higher than those in the non-Alliin intervention group (median 5.71 nmol/g, IQR 4.75 to 6.67, mean 5.85 nmol/g) (p=0.0358).

The median concentration of detected Alliin in patients consuming an Alliin-containing intervention in the TZ was 6.74 nmol/g (IQR 5.19 to 9.09), which was not deemed significantly higher than that of the non-Alliin intervention group (median 5.60 nmol/g, IQR 4.61 to 6.14, mean 5.58 nmol/g) (p=0.0696).

SAC was detected in 14 of 20 patients consuming an Alliin-containing intervention, compared to 9 of 19 in the non-Alliin containing group. The median concentration of detected SAC in patients consuming an Alliin-containing intervention in the TZ was 0.37 nmol/g (IQR 0.00 to 0.50, mean 0.42

nmol/g), which was not significantly different to those in a non-Alliin intervention group (median 0.00 nmol/g, IQR 0.00 to 0.38, mean 0.20 nmol/g) (p=0.0871). However, this data does show a tendency towards effect in the treated group.
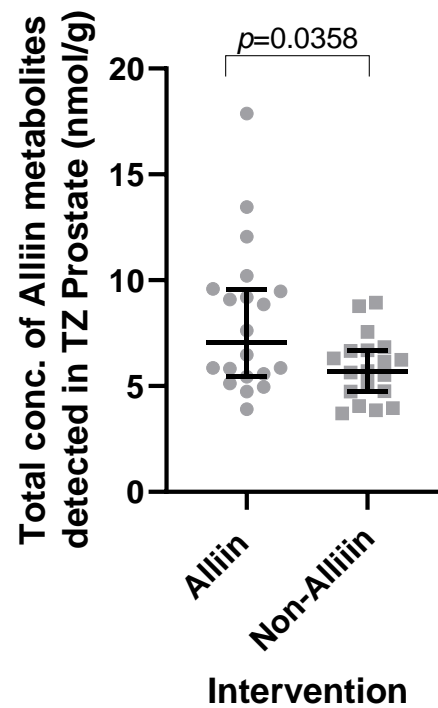
Figure 3. 30 Total concentration of all Alliin metabolites detected in the transition zone of the prostate in patients consuming an Alliin-containing intervention (n=20) compared to a non-Alliin containing intervention (n=19). Metabolites include Alliin, S-allyl-cysteine (SAC) and γ-glutamyl-S-ally-L-cysteine (γ-SAC). Results are shown as median ± interquartile range. Analysis using Mann-Whitney.
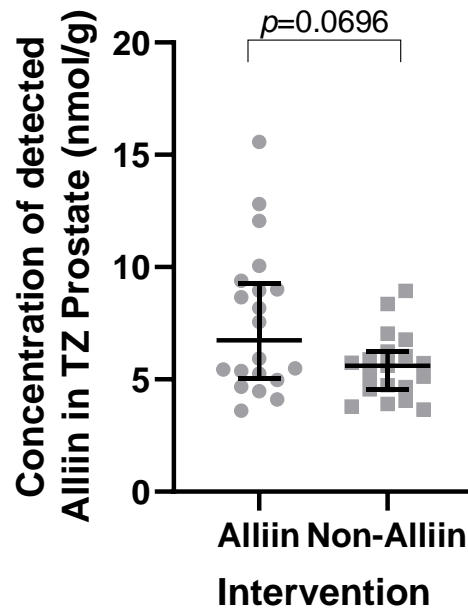
Figure 3. 31 Concentration of Alliin detected in the transition zone of the prostate in patients consuming an Alliin-containing intervention (n=20) compared to a non-Alliin containing intervention (n=19). Results are shown as median ± interquartile range. Analysis using Mann-Whitney.
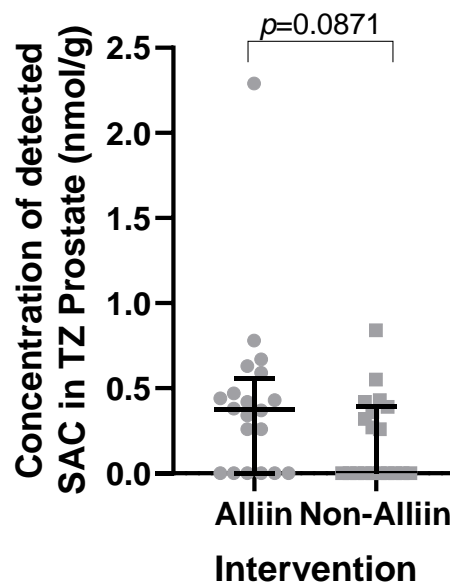
Figure 3. 32 Concentration of SAC detected in the transition zone of the prostate in patients consuming an Alliin-containing intervention (n=20) compared to a non-Alliin containing intervention (n=19). Results are shown as mean ± SD. Results are shown as median ± interquartile range. Analysis using Mann-Whitney.

3.5.2.4 There is no evidence that the concentration of Alliin accumulation is higher in the Peripheral Zone compared to the Transition Zone or that there is any correlation between zones

As was demonstrated for ITCs, to ascertain whether the concentration of accumulated prostate metabolites differed between zones, paired analysis of prostate samples (from the PZ and TZ) of patients consuming an Alliin-containing intervention were analysed (figures 3.33, 3.34 and 3.35).

No significant difference was demonstrated in the concentration of Alliin detected between the PZ and TZ in patients consuming Alliin ($p=0.0967$) and there is no evidence of a correlation between the two zones ($r^2 = 0.0013$). In addition, there was not found to be any correlation between the concentration of SAC metabolites found in the PZ compared to the TZ. Total metabolite concentrations were not significantly different between the two zones.
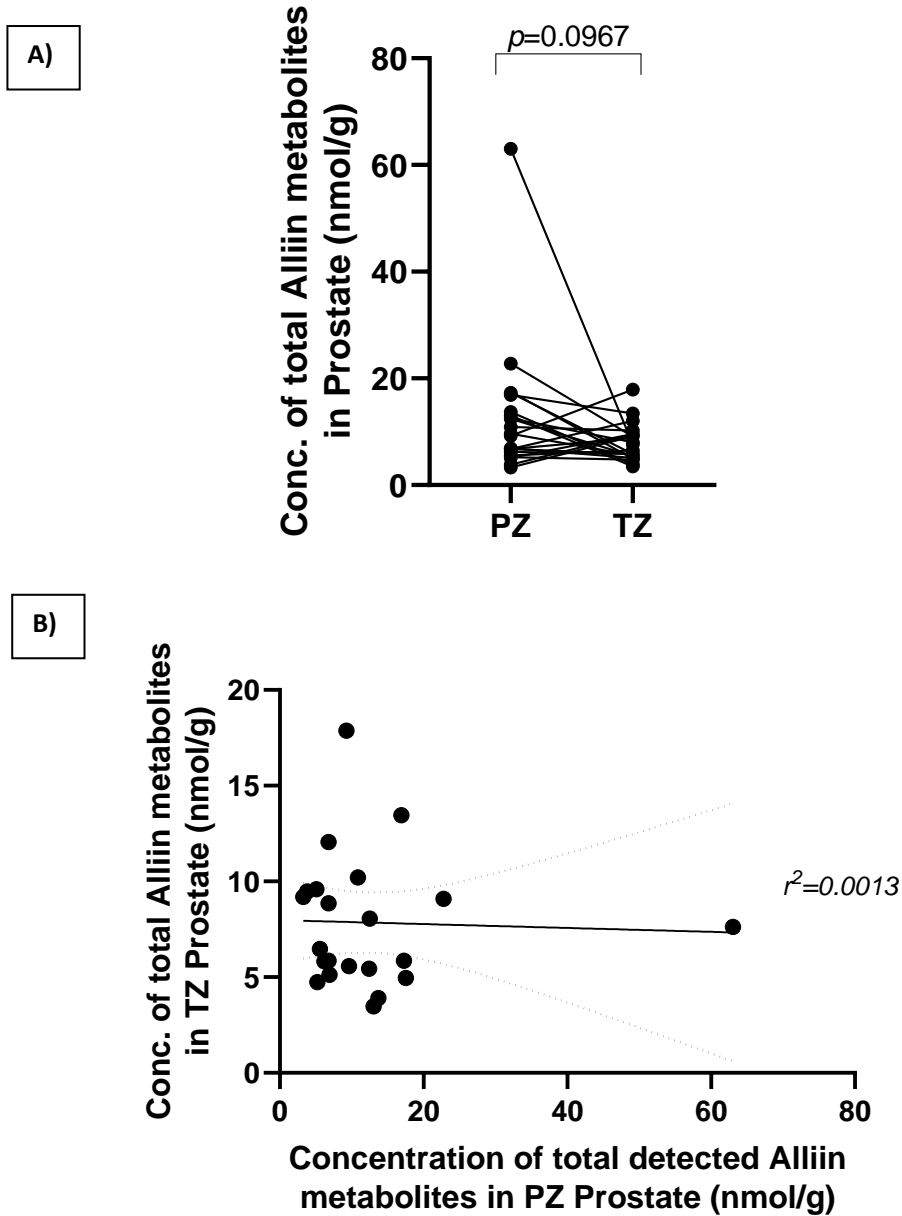
Figure 3. 33 A) *Concentration of all Alliin-metabolites detected in the peripheral zone vs. the transition zone of the prostate in patients consuming an Alliin-containing intervention (n=20). Results are shown as paired samples. Analysis using paired T-test. And B) Data presented as linear regression, r^2 = 0.0013.*
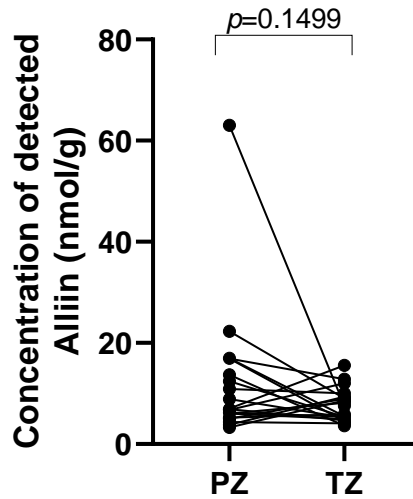
Figure 3. 34 Concentration of Alliin detected in the peripheral zone vs. the transition zone of the prostate (n=20) in patients consuming an Alliin-containing intervention. Results are shown as paired samples. Analysis using paired T-test.
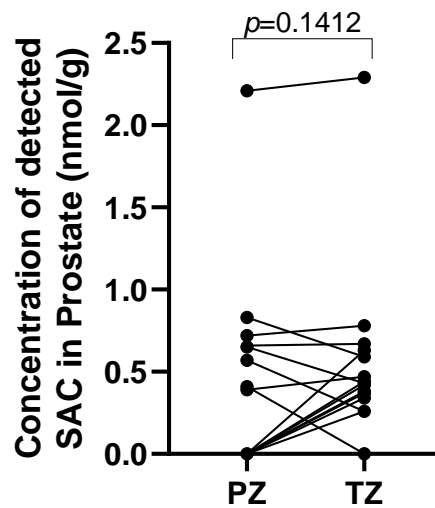
Figure 3. 35 Concentration of SAC detected in the peripheral zone vs. the transition zone of the prostate (n=20) in patients consuming an Alliin-containing intervention. Results are shown as paired samples. Analysis using paired T-test.

3.5.3 There is no correlation between excreted urinary metabolites and those detected in Prostate Tissue

Given the results previously demonstrating a significant concentration of urinary excreted SFN and metabolites (p<0.0001) and Alliin metabolites (p=0.0039) in participants consuming GFN- and Alliin-containing interventions respectively, it would be reasonable to hypothesise that the concentration of metabolites detected in the urine would correlatee with prostatic accumulation, should the theory of urinary reflux into the PZ be true. Interestingly however, this was not demonstrated for either intervention.
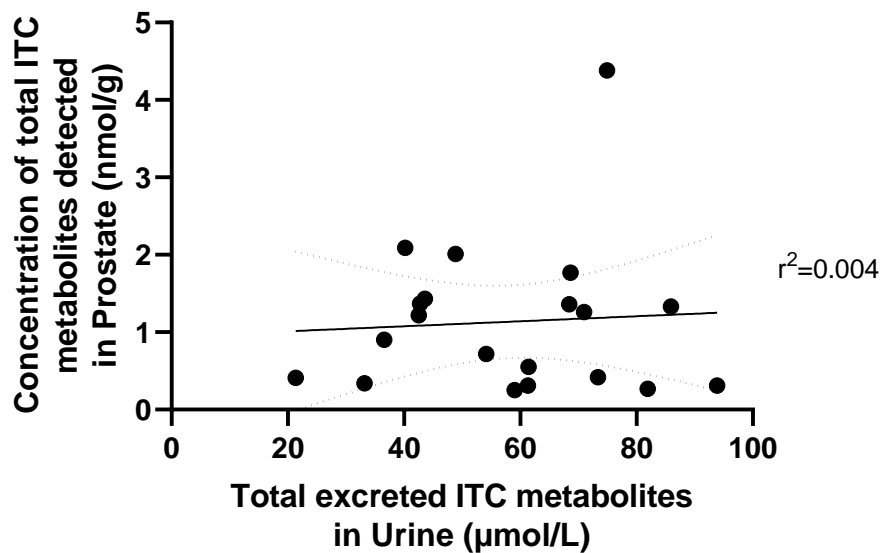
Figure 3. 36 Total concentration of ITC metabolites detected in the prostate vs. the concentration of total excreted ITCs in urine, in patients consuming a glucoraphanin intervention (n=20). Urinary metabolites include Sulforaphane and the Sulforaphane metabolites including sulforaphane-cysteine, sulforaphane-NAC, and erucin-NAC. Prostatic metabolites include sulforaphane and the Sulforaphane metabolite sulforaphane-NAC. Data presented as linear regression, $r^2 = 0.004$.
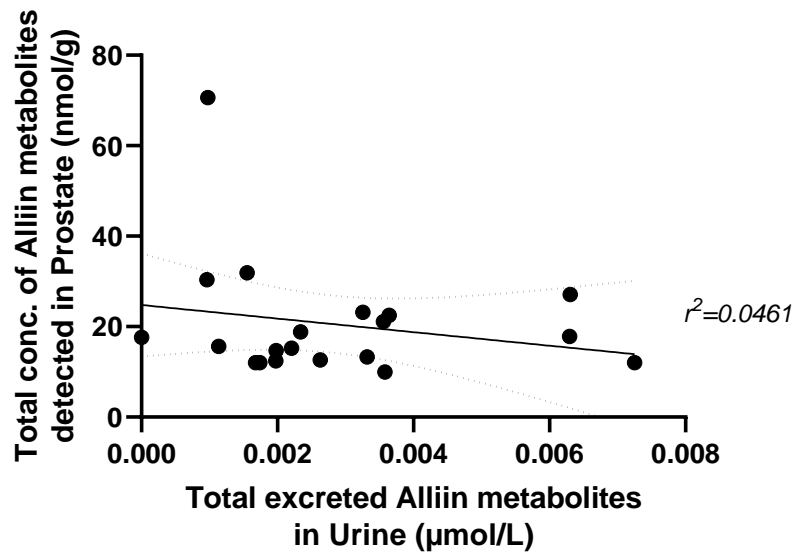
Figure 3. 37 Total concentration of Alliin metabolites detected in the prostate vs. the concentration of total excreted Alliin metabolites in urine, in patients consuming an Alliin intervention (n=20). Metabolites include; Alliin, S-allyl-cysteine (SAC), N-acetyl-S-allyl-cysteine (NAC-SAC) and γ-glutamyl-S-ally-L-cysteine (γ-SAC). Data presented as linear regression, r^2 = 0.0461.

Table 3. 3 Summary table of the concentration of Alliin and metabolites detected in the peripheral and transition zones of the prostate, the total prostate (nmol/g), and urine (μmol/L) of participants consuming an Alliin-containing intervention (n=20) vs. a non-Alliin containing intervention (n=19). Metabolites include; Alliin, S-allyl-cysteine (SAC) and γ-glutamyl-S-ally-L-cysteine (γ-SAC). Results are shown as mean ± standard deviation and median with IQR due to the variation in the normality of distribution of the data.

	Alliin-Containing Intervention										
	PZ (nmol/g)			TZ (nmol/g)			Total Prostate (nmol/g)				Urine (μmol/L)
	Alliin	SAC	γ-SAC	Alliin	SAC	γ-SAC	Alliin	SAC	γ-SAC	Total Metabolites	Total Metabolites
Mean	12.13 ± 13.13	0.32 ± 0.54	0.04 ± 0.07	7.58 ± 3.25	0.42 ± 0.51	0.06 ± 0.05	19.71 ± 13.49	0.74 ± 1.01	0.10 ± 0.07	20.55 ± 13.39	0.003 ± 0.002
Median	6.99	0.00	0.00	6.74	0.37	0.06	15.75	0.42	0.08	16.61	0.002
IQR	8.69	0.59	0.06	3.91	0.50	0.06	9.79	0.72	0.08	10.07	0.002
	Non Alliin-Containing Intervention										
	PZ (nmol/g)			TZ (nmol/g)			Total Prostate (nmol/g)				Urine (μmol/L)
	Alliin	SAC	γ-SAC	Alliin	SAC	γ-SAC	Alliin	SAC	γ-SAC	Total Metabolites	Total Metabolites
Mean	32.81 ± 63.52	0.30 ± 0.50	0.29 ± 0.92	5.58 ± 1.46	0.20 ± 0.25	0.07 ± 0.07	38.39 ± 63.81	0.50 ± 0.61	0.35 ± 0.92	39.25 ± 64.14	0.002 ± 0.003
Median	11.60	0.00	0.00	5.60	0.00	0.05	18.09	0.36	0.09	18.60	0.001
IQR	8.05	0.58	0.10	1.53	0.38	0.09	8.18	0.74	0.14	8.42	0.001

3.5.4 Analysis of Combination Supplementation

3.5.4.1 Consuming GFN in combination with Alliin had no impact on the levels of SFN and SFN-NAC detected in the prostate

The Norfolk-ADaPt study was designed based upon the assumption that there is no reason to believe that consuming GFN or Alliin metabolites in combination with each other, would impact the accumulation of either metabolites in the urine or prostate. However, the use of the factorial design gives us the opportunity to test this assumption.

As was expected, there was no difference in the concentration of detected SFN or SFN-metabolites detected in the prostate of patients consuming GFN with placebo, compared with those consuming GFN in combination with Alliin (see table 3.4).
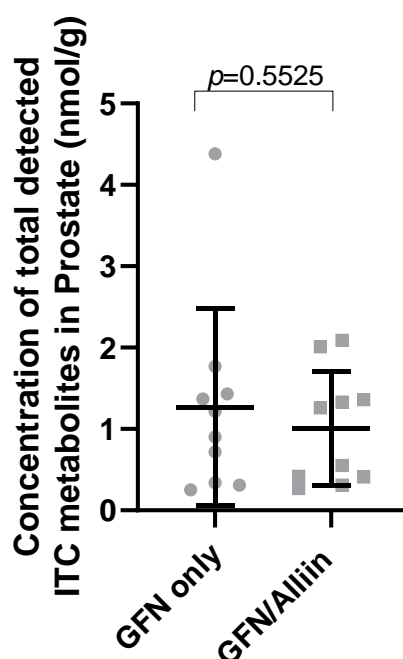
Figure 3. 38 Total concentration of detected ITC metabolites (SFN and SFN-NAC) in the prostate in patients consuming glucoraphanin with placebo (n=10) vs. glucoraphanin + Alliin (n=10). Results are shown as mean ± SD. Analysis using two-tailed unpaired T-test.
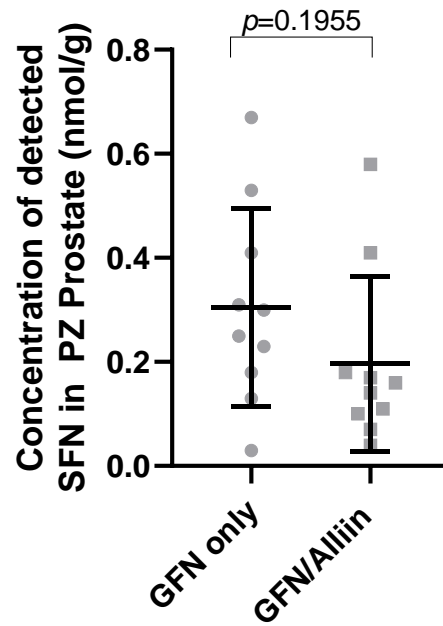
Figure 3. 39 Concentration of SFN detected in the peripheral zone of the prostate (n=10) in patients consuming glucoraphanin + placebo (n=10) vs. glucoraphanin + alliin (n=10) intervention. Results are shown as mean ± SD. Analysis using two-tailed unpaired T-test.
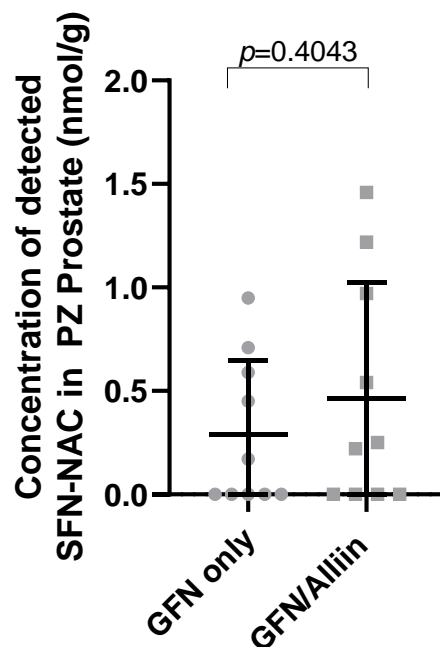
Figure 3. 40 Concentration of SFN-NAC detected in the peripheral zone of the prostate (n=10) in patients consuming glucoraphanin + placebo (n=10) vs. glucoraphanin + alliin intervention (n=10). Results are shown as mean ± SD. Analysis using two-tailed unpaired T-test.
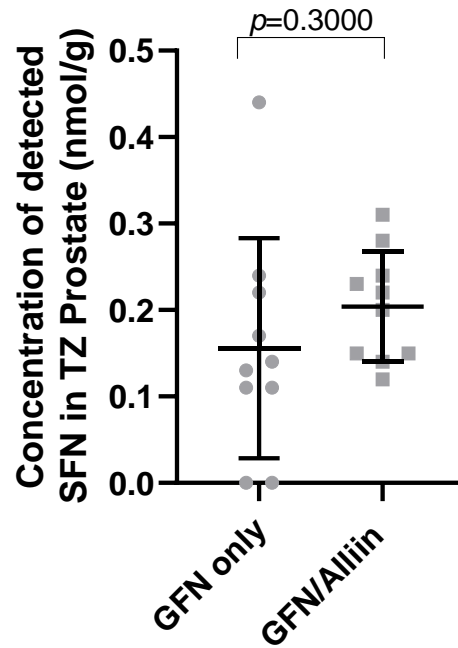
Figure 3. 41 Concentration of SFN detected in the transition zone of the prostate in patients consuming glucoraphanin + placebo (n=10) vs. glucoraphanin + alliin (n=10) intervention. Results are shown as mean ± SD. Analysis using two-tailed unpaired T-test.
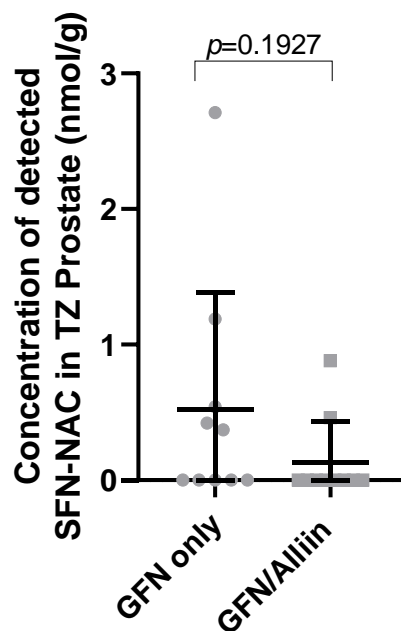
Figure 3. 42 Concentration of SFN-NAC detected in the transition zone of the prostate in patients consuming glucoraphanin + placebo (n=10) vs. glucoraphanin + alliin intervention (n=10). Results are shown as mean ± SD. Analysis using two-tailed unpaired T-test.

Table 3. 4 Summary table of the concentration of SFN and metabolites detected in the peripheral and transition zones of the prostate and the total prostate (nmol/g), of participants consuming a GFN with placebo intervention (n=10) vs. a GFN and Alliin combination intervention (n=10). Metabolites include Sulforaphane and N-acetyl-S-allyl-cysteine (NAC-SAC). Results are shown as mean ± standard deviation and median with IQR due to the variation in the normality of distribution of the data.

	GFN / Placebo Intervention						
	PZ (nmol/g)		TZ (nmol/g)		Total Prostate (nmol/g)		
	SFN	SFN-NAC	SFN	SFN-NAC	SFN	SFN-NAC	Total Metabolites
Mean	0.30 ± 0.19	0.29 ± 0.36	0.16 ± 0.13	0.52 ± 0.86	0.46 ± 0.28	0.81 ± 1.01	1.27 ± 1.21
Median	0.28	0.09	0.14	0.18	0.38	0.57	1.06
IQR	0.19	0.56	0.10	0.51	0.27	0.84	0.98
	GFN / Alliin Intervention						
	PZ (nmol/g)		TZ (nmol/g)		Total Prostate (nmol/g)		
	SFN	SFN-NAC	SFN	SFN-NAC	SFN	SFN-NAC	Total Metabolites
Mean	0.20 ± 0.17	0.47 ± 0.56	0.20 ± 0.06	0.13 ± 0.30	0.40 ± 0.19	0.60 ± 0.56	1.00 ± 0.70
Median	0.15	0.24	0.21	0.00	0.35	0.57	0.91
IQR	0.08	0.86	0.09	0.00	0.10	0.94	0.94

3.5.4.2 Consuming Alliin in combination with Glucoraphanin had no impact on the levels of Alliin metabolites detected in the prostate

As was demonstrated for SFN and metabolites, no difference was detected for the concentration of Alliin and Alliin metabolites detected in the prostate of patients consuming Alliin with placebo, compared with those consuming Alliin in combination with GFN (see table 3.5).
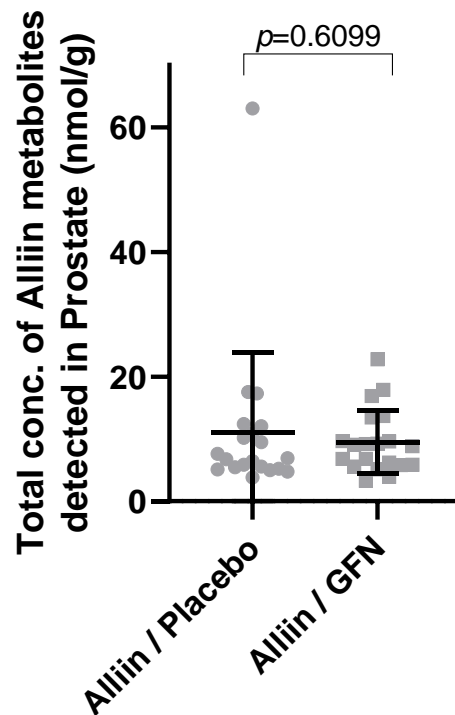
Figure 3. 43 Concentration of total Alliin metabolites detected in the prostate in patients consuming Alliin + placebo (n=10) vs. Alliin + glucoraphanin (n=10) intervention. Metabolites include Alliin, S-allyl-cysteine (SAC) and γ-glutamyl-S-ally-L-cysteine (γ-SAC). Results are shown as mean ± SD. Analysis using two-tailed unpaired T-test.
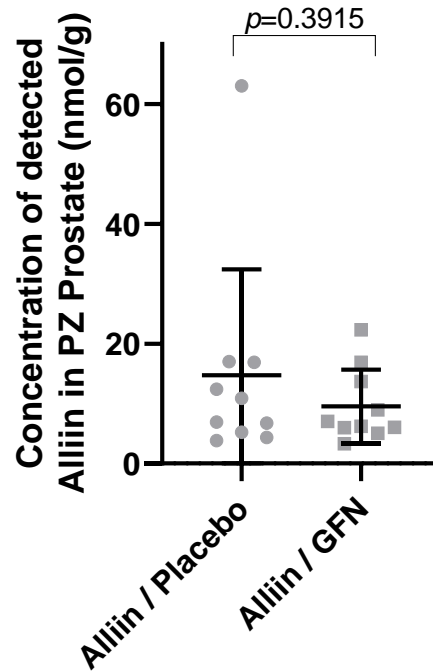
Figure 3. 44 Concentration of Alliin detected in the peripheral zone of the prostate in patients consuming Alliin + placebo (n=10) vs. Alliin + glucoraphanin (n=10) intervention. Results are shown as mean ± SD. Analysis using two-tailed unpaired T-test.
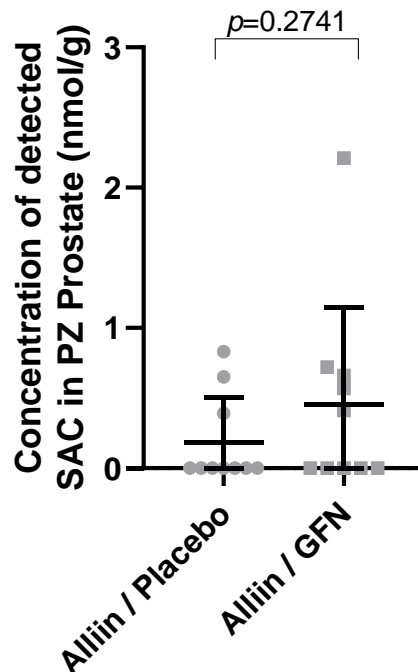
Figure 3. 45 Concentration of SAC detected in the peripheral zone of the prostate in patients consuming Alliin + placebo (n=10) vs. Alliin + glucoraphanin (n=10) intervention. Results are shown as mean ± SD. Analysis using two-tailed unpaired T-test.
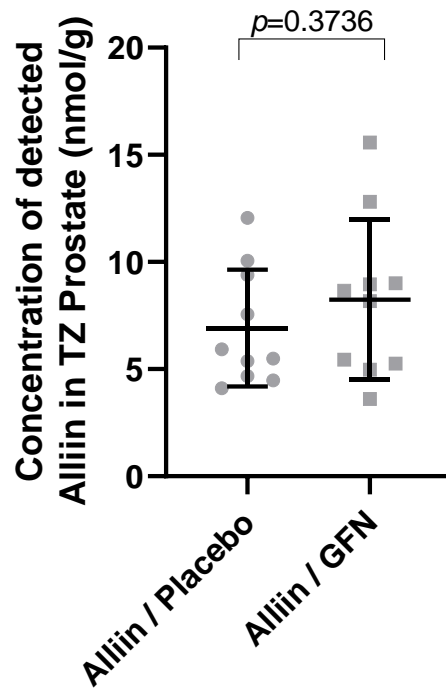
Figure 3. 46 Concentration of Alliin detected in the transition zone of the prostate in patients consuming Alliin + placebo (n=10) vs. Alliin + glucoraphanin (n=10) intervention. Results are shown as mean ± SD. Analysis using two-tailed unpaired T-test.
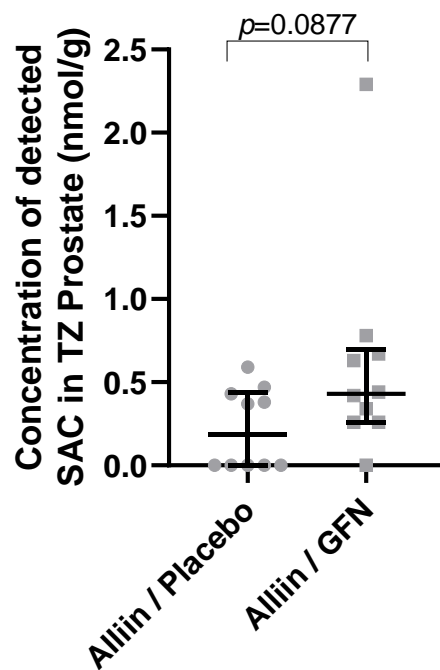
Figure 3. 47 Concentration of SAC detected in the transition zone of the prostate in patients consuming Alliin + placebo (n=10) vs. Alliin + glucoraphanin (n=10) intervention. Results are shown as median ± interquartile range. Analysis using Mann-Whitney.

Table 3. 5 Summary table of the concentration of Alliin and metabolites detected in the peripheral and transition zones of the prostate and the total prostate (nmol/g) of participants consuming an Alliin with placebo intervention (n=10) vs. an Alliin and GFN combination intervention (n=10). Metabolites include; Alliin, S-allyl-cysteine (SAC) and γ-glutamyl-S-ally-L-cysteine (γ-SAC). Results are shown as mean ± standard deviation and median with IQR due to the variation in the normality of distribution of the data.

	Alliin / Placebo Intervention									
	PZ (nmol/g)			TZ (nmol/g)			Total Prostate (nmol/g)			
	Alliin	SAC	γ-SAC	Alliin	SAC	γ-SAC	Alliin	SAC	γ-SAC	Total Metabolites
Mean	14.73	0.19	0.03	6.91	0.22	0.06	21.64	0.41	0.09	22.14
SD	± 17.66	± 0.32	± 0.09	± 2.73	± 0.24	± 0.04	± 17.88	± 0.53	± 0.08	± 17.68
Median	8.91	0.00	0.00	5.71	0.18	0.06	18.31	0.18	0.07	18.34
IQR	10.17	0.29	0.00	4.07	0.41	0.03	9.24	0.74	0.03	9.77
	Alliin / GFN Intervention									
	PZ (nmol/g)			TZ (nmol/g)			Total Prostate (nmol/g)			
	Alliin	SAC	γ-SAC	Alliin	SAC	γ-SAC	Alliin	SAC	γ-SAC	Total Metabolites
Mean	9.54	0.46	0.04	8.25	0.61	0.07	17.78	1.07	0.11	18.96
SD	± 6.11	± 0.69	± 0.05	± 3.72	± 0.63	± 0.06	± 7.50	± 1.28	± 0.07	± 7.74
Median	6.63	0.21	0.03	8.41	0.43	0.06	14.19	0.54	0.10	15.41
IQR	6.50	0.64	0.07	3.68	0.38	0.08	8.85	0.80	0.11	11.60

3.6 Discussion

Despite the wealth of information surrounding the behaviour of Glucoraphanin and Alliin metabolites in the urinary system, studies have yet to determine how the prostate may become exposed to these compounds.

For the first time, SFN and SFN metabolites were detected in human prostate to significantly higher levels in patients consuming a GFN-containing intervention (p=0.0023) compared to a placebo intervention. Given the high proportion of excreted urinary metabolites found in participants consuming a GFN-intervention in the Norfolk-ADaPt study, it is reasonable to expect that the prostate is exposed to these compounds from the urinary system, with particular reference to urinary reflux. However, there are two potential flaws in this hypothesis; Firstly, previous evidence suggests that the reflux of compounds from the urine into the prostate is more likely to occur in the PZ, given the angle of the ducts draining this zone (3). In this case, it would be expected therefore, that the concentration of metabolites detected in the prostate would be higher in the PZ compared to the TZ, a finding that was not demonstrated in this analysis. Secondly, as has previously been documented, not all SFN metabolites are excreted in the urine (141, 255, 269, 295), and hence the prostate may be exposed to these compounds via an alternative route. The pharmacokinetic behaviour of SFN in plasma is well documented, and it may be possible that the prostate is also exposed to these compounds via the systemic circulation (255, 295).

The findings of this study are in contrast to previous findings of the SAP study, in which participants consumed a GFN-rich brocoli soup for a period of at least 4 weeks prior to their prostate biopsy. The difference in findings is likely due to the dose of GFN consumed and the timings of the intervention; participants in the SAP study consumed one portion of the GFN-rich study soup three times *per week,* totaling 840 µmol of GFN (133). In the ADaPt study, the consumption of GFN in the form of Broccomax was 724.22 µmol per week. However, unlike the soup (in which myrosinase would have been denatured in the manufacturing process, and did not contain added myrosinase enzyme), Broccomax capsules contain activated myrosinase, which would enable a greater conversion of GFN to the active compound SFN, and removes the potential inter-individual variation of metabolism secondary to myrosinase-producing bacterial microflora present in the colon (313). In addition, Broccomax capsules were consumed daily, and all participants were instructed to consume their final capsules in the morning of the day prior to their biopsy procedure, a factor not considered in the SAP study.

More recently, Zhang *et al.* demonstrated that SFN metabolites were detected in the prostate of only 3 patients (out of 50) who were consuming BSE as part of a double-blinded intervention study (297). The small number of patients with detectable SFN therefore was not significant. In this study, participants consumed 2 myrosinase-treated BSE capsules at 12 hourly intervals, providing a total daily dose of 200 µmol SFN, for a period of 4-8 weeks (mean 4.4 weeks) prior to their prostate biopsy procedure. In comparison, in the ADaPt study, SFN and/or SFN metabolites were detected in all but 2 participants consuming a GFN-containing intervention (n=18). It is plausible that in the Zhang study, providing a lower dose of SFN at such short intervals, may not have been sufficient to enable prostatic accumulation, whereas giving the total dose once per day in the ADaPt study may have enabled effective cumulative exposure, and hence accumulation. Additionally, unlike in the ADaPt study, Zhang *et. al*. did not specify the the time of the final dose prior to the biopsy procedure.

The majority of literature surrounding the detection of Alliin metabolites in urine, blood and tissue, describe the use of highly sensitive methods such as GS-MS/MS (299). To our knowledge, this is the first time that Alliin metabolites have been detected in the prostate using the LC-MS/MS method. The concentration of detected Alliin metabolites in urine was very small, albeit detectable, and significantly higher in patients consuming an Alliin-containing intervention compared a non-Alliin containing intervention. This was driven by the urinary metabolite NAC-SAC, which is well documented to be a good urinary marker of garlic consumption (308). However, although these metabolites were detected in the prostate, the concentration of total Alliin metabolites in the TZ was the only statistically significant finding when comparing patients consuming an Alliin intervention to a non-Alliin containing intervention. This appears to be driven by the accumulation of SAC which in itself did not give a statistically significant result, and should therefore be treated with caution. This finding is nonetheless interesting; although urinary Alliin metabolites were significantly higher in the treatment group, the concentrations detected were very low (although this may simply demonstrate our inability to detect them using LCMS-MS). Given the significant accumulation in the TZ, and not in the PZ (when analysing treatment vs. control in each zone separately), this finding may represent a greater systemic distrubution of Alliin metabolites in the plasma rather than via the urine, for the reasons explained above. Plasma kinetics were not undertaken in the Norfolk-ADaPt study, but could be assessed in future studies to analyse this potential link.

The prostate has a complex and vast arterial network via the prostatic arteries which are mainly derived from the internal iliac arteries, with other branches arising from the middle rectal and pudendal arteries. The fact that up to 60% of men demonstrate considerable anatomoses between

prostatic pedicles and surrounding arteries, makes systemic exposure to the prostate a valid hypothesis (314). This is a potential area worthy of analysis.

Alliin was detected to some degree in every patient, irrespective of treatment. This is an interesting and unexpected finding, especially as some participants recorded consuming little to no alliacious vegetables. However, of those patients with no alliacious vegetable intake recorded, their cruciferous vegetable questionnaires revealed that they did consume products such as mustard. Although mustard is from the *brassicaceae* family, it's genus is 'alliaria', or 'resembling garlic', and it is therefore plausible that such related compounds may be contributing to this result, and may in fact explain the high concentrations of Alliin metabolites detected in 2 participants in the non-Alliin containing group

There is vast documentation which suggests that GSTM1- positive individuals gain more advantage from sulphur-containing dietary bioactive compounds. However, results from studies undertaken at the QIB differ; the significant differences in plasma and urine SFN metabolite concentrations between GSTM1 positive and null individuals has been demonstrated in the analysis of short cumulative times, with the greatest peaks seen in GSTM1 positive individuals up to 6-hours post GFN consumption (141). In contrast, a further study failed to demonstrate any significant difference in either plasma pharmacokinetic parameters, urinary excretion, or individual SFN metabolites in plasma or urine (295). The results of the ADaPt study are in keeping with these latter findings; no difference was demonstrated in the levels of urinary or prostatic metabolites when stratified by genotype. The reason for this finding may be two-fold; Firstly, the significant findings discussed above demonstrated a significant difference in the first 6-hours post ingestion, whereas the ADaPt study analysed total 24-hour urine collections (with no cumulative time point analysis). It may therefore be the case that although the metabolism of sulphur-containing compounds varies following ingestion in GSTM1- positive individuals, the overall excretion levels are unaffected, and the mechanism of it's physiological advantage is not in fact related to it's effect on the compounds' metabolism. This finding was also demonstrated for Alliin metabolites, although allium vegetables are also documented to demonstrate an ability to induce and upregulate GSTs in humans (315). It is also plausible however, that a substantial effect of GSTM1 genotype in the metabolism of GFN and Alliin was undetectable with the sample size used for this analysis.

3.7 Conclusion

This chapter, for the first time, demonstrates the ability of SFN metabolites to significantly accumulate within the prostate tissue of men consuming high dose GFN dietary supplementation. The significant prostatic accumulation of Alliin metabolites was demonstrated only in the single subgroup analysis of the TZ. Given the wealth of documentation reporting the significance of these dietary compounds in reducing the risk, or progression of PCa, this work significantly contributes to our understanding of a potential mechanistic explanation of this link. The following chapters will therefore explore whether the accumulation of these compounds leads to an attenuation of downstream functional biological pathways associated with PCa.

Chapter Four

Transcriptional Changes between the

Peripheral and Transition Zones of the Prostate

in Men Enrolled in the Norfolk-ADaPt Study

(Placebo Analysis)

4.1 Introduction

The peripheral zone (PZ) of the prostate is the site of 70-80% of prostate cancers (PCa) (2). Anatomically (other than its proximity to the urethra) and histologically, the PZ is difficult to distinguish from the other prostatic zones described by McNeal (2, 316) and hence the reason for this increased susceptibility remains unclear.

Not only is the PZ more likely to be the site of PCa, but PCas between the peripheral and transition zones tend to have very different characteristics, which suggest a fundamental difference in the tissue of origin (317). PCa in the TZ for example, tends to present later than PZ tumours, with a greater tumour volume and PSA (318). This is largely down to its position and hence difficulty in palpation on DRE or access during needle biopsy. Despite these factors, PCas in the TZ are known to be associated with lower Gleason scores, lower volumes of high-grade disease and lower rates of vascular, lymphatic and extracapsular invasion, thus resulting in better clinical outcomes, and higher levels of biochemical recurrence-free survival rates (318-321). In comparison to TZ tumours however, PZ tumour volume is (even after adjusting for Gleason score) an independent predictor of biochemical recurrence, metastasis and mortality (320, 322).

Irrespective of cancer site, increased tumour volumes tend to be associated with a more aggressive phenotype secondary to rapid proliferation rates and therefore an increased risk of mutation acquisition (323, 324). For this reason, tumour volumes are directly associated with a worse clinical outcome. The fact that the TZ does not display this same behaviour, having a lower proliferation index and maintaining a diploid DNA status even at larger tumour volumes compared to PZ tumours, suggests that the TZ is potentially less susceptible to the genomic alterations involved in the development and progression of PCa (325, 326). This theory is strengthened by the evidence that Gleason 4 patterns evolve clonally from those of Gleason 3 based on acquired mutations and genomic structural alterations (327). As a result, it may be that the TZ environment preferentially favours Gleason 3 disease which is rarely able to clonally evolve to Gleason 4 disease.

More recently, emerging evidence has described a variety of potential hypotheses to aid in elucidating the association between the PZ and its increased propensity for PCa.

4.1.1 The Transcriptional Differences between the Peripheral and Transition Zones of the Prostate Gland

Given the limited knowledge regarding the difference between the PZ and TZ of the prostate in terms of gene and protein expression, it is plausible that the higher incidence of PCa in the PZ is due to fundamental transcriptomic differences in these tissues (328). However, proteome analysis of the prostate has previously demonstrated that despite the difference in terms of incidence of cancer and hyperplasia, both the PZ and TZ have epithelium with very similar major protein expression profiles (329). Additionally, immuno-histochemical analysis has paradoxically shown that both zones appear to have a similar proliferative index and incidence of apoptosis (330). Given these findings that epithelial cells of both the PZ and TZ may be equally susceptible to the *initial* events of hyperplasia, it may be postulated that other events are responsible for the increased incidence of PCa development and progression within the PZ, such as hormonally-driven growth promotion or epigenetic silencing of protective genes.

Differential gene expression profiling of prostate tissue has previously demonstrated significant intra-individual gene expression patterns between the PZ and TZ. Noel *et. al.* has previously described 43 out of 24,325 genes which are differentially expressed between the PZ and TZ, and reported a higher expression of genes associated with cell adhesion, signal transduction and neurogenesis in the PZ, which may confer a survival benefit of tumour cells in this zone (331). Additionally, another large-scale study (utilising microarray analysis) demonstrated that 346 of 15,000 investigated genes were differentially expressed between the PZ and TZ; 5 of which overlap with the results of Noel *et. al* (332). In both cases, RNA was extracted from radical prostatectomy or cystoprostatectomy specimens.

More recently, whole-genome RNA sequencing and high-throughput metabolic profiling of non-cancerous tissue from the PZ and TZ of patients undergoing total prostatectomy has demonstrated that the transcription of genes involved in lipid biosynthesis and fatty acid catabolic activity, is higher in the PZ (333). It may be postulated that these well-known metabolic alterations in PCa are indeed upregulated to a greater degree in the PZ, and hence provide a more accommodating environment for cancer growth within this zone.

Differences in the expression of genes related to hormone metabolism have also been described as a potential explanation for the risk of PCa in the different prostatic zones. Specifically, histopathological and real-time PCR studies have shown that the genes CYP1B1 and CYP19 (pathways related to oestrogen metabolism) appear to be expressed to a greater degree in the PZ of the prostate (334-336). This may provide an insight into the role for oestrogen-related metabolites produced by these pathways in the development of PCa.

This chapter aims to assess the differences between the transcriptional profiles of the PZ compared to the TZ. Unlike previous evidence which has analysed the transcriptional signature of prostate tissue following prostatectomy in patients with PCa requiring radical treatment, this chapter seeks to analyse the transcriptional differences from biopsy samples of patients with either a low-risk PCa on 'active surveillance' or under investigation for a potential PCa. In this way, it is hypothesised that any differences detected between the PZ and TZ are more likely to explain early transcriptional changes which may occur in the prostate microenvironment in the development of PCa.

4.2 Aims

- To characterise the transcriptional signatures of the peripheral and transition zones from prostate biopsies of patients consuming a placebo intervention in the 'Norfolk-ADaPt' trial.

4.3 Materials and Methods

The methods below describe the processes used for all samples, including the control samples (patients consuming a placebo intervention) and the samples from patients consuming the GFN or Alliin supplements (described in chapter five), as this initial analysis was standardised for all samples.

4.3.1 Sample Processing

As previously described in Chapter 2, ethical approval for the use of urine and prostate from the 'Norfolk-ADaPt' study volunteers was granted by the East of England – Cambridge East REC in June 2019. Written informed consent was obtained for study participation and tissue banking consent at the Norwich Biorepository.

On the biopsy day, four prostate biopsy cores (two from each of the PZ and TZ) were placed directly into RNAlater^{TM} solution and stored at 5 ^{o}c for 24 hours. After 24 hours, samples were removed from

the RNAlater™ solution, transferred into new labelled cryovials and stored at -80 °c until required for analysis.

4.3.2 RNA Extraction and Quality Control

RNA from biopsy cores was extracted using the Qiagen TissueRuptor and Qiagen RNeasy Mini kit with on-column Qiagen DNase I treatment. RNA was extracted from one biopsy core from the PZ and one from the TZ for each patient.

All glass slides and TissueRuptor probes were autoclaved, and sterile scalpels were used. Cores were removed from -80 °C, dabbed on tissue paper to remove excess RNAlater™, placed on a glass slide and cut into smaller pieces using a scalpel. In between samples, RNAzap™ was used to clean the scalpel and slide. Tissues were then weighed in a 2mL eppendorf tube and 600 µl buffer RLT (with β-Mercaptoethanol) (Qiagen Inc.) was added. TissueRuptor was used to homogenise each sample for 20 secs at a speed of 6-7. Samples were centrifuged, and RNA extracted according to the RNeasy manufacture's protocol. RNA was eluted in 30 µl H_2O. 1 µl of each RNA extraction was analysed on the nanodrop™ spectrophotometer (ThermoFisher) to ascertain the RNA yield and 260/280 ratio.

4.3.3 RNA Sequencing and Processing

Prostate tissue cores of between 4.2 and 10.26 mg from each patient were homogenized with a Qiagen TissueRuptor before total RNA was extracted with the Qiagen RNeasy Mini kit as described above.

Samples were sent to Macrogen Europe, where they were first ribodepleted with the Ribo-Zero Magnetic Gold rRNA Removal Kit (Illumina) before constructing Illumina barcoded TruSeq RNA libraries. Sequencing of 84 samples (39 patients' x 2 zones, plus 6 RNeasy microbial controls for future analysis) was performed on an Illumina NovaSeq600 to generate 151-bp paired-end reads, with at least 40 million reads per sample.

The RNA-sequencing data analysis was performed by the QIB bioinformatician Dr Perla Troncoso Rey. The analysis was divided into two steps: processing the raw RNA-sequencing data to estimate genes counts and then the comparative analysis of the transcriptomics data. Data processing was performed following the protocol for the *"new Tuxedo"* suite for short reads (337) using the HPC

environment managed by *the Norwich Bioscience Institute's Computing Infrastructure for Science* (NBI's CiS) (338). The new Tuxedo suit includes computational tools for the alignment of RNA-seq reads to a reference genome, the assembly of transcripts, quantification of gene and transcript expression and differential expression analysis.

The first part of the analysis started with the processing of raw RNA-seq data to remove Illumina adapter sequences, low-quality and short reads using *Trim Galore!* v.0.6.5 (339) (340). Adaptor sequences were removed with an overlap of minimum 5 bases (*--stringency 5*). Due to the imperfect nature of the sequencing process and limitations of the optical instruments, base calling will always have inherent uncertainty. For this reason, FASTQ files store the DNA sequence of each read together with a position-specific quality score (the 'Phred33' score) that represents the error probability, i.e., how likely it is that an individual base call may be incorrect. For this analysis the quality control (based on the 'Phred33' score) removed reads with a quality of less than 30 (-q 30) and reads shorter than 60 bp (-length 60).

The alignment of high-quality reads was performed with *HISAT2* v.2.1.0 (341) to the ensembl's human reference genome GRCh38, release 97 (July 2019) (342). *HISAT2* is an ultrafast splice-aware aligner based on the principles of some of the most widely used aligners; the Burrows-Wheeler aligner (BWA) and Bowtie (343), which uses the Burrow-Wheeler transform to store the reference genome in a highly compressed form. Using the Ferragina-Manzini, FM, indexing, Bowtie and BWA can search a genome very rapidly.

The alignments were then assembled into full-length transcripts and quantified in each sample using *StringTie* v.1.2.2 (337). *StringTie* creates as many isoforms as needed to explain the data, and estimates the expression levels of all known genes and transcripts. After the initial assembly, the assembled transcripts were merged together to create a uniform set of transcripts for all samples. The merged transcripts were then compared to the reference human annotation and statistics on this comparison were calculated using *gffcompare* v.0.9.8 (344). Finally, the read alignments and the merged transcripts were used to re-estimate abundances (where necessary) and create transcript and gene counts for further analyses.

The complete bioinformatics pipeline, differential gene expression (DGE) analyses, and statistical analysis follow the QIB's GitHub repository for RNA-seq analysis in the following link: https://github.com/quadram-institute-bioscience/ADAPT-RNA-seq-Analysis.

The table below shows the processing of RNAseq data, including the % reads with adaptors, reads passing quality control, and overall alignment for each prostate sample (n=78) analysed.

Table 4. 1 Processing Raw Data Statistics

Sample	Number of Reads	Reads with adapter	% Reads with adapter	Pass QC	% Pass QC	Uniquely Aligned	% Uniquely Aligned	Multimapped	% Multimapped	Overall Alignment
1P	41,869,227	7,468,727	17.80	41,226,895	98.47	36,804,144	89.27%	1,753,335	4.25%	97.54%
1T	49,219,673	9,589,371	19.50	48,493,418	98.52	43,481,455	89.66%	2,041,219	4.21%	97.66%
2P	49,111,268	10,105,098	20.60	48,503,060	98.76	43,654,974	90.00%	1,955,848	4.03%	97.93%
2T	49,279,372	9,432,661	19.10	48,527,797	98.47	43,049,336	88.71%	2,659,118	5.48%	97.59%
3P	41,742,264	8,774,699	21.00	41,186,326	98.67	37,317,293	90.61%	1,476,698	3.59%	97.77%
3T	49,515,461	10,253,074	20.70	48,763,321	98.48	43,852,470	89.93%	1,994,497	4.09%	97.57%
4P	41,275,366	7,663,556	18.60	40,607,729	98.38	36,415,488	89.68%	1,533,749	3.78%	97.54%
4T	49,301,134	10,660,872	21.60	48,660,950	98.70	43,973,052	90.37%	2,200,464	4.52%	97.87%
5P	49,414,761	8,498,307	17.20	48,775,152	98.71	44,408,019	91.05%	2,000,465	4.10%	97.99%
5T	40,936,230	8,541,922	20.90	40,349,854	98.57	36,085,348	89.43%	1,747,880	4.33%	97.65%
6P	49,600,350	9,099,402	18.30	48,891,417	98.57	44,355,115	90.72%	1,844,195	3.77%	97.83%
6T	43,472,252	8,057,570	18.50	42,912,616	98.71	38,752,249	90.31%	1,588,549	3.70%	97.70%
7P	41,380,141	8,231,308	19.90	40,824,393	98.66	36,980,122	90.58%	1,430,088	3.50%	97.79%
7T	42,278,473	9,913,553	23.40	41,729,381	98.70	37,371,836	89.56%	1,876,385	4.50%	97.61%
8P	49,501,218	10,951,887	22.10	48,804,832	98.59	43,616,072	89.37%	1,808,207	3.70%	97.45%
8T	49,342,484	9,520,661	19.30	48,705,489	98.71	44,213,027	90.78%	1,964,912	4.03%	97.92%
9P	49,331,958	8,932,760	18.10	48,663,291	98.64	43,880,972	90.17%	2,091,650	4.30%	97.92%
9T	42,220,757	8,621,611	20.40	41,737,842	98.86	37,657,473	90.22%	1,835,397	4.40%	98.03%
10P	41,644,342	10,080,085	24.20	41,100,288	98.69	37,026,062	90.09%	1,592,992	3.88%	97.66%
10T	42,989,195	8,083,308	18.80	42,464,002	98.78	38,390,277	90.41%	1,644,338	3.87%	97.81%
11P	43,964,626	11,394,700	25.90	43,408,045	98.73	38,892,347	89.60%	2,223,923	5.12%	98.05%
11T	49,321,196	9,289,959	18.80	48,742,729	98.83	44,553,895	91.41%	1,759,537	3.61%	97.99%
12P	42,176,216	9,229,886	21.90	41,573,568	98.60	37,053,281	89.13%	2,217,716	5.33%	97.66%
12T	41,508,406	8,083,206	19.50	40,956,799	98.67	37,386,900	91.28%	1,456,102	3.56%	97.96%
13P	42,149,352	7,413,382	17.60	41,566,527	98.62	37,588,883	90.43%	1,403,153	3.38%	97.66%
13T	49,467,325	8,736,590	17.70	48,707,367	98.46	43,712,784	89.75%	1,645,388	3.38%	97.54%
14P	49,344,524	8,822,605	17.90	48,597,845	98.49	43,365,478	89.23%	1,769,139	3.64%	97.51%
14T	41,804,791	6,874,501	16.40	41,234,969	98.64	37,491,644	90.92%	1,259,906	3.06%	97.74%
15P	49,536,877	9,244,210	18.70	48,948,562	98.81	44,279,164	90.46%	2,170,005	4.43%	98.09%
15T	49,611,599	9,508,635	19.20	48,988,729	98.74	44,581,889	91.00%	1,743,803	3.56%	97.86%
16P	49,356,043	9,119,267	18.50	48,705,522	98.68	44,101,617	90.55%	1,912,100	3.93%	97.89%
16T	49,149,367	9,760,865	19.90	48,506,466	98.69	44,324,005	91.38%	1,583,012	3.26%	97.90%
17P	49,516,267	8,738,014	17.60	48,833,618	98.62	44,240,910	90.60%	1,900,166	3.89%	97.92%
17T	49,519,204	9,368,731	18.90	48,880,873	98.71	44,447,835	90.93%	1,778,934	3.64%	97.88%
18P	49,416,508	9,765,511	19.80	48,859,819	98.87	44,317,448	90.70%	1,745,320	3.57%	97.69%
18T	42,420,057	8,150,986	19.20	41,763,337	98.45	37,700,615	90.27%	1,558,270	3.73%	97.71%
19P	49,198,192	8,280,659	16.80	48,562,109	98.71	44,021,830	90.65%	1,859,339	3.83%	97.86%
19T	41,662,395	8,316,453	20.00	41,210,169	98.91	37,398,155	90.75%	1,656,038	4.02%	97.93%
20P	49,650,309	8,900,082	17.90	48,924,219	98.54	43,514,468	88.94%	2,337,089	4.78%	97.67%
20T	49,310,985	10,117,420	20.50	48,506,446	98.37	43,007,227	88.66%	2,030,589	4.19%	97.33%
21P	49,655,447	9,302,560	18.70	49,011,819	98.70	44,093,625	89.97%	2,087,597	4.26%	97.94%
21T	42,178,526	7,921,766	18.80	41,587,732	98.60	37,030,970	89.04%	1,600,813	3.85%	97.53%
22P	41,100,603	7,883,203	19.20	40,531,674	98.62	36,601,367	90.30%	1,604,159	3.96%	97.63%
22T	41,400,534	7,838,733	18.90	40,810,795	98.58	36,666,986	89.85%	1,467,619	3.60%	97.56%
23P	49,480,024	9,063,021	18.30	48,860,422	98.75	44,382,596	90.84%	1,922,258	3.93%	97.96%
23T	49,193,033	9,280,848	18.90	48,544,447	98.68	43,971,494	90.58%	1,662,439	3.42%	97.85%
24P	49,524,634	9,735,796	19.70	48,901,901	98.74	44,085,181	90.15%	2,189,283	4.48%	97.93%
24T	49,482,945	10,396,605	21.00	48,809,012	98.64	44,414,919	91.00%	1,607,206	3.29%	97.75%
25P	49,579,842	11,261,522	22.70	48,897,920	98.62	43,622,054	89.21%	2,484,262	5.08%	97.74%
25T	49,355,082	10,015,449	20.30	48,675,838	98.62	43,921,820	90.23%	1,996,862	4.10%	97.47%
26P	41,852,101	8,838,485	21.10	41,231,274	98.52	36,889,706	89.47%	1,664,626	4.04%	97.63%
26T	49,373,914	10,672,154	21.60	48,752,147	98.74	43,991,114	90.23%	2,235,185	4.58%	97.84%
27P	43,361,211	11,583,479	26.70	42,718,524	98.52	37,841,848	88.58%	2,460,283	5.76%	97.63%
27T	41,272,675	7,153,619	17.30	40,674,955	98.55	36,746,841	90.34%	1,549,797	3.81%	97.76%
28P	49,419,374	9,863,290	20.00	48,667,144	98.48	43,471,637	89.32%	2,338,542	4.81%	97.80%
28T	49,393,852	9,071,149	18.40	48,678,634	98.55	44,125,620	90.65%	1,640,290	3.37%	97.75%
29P	49,303,061	8,509,756	17.30	48,593,522	98.56	44,062,511	90.68%	1,802,443	3.71%	97.81%
29T	49,409,310	9,779,669	19.80	48,694,532	98.55	43,854,865	90.06%	2,055,716	4.22%	97.80%
30P	49,521,042	8,940,526	18.10	48,873,904	98.69	44,351,829	90.75%	2,277,014	4.66%	98.19%
30T	49,228,096	10,303,499	20.90	48,573,804	98.67	43,730,837	90.03%	2,246,013	4.62%	98.03%
31P	49,141,742	9,671,187	19.70	48,431,889	98.56	43,581,000	89.98%	1,928,890	3.98%	97.73%
31T	41,510,881	7,926,382	19.10	40,840,198	98.38	36,134,144	88.48%	1,807,417	4.43%	97.40%
32P	49,319,400	9,198,709	18.70	48,584,092	98.51	43,386,418	89.30%	2,291,700	4.72%	97.65%
32T	41,187,746	8,689,135	21.10	40,600,382	98.57	36,127,731	88.98%	1,940,725	4.78%	97.70%
34P	49,484,532	9,347,246	18.90	48,740,757	98.50	43,798,911	89.86%	1,787,448	3.67%	97.55%
34T	49,407,413	10,572,338	21.40	48,646,471	98.46	43,753,593	89.94%	2,050,409	4.21%	97.57%
35P	41,512,069	7,583,290	18.30	40,857,942	98.42	36,426,505	89.15%	1,575,267	3.86%	97.59%
35T	49,601,858	9,548,134	19.20	48,813,559	98.41	43,854,512	89.84%	1,877,699	3.85%	97.62%
36P	42,060,186	7,925,812	18.80	41,504,762	98.68	37,984,543	91.52%	1,504,575	3.63%	97.96%
36T	49,659,252	10,521,081	21.20	48,980,748	98.63	44,250,582	90.34%	1,920,762	3.92%	97.71%
37P	41,617,794	6,909,071	16.60	40,999,214	98.51	37,105,313	90.50%	1,381,599	3.37%	97.50%
37T	42,448,044	6,805,724	16.00	41,802,555	98.48	37,696,694	90.18%	1,469,569	3.52%	97.60%
38P	49,121,289	10,810,720	22.00	48,323,041	98.37	43,472,257	89.96%	1,694,646	3.51%	97.43%
38T	41,038,393	7,478,100	18.20	40,401,301	98.45	36,199,988	89.60%	1,616,773	4.00%	97.68%
39P	49,135,787	9,457,125	19.20	48,319,698	98.34	42,192,659	87.32%	1,999,661	4.14%	97.05%
39T	42,413,975	8,542,046	20.10	41,874,771	98.73	38,099,965	90.99%	1,662,116	3.97%	97.93%
40P	49,382,379	8,306,257	16.80	48,843,003	98.91	45,151,473	92.44%	1,302,627	2.67%	98.22%
40T	42,281,474	8,096,598	19.10	41,760,881	98.77	37,962,474	90.90%	1,281,200	3.07%	97.95%

[1]The table shows the statistics for the first two steps of the processing of the raw RNA-sequencing data: quality control and alignment. Quality control of the data started by scanning the sequencing data to find and remove adapter sequences from the raw reads (column "Reads with adapter"), then removed low quality bases (<30) and reads that are too short (<60bp). The total number of reads with high-quality and its percentage from the total number of raw reads are shown in the columns Pass QC and % Pass QC respectively. The high-quality reads were then aligned to the reference genome. The number of reads that are mapped to only one location in the reference genome are shown in the column "Uniquely aligned". Some reads were aligned to more than one location and those are specified in the "Multimapped" column. The column "Overall Alignment" corresponds to the percentage of all reads with a valid alignment, which considers unique alignments, multimapped alignments and discordantly alignments (where both mates align uniquely but does not satisfy the paired-end constraint).

4.3.4 Comparative Analysis of Transcriptomics Data

4.3.4.1 Pre-Filtering

The statistical analysis of the gene expression data was performed with R studio and the differential expression analysis was undertaken using DESeq2 v.1.24.0 (345).

The gene expression data contains 60,617 transcripts, which includes all genes in the assembly, including protein coding genes, non-coding genes and pseudo-genes.

The analysis begun by removing low expressed genes. Although pre-filtering gene counts is not necessary before running analysis in DESeq2, pre-filtering was undertaken for multiple reasons; to remove low counts which may influence results, to reduce the memory size of the data, and to increase the speed of the transformation and testing functions within DESeq2 itself. For analysis of the control (placebo intervention) samples, a minimal pre-filtering was applied to remove lowly-expressed genes, keeping only genes with at least 10 counts per sample, for at least 9 samples in total (i.e. the size of each comparison group). The genes remaining after the removal of the lowly-expressed are used in all the following analyses.

4.3.4.2 Exploratory Analysis of Gene Expression Profiles

One initial method used to visualise similarities and differences between samples is the principal component analysis (PCA). Using this transformation method, the data points (a samples' expression profile) are commonly projected onto only the first few components to allow for easier visualisation while preserving as much as the data's variation as possible. PCA plots show similarities and differences between samples in an unsupervised manner. Because PCA is particularly useful for high dimensional data, typically the genes with higher variance (after pre-filtering) are included (n=500). The data is reduced in dimensions and principal components (PCs) are formed which are plotted. The PCs account for the varied influences of the original characteristics.

Methods for exploratory analysis of multi-dimensional data (such as clustering and principal component analysis ((PCA)), work best for homoscedastic data, where the variance of an observable quantity (i.e., the expression strength of a gene) does not depend on the mean. Because variance grows with the mean with RNA-sequenced data, DESeq2 provides two transformations to produce more homoscedastic data: the variance stabilising transformation (VST) and the rlog. VST attempts to create data that is more approximately normally distributed than the original data (or at least has more constant variance), so that a variable value is not related to the mean value. VST is recommended for medium to large datasets, as it is much faster to compute and is less sensitive to high count outliers than the rlog. These transformations are functions of DESeq2 which are provided for application and visualisation of the data only, but are not used for differential testing (which uses the raw untransformed counts).

To visually explore the similarity of transcriptional profiles between samples, heatmaps and hierarchical clustering in the form of dendrograms were used. This was undertaken using the R library *pheatmap* (version 1.0.12) on the count matrix. Heatmaps of the sample-to-sample distances are plotted using dendrograms to give an overview over similarities and dissimilarities between samples, showing how the samples are clustered into groups. Initially, all samples are in a separate cluster, and at each step a hierarchical algorithm is applied, which informs us of similarity or dissimilarity (distance or height) of the samples. At each of these steps, the two clusters that are most similar are joined into a single cluster, and once fused the samples are not separated. The height of the dendrogram (or vertical axis) indicates the order in which clusters were joined. The vertical position of the split, shown by the short horizontal bar, demonstrates the distance (or dissimilarity) between two clusters.

4.3.4.3 Differential Expression Analysis

DESeq2 takes the unnormalized gene expression data as input, where each entry indicates the number of sequencing reads that have been mapped to a gene in a sample. For each gene, DESeq2 fits a generalised linear model, GLM, as follows (345).

The read counts K_{ij} are modelled as a negative binomial distribution with a mean μ_{ij} and a dispersion α_i. The mean is taken as a quantity q_{ij} proportional to the concentration of cDNA fragments from the gene in the sample, scaled by a normalisation factor s_{ij}, such that: $\mu_{ij} = s_{ij} q_{ij}$.

The differential expression analysis workflow with DESeq2 comprises three main steps: estimation of size factors, estimation of dispersion and negative binomial GLM fitting and Wald statistics. The analysis is performed using the function *DESeq* with no replacement of outliers (*minReplicatesForReplace = Inf)* that automatically runs all the steps. A description of the functions called internally by *DESeq* in each of these steps are described next:

4.3.4.3.1 Estimation of size factors (using function *estimateSizeFactors*)

DESeq2's function *estimateSizeFactors* uses the median ratios method to estimate a normalisation factor for each sample, or *size factors*. These normalisation factors are the median ratio of the samples over a "pseudo-sample", where for each gene, is the geometric mean of all samples. Estimating size factors is performed as follows:

1) Calculate a pseudo-reference sample geometric mean for each gene, that is equal to the geometric mean across all samples

2) Calculate the ratio of each sample to the reference: for every gene in a sample, the ratios sample/reference are calculated. This is performed for each sample in the dataset.

3) Calculate the *size factor*, which is the median value of all ratios for a given sample for that sample.

4) Calculate the normalised count values using the normalisation factor: this is performed dividing each raw count value in a given sample by that sample's normalisation factor.

4.3.4.3.2 Estimation of dispersion (using function *estimateDispersions*)

It is important to identify genes that have significantly different mean expression between groups, taking into account the variation between replicates (within groups) and considering that the

variation within a group will increase with the mean expression. For these reasons, DESeq2 uses a measure of variation called dispersion, instead of using variance to identify Differentially Expressed genes, which accounts for the variance and expression level of a gene. Thus, the dispersion estimates the variance in gene expression for a given mean value. After estimating the dispersion, DESeq2 fits a curve to the gene-wise dispersion estimates. This curve provides an estimate for the expected dispersion value for genes with similar expression but does not represent deviations of individual genes from this overall trend (345).

4.3.4.3.3 Shrinkage method

DESeq2 uses a method to shrink the gene-wise dispersion estimates toward the expected dispersion values to reduce false positives in the analysis. Genes with low and slightly high dispersion estimates are shrunken towards the curve (estimate of the expected dispersion value for genes of a given mean expression). These shrunken and more accurate values are used for fitting the model and differential expression testing. However, genes with extremely high dispersion values are not shrunken. This is due to the probability that the gene does not follow the modelling assumptions and has higher variability than others for biological or technical reasons.

For shrinkage estimation, the Approximate Posterior Estimation for GLM method, APEGLM, was used (346).

4.3.4.3.4 Negative binomial GLM fitting and Wald statistics (nbinomWaldTest)

The final step in the DESeq2 workflow is to fit the Negative Binomial model for each gene and perform differential expression testing. DESeq2 uses the following formula as the model for each gene as shown in eq. 1:

$$K_{ij} \sim NB(s_{ij}q_{ij}, \alpha_i)$$

where:

K_{ij} represents the counts for gene i in sample j

$s_{ij}\,q_{ij}$ this is the fitted mean distribution: normalised counts (q_{ij}) scaled by a normalisation factor (s_{ij})

α_i gene-specific dispersion parameter

For hypothesis testing, the null hypothesis for each gene is that there is no differential expression across groups: *LFC = 0*. DESeq2 uses the Wald test, a hypothesis test, where the estimated standard error of a log2 fold change is used to test if it is equal to zero. DESeq2 uses the Wald test as follows: takes the LFC and divides it by its standard error, resulting in a z-statistic; the z-statistic is compared to a standard normal distribution, and a p-value is computed reporting the probability that the z-statistic could be observed at random; and if the p-value is small we reject the null hypothesis as there is evidence against that the gene is indeed differentially expressed.

DESeq2 uses an Independent Filtering function which helps to reduce the number of genes tested by removing genes unlikely to be significantly differentially expressed prior to testing, such as those with low number of counts and outliers. A significance cutoff of 0.1 was used to optimise the independent filtering. Independent filtering uses a low mean threshold that is empirically determined from the data. Using this threshold, significantly differentially expressed genes can be increased by reducing the number of genes tested.

The p values from the Wald Test are corrected for multiple testing using the False Discovery Rate (FDR) method based on the Benjamini-Hochberg (BH) algorithm.

Initially, extracted differentially expressed genes were used to produce Mean Average (MA) plots (an application of a Bland-Attman plot). MA plots are 2-D scatter plots used for the visualisation of genomic data and provide a useful overview for a two-group comparison. They allow the visualisation and identification of gene expression changes from two groups in terms of log fold change (M – on Y-axis) and the log of the mean of normalised expression counts over all samples (A – on X-axis). By producing MA plots, we can visualise the degree of differentially expressed genes and in which direction; genes with similar expression in both groups will cluster around M=0 value (i.e. no significant difference in expression), whereas points away from M=0 line indicate significantly differentially expressed genes (upregulated or downregulated if above or below the line respectively).

Volcano plots were subsequently formed using R library *EnhancedVolcano* version 1.8.0. Volcano plots are a useful visualisation tool to display the results of a differential expression analysis which allows for a visual identification of genes with large fold changes that are also statistically significant. The volcano plot shows the statistical significance, P value, versus the change represented by the fold change.

4.3.4.4 Functional analysis

Functional analyses of paired differential gene expression (DGE) was undertaken using the gene set enrichment analysis (GSEA) software (22) using the Hallmark gene sets (50 gene sets in total) within the available Molecular Signatures Database (MSigDB,version6.1). This Hallmark gene set was chosen as it summarises and represents specific well-defined biological states in cancer. DGE lists for all genes were ranked according to their P value, modified using the rank–rank hypergeometric overlap (RRHO) algorithm (347). All genes were inputted into the GSEA tool to look at groups of genes which are changing in the same direction, even when modest. Ranking of the genes were calculated as the log10-transformed P value, multiplied by the sign of the log fold change. The sign of the log fold change, represented the direction of the change: positive for upregulated over time, and negative for downregulated over time. By using the RRHO method we explored the functional consequences of the paired changes in gene expression without being constrained by a given statistical threshold. The ranked DGE list was then submitted to GSEA and statistical significance of enriched pathways was set at an FDR-adjusted P value <0.05. Normalized enrichment scores for each individual pathway and their associated FDRadjusted P value for each intervention was reported.

4.4 Results

To explore whether there is a difference between the transcription of genes in the PZ and TZ as suggested in recent studies, the samples from the control group (placebo intervention) were analysed. A total of 18 paired control samples (9 from the PZ and 9 from the TZ) collected from nine patients were analysed. These patients consumed 2 placebo capsules once per day for >28 days prior to their biopsy procedure. This intervention will be described as the "placebo-intervention" throughout.

4.4.1 Assessing the Transcriptional Similarity of the Prostate Zones

As discussed above, pre-filtering of gene counts was undertaken. As demonstrated in table 4.2, the gene expression data for the control samples contained 60617 transcripts (i.e. all genes in the assembly, including protein coding genes, non-coding genes etc.). Pre-filtering as described above removed 35,149 lowly expressed genes, leaving 25,468 genes for analysis.

Table 4. 2 Filtering lowly expressed transcripts

Zone	Number of Transcripts	Low Expressed Transcripts	Expressed Transcripts
PZ and TZ Control Samples	60,617	35,149	25,468

expressed genes refers to the number of genes that were used for the analysis.

Principle component analysis (PCA) was undertaken using the VST transformed data. As described above, this method demonstrates similarities and differences between samples in an unsupervised manner. Because PCA is particularly useful for high dimensional data, the top 500 transcripts were included, selected by the higher variance across samples. Figure 4.1 shows the PCA of the placebo intervention samples from both the PZ and TZ. Ellipses were added to the plots for visualisation purposes only and are not part of the DESeq2 analysis.
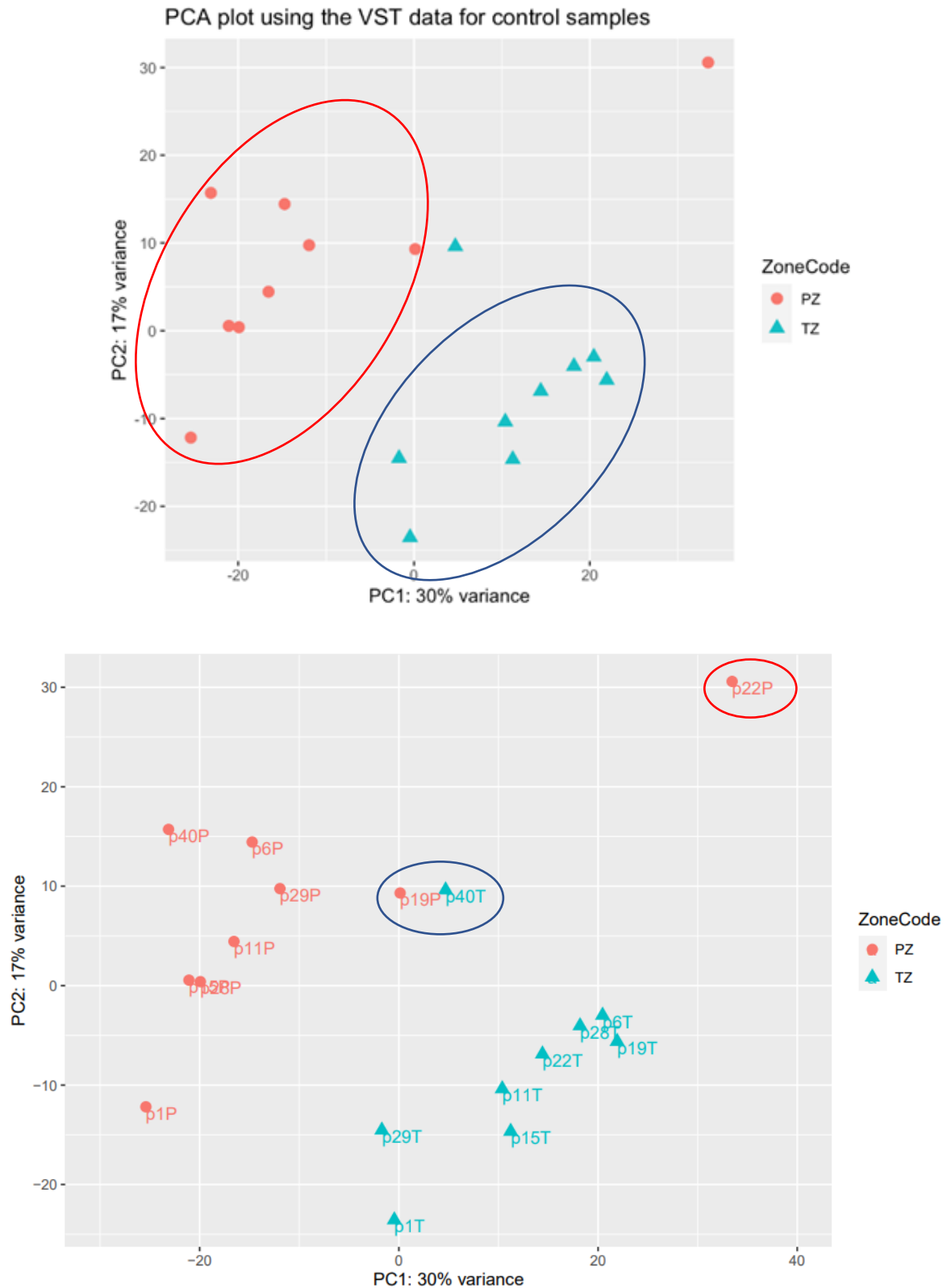
Figure 4. 1 A) PCA plot of peripheral zone (PZ – shown in red) and transition zone (TZ – shown in blue) placebo intervention samples (n=18 paired samples from 9 patients). The PCA plot is formed using the top 500 transcripts selected by the highest variance across samples. Clear separation is demonstrated and highlighted between the two zones. B) Same PCA plot demonstrating two transcriptionally similar samples from differing

prostate zones (19P and 40T, highlighted in the blue circle), and one outlier samples (labelled 22p and highlighted in red circle). Blue and red ellipses are manually added following analysis for visual purposes only and are not an internal function of the analysis.

Figure 4.1a demonstrates that the placebo intervention samples from the PZ and the TZ of the prostate cluster into two distinct groups (PZ – red dots in red circle, and TZ – blue triangles in blue circle), demonstrating that they are indeed transcriptionally different. In addition, this figure demonstrates that the transcriptional variability between the two zones within an individual is greater than the inter-individual variability for the same zone (i.e. transcriptionally, an individual's PZ is more similar to the PZ of another individual, than it is to its own TZ). Figure 4.1b highlights three individual samples. The samples from two participants (19P and 40T) appear to be transcriptionally very similar to one another as demonstrated by their proximity on the PCA plot. Another sample (22P) appears as an outlier on the PCA plot, being transcriptionally dissimilar to the other samples.

To analyse the similarity of the transcriptional profiles between samples, hierarchical clustering in the form of a dendrogram was produced. Clustering is undertaken using the normalised counts for all 25,468 expressed genes.
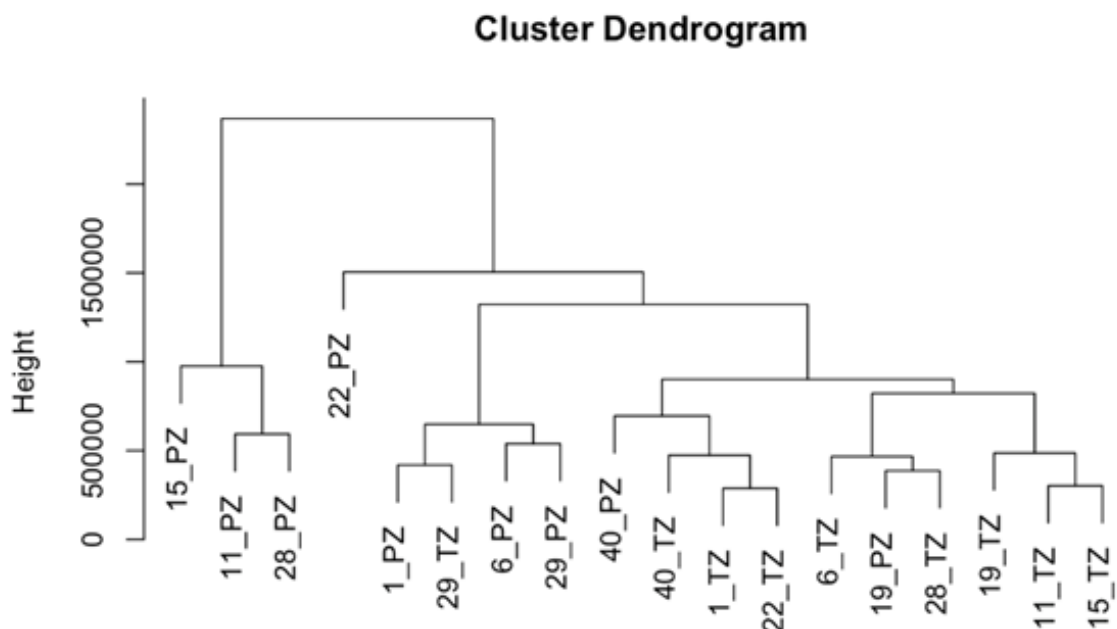
Figure 4. 2 Dendrogram showing the hierarchical clustering of expressed genes in the peripheral and transition zone of the prostate in control (placebo intervention) samples. Clustering is undertaken using the normalised counts for all 25,468 expressed genes.

As demonstrated in figure 4.2, four clusters occur at the approximate same vertical distance, and samples from the TZ generally cluster together independently of the PZ. This confirms the previous observation that inter-individual variability between zones is high. There are samples from two participants (19P and 40T) which appear to be clustered with samples from other zones on this dendrogram, which were also closely associated with each other on the PCA plot in figure 4.1b. Interestingly, the sample 22PZ which was identified in figure 4.1b as transcriptionally dissimilar to other samples, appears as an individual cluster (at a much greater height (or distance)).

4.4.2 Differential Expression Analysis

Following DESEq2 independent filtering, differential expression analysis was undertaken to determine whether individual genes are differentially expressed between the TZ and PZ.

Initially, extracted differentially expressed genes were used to produce MA plots.

Figure 4.3 demonstrates the differentially expressed genes between the TZ and PZ in placebo intervention samples following normalisation based on shrinkage estimation of log2 fold changes (LFCs). This MA-plot shows that there are differentially expressed genes in both directions of the M=0 line, with the majority of log fold difference between 0 and 2. Red dots above the M=0 line represents upregulated differentially expressed genes with an FDR-adjusted P value ≤ 0.1, compared to red dots below the M=0 lines representing downregulated differentially expressed genes with an FDR-adjusted P value ≤ 0.1.
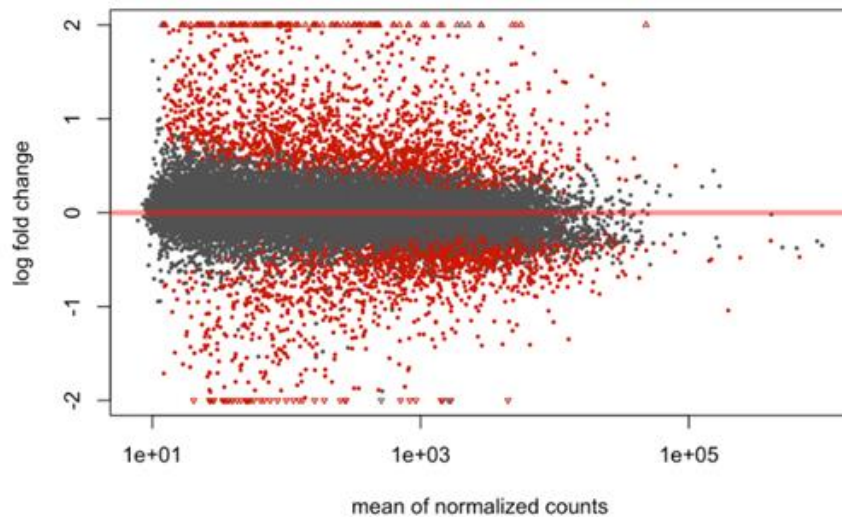
Figure 4. 3 MA plot of differentially expressed genes between the peripheral and transition zones of the prostate in patients consuming a placebo intervention (following transformation of normalised counts with log2-fold shrinkage). Each dot represents one transcript (n=25,468). The red dots indicate differentially expressed genes with an FDR-adjusted P value ≤ 0.05 (n=3,902).

Using the Benjamini-Hochberg (BH) method for multiple testing, the adjusted P values are used to define statistically significant differentially expressed genes.

In this analysis 25,468 genes are expressed (i.e. lowly-expressed genes removed). Of these genes, 25,343 genes pass the Wald test (a test for coefficients in a regression model) and return adjusted p-values according to the Benjamini-Hochberg method to control the false discovery rate (FDR). Table 4.3 below demonstrates that 14,821 genes were differentially expressed between the TZ and PZ (FDR-adjusted P value ≤ 0.5). At FDR-adjusted P value ≤ 0.01, 1,796 genes were differentially expressed, of which 1,139 demonstrate a higher expression and 657 demonstrate a lower relative expression in the TZ compared to the PZ. This is an interesting finding which supports previous evidence that more genes are preferentially expressed in the TZ than the PZ (331).

Table 4. 3 Number of genes differentially expressed in the transition vs peripheral zone of the prostate in participants consuming a placebo intervention.

	Control Samples: TZ vs. PZ
Genes that pass Wald Test	25,343
FDR-adjusted P value²	
≤ 0.5	14,821 (6737↑ 8084↓)
≤ 0.2	8,750 (3839↑ 4911↓)
≤ 0.1	5,815 (2,624↑ 3,191↓)
≤ 0.05	3,902 (1,943↑ 1,959↓)
≤ 0.01	1,796 (1,139↑ 657↓)

[1]FDR, false discovery rate; ↑ indicates a higher gene expression in the transition zone compared to the peripheral zone. ↓ indicates a lower gene expression in the transition zone compared to the peripheral zone. [2]Wald test, adjusted for multiple testing correction by Benjamini–Hochberg.

To visually analyse and identify the differentially expressed genes with large fold changes, a volcano plot was produced. This type of scatterplot demonstrates both the statistical significance (P value ≤ 0.05) vs. the magnitude of fold change. The volcano plot shows the 24,849 genes which passed the BH multiple testing correction by their P value and log2fold change. The horizontal line is drawn at the statistical significance threshold of 0.05 and the vertical lines are drawn at the negative and positive values of a log2 fold change of 1. In the volcano plot, the most statistically significant genes are towards the top of the plot, the most up-regulated genes are to the right, and the most down-regulated genes are to the left. The plot shows the non-significant genes as grey dots. Blue dots

represent genes with a P value < 0.05 but with small changes, and the red dots represent genes with a P value < 0.05 and a log2 fold change > 1.

Figure 4.4 highlights the majority of significantly differentially expressed genes with a significant fold change are to the right-hand side (demonstrating an increased relative expression).
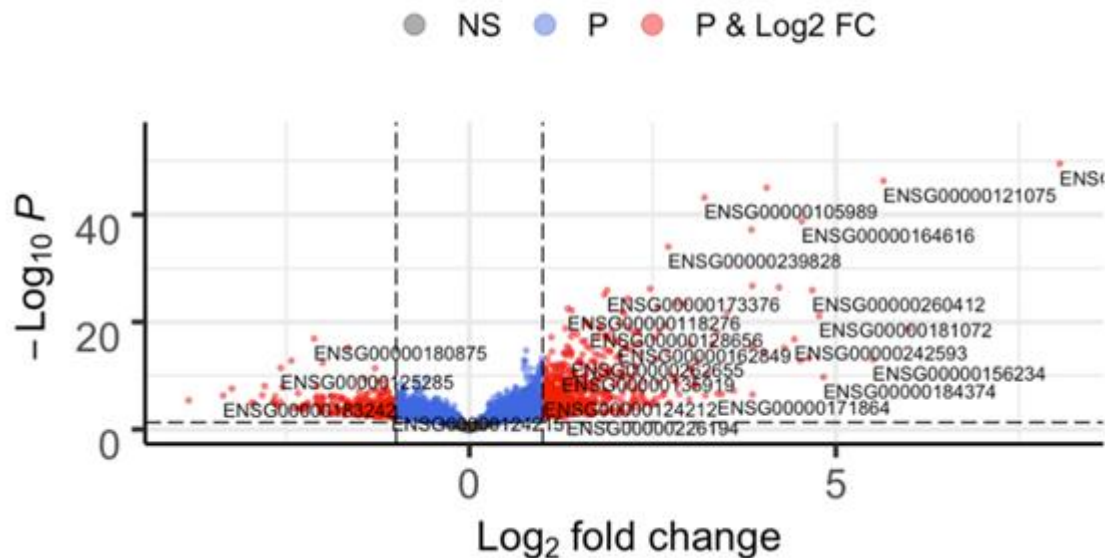
Figure 4. 4 Volcano plot demonstrating the 24,849 genes which passed the BH multiple testing correction by their P value and log2fold change in the transition vs peripheral zone of the prostate in patients consuming a placebo intervention. The most statistically significant genes are towards the top of the plot. Positive fold changes demonstrating a higher expression in the transition zone compared to the peripheral zone are shown on the right-hand side, whereas negative fold changes (demonstrating a lower expression in the transition zone compared to the peripheral zone) are on the left-hand side. The plot shows the non-significant genes as grey dots. The blue dots represent genes with a P value < 0.05 but with small changes, and the red dots represent genes with a P value < 0.05 and a log2 fold change > 1.

4.4.2.1 Analysis of Individual Genes

Results of the differential expression test discussed above, demonstrated 3,902 genes which were differentially expressed between the TZ and PZ of the prostate in patients consuming a placebo intervention (FDR-adjusted P value <0.05). The top 50 genes are demonstrated in table 4.4. Highlighted genes are those which have also been shown to be differentially expressed in previous literature; these include BMP5, NELL2 and FOXF2, all of which were preferentially expressed in the

TZ (as demonstrated by a positive log2fold change). GREM2 (a DAN family BMP antagonist) demonstrated preferential expression in the PZ compared to the TZ (as represented by a negative log2fold change). Interestingly, the top 49 genes are all preferentially expressed in the TZ compared to the PZ.

BMP5 and NELL2 are both associated with neurogenesis, signal transduction and cell motility and development. FOXF2 (Forkhead box F2) is associated with the regulation of transcription, organ morphogenesis and vasculogenesis, and is known to be preferentially expressed in the TZ of the prostate, compared to the PZ, and indeed PCa, where it's expression is typically decreased.

Table 4. 4 The top fifty differentially expressed genes between the transition and peripheral zone of the prostate in patients consuming a placebo intervention. Genes highlighted in blue demonstrate genes which have also been highlighted as significant in previous literature.

ensemblID	GeneSymbol	log2FoldChange	padj
ENSG00000112175	BMP5	8.055	<0.001
ENSG00000121075	TBX4	5.649	<0.001
ENSG00000184613	NELL2	4.056	<0.001
ENSG00000105989	WNT2	3.206	<0.001
ENSG00000164616	NA	4.535	<0.001
ENSG00000162989	KCNJ3	3.848	<0.001
ENSG00000239828	NA	2.714	<0.001
ENSG00000287900	NA	3.860	<0.001
ENSG00000100427	MLC1	4.223	<0.001
ENSG00000137273	FOXF2	2.465	<0.001
ENSG00000173376	NDNF	1.878	<0.001
ENSG00000260412	NA	4.678	<0.001
ENSG00000242759	LINC00882	1.841	<0.001
ENSG00000170381	SEMA3E	2.160	<0.001
ENSG00000138207	RBP4	2.833	<0.001
ENSG00000138483	CCDC54	2.943	<0.001
ENSG00000146250	PRSS35	2.573	<0.001
ENSG00000118276	B4GALT6	1.342	<0.001
ENSG00000044524	EPHA3	1.394	<0.001
ENSG00000072657	TRHDE	2.087	<0.001
ENSG00000164879	CA3	3.516	<0.001
ENSG00000164176	EDIL3	2.108	<0.001
ENSG00000181072	CHRM2	4.772	<0.001
ENSG00000135333	EPHA7	1.587	<0.001
ENSG00000111452	ADGRD1	2.043	<0.001
ENSG00000272636	DOC2B	1.619	<0.001
ENSG00000128482	RNF112	2.660	<0.001
ENSG00000128656	CHN1	1.645	<0.001
ENSG00000133067	LGR6	2.156	<0.001
ENSG00000077063	CTTNBP2	1.782	<0.001
ENSG00000180616	SSTR2	1.775	<0.001
ENSG00000046889	PREX2	1.308	<0.001
ENSG00000145681	HAPLN1	5.995	<0.001
ENSG00000184985	SORCS2	1.410	<0.001
ENSG00000171004	HS6ST2	2.220	<0.001
ENSG00000250320	NA	1.939	<0.001
ENSG00000119630	PGF	2.585	<0.001
ENSG00000145777	TSLP	2.286	<0.001
ENSG00000146151	HMGCLL1	2.318	<0.001
ENSG00000188176	SMTNL2	3.379	<0.001
ENSG00000115896	PLCL1	1.471	<0.001
ENSG00000137726	FXYD6	1.853	<0.001
ENSG00000108381	ASPA	1.863	<0.001
ENSG00000138395	CDK15	1.748	<0.001
ENSG00000187955	COL14A1	1.386	<0.001
ENSG00000005249	PRKAR2B	1.118	<0.001
ENSG00000095303	PTGS1	2.510	<0.001
ENSG00000180875	GREM2	-2.120	<0.001

In addition to the genes highlighted in table 4.4, table 4.5 highlights other genes of interest which have previously been described as differentially expressed between the prostate zone, which were also confirmed to be significant in the current analysis. The finding of preferential expression of AMACR in the PZ is most noteworthy, and has not previously been described in the 'normal' transcriptional signature of the PZ.

Table 4. 5 Table of genes of interest which are differentially expressed between the transition and peripheral zone of the prostate in patients consuming a placebo intervention. Highlighted in blue are genes which are preferentially expressed in the transition zone compared to the peripheral zone (as represented by a positive fold change). Highlighted in orange are genes which are preferentially expressed in the peripheral zone compared to the transition zone (as represented by a negative fold change). Reference refers to the previous literature in which an association was previously described (either gene family or specifically).

ensemblID	GeneSymbol	log2FoldChange	padj	Reference
ENSG00000112175	BMP5	8.055	8.21E-46	Noel *et. al.* 2008
ENSG00000184613	NELL2	4.056	8.00E-42	Noel *et. al.* 2008
ENSG00000137273	FOXF2	2.465	1.60E-23	Van Der Heul-Nieuwenhuijsen *et. al.* 2009
ENSG00000180875	GREM2	-2.120	6.41E-15	Noel *et. al.* 2008
ENSG00000117594	HSD11B1	1.877	2.41E-09	Noel *et. al.* 2008
ENSG00000196154	S100A4	1.518	2.76E-07	Noel *et. al.* 2008
ENSG00000158163	DZIP1L	0.819	4.06E-05	Zhao *et. al.* 2009
ENSG00000106483	SFRP4	-1.344	0.000539	Noel *et. al.* 2008
ENSG00000147394	ZNF185	-0.879	0.00066	Noel *et. al.* 2008
ENSG00000120057	SFRP5	-2.049	0.001047	Noel *et. al.* 2008
ENSG00000242110	AMACR	-1.151	0.020546	n/a
ENSG00000145423	SFRP2	0.695	0.038229	Noel *et. al.* 2008
ENSG00000104332	SFRP1	-0.538	0.043805	Noel *et. al.* 2008
ENSG00000197614	MFAP5	-2.550	1.18E-06	Shaikhibrahim *et. al.* 2012
ENSG00000170927	PKHD1	-0.953	0.025958	Shaikhibrahim *et. al.* 2012
ENSG00000106819	ASPN	-2.003	9.74E-11	Shaikhibrahim *et. al.* 2012

4.4.3 Gene Set Enrichment Analysis

To ascertain which functional pathways were differentially regulated in the TZ and PZ of the prostate in placebo samples, gene set enrichment (GSEA) was undertaken. GSEA considers all the genes expressed in the analysis which passed the Wald test (and hence returned a P value), ranked by P value and sign of fold change, compared to the Molecular Signatures Database (MSigDN) hallmark gene set.

Table 4.6 shows the GSEA of changes in the TZ compared to the PZ of the prostate. The hallmark database contains 50 sets, and of these, 25 sets were significantly different (returning a q.value ≤ 0.05) in this analysis. 10 sets demonstrated a positive normalised enrichment score (NES) and represent upregulated pathways in the TZ compared to the PZ (highlighted in blue). The remaining 15 sets demonstrate a negative NES, representing a downregulation in pathways in the TZ compared to the PZ.

In keeping with previous results, this analysis demonstrates that fatty acid metabolism and cholesterol homeostasis are less preferentially expressed in the TZ compared to the PZ, which may confer a more favourable environment within the PZ for the development and progression of PCa. Hormonal pathways such as the androgen and oestrogen response are also downregulated in the TZ compared to the PZ. Epithelial mesenchymal transition (EMT), which is significantly upregulated in the TZ compared to the PZ, may provide a hypothesis for the propensity towards BPH in the TZ over PCa. In addition, downregulated sets in the TZ compared to the PZ are more consistent with reduced risk of carcinogenesis, which may also support the evidence that the TZ is transcriptionally less likely to develop cancer.

Table 4. 6 Gene set enrichment of changes that occurred in transition zone compared to the peripheral zone of the prostate in participants consuming a placebo intervention (q.value ≤ 0.05). Highlighted in blue are the 10 gene sets upregulated in the transition zone compared to the peripheral zone with a positive normalised enrichment score. The remaining 15 sets are downregulated in the transition zone compared to the peripheral zone with a negative normalised enrichment score. Pathway analysis was conducted using the GSEA software analysed by the Hallmark database.

Set.Name	SIZE	NES	QVALUE
EPITHELIAL_MESENCHYMAL_TRANSITION	191	2.337	<0.001
UV_RESPONSE_DN	144	1.984	0.001
MYOGENESIS	177	1.907	0.002
KRAS_SIGNALING_UP	182	1.897	0.002
NOTCH_SIGNALING	32	1.849	0.003
COAGULATION	106	1.787	0.004
ANGIOGENESIS	31	1.689	0.011
IL6_JAK_STAT3_SIGNALING	80	1.652	0.014
ALLOGRAFT_REJECTION	175	1.540	0.039
COMPLEMENT	179	1.505	0.049
MYC_TARGETS_V1	196	-2.220	<0.001
OXIDATIVE_PHOSPHORYLATION	200	-2.206	<0.001
PROTEIN_SECRETION	96	-2.123	<0.001
CHOLESTEROL_HOMEOSTASIS	72	-2.041	<0.001
ANDROGEN_RESPONSE	99	-2.006	<0.001
UNFOLDED_PROTEIN_RESPONSE	109	-1.922	<0.001
DNA_REPAIR	148	-1.869	<0.001
MTORC1_SIGNALING	198	-1.786	0.001
PEROXISOME	98	-1.758	0.001
HEME_METABOLISM	173	-1.631	0.006
MYC_TARGETS_V2	58	-1.630	0.005
ESTROGEN_RESPONSE_EARLY	196	-1.596	0.007
FATTY_ACID_METABOLISM	144	-1.567	0.008
P53_PATHWAY	192	-1.446	0.025
REACTIVE_OXYGEN_SPECIES_PATHWAY	48	-1.444	0.023

[1]IL6, interleukin 6; JAK, Janus Kinase; KRAS, V-Ki-Ras2 Kirsten Rat Sarcoma 2 Viral Oncogene Homolog; MSigDb, Molecular Signature Database; MTORC1, mammalian target of rapamycin complex 1; MYC, myelocytomatosis; NES, normalized enrichment score; UV, ultraviolet. SIZE refers to the numbers of genes in the pathway. UV response DN refers to genes that are down regulated by UV radiation. UV response UP refers to genes that are up regulated by UV radiation. KRAS signalling UP refers to genes that are up regulated by KRAS signalling.

[2]Q value, false discovery rate using Benjamini-Hochberg (BH) adjustment.

[3]GSEA by GSEA software version 4.0.3, on all genes ranked by the significance of fold change.

4.5 Discussion

The transcriptional differences between the PZ and TZ of the prostate have previously been analysed using whole-genome RNA sequencing and high-throughput metabolic profiling samples from whole prostate following prostatectomy or cystoprostatectomy in patients with PCa requiring radical treatment. This chapter however, sought to analyse the transcriptional differences from biopsy samples in the PZ and TZ of patients with either known PCa on 'active surveillance' for low risk disease, or under investigation for a potential PCa, using RNA-sequencing techniques. The propensity for PCa in the PZ of the prostate is largely unexplained. This chapter demonstrates the potential transcriptional changes in the pathway of PCa progression and demonstrates a potential transcriptional hypothesis for this phenomenon.

Analysis of control samples from the Norfolk-ADaPt study, supports previous evidence which suggests that the PZ and TZ are transcriptionally different. This is demonstrated across all areas of the sample analysis. A clear pattern of separation was initially demonstrated in the PCA plot (figure 4.1), which highlighted that TZ samples and PZ samples cluster independently of one another. In addition, this plot demonstrates that not only are paired samples from the TZ and PZ of individuals transcriptionally very different, but that samples from the PZ of multiple individuals all tend to cluster together, the same as for the samples from the TZ. This not only suggests that the transcriptional signature of the PZ and TZ is different amongst individuals, but that all samples from the PZ (from multiple individuals) are very similar, and vice versa.

Differential expression analysis confirmed that multiple genes are differentially expressed between the TZ and PZ, both with an increased and decreased relative expression, suggesting that the prostate zones have a very unique transcriptional signature. However, figure 4.3 highlights that the majority of differentially expressed genes appear to have an increased relative expression. Table 4.3 confirmed that 14,821 genes were differentially expressed between the TZ and PZ (padj ≤ 0.5), of which 1,796 genes remained differentially expressed at padj ≤ 0.01. Of these genes, 1,139 genes demonstrated preferential expression in the TZ compared to the PZ, and 657 demonstrated preferential expression in the PZ compared to the TZ. This interesting finding has also previously

been observed by Noel *et. al*, who noted that the majority of differentially expressed genes between the two prostate zones are preferentially expressed in the TZ compared to the PZ (331).

Of the individually differentially expressed genes between the two zones, many genes previously shown to be preferentially expressed in the PZ compared to the TZ in previous studies were also demonstrated in this analysis. These included ZNF185, SFRP4, MFAP5, PKHD1 and ASPN.

ZNF185, a zinc-finger protein, which belongs to the LIM superfamily of proteins (348), has previously been shown to be preferentially expressed in the PZ of the prostate (331) a finding which was also demonstrated in this study (log2fold change -0.879 TZ to PZ padj 0.001). The LIM superfamily is one of the most abundant groups of proteins, which have a variety of diverse roles including cytoskeletal organisation, cell differentiation, DNA repair and transcriptional regulation (349). ZNF185 itself has been demonstrated to function in the focal adhesion pathway (348). Interestingly, ZNF185 has been shown to inhibit prostate tumour cell growth and has been identified as a candidate tumour suppressor protein, by associating with the actin cytoskeleton via its N-terminal region (350). ZNF185 expression decreases during PCa progression which is thought to be mainly due to its epigenetic silencing via methylation of CpG dinucleotides (351). As such, epigenetic alterations resulting in transcriptional silencing may therefore be a useful biomarker of PCa progression.

As previously demonstrated by Noel *et. al.* (331), SFRP4 demonstrated preferential expression in the PZ compared to the TZ in this analysis (log2fold change -1.344 TZ to PZ padj 0.001). SFRP4 belongs to the family of secreted frizzled-related proteins, which bind to and inhibit Wnt signalling (352). Wnt signalling is known have an important role in the development of cancers, where it becomes highly activated, and as such is a potential therapeutic target in multiple cancer types (352, 353). As a result, SFRPs are generally thought to be tumour suppressors. SFRP4 itself is also thought of as a tumour suppressor (354), however, in relation to PCa the evidence is mixed. Studies have demonstrated that the increased expression of SFRP4 is associated with aggressive and recurrent disease (355-357) (and correlates with citrate and spermine concentrations) (358), whereas immunohistochemical staining of SFRP4 protein levels have been associated with a good prognosis (359, 360). It has been suggested that methylation silencing of SFRP4 may result in aberrant Wnt activation, inhibition of apoptosis and hence cancer progression (361). SFRP4 is an interesting candidate and certainly warrants further investigation.

Previously, clustering analysis based on gene function from the pooling of microarray RNA samples from normal prostate tissue, has demonstrated the preferential expression of 9 genes in the PZ compared to the TZ (362), 3 of which (MFAP5, PKHD1 and ASPN) were also significantly differentially expressed in the same way in this analysis. MFAP5 (microfibrillar-associated protein 5) is a

component of the extracellular matrix, interacting with elastin-associated microfibrils and fibrillin, and has a function in tissue development and cancer progression. MFAP5 expression is upregulated (and secreted by tumour cells) in multiple cancer types, where it promotes tumour cell survival, angiogenesis and metastasis (363-366). Similarly, ASPN (asporin) is expressed in the tumour-associated stroma (367-369), surrounding tumour cells, which appears to correlate with PCa aggressiveness and progression (370). The finding that these genes are preferentially expressed in the PZ compared to the TZ may suggest a preferable stromal and surrounding environment for the development of cancer clones.

One of the most significant findings in this analysis however, is the preferential expression of AMACR in the PZ (TZ to PZ -1.151 padj. 0.021). As previously discussed in chapter one, AMACR is required for the utilisation of fatty acids via β-oxidation, in order to enable cell growth and proliferation, as well as providing an energy source (44). AMACR is reportedly overexpressed in all grades of PCa in the PZ, and also in high-grade dysplasia (PIN) and has therefore been proposed as a new molecular marker for PCa (371-375). The expression of AMACR in the current analysis is interesting, as all biopsy samples were taken *away* from areas which were known to contain, or were suspicious for PCa. This finding may therefore represent the following; either biopsy samples did contain areas of PIN or PCa, or the PZ preferentially expresses higher levels of AMACR which signifies an increased susceptibility to PCa in this zone. Interestingly, previous research analysing AMACR expression in the TZ, has demonstrated that some carcinomas indeed arise from AMACR-positive transition lesions, and that upregulation of this enzyme may in fact *precede* any morphological evidence of neoplastic transformation (375). This finding also supports the evidence that PCa arises from multiple clones, as part of the field cancerisation effect, whereby the development of multi-focal premalignant molecular lesions precede detectable histological change (375).

Consistent with Noel *et. al.*, preferentially expressed genes in the TZ included NELL2 (+4.056 padj<0.0001), S100A4 (+1.518 padj. <0.0001) and BMP5 (+8.055 padj. <0.0001). Indeed, BMP5 was the most significantly differentially expressed gene in this analysis, and NELL2 the third most significantly differentially expressed gene. Other markers previously shown to be overexpressed in the TZ of normal prostate tissue (and subsequently downregulated in PCa cells and tissue) were also confirmed in this study, including CCDC8 (+0.691 adj. p<0.003), HOXD13 (0.718 adj.p<0.004), SPON1 (+1.385 <0.0001), PTGS1 (+2.510 padj <0.0001), HSD11B1 (+1.877 padj<00001), SYNPO 0.881 padj. 0.003) and UNC5B (1.095 padj. <0.0001).

The preferential expression of BMP5 in the TZ has been demonstrated in previous studies (331, 376). BMP5 (bone morphogenetic protein-5) is a member of the transforming growth factor-β (TGF-β)

superfamily, which comprise regulators of epithelial-mesenchymal transition (EMT), cell differentiation, apoptosis and stem cell homeostasis (377). BMP5 expression is specifically known to induce ectopic bone and cartilage formation, and has hence received interest with regards to bone metastasis in breast and PCa (378, 379). Interestingly however, BMP5 is known to be one of the most highly expressed genes in prostate basal stem cells where it appears to promote basal cell homeostasis, and its preferential expression in the TZ may therefore also highlight its role in the development of BPH in this zone (380-382).

NELL2 (neural epidermal growth factor-like 2) belongs to the family of multimodular extracellular glycoproteins, and is predominantly expressed in the nervous system where it is known to function in neurogenesis and signal transduction (383, 384). However, NELL2 has also been shown to be highly expressed in non-cancerous human renal tubules, with a significantly lower expression in renal cell carcinoma (RCC) (385) where they bind RCC cells to cell surface receptors and transduce intracellular signalling. NELL2 is also considered a candidate biomarker for bladder cancer. Regarding the prostate, NELL2 expression has been shown to be upregulated in BPH, where it appears to contribute to alterations in epithelial-stromal homeostasis (386). The preferential expression of NELL2 in the TZ may therefore provide a further explanation to the predilection of BPH in this zone.

The preferential expression of S100A4 in the TZ of the prostate has previously been described (379) and is supported in this study ((log2fold change +1.5180 TZ to PZ padj <0.001). S100A4 (a member of the S100 calcium-binding protein family) also known as FSP1 (fibroblast-specific protein 1) is expressed by fibroblasts and induced by epidermal growth factor (EGF) and TGF-β1 cytokines associated with fibrosis (387). Experimental evidence suggests that fibroblasts which express this gene may be derived from epithelial cells through epithelial-mesenchymal transformation during fibrosis (388, 389). Not only has S100A4 been shown to be preferentially expressed in the TZ of the prostate, but also significantly upregulated in BPH tissue (where stromal-epithelial ratio significantly increases (390)) when compared to normal TZ tissue (391). Conversely however, given the theory that the stromal microenvironment contributes to tumourigenesis in cancers of epithelial origin (392), S100A4 overexpression has also been associated with PCa progression and metastasis, where it is a potential candidate biomarker for early PCa diagnosis and prognostics. This is achieved via the downregulation of E-cadherin and modulation of MMPs and integrins, vital for cell invasion and metastasis by the induction of the EMT (393, 394).

The extent of differentially expressed genes between the peripheral and transition zones in this analysis contrasts with previous studies, which report lower numbers. The differences may be due to tissue processing, RNA extraction and/or analytical techniques. Firstly, compared to previous

literature, this chapter described the transcriptional analysis from prostate biopsy samples, rather than samples taken from an extracted prostatectomy or cystoprostatectomy specimen. In this analysis, the biopsy tissue was immediately (within 30 seconds) placed into RNAlater solution (without further physical insult) to prevent RNA degradation. In comparison to prostatectomy or cystoprostatectomy samples used in previous studies (331, 332, 362), in which specimens are generally processed any time up to 1 hour following surgical extirpation of the gland. However, surprisingly, evidence suggests that there is indeed little overall increase in gene expression variability between 0 and 1-hour ischaemic time of the whole prostate (demonstrated by a negligible change between MA-plots at these time points) (395). Despite this, four reference genes associated with ischaemia have been noted to be increased 1 hour following extirpation (395). It is important to highlight however, that "time 0" samples from the prostate in this described study, were still analysed following tissue transportation to a nearby laboratory and processed – it is likely that initial ischaemic events will occur even prior to extirpation following devascularisation of the prostate (approximately 30 mins in the case of a prostatectomy), which the methods used in this current analysis avoid. One of the four ischaemic reference genes included in the previous analysis which demonstrated an upregulation with increased ischaemic time, was activating transcription factor 3 (ATF3) (395). ATF3 was also preferentially expressed in the PZ compared to the TZ in this analysis (TZ to PZ log2fold change -0.548, adjp=0.022), but despite being upregulated in most tissue types following ischaemic insult (including the heart, kidney, brain and liver) (396), it has not been shown to be related to prostate tissue specifically. In addition to the processing time, the difference in the amount of significantly expressed genes in this analysis may be due to the analytical methods used; for example, a previous study has only presented genes which were found to be highly differentially expressed with a criteria of >10-fold increase or decrease and a P value <0.001 (362), a criteria not used in this analysis.

The large number of differentially expressed genes also raised the possibility that downstream biological pathways may be significantly different between the peripheral and transition zone. This was confirmed in the GSEA (shown in table 4.4), which returned 25 significantly altered gene sets. Of these sets, 10 were shown to have an increased expression in the TZ compared to the PZ, whereas 15 were downregulated in the TZ compared to the PZ. Of particular interest, GSEA confirms that cholesterol synthesis and fatty acid metabolism (characteristic of PCa) are preferentially expressed in the PZ, which is consistent with previous findings suggesting that the PZ may provide an ideal micro-environment for the development and progression of PCa (333). The link between cholesterol synthesis and PCa is well researched and was described in chapter one. Initially thought of as a metabolic by-product, cholesterol has been shown to have multiple cellular functions, not only as a

precursor for steroid hormones and bile acids as previously described, but also in enhancing cellular structural integrity, signal transduction and cell signalling (56, 397, 398). Via these functions, cholesterol is therefore essential for cellular proliferation, and its role in uncontrolled cell growth of cancer cells appears to be most significant in the development of PCa (49, 56). *In vivo*, animal, epidemiological and human studies have all associated high cholesterol levels with an increased risk of PCa, whilst the use of cholesterol-lowering drugs (statins) has been shown to reduce the risk of advanced PCa (49, 399, 400) (56).

GSEA also demonstrated that the androgen response pathway is downregulated in the TZ compared to the PZ. This significant finding further supports the evidence that the PZ is transcriptionally more susceptible to the development of PCa. As previously discussed, the androgen receptor (AR) is one of the main regulators of prostate cell growth and development (401), recognising androgens including testosterone and 5α-dihydrotestosterone (DHT, a potent AR activator). Briefly, the AR is bound to a heat-shock protein in the cytosol, deeming it inactive. Upon binding to DHT, the heat-shock chaperone is displaced, which enables the AR to phosphorylate and migrate to the nucleus whereby it is able to bind androgen-response elements (AREs) (402). This binding causes the upregulation of target genes vital for prostate cellular physiology. The AR receptor is hence vital for PCa initiation and growth (401) and is observed throughout progression in both hormone-sensitive and hormone refractory courses (401, 403-405), which makes it a significant target in the treatment of PCa. Interestingly, the AR is also known to be involved in promoting cholesterol accumulation by utilising the transcription factors involved in cholesterol homeostasis to regulate SREBP-2 and LXR (via the activation and inhibition respectively) (406). Although the AR is highly heterogenous (403) the finding that both the androgen response and cholesterol and fatty acid synthesis gene sets are downregulated in the TZ compared to the PZ, may go some way to explaining the predilection of PCa development in the PZ.

Interestingly, GSEA in this chapter also demonstrated that the oestrogen response is downregulated in the TZ compared to the PZ. More recently, the role of oestrogens in the development of PCa has been increasingly suggested, including its interaction with the androgen receptor. Rodent models of prostate neonatal oestrogenisation suggest an epigenetic basis for oestrogen imprinting in PCa, most notably regarding DNA and histone modifications resulting in gene silencing, particularly of tumour-suppressor genes (407-411). Additionally, chronic exposure to oestrogen causes an increase in prolactin levels, which has recently been shown to alter gene expression and inflammatory changes implicated in PCa development (412-415). These changes have been demonstrated to support tumour proliferation, chemo-resistance and the survivability associated with hormone resistance (416). The upregulation of the oestrogen response pathway demonstrated in the PZ compared to

the TZ in this study therefore supports the evidence for a hormonal hypothesis for the predilection of PCa in this zone.

In addition to this, potentially oncogenic gene sets are also upregulated in the PZ compared to the TZ, including Myc (commonly activated in PCa), the p53 pathway and DNA repair.

The findings in the GSEA also support the differential expression analysis in potentially explaining the propensity of the TZ towards BPH rather than carcinogenesis. Epithelial mesenchymal transition (EMT) was significantly upregulated in the TZ compared to the PZ, as well as myogenesis. Historically, BPH has been thought to be a proliferative stromal disease (417), where excessive proliferation of the epithelial and stromal cells in the TZ and periurethral glands lead to the presence of hypertrophic basal cells, an increase in stromal mass, and enhanced extracellular matrix deposition (418). More recently, sequencing of human BPH tissue has also demonstrated the upregulated expression of EMT markers, along with the loss of expression of E-cadherin or cytokeratin 8 (CK8) (hallmark features of BPH) (419, 420). Further analysis is required to investigate the transcriptional signature of the TZ and its propensity towards BPH.

As previously discussed, the use of biopsy tissue for this analysis rather than prostatectomy specimens has major advantages. However, one limitation of using biopsy tissue is the possibility of including many cell types in the analysis. For example, as previously described, it is the glandular (secretory) epithelial cells of the PZ which demonstrate a unique metabolism and ability to accumulate and secrete (rather than oxidise) large concentrations of citrate, rather than epithelial cells in general. There is the possibility of including many cell types into one biopsy sample, which would result in the quantification of mean gene expression across different cell types. In order to overcome this potential limitation, single cell RNA sequencing could be utilised in future analyses.

4.6 Conclusion

This chapter demonstrates that the PZ and TZ possess unique transcriptional signatures. Transcriptional analysis suggests that the PZ may indeed be 'primed' for carcinogenesis to a greater extent than the TZ, due to the higher relative expression of genes involved in PCa development and progression, most notably including AMACR and others involved in fatty acid and cholesterol metabolism, as well as those associated with the androgen pathway. Additionally, this analysis also supports previous evidence in providing a potential transcriptional explanation for the TZ's propensity towards BPH.

Chapter Five

Transcriptional Changes in the Prostate of Men

Enrolled in the Norfolk-ADaPt Study – The

Effect of Alliin and Glucoraphanin Dietary

Supplementation

5.1 Introduction

The previous chapter demonstrated that the peripheral and transition zones of the prostate have unique transcriptional profiles, which may explain the propensity of the different zones to PCa or BPH. This chapter builds upon these findings by exploring the potential transcriptional effects that a short-term intervention of GFN and/or Alliin may have on the prostate.

5.1.1 Transcriptional Alterations in Response to Dietary Bioactive Compounds

5.1.1.1 Glucoraphanin

As discussed in chapter 1, SFN has been shown to provide multi-modal influences on a wide variety of metabolic and cell-signalling pathways involved in cancer; including the induction of antioxidant pathways, cell cycle regulation, induction of apoptosis, inhibition of inflammation and angiogenesis, and detoxification of carcinogens (100). Additionally, SFN has been shown to alter fatty acid metabolism (107) and interact with AR chaperones via the inhibition of HDAC enzymes (109-111). The transcriptomic effects of GFN are thought to be largely due to the action of SFN on the transcription factor nrf-2. Nrf-2 is controlled by a complex transcriptional and epigenetic network that ensures an increase in its activity during redox alterations, inflammation, and growth factor and nutrient fluxes, and therefore orchestrates a response to multiple forms of stress whilst regulating the cellular redox status (421). As described in chapter one, *in vitro* studies have shown that SFN causes the dissociation of the nrf-2:keap1 complex, allowing nrf-2 to translocate to the nucleus and exhibit its downstream anti-oxidant effects (102, 103). In addition, nrf-2 has also been shown to act as a metabolic regulator, directing metabolic reprogramming during stress. In this way, nrf-2 can control the activity of a wide range of genes involved in metabolism, resulting in an inhibition of lipogenesis, supporting β-oxidation of fatty acids, and increasing NADPH regeneration (421-423). The way in which nrf-2 acts to regulate these genes however, is not fully understood.

Despite the abundance of evidence from *in vitro* and animal studies, evidence from human studies is currently limited. In one recent human study, the effect of GFN on the transcriptomic profile of human prostate cancer was demonstrated as part of a 12-month dietary intervention study (the ESCAPE study). In this study, GFN in the form of a GFN-rich broccoli soup demonstrated a dose-dependent suppression of oncogenic pathways using high-throughput RNA sequencing approaches

(424). Gene set enrichment analysis in this study demonstrated significant enrichment in pathways such as the inflammatory response, angiogenesis, apoptosis and androgen response; all associated with risk of carcinogenesis. Further human intervention studies are paramount to shed light on the impact of these compounds on the prostate tissue; in particularly whether delivering a higher concentration of the active compound of interest (SFN), and for a short period of time, can elicit the transcriptional effects of interest.

5.1.1.2 Alliin

Garlic constituents including Alliin and its metabolites have been shown *in vitro* to influence a multi-modal range of epigenetic features, including detoxification, induction of apoptosis, cell-cycle arrest and modulation of hydrocarbon and nitrosamine metabolism (124-127). However, unlike GFN, its effect on the transcriptional signature of human prostate is currently lacking.

Hallmark epigenomic alterations (heritable changes in gene function that occur without a change in DNA sequence) in PCa include alterations in histone acetylation and methylation, and excessive deacetylase activity – also predictors of PCa recurrence (425). Under normal circumstances, histone acetylation typically results in an 'open' chromatin configuration which facilities transcription factor access to DNA and gene transcription. Acetylation and deacetylation of histones are generally associated with activation and deactivation respectively; a balanced regulatory process enabling the appropriate level of transcription (426, 427). Acetylation and deacetylation of histones is catalyzed by histone acetyltransferases (HATs) and histone deacetylases (HDACs) respectively. Therefore, the overexpression and hence increased activity of HDACs repress transcription and can result in dysregulation of the cell cycle, apoptosis and differentiation, via the silencing of tumour suppressor genes (428, 429). As such, HDAC inhibitors are gaining increased interest in the potential treatment of PCa, given that PCa tumour cells treated *in vitro* with histone deacetylase inhibitors are more susceptible to cytotoxic T-lymphocyte (CTL) killing. Allyl derivatives have been shown to induce histone acetylation and HDAC inhibition in a variety of human cancer cells, including PCa (430), via increased CDKN1A gene expression, leading to a reduction in proliferation and angiogenesis.

Alliin metabolites have also been documented to play a role in bioactivation and detoxification, via their ability to induce NADPH:quinone oxidoreductase (NQO1) (an enzyme involved with the removal of quinones associated with carcinogenesis). Similar to isothiocyanates, this inductive effect appears to be mediated by the antioxidant response element enhancer sequence bound by nrf-2 in

the NQO1 and the heme oxygenase 1 (HO1) gene promoter regions. Nrf-2 therefore appears important in the transcriptional effects of both cruciferous and alliaceous vegetables.

The immunomodulatory effects of Allyl metabolites may also provide a desirable effect on PCa pathogenesis and progression (431-433). The phagocytosis of apoptotic PCa cells causes a polarisation of PCa-associated macrophages towards an M2 anti-inflammatory phenotype, leading to a high expression of the cytokine TGF-β1 RNA (434). As discussed in chapter one, the presence of PCa-associated macrophages and propensity for M2 phenotype, as well as increased levels of TGF-B1, promote PCa invasion and proliferation, and are associated with worse disease outcomes, including invasive tumour phenotype, metastasis and recurrence. Additionally, T-cell subsets appear important in anti-tumour response; T-regulatory cells (T-regs) which accumulate in both the plasma and tumour tissue in PCa, appear to inhibit T-helper cells (THCs) and deprive them of IL-2 (a contributing factor of PCa immune escape) (434). Increased levels of IL-2 also promotes a pro-inflammatory M1 macrophage phenotype over M2. IL-2 and TGF-B1 are therefore promising candidates for immune recognition and PCa tumour targeting. Garlic extracts have been reported to cause an upregulation in multiple cytokine release, including IL-2, TNFα and IFNγ, in a variety of cancers, suggesting the induction of a Th1-type immune response (432, 433, 435, 436).

As is the case for GFN, despite the abundance of literature demonstrating the variety of mechanisms by which these bioactives may exert their effect in cell and animal model systems (as supported by epidemiological studies), human intervention studies utilising these compounds are extremely limited. In addition, as previously described, *in vitro* concentrations cannot directly be paralleled to human studies, and basic anatomical differences in animal models make any findings difficult to interpret on a more mechanistic level.

To ascertain whether the currently known evidence also applies to human tissue following the ingestion of these bioactive compounds, requires well-designed human intervention studies. This chapter aims to explore whether treatment with GFN and/or Alliin interventions alter the transcriptional environment of the prostate, which may lead to the downstream changes in functional biological pathways associated with PCa development and/or progression. Given the vast differences demonstrated between the transcriptional signatures of the peripheral and transition zones, and their differing propensities towards incidence of PCa, RNA-sequenced data of samples from both zones were analysed independently.

5.2 Aims

- To investigate the effects of GFN and Alliin interventions in the peripheral and transition zone of the prostate using next generation RNA sequencing

- To explore whether an intervention with GFN and/or Alliin causes an upregulation in nrf-2 regulated genes

5.3 Materials and Methods

All steps in the RNAseq analysis are as previously described in chapter four, apart from alterations in the codes used for differential expression analysis in the comparison of samples from patients who were consuming GFN and/or Alliin samples. These steps are detailed below.

5.3.1 Differential Expression Analysis

Differential Expression analysis was performed with R studio using DESeq2.

The gene expression data contained 60,617 genomic features, which includes all genes in the assembly, including protein coding genes, non-coding genes and pseudo-genes.

The statistical analysis starts by removing low expressed genes. The peripheral and transition zone analysis were undertaken separately. Genes with less of 10 counts for at least 19 samples in each analysis were removed. In the following table, the column "Expressed" represents the number of genes that were used for the analysis, for each of the zones.

Table 5. 1 Filtering lowly expressed genes in the samples derived from the peripheral zone (PZ) and transition zone (TZ)

Zone	Number of Genes	Low Expressed Genes	Expressed Genes
PZ	60,617	35,317	25,300
TZ	60,617	34,985	25,632

Differential testing was conducted with DESeq2 in each zone separately to test for the main effect of the treatments, GFN and alliin. This experiment used a 2^2-factor design. Before using the *DESeq* function to solve the linear model defined in chapter 4, equation1, we specified the following design formula which contains factors for each of the treatments:

$$design = \sim GFN + alliin$$

This experiment design informs the statistical model to account for the variation in the mean expression data for each treatment.

A differential expression test was also conducted to test whether there is any significant interaction between the treatments, using the design formula:

$$design = \sim GFN + alliin + GFN:alliin$$

The test using the interaction term, allow us to test whether the log2 fold change in a treatment is influenced by the other treatment, this is, if the effect seen by GFN is *different* based on alliin and vice versa.

For this analysis, DESeq2's automatic replacement of counts with large Cook's distance was disabled, as previously discussed in chapter 4.

To account for possible bias in fold change due to low counts of highly variable counts that can result in ineffective ranking of counts by effect size, the Approximate Posterior Estimation for GLM method, APEGLM was used (346).

5.4 Results

Given the transcriptional differences demonstrated between control samples in the individual zones, the PZ and TZ samples from patients consuming Alliin and/or GFN interventions were subsequently analysed separately. The following results discuss the analysis of samples from the PZ of patients enrolled in the 'Norfolk-ADaPt' study. The analysis of samples from the TZ is presented in section 5.4.2.

5.4.1 Peripheral Zone

5.4.1.1 Assessing the Effect of Dietary Interventions on the Transcriptional Profile

One of the typical first steps in RNA-seq analysis is to examine the overall similarity between samples, which allows us to determine whether there is overall similarity between the gene expression in samples by calculating sample-to-sample distances. The Poisson distances is one option for calculating sample distances; it uses the raw gene counts, and it is a measure of dissimilarity between counts. This measure of dissimilarity is commonly used as it takes into consideration the variance of the data when calculating the distances between samples (437). The Poisson dissimilarity matrix is calculated using the function PoissonDistance function from the library PoiClaClu version 1.0.2.1.

The sample distances can be visualised in a heatmap, which could be seen as a symmetric matrix of the distances, D, where each value d_{ij} represents the distance (pairwise dissimilarity) between sample i and sample j, where the larger the distance, the more dissimilar the two samples are.

The plot below, compares each sample in a symmetrical way (i.e. column vs. row) and demonstrates no obvious similarities between samples in the four treatment groups (as confirmed by the treatment codes on the right-hand side). For example, the dark cluster at the top left of the plot shows similarities between gene expression in 16 samples, which are however from multiple treatment groups.
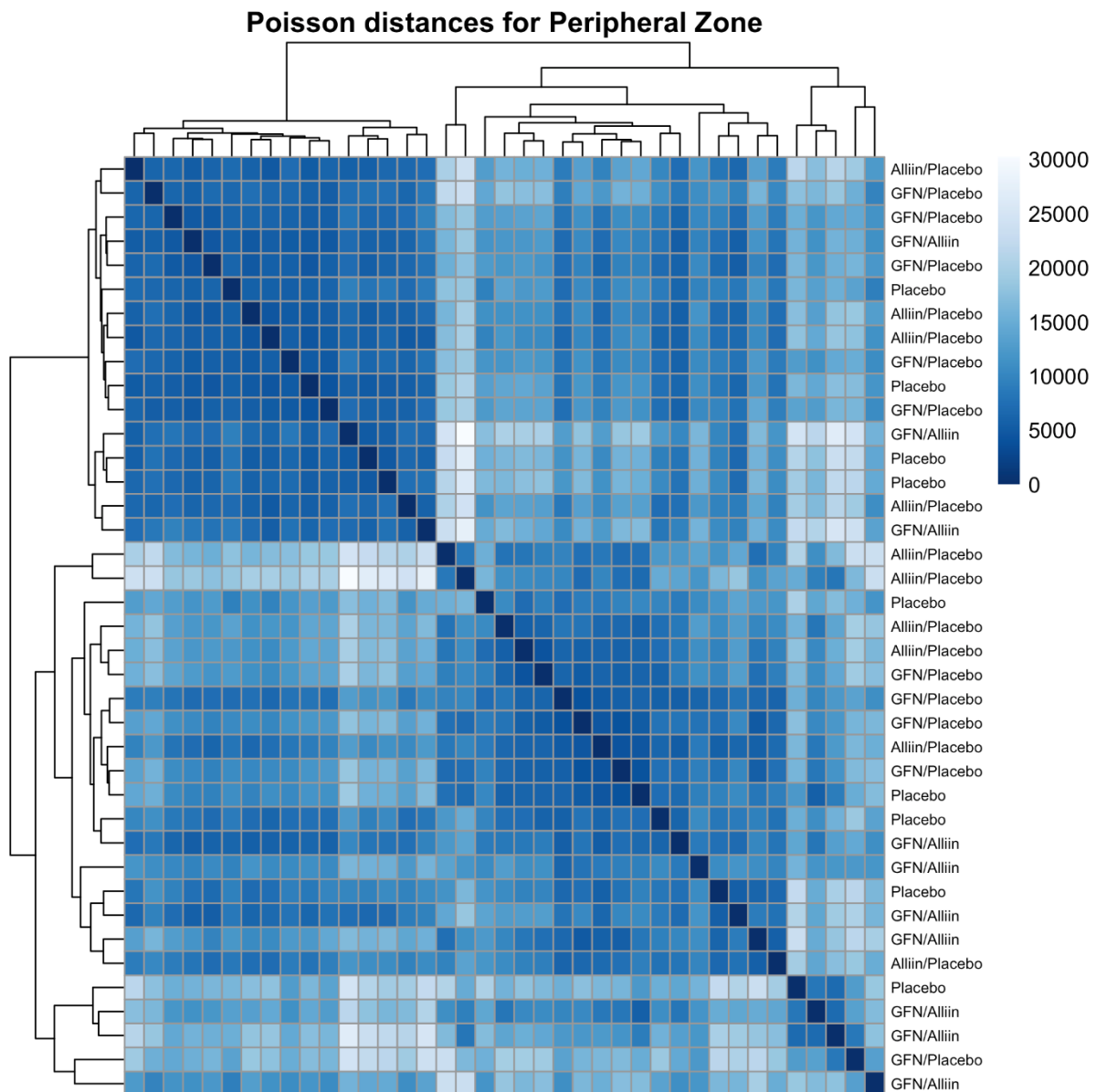
Figure 5. 1 Heatmap of sample-to-sample distribution of all samples in the peripheral zone by intervention using Poisson distances. Colour represents the Poisson distance between two given samples; a small Poisson distance (dark blue), represents low dissimilarity between samples (for example the dark blue diagonal line is a sample compared to itself and is hence the same), in contrast, a large Poisson distance (light blue), represents large dissimilarity.

As previously described in chapter four, another way to visualise sample-to-sample distances is via the formation of PCA plots, whereby similarities and differences between samples are demonstrated in an unsupervised manner. Here, a PCA plot was initially produced using VST transformed data to ascertain whether there was any clustering between control samples (placebo intervention) compared to those consuming any intervention (i.e. GFN or Alliin supplements). Ideally, in this plot,

we would like to see 3 separate clusters of samples (one of each placebo, GFN, and Alliin samples). As discussed in chapter four, we use the VST transformed data to ensure there is a roughly equal contribution from all genes.

Figure 5.2 shows the PCA plot for all control (placebo/placebo) samples (shown in blue n=9) vs. all intervention samples (shown in red n=30). There is some clustering in the control samples (blue triangles, highlighted within the blue circle) with more variation in samples from patients consuming interventions (red circles), however, this difference is not enough to separate and analyse. The same placebo sample previously highlighted as an outlier in chapter four (figure 4.4), is again demonstrated as the blue triangle external to this cluster.
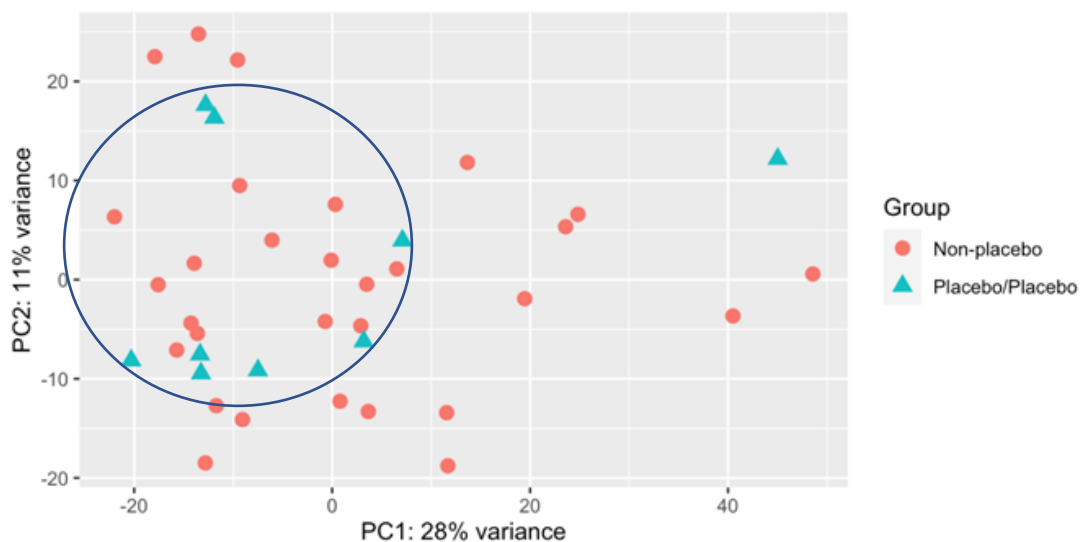
Figure 5. 2 Principle component analysis of control samples (blue triangles n=9) vs. all interventions (red dots, n=30) in the peripheral zone. Some clustering is demonstrated in the control group (placebo intervention) highlighted within the blue circle. More variation is demonstrated in the treatment groups. The blue ellipsis is added manually following analysis for visual purposes only and is not an internal function of the analysis.

By highlighting and labelling the samples in a different manner, a PCA plot was produced to demonstrate the samples from participants consuming GFN-containing supplements, vs. any intervention not containing GFN. Figure 5.3 shows the PCA plot for participants consuming GFN (blue squares and crosses, n=20) vs. participants consuming an intervention containing no GFN (red dots and triangles, n=19). There appears to be some similarities between the variation in gene expression in those consuming GFN/placebo (blue squares, clustered in the blue circle). However,

when GFN is combined with Alliin (blue crosses), this separation disappears and there is greater

variation between samples (samples shown in red circle)
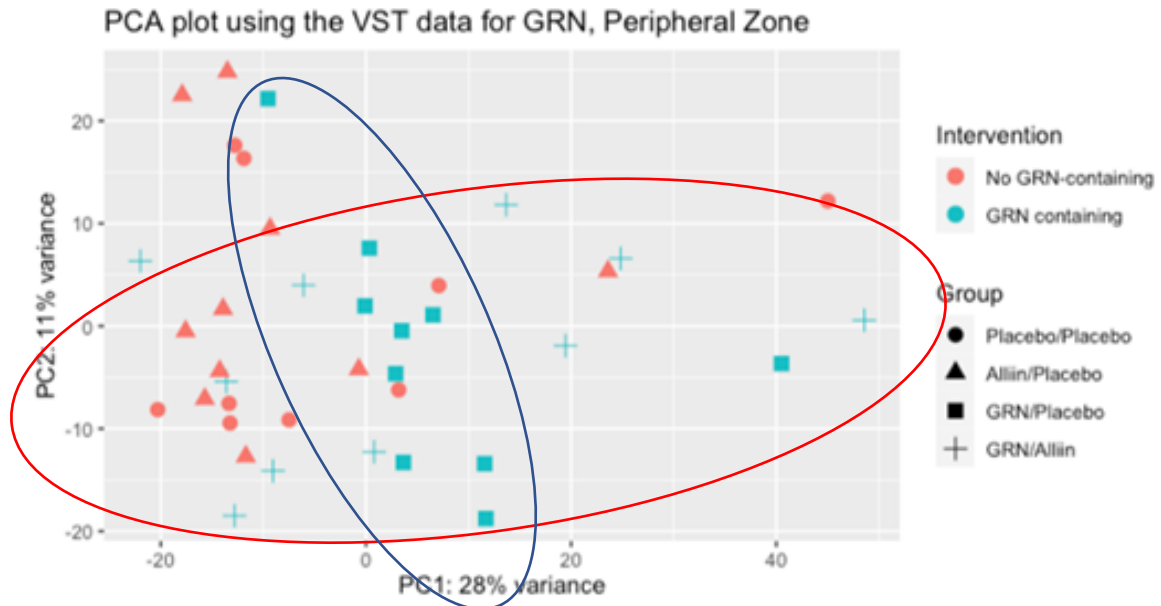
Figure 5. 3 Principle component analysis of glucoraphanin-containing intervention (blue squares and crosses

n=20) vs. a non GFN-containing intervention (red dots and triangles n=19) in the peripheral zone. The blue circle

highlights some clustering of samples in the GFN/Placebo intervention group (blue squares), which appears to

disappear in samples where GFN is combined with Alliin (blue crosses). Blue and red ellipses are manually

added following analysis for visual purposes only and is not an internal function of the analysis.

By again highlighting the samples in a different manner, figure 5.4 shows the PCA plot for the same

samples for participants consuming Alliin (blue triangles and crosses, n=20) vs. participants

consuming an intervention containing no Alliin (red dots and squares, n=19). There appears to be

some similarities between the variation in gene expression in those consuming Alliin/placebo (blue

triangles), with greater variation in samples from those consuming GFN/Alliin combination as

previously demonstrated (blue crosses).

PCA plot using the VST data for Alliin, Peripheral Zone
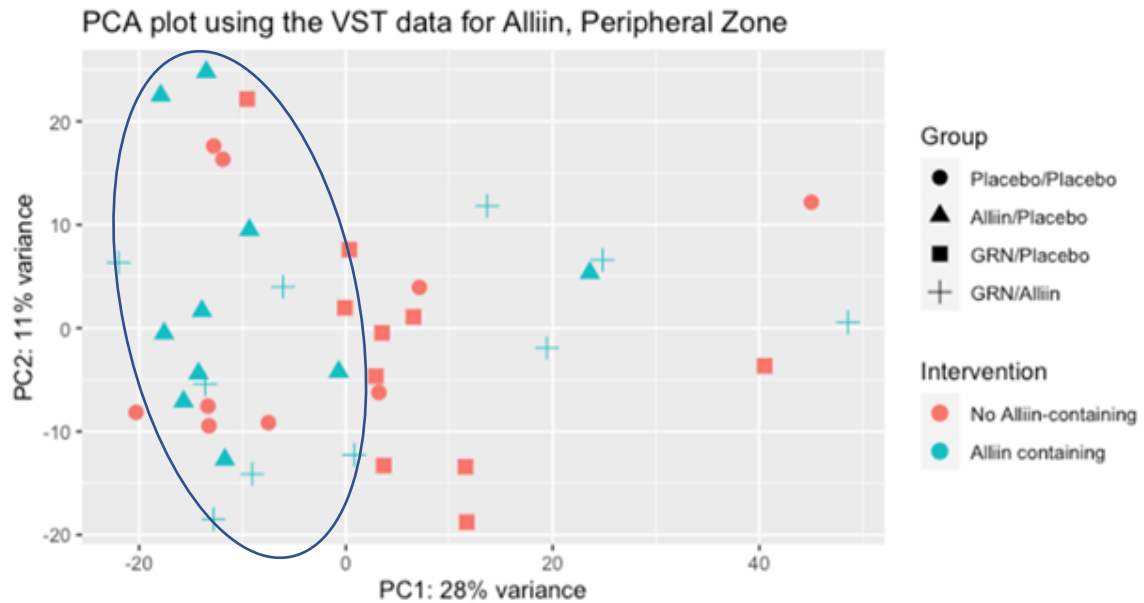
Figure 5. 4 Principle component analysis of Alliin-containing intervention (blue triangles and crosses n=20) vs. Non-Alliin containing intervention (red dots and squares n=19) in the peripheral zone. More similarity is seen between samples in the Alliin/Placebo group (as highlighted in the blue clustering circle) compared to an increased variability in the Alliin/GFN combination group. The blue ellipsis is added manually following analysis for visual purposes only and is not an internal function of the analysis.

5.4.1.2 Differential Expression Analysis

Following DESEq2 independent filtering, differential expression analysis was undertaken to determine whether the GFN and/or Alliin interventions caused the differential expression of individual genes.

As previously discussed in chapter four, independent filtering is undertaken to remove weakly expressed genes, preventing them having an influence on the multiple-testing procedure. Extracted differentially expressed genes were then again used to produce a MA plots, this time to visualise and identify gene expression changes between the treatment groups within the PZ, in terms of log fold change (M – on Y-axis) and the log of the mean of normalised expression counts over all samples (A – on X-axis).

Figure 5.5 demonstrates the differentially expressed genes following a GFN-containing intervention compared to a non-GFN containing intervention following normalisation based on log fold changes (LFCs). The MA-plot shows that there are differentially expressed genes in both directions of the

M=0 line, with the majority of log fold change between 0 and 2. The four red dots above the M=0 line represent 4 differentially expressed genes with an FDR-adjusted p value ≤ 0.1. An MA-plot for differentially expressed genes following an Alliin-containing intervention vs. a non-Alliin containing intervention is shown in figure 5.6. In comparison, there is only one red dot representing a significantly differentially expressed gene with an FDR-adjusted p value ≤ 0.1, which is below the M=0 line and therefore downregulated.
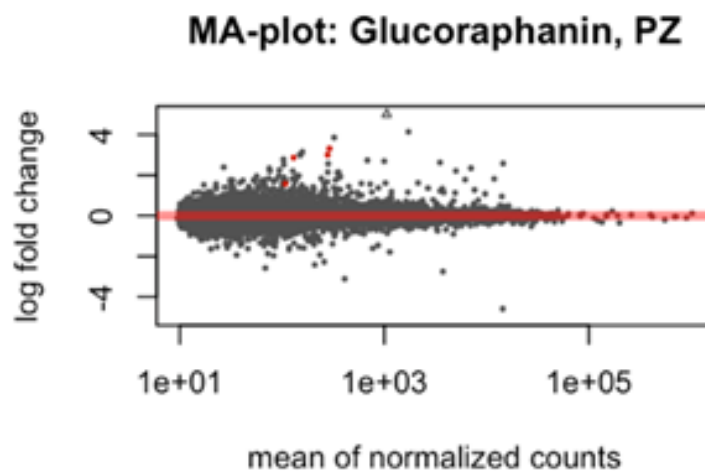
Figure 5. 5 Heatmap of differentially expressed genes in participants consuming a glucoraphanin-containing intervention vs. a non-glucoraphanin intervention (following transformation of normalised counts with log-fold shrinkage) in the peripheral zone. Each dot represents one genomic feature (n=25,300). The red dots indicate four differentially expressed genes (upregulated) with an FDR-adjusted p value ≤ 0.1.

MA-plot: Alliin, PZ
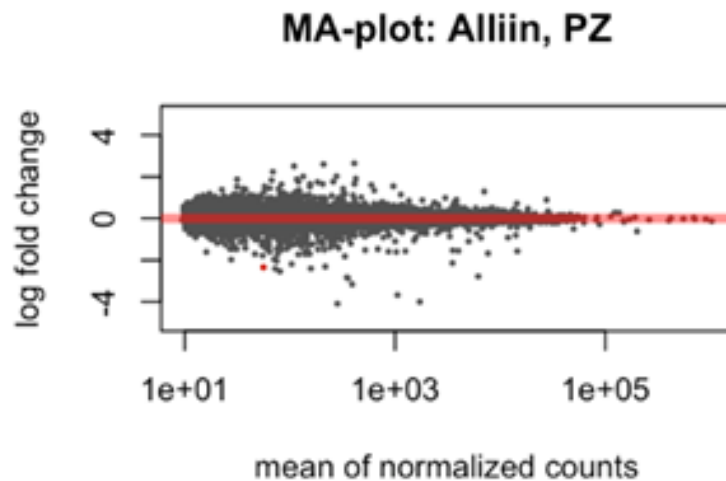
Figure 5. 6 Heatmap of differentially expressed genes in participants consuming an Alliin-containing intervention vs. a non-Alliin intervention (following transformation of normalised counts with log-fold shrinkage) in the peripheral zone. Each dot represents one genomic feature (n=25,300). The red dot indicates one differentially expressed gene (downregulated) with an FDR-adjusted p value ≤ 0.1.

As was eluded to in the MA plots, differential expression analysis demonstrated that different numbers of genes are differentially expressed for the two different interventions in the PZ. The below table demonstrates the numbers of differentially expressed genes at differing levels of significance in the PZ for participants consuming GFN-containing interventions compared to a non-GFN containing intervention, and Alliin-containing interventions vs. non-Alliin containing interventions.

In the PZ, 25,300 expressed genes pass independent filtering. Of these genes, 25,136 genes pass the Wald test (the hypothesis test used by DESeq2). The p values returned by the Wald Test are corrected for multiple testing using the False Discovery Rate (FDR) method based on the Benjamini-Hochberg, BH, algorithm.

Table 5.2 below demonstrates that 21 genes were differentially expressed in response to a GFN-containing intervention compared to a non-GFN containing intervention (padj ≤ 0.5), and 4 genes are differentially expressed at padj ≤ 0.1. In comparison, only 4 genes were differentially expressed in response to an Alliin-containing intervention compared to a non-Alliin containing intervention (padj ≤ 0.5), and only 1 gene was differentially expressed at padj ≤ 0.1.

Table 5. 2 Number of genes differentially expressed in participants consuming a glucoraphanin-containing intervention vs. non-glucoraphanin containing intervention (column 'Glucoraphanin PZ') and in participants consuming an Alliin-containing vs. non-Alliin containing intervention (column 'Alliin PZ') in the peripheral zone [1]

FDR-adjusted P value[2]	Glucoraphanin PZ	Alliin PZ
≤ 0.5	21 (18↑ 3↓)	4 (0↑ 4↓)
≤ 0.2	13 (13↑ 0↓)	3 (0↑ 3↓)
≤ 0.1	4 (4↑ 0↓)	1 (0↑1↓)
≤ 0.05	3 (3↑ 0↓)	1 (0↑1↓)
≤ 0.01	2 (2↑ 0↓)	0 (0↑0↓)

[1]FDR, false discovery rate; ↑ indicate upregulation in gene expression. ↓ indicate downregulation in gene expression.

[2]Wald test, adjusted for multiple testing correction by Benjamini–Hochberg.

This data highlights two interesting observations; GFN-containing interventions appear to have a greater impact on the differential expression of genes in the PZ than Alliin; and GFN and Alliin interventions appear to be working in different (and opposing) ways i.e. GFN appears to be causing an increase in expression (upregulation) of the differentially expressed genes, compared to Alliin, in which expression of differentially expressed genes is decreased (downregulated).

In order to assess the commonalities in differentially expressed genes among the two intervention types, Venn diagrams were constructed (see figure 5.7).

Figure 5. 7 Differentially expressed genes in the peripheral zone following GFN and Alliin containing interventions compared to a non GFN or Alliin containing intervention. A) with adj p.value <0.5, B) adj. p.value <0.1 and C) adj. p.value <0.05. P values adjusted for multiple testing correction by Benjamini–Hochberg. The bottom right number represents total number of genes that return a p-value minus the number of genes with p-value smaller than the described threshold.

Figure 5.7 demonstrates that even at a relatively high adj. p value (<0.5), there are no commonalities in the differentially expressed genes following an intervention with either treatment. i.e. none of the differentially expressed genes in the GFN group were also differentially expressed in the Alliin group, and vice versa. This interesting observation highlights that not only are GFN and Alliin working in an opposing manner (GFN appears to cause increased relative expression of differentially expressed genes whereas Alliin causes a decreased relative expression) as demonstrated in table 5.2, but that

they are in fact working in completely independent ways, by altering the expression of entirely different genes.

To elucidate these expressional changes further, the top 10 differentially expressed genes were then filtered and analysed.

5.4.1.3 Top 10 Differentially Expressed Genes

5.4.1.3.1 Glucoraphanin

Differential expression analysis demonstrates that consuming GFN causes the increased expression of several genes as discussed above. The top ten differentially expressed genes in participants consuming a GFN-containing intervention are shown in table 5.3. Only the top four genes are significantly differentially expressed (padj ≤ 0.1), and all demonstrate a positive log fold change (upregulation in expression).

Table 5. 3 The top ten differentially expressed genes in the peripheral zone of patients consuming a GFN-containing intervention (n=20) compared to a non-GFN containing intervention (n=19).

ensemblID	Gene Name	log2FoldChange	lfcSE	padj	Description
ENSG00000242534	IGKV2D-28	2.752	0.621	0.004	immunoglobulin kappa variable 2D-28
ENSG00000244116	IGKV2-28	3.044	0.685	0.004	immunoglobulin kappa variable 2-28
ENSG00000211947	IGHV3-21	2.541	0.696	0.025	immunoglobulin heavy variable 3-21
ENSG00000181847	TIGIT	1.392	0.385	0.065	T cell immunoreceptor with Ig and ITIM domains
ENSG00000211900	IGHJ6	2.414	0.730	0.114	immunoglobulin heavy joining 6
ENSG00000211679	IGLC3	2.296	0.690	0.114	immunoglobulin lambda constant 3 (Kern-Oz+ marker)
ENSG00000211659	IGLV3-25	2.720	0.849	0.123	immunoglobulin lambda variable 3-25
ENSG00000211892	IGHG4	2.322	0.728	0.123	immunoglobulin heavy constant gamma 4 (G4m marker)
ENSG00000198535	C2CD4A	2.034	0.669	0.126	C2 calcium dependent domain containing 4A
ENSG00000253755	IGHGP	2.345	0.755	0.126	immunoglobulin heavy constant gamma P (non-functional)

[1]Padj = FDR-adjusted p value,

[2]lfcSE = log2fold change standard error

Table 5.3 demonstrates that all differentially expressed genes are involved in immune regulation, in particular antigen binding via the variable region of immunoglobulins. This is an interesting finding given the known mechanisms of immune evasion associated with cancer development, and particularly PCa (as described in chapter 1). The increased expression of TIGIT (log2foldchange 1.392 padj 0.065) is of particular interest with regards to PCa, given its emerging interest as a potential target in cancer immunotherapy, and is discussed further in section 5.5 'discussion'.

5.4.1.3.2 Alliin

The top ten differentially expressed genes in participants consuming an Alliin-containing intervention are shown in table 5.4. Only one gene (mesothelin) is significantly differentially expressed (padj ≤ 0.1), although with a negligible negative log fold change (downregulation).

Table 5. 4 The top ten differentially expressed genes in the peripheral zone of patients consuming an Alliin-containing intervention (n=20) compared to a non-Alliin containing intervention (n=19).

ensemblID	Gene Name	log2FoldChange	lfcSE	padj	Description
ENSG00000102854	MSLN	0.000	0.001	0.012	mesothelin
ENSG00000211677	IGLC2	-2.450	0.678	0.115	immunoglobulin lambda constant 2
ENSG00000211676	IGLJ2	0.000	0.001	0.148	immunoglobulin lambda joining 2
ENSG00000114854	TNNC1	0.000	0.001	0.410	troponin C1, slow skeletal and cardiac type
ENSG00000127249	ATP13A4	1.124	0.458	0.707	ATPase 13A4
ENSG00000196796	NPIPB10P	0.782	0.297	0.707	nuclear pore complex interacting protein family, member B10, pseudogene
ENSG00000196436	NPIPB15	1.241	0.489	0.707	nuclear pore complex interacting protein family member B15
ENSG00000100626	GALNT16	0.372	0.150	0.707	polypeptide N-acetylgalactosaminyltransferase 16
ENSG00000264230	ANXA8L1	-0.853	0.343	0.707	annexin A8 like 1
ENSG00000259976	AC093010.2	-1.215	0.430	0.707	novel transcript

[1]*Padj = FDR-adjusted p value,*

[2]*lfcSE = log2fold change standard error*

5.4.1.4 Effect of intervention on nuclear factor (erythroid-derived 2)-like 2–regulated

genes

As discussed in section 5.1, both Sulforaphane and Alliin metabolites are documented to be Nrf-2 inducers. From the RNA sequenced data, the expression of previously defined Nrf-2 target genes were therefore extracted (98). Table 5.5 lists these genes with their corresponding adj-p-values. No change in expression was demonstrated in any Nrf-2-regulated genes in either the GFN or Alliin interventions (Benjamini–Hochberg FDR-adjusted P value ≤ 0.1).

Table 5. 5 Expression of Nrf-2 associated genes in participants consuming a GFN-containing intervention vs. non-GFN containing intervention, and an Alliin vs. non-Alliin containing intervention in the peripheral zone. No significant change in expression is demonstrated in either group.

Gene Name	EnsemblID	GRN			Alliin		
		log2foldchange	pvalue	padj	log2foldchange	pvalue	padj
ALDH1A1	ENSG00000165092	0.000	0.767	1.000	0.000	0.083	1.000
GSTP1	ENSG00000084207	0.000	0.250	1.000	0.000	0.250	1.000
ME1	ENSG00000065833	0.000	0.417	1.000	0.000	0.543	1.000
NQO1	ENSG00000181019	0.000	0.550	1.000	0.000	0.893	1.000
ABCC3	ENSG00000108846	0.000	0.751	1.000	0.000	0.746	1.000
AKR1B1	ENSG00000085662	0.000	NA	NA	0.000	NA	NA
GPX2	ENSG00000176153	0.000	0.072	1.000	0.000	0.105	1.000
ABCC5	ENSG00000114770	0.000	0.459	1.000	0.000	0.737	1.000
PNPLA2	ENSG00000177666	0.000	0.682	1.000	0.000	0.364	1.000
ACOX2	ENSG00000168306	0.000	0.381	1.000	0.000	0.072	1.000
ABCC4	ENSG00000125257	0.000	0.331	1.000	0.000	0.700	1.000
MGST1	ENSG00000008394	0.000	0.738	1.000	0.000	0.643	1.000
LIPH	ENSG00000163898	0.000	0.498	1.000	0.000	0.185	1.000
BLVRA	ENSG00000106605	0.000	0.609	1.000	0.000	0.850	1.000
FECH	ENSG00000066926	0.000	0.964	1.000	0.000	0.871	1.000
SLC7A11	ENSG00000151012	0.000	0.411	1.000	0.000	0.434	1.000
CEBPB	ENSG00000172216	0.000	0.846	1.000	0.000	0.958	1.000
ACOT8	ENSG00000101473	0.000	0.321	1.000	0.000	0.870	1.000
AHR	ENSG00000106546	0.000	0.846	1.000	0.000	0.986	1.000
NFE2L2	ENSG00000116044	0.000	0.248	1.000	0.000	0.588	1.000
G6PD	ENSG00000160211	0.000	0.993	1.000	0.000	0.341	1.000
PPARG	ENSG00000132170	0.000	0.858	1.000	0.000	0.644	1.000
UGDH	ENSG00000109814	0.000	0.081	1.000	0.000	0.851	1.000
HMOX1	ENSG00000100292	0.000	0.244	1.000	0.000	0.832	1.000
PGD	ENSG00000142657	0.000	0.418	1.000	0.000	0.442	1.000
AKR1C1	ENSG00000187134	0.000	0.254	1.000	0.000	0.030	1.000
TXNRD1	ENSG00000198431	0.000	0.469	1.000	0.000	0.900	1.000
TALDO1	ENSG00000177156	0.000	0.680	1.000	0.000	0.991	1.000
ABCC1	ENSG00000103222	0.000	0.746	1.000	0.000	0.716	1.000
ACOX1	ENSG00000161533	0.000	0.819	1.000	0.000	0.819	1.000
ACOT7	ENSG00000097021	0.000	0.487	1.000	0.000	0.741	1.000
PRDX6	ENSG00000117592	0.000	0.645	1.000	0.000	0.994	1.000
GLRX	ENSG00000173221	0.000	0.978	1.000	0.000	0.256	1.000
BLVRB	ENSG00000090013	0.000	0.927	1.000	0.000	0.982	1.000
GCLM	ENSG00000023909	0.000	0.388	1.000	0.000	0.668	1.000
PLA2G7	ENSG00000146070	0.000	0.737	1.000	0.000	0.883	1.000
EPHX1	ENSG00000143819	0.000	0.756	1.000	0.000	0.525	1.000
GCLC	ENSG00000001084	0.000	0.048	1.000	0.000	0.460	1.000
SRXN1	ENSG00000271303	0.000	0.654	1.000	0.000	0.641	1.000
TKT	ENSG00000163931	0.000	0.758	1.000	0.000	0.635	1.000
PPARGC1B	ENSG00000155846	0.000	0.136	1.000	0.000	0.139	1.000
ABCB6	ENSG00000115657	0.000	0.911	1.000	0.000	0.538	1.000
CBR1	ENSG00000159228	0.000	0.722	1.000	0.000	0.579	1.000
RXRA	ENSG00000186350	0.000	0.502	1.000	0.000	0.325	1.000
PTGR1	ENSG00000106853	0.000	0.615	1.000	0.000	0.924	1.000
KEAP1	ENSG00000079999	0.000	0.713	1.000	0.000	0.476	1.000
ALDH7A1	ENSG00000164904	0.000	0.776	1.000	0.000	0.685	1.000
SLC6A9	ENSG00000196517	0.000	0.434	1.000	0.000	0.279	1.000
GLS	ENSG00000115419	0.000	0.338	1.000	0.000	0.692	1.000
GPX4	ENSG00000167468	0.000	0.883	1.000	0.000	0.386	1.000
FTH1	ENSG00000167996	0.000	0.775	1.000	0.000	0.113	1.000
IDH1	ENSG00000138413	0.000	0.537	1.000	0.000	0.857	1.000
PRDX1	ENSG00000117450	0.000	0.977	1.000	0.000	0.726	1.000

5.4.1.5 Gene Set Enrichment Analysis

Although the number of genes differentially expressed by each intervention in the PZ was limited (as demonstrated in table 5. 2), there is a possibility that small consistent changes in important functional pathways could be occurring. In order to identify whether this was the case, GSEA was undertaken across all genes that passed the Wald Test (n=25,300), which were then mapped to unique ensembl IDs (n=25,057) ranked by their fold change and FDR adjusted P-value, as previously described (chapter 4 section 4.3.4.3). The number of genes that pass the Wald Test and genes that have a unique ensembl ID is different because the same ensembl ID is sometimes assigned to more than one gene name (for example if a gene has different transcripts).

Table 5.6 shows the GSEA of changes that occurred with an intervention containing GFN compared to a non-GFN containing intervention, and an Alliin-containing intervention compared to a non-Alliin containing intervention in the PZ. 26 of 42 gene sets returned a FDR-adjusted P value ≤ 0.05 in at least one compound in the PZ. A total of 9 gene sets (in white) are significant for both compounds in the PZ. 17 gene sets (highlighted in blue) are significant in the GFN-containing intervention group only. No gene sets were uniquely significant for the Alliin-containing intervention group only.

Table 5. 6 Gene set enrichment of changes that occurred in the treatments groups (FDR-adjusted P value ≤ 0.05); GFN-containing intervention compared to a non-GFN containing intervention, and an Alliin-containing intervention compared to a non-Alliin containing intervention in the peripheral zone. Sets in white boxes highlight the 9 sets which are significant for both compounds. Highlighted in blue are the 17 gene sets significant only for GFN. Pathway analysis was conducted using the GSEA software analysed by the Hallmark database.

Msig Db Pathway	GFN-Containing Intervention		Alliin-Containing Intervention	
	NES	padj	NES	padj
INTERFERON_GAMMA_RESPONSE	2.813	<0.001	-2.382	<0.001
INTERFERON_ALPHA_RESPONSE	2.475	<0.001	-2.648	<0.001
MYC_TARGETS_V2	1.954	<0.001	-1.925	<0.001
ALLOGRAFT_REJECTION	3.017	<0.001	-2.189	0.001
E2F_TARGETS	2.244	<0.001	-1.669	0.008
G2M_CHECKPOINT	2.139	<0.001	-1.540	0.023
TNFA_SIGNALING_VIA_NFKB	2.121	<0.001	-1.416	0.061
INFLAMMATORY_RESPONSE	2.382	<0.001	-1.356	0.088
MTORC1_SIGNALING	2.010	<0.001	-1.250	0.180
IL2_STAT5_SIGNALING	2.299	<0.001	-0.906	0.975
IL6_JAK_STAT3_SIGNALING	2.510	<0.001	-0.766	1.000
MYC_TARGETS_V1	1.928	<0.001	-2.146	0.001
COMPLEMENT	1.842	0.001	0.927	0.756
KRAS_SIGNALING_UP	1.808	0.001	-0.916	0.977
PI3K_AKT_MTOR_SIGNALING	1.775	0.001	-0.848	1.000
DNA_REPAIR	1.671	0.004	-1.743	0.005
UNFOLDED_PROTEIN_RESPONSE	1.592	0.008	-1.004	0.683
REACTIVE_OXYGEN_SPECIES_PATHWAY	1.527	0.016	-1.064	0.513
COAGULATION	1.510	0.017	1.133	0.535
ESTROGEN_RESPONSE_LATE	1.486	0.021	-1.307	0.125
XENOBIOTIC_METABOLISM	1.488	0.021	1.157	0.534
UV_RESPONSE_UP	1.465	0.025	-0.860	1.000
APOPTOSIS	1.423	0.036	-1.414	0.058
PEROXISOME	1.412	0.038	-0.752	1.000
P53_PATHWAY	1.403	0.039	-1.996	<0.001
GLYCOLYSIS	1.389	0.043	-0.766	1.000

[1]*E2F, E2 Factor; G2M, G2-M DNA damage checkpoint; GFN, glucoraphanin; IL2, interleukin 2; IL6, interleukin 6; JAK, Janus Kinase; KRAS, V-Ki-Ras2 Kirsten Rat Sarcoma 2 Viral Oncogene Homolog; MSigDb, Molecular Signature Database; MTORC1, mammalian target of rapamycin complex 1; MYC, myelocytomatosis; NES, normalized enrichment score; PI3K_AKT, Phosphoinositide 3-kinase_Protein kinase B; TNFA, tumor necrosis factor α; UV, ultraviolet. SIZE refers to the numbers of genes in the pathway. UV response DN refers to genes that are down regulated by UV radiation. UV response UP refers to genes that are up regulated by UV radiation. KRAS signalling UP refers to genes that are up regulated by KRAS signalling.*

[2]*padj, false discovery rate using Benjamini-Hochberg (BH) adjustment.*

[3]*GSEA by GSEA software version 4.0.3 on all genes ranked by the significance of fold change.*

Interestingly, as was also demonstrated in the differential expression analysis, Alliin and GFN interventions appear to be working in an opposing manner. 9 gene sets are significantly enriched (FDR-adjusted P value ≤ 0.05) in both the GFN-containing and Alliin-containing intervention groups. They include Interferon Alpha and Gamma, Myc Targets V1 and V2, Allograft rejection, E2F targets, G2M checkpoint, DNA repair and P53 pathway. In response to GFN, these 9 sets demonstrate upregulation (as evidenced by positive normalised enrichment scores from 1.4 to 3). In contrast, in response to Alliin, these enriched gene sets demonstrate downregulation (as evidenced by negative normalised enrichment scores from -1.5 to -2.6). The 17 gene sets which are significantly enriched only the GFN-containing intervention group all demonstrate upregulation.

26 gene sets in total are therefore significantly enriched in patients consuming a GFN-containing intervention. As demonstrated, these sets comprise a wide variety of pathways associated with cancer, including cell cycle progression, apoptosis, DNA repair, inflammatory and immune pathways. This pattern may not be unexpected given the multi-modal influence that these dietary metabolites have been shown to have *in vitro*.

The remaining 16 gene sets which were not significantly enriched in the PZ by either intervention are shown in table 5.7. Interestingly, pathways such as fatty acid metabolism and cholesterol homeostasis (products of which are known to be both upregulated in PCa and shown to be upregulated in control samples in the PZ compared to the TZ in the previous chapter), are not significantly enriched by either a GFN or Alliin containing intervention.

*Table 5. 7 The 16 gene sets which were **not** significantly altered in either a GFN-containing intervention vs. non-GFN containing intervention, or Alliin-containing intervention vs. non-Alliin containing intervention in the peripheral zone (FDR-adjusted P value > 0.05).*

Msig Db Pathway	GFN-Containing Intervention		Alliin-Containing Intervention	
	NES	padj	NES	padj
MYOGENESIS	-1.503	0.080	1.315	0.454
EPITHELIAL_MESENCHYMAL_TRANSITION	-1.327	0.085	1.398	0.397
FATTY_ACID_METABOLISM	1.300	0.090	-0.917	1.000
SPERMATOGENESIS	1.226	0.160	1.130	0.479
OXIDATIVE_PHOSPHORYLATION	1.172	0.231	-0.554	1.000
APICAL_SURFACE	-1.154	0.242	-1.107	0.451
ESTROGEN_RESPONSE_EARLY	1.105	0.338	0.940	0.774
BILE_ACID_METABOLISM	1.018	0.500	-0.870	1.000
KRAS_SIGNALING_DN	1.012	0.501	-1.190	0.266
ANGIOGENESIS	-1.022	0.504	0.911	0.749
CHOLESTEROL_HOMEOSTASIS	1.004	0.507	-0.813	1.000
ANDROGEN_RESPONSE	0.888	0.776	-1.071	0.520
HEME_METABOLISM	0.873	0.792	0.750	0.942
ADIPOGENESIS	0.805	0.906	0.782	0.964
PROTEIN_SECRETION	0.784	0.914	-0.546	0.999
NOTCH_SIGNALING	-0.611	0.996	1.201	0.581

[1]KRAS, V-Ki-Ras2 Kirsten Rat Sarcoma. KRAS signalling DN refers to genes that are down regulated by KRAS signalling. SIZE refers to the numbers of genes in the pathway. UV response DN refers to genes that are down regulated by UV radiation. UV response UP refers to genes that are up regulated by UV radiation.

[2]padj, false discovery rate using Benjamini-Hochberg (BH) adjustment.

[3]GSEA by GSEA software version 4.0.3 on all genes ranked by the significance of fold change.

5.4.2 Transition Zone

The following results describe the RNA-sequencing analysis of samples from the TZ of patient's enrolled on the 'Norfolk-ADaPt' study.

5.4.2.1 Assessing the Effect of Interventions on the Transcriptional Profile

As previously discussed, symmetric matrix or 'heatmaps' were formed to enable initial visualisation of samples following transformation, using Poisson distances. Figure 5.8, compares each sample in a symmetrical manner (column vs. row). Similar to the matrix previously presented for the PZ, there are no obvious clustering or similarities between samples.
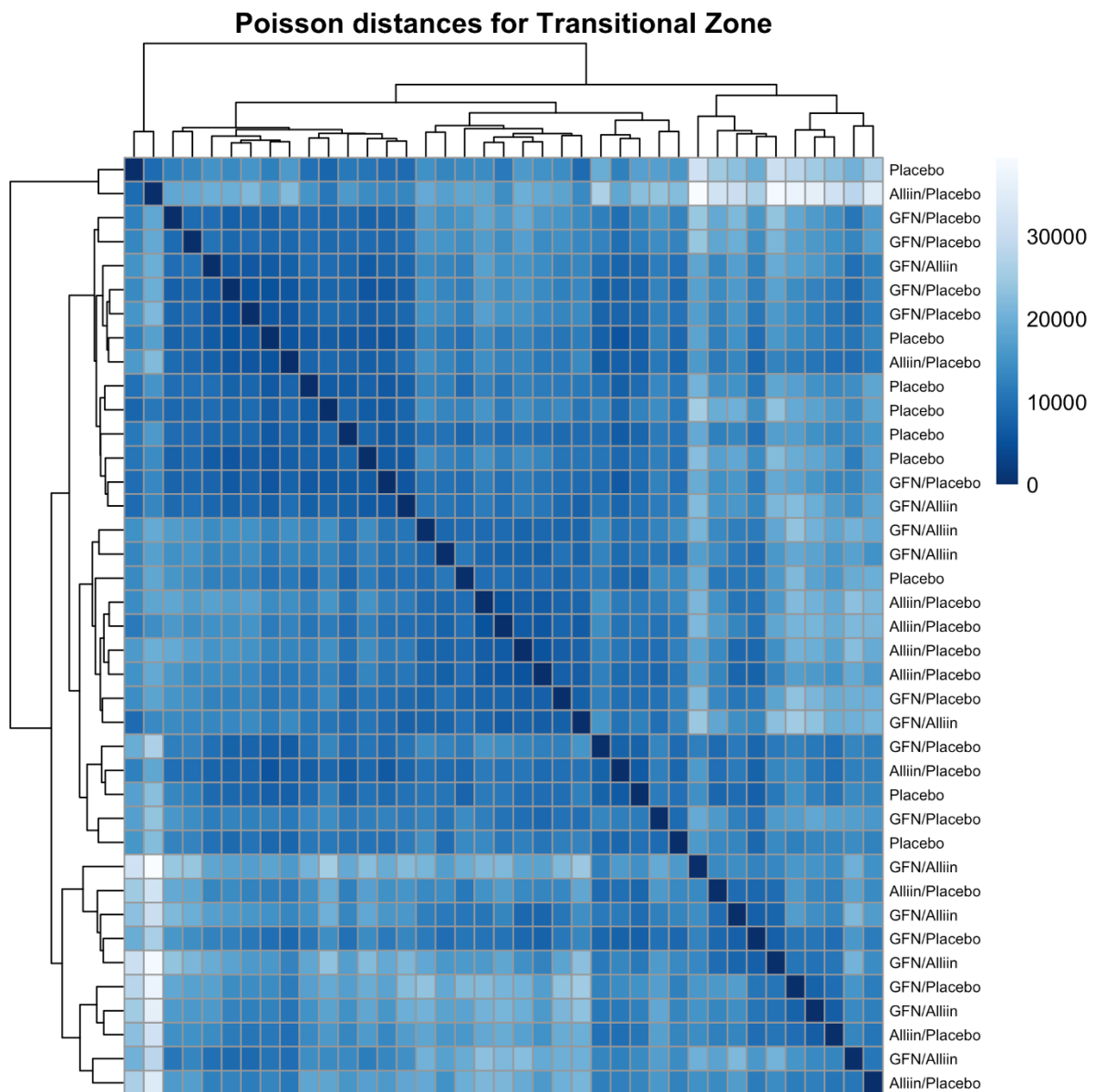
Figure 5. 8 Heatmap of sample-to-sample distribution of all samples in the transition zone by intervention using Poisson distances. Colour represents the Poisson distance between two given samples; a small Poisson distance (dark blue), represents low dissimilarity between samples (for example the dark blue diagonal line is a sample compared to itself and is hence the same), in contrast, a large Poisson distance (light blue), represents large dissimilarity.

PCA plots were then formed, whereby similarities and differences between samples are demonstrated in an unsupervised manner. A PCA plot was initially produced to ascertain whether there was any clustering between control samples (placebo/placebo) compared to those consuming

any intervention (i.e. GFN or Alliin supplements) in the TZ. Ideally, in this plot, we would like to see 3 separate clusters of samples (one of each placebo, GFN, and Alliin samples).

Figure 5.9 shows the PCA plot for all control (placebo/placebo) samples (shown in blue n=9) vs. all intervention samples (shown in red n=30) in the TZ. There is obvious clustering in the control samples (blue triangles, highlighted within the blue circle) with significantly more variation in samples from patients consuming interventions (red circles).
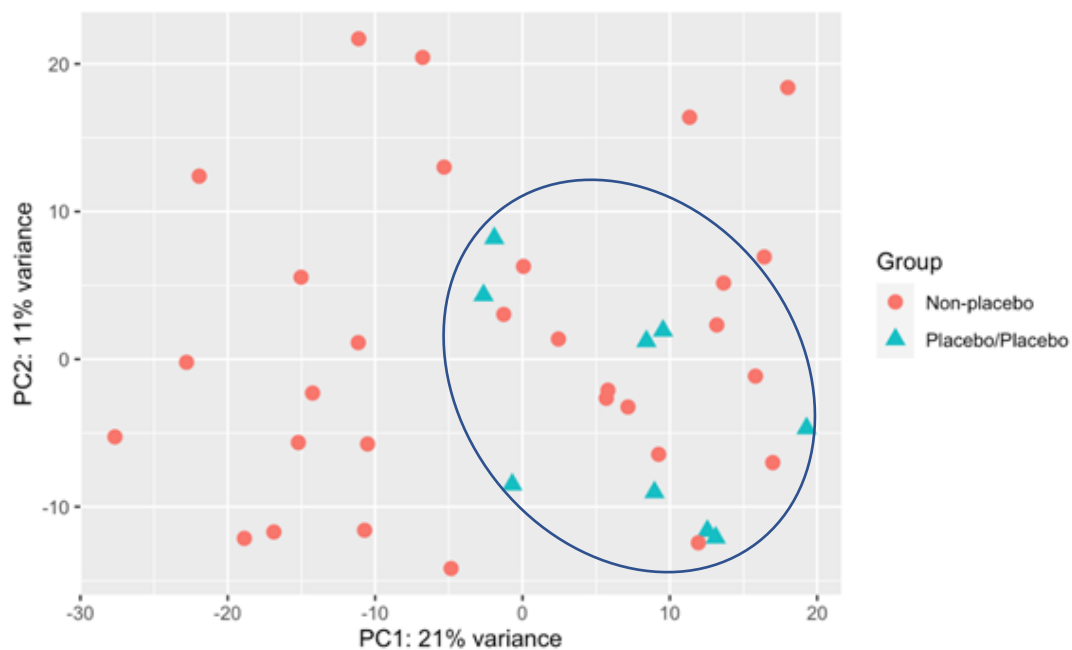
Figure 5. 9 Principle component analysis of control samples (blue triangles n=9) vs. all other interventions (red dots, n=30) in the transition zone. Clustering is demonstrated in the control group (placebo intervention) highlighted within the blue circle. More variation is demonstrated in the intervention groups. The blue ellipsis is added manually following analysis for visual purposes only and is not an internal function of the analysis.

By analysing and highlighting the samples in a different manner, a PCA plot was produced to demonstrate the samples from participants consuming GFN-containing supplements, vs. any intervention not containing GFN.

Figure 5.10 shows the PCA plot for participants consuming GFN (blue squares and crosses, n=20) vs. participants consuming an intervention containing no GFN (red dots and triangles, n=19). Similar to the results demonstrated for the PZ, there appears to be some similarities between the variation in gene expression in those consuming GFN/placebo (blue squares, clustered in the blue circle).

However, when GFN is combined with Alliin (blue crosses), this separation again seems to disappear and there is greater variation between samples (samples shown in red circle).
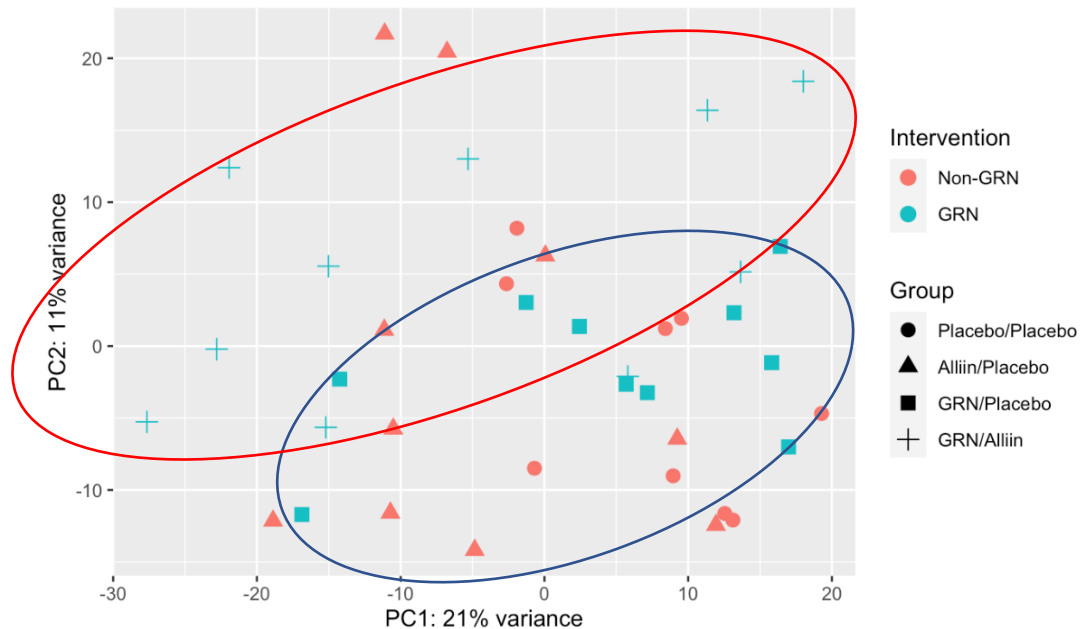
Figure 5. 10 Principle component analysis of glucoraphanin-containing intervention (blue squares and crosses n=20) vs. a non GFN-containing intervention (red dots and triangles n=19) in the transition zone. The blue circle highlights some clustering of samples in the GFN/Placebo intervention group, which seems to disappear in samples where GFN is combined with Alliin. The blue and red ellipses are added manually following analysis for visual purposes only and is not an internal function of the analysis.

By again highlighting the samples in a different manner, figure 5.11 shows the PCA plot for the same samples for participants consuming Alliin (blue triangles and crosses, n=20) vs. participants consuming an intervention containing no Alliin (red dots and squares, n=19).

As previously demonstrated on figure 5.10, samples from participants consuming a combination intervention of GFN and Alliin (blue crosses) demonstrate significant variance. Alliin treatment alone (blue triangles) does show some clustering demonstrating some similarity between samples (highlighted in the blue circle), although two samples lie outside this cluster on the y axis (highlighted in the red circle).
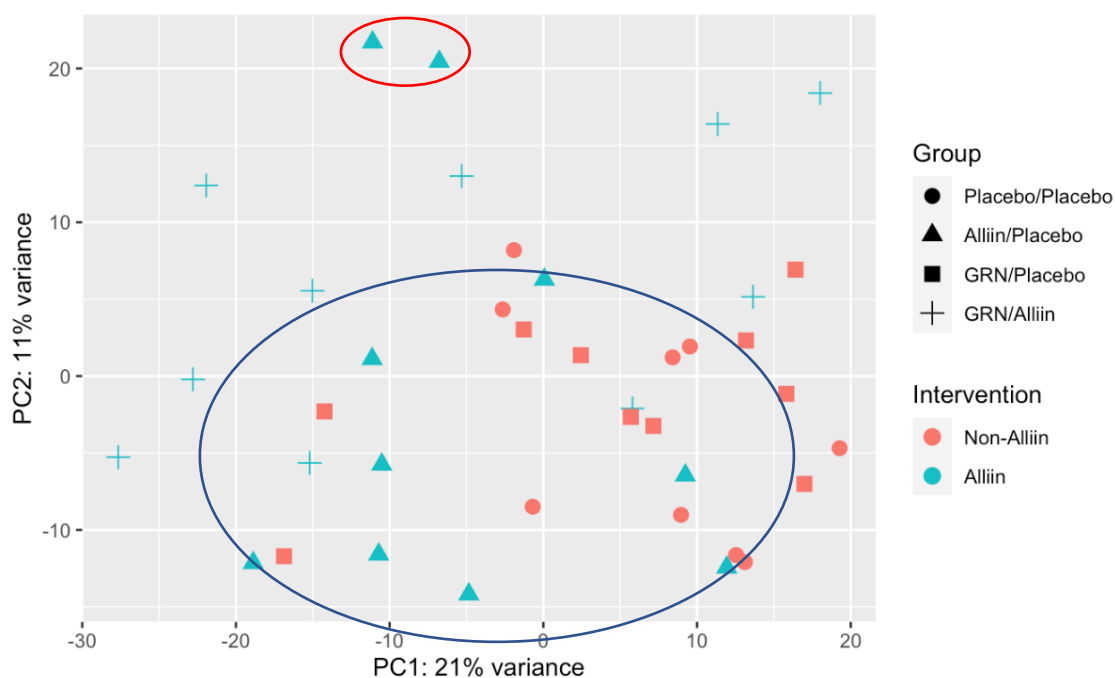
Figure 5. 11 Principle component analysis of Alliin (blue triangles and crosses n=20) vs. No Alliin (red dots and squares n=19) in the transition zone. More similarity is seen between samples in the Alliin/Placebo group (as highlighted in the blue clustering circle) compared to an increased variability in the Alliin/GFN combination group. Blue and red ellipses are manually added following analysis for visual purposes only and is not an internal function of the analysis.

5.4.2.2 Differential Expression Analysis

Following DESEq2 independent filtering, differential expression analysis was undertaken to determine whether interventions caused the differential expression of individual genes in the TZ.

Extracted differentially expressed genes were used to produce a MA plots, to visualise and identify gene expression changes between the treatment groups within the TZ, in terms of log fold change (M – on Y-axis) and the log of the mean of normalised expression counts over all samples (A – on X-axis).

Figure 5.12 demonstrates the differentially expressed genes following a GFN-containing intervention compared to a non-GFN containing intervention in the TZ. Normalisation was undertaken by DESeq2 based on shrinkage estimation of log fold changes (LFCs). The MA-plot shows that there are

differentially expressed genes in both directions of the M=0 line, with the majority of log fold change between 0 and 2. There are two red dots above the M=0 line which represent 2 differentially expressed genes (representing upregulation) with an FDR-adjusted p value ≤ 0.1, and two red dots below the M=0 line which represent 2 differentially expressed genes (representing downregulation) with an FDR-adjusted p value ≤ 0.1. An MA-plot for differentially expressed genes following an Alliin-containing intervention vs. a non-Alliin containing intervention in the TZ is shown in figure 5.13. In comparison, there are numerous red clusters both above and below the M=0 line, representing multiple significantly differentially expressed genes (both up and downregulated) with an FDR-adjusted p value ≤ 0.1.
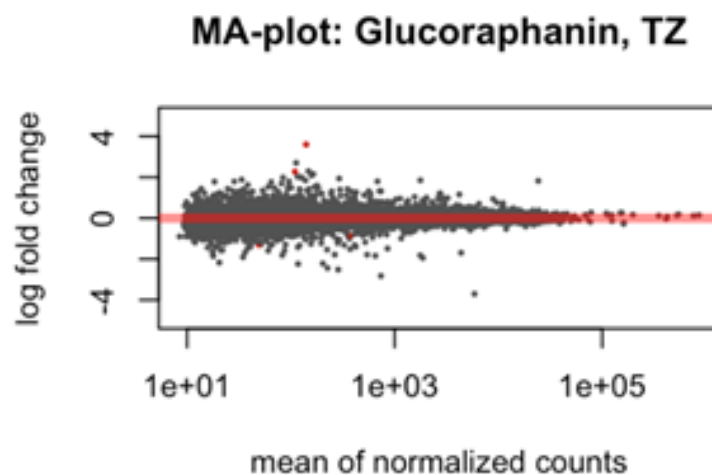
Figure 5. 12 Heatmap of differentially expressed genes in participants consuming a Glucoraphanin-containing intervention vs. a non-glucoraphanin containing intervention (following transformation of normalised counts with log-fold shrinkage) in the transition zone. Each dot represents one genomic feature (n=25,632). The red dots indicate two differentially expressed genes (upregulated) with an FDR-adjusted p value ≤ 0.1.
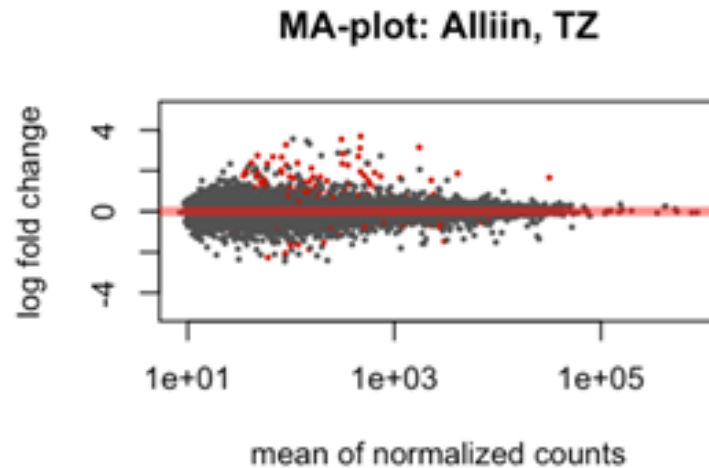
Figure 5. 13 Heatmap of differentially expressed genes in participants consuming an Alliin-containing intervention vs. a non-Alliin containing intervention (following transformation of normalised counts with log-fold shrinkage) in the transition zone. Each dot represents one genomic feature (n=25,632). The red dots indicate differentially expressed genes with an FDR-adjusted p value ≤ 0.1 either upregulated (above the M=0 line) or downregulated (below the M=0 line).

These MA plots highlight a very interesting finding. There appears to be a significant amount of differentially expressed genes as a result of Alliin treatment in the TZ. From initial glance, the majority of significantly expressed genes are upregulated (as demonstrated by the red dots above the M=0 line). This is further analysed in the next section.

5.4.2.3 Differentially Expressed Genes in the Transition Zone

Differential expression analysis demonstrated that different numbers of genes are differentially expressed for the two different interventions. The below table demonstrates the numbers of differentially expressed genes at differing levels of significance in the TZ for participants consuming a GFN-containing intervention compared to a non-GFN containing intervention, and an Alliin-containing intervention vs. non-Alliin containing intervention.

In the TZ, 25,632 expressed genes pass independent filtering. Of these genes, 25,572 genes pass the Wald test (the hypothesis test used by DESeq2). The p values returned by the Wald Test are corrected for multiple testing using the False Discovery Rate (FDR) method based on the Benjamini-Hochberg, BH, algorithm.

Table 5.8 below demonstrates that 302 genes were differentially expressed in response to a GFN-containing intervention compared to a non-GFN containing intervention (padj ≤ 0.5), but only 4 genes are differentially expressed at padj ≤ 0.1. In stark comparison however, 4061 genes were differentially expressed in response to an Alliin-containing intervention compared to a non-Alliin containing intervention (padj ≤ 0.5), and 145 genes remained differentially expressed at padj ≤ 0.1.

Table 5. 8 Number of genes differentially expressed in participants consuming a glucoraphanin-containing intervention vs. non-glucoraphanin containing intervention (column 'Glucoraphanin TZ') and in participants consuming an Alliin-containing vs. non-Alliin containing intervention (column 'Alliin TZ') in the transition zone [1]

FDR-adjusted P value[2]	Glucoraphanin TZ	Alliin TZ
≤ 0.5	302 (136↑ 166↓)	4061 (1978↑ 2083↓)
≤ 0.2	30 (11↑ 19↓)	563 (262↑ 301↓)
≤ 0.1	4 (2↑ 2↓)	145 (88↑ 57↓)
≤ 0.05	2 (1↑ 1↓)	42 (37↑ 5↓)
≤ 0.01	1 (1↑ 0↓)	10 (9↑ 1↓)

[1]*FDR, false discovery rate; ↑ indicate upregulation in gene expression. ↓ indicate downregulation in gene expression.*

[2]*Wald test, adjusted for multiple testing correction by Benjamini–Hochberg.*

This data highlights an interesting observation which was initially eluded to in figure 5.13; Alliin-containing interventions appear to have a greater impact on the differential expression of genes in the TZ than GFN. This finding is in keeping with the hypothesis that Alliin would have a greater effect on the transcriptional signature of the TZ given that Alliin was detected in the TZ of the prostate to significantly higher levels in those consuming an Alliin-containing intervention compared to a non-Alliin containing intervention.

In order to assess the commonalities in differentially expressed genes among the two treatment groups, Venn diagrams were constructed (see figure 5.14).
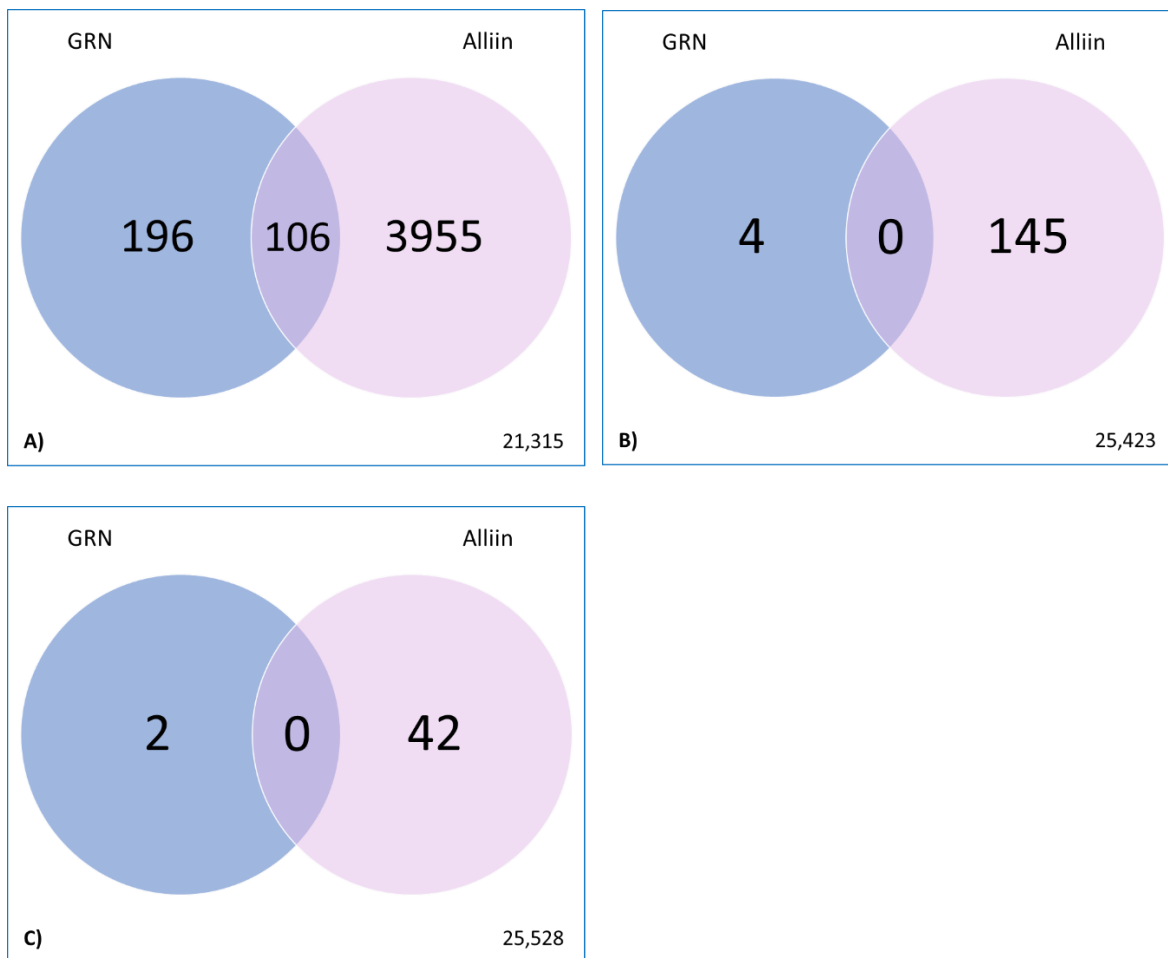
Figure 5. 14 Differentially expressed genes in the transition zone following GFN and Alliin containing interventions compared to a non -GFN or -Alliin containing intervention. A) with an FDR-adjusted p value <0.5, B) an FDR-adjusted p value <0.1 and C) an FDR-adjusted p value <0.05. P values adjusted for multiple testing correction by Benjamini–Hochberg. The bottom right number represents total number of genes that return a p-value minus the number of genes with p-value smaller than the described threshold.

Figure 5.14 A) demonstrates that at an FDR-adjusted p value <0.5, 106 of the 4363 differentially expressed genes in the TZ are differentially (and commonly) expressed in both groups (GFN and Alliin). This observation contrasts with the findings demonstrated in figure 5.7, where no differentially expressed genes were commonly expressed between treatments in the PZ. At slower FDR-adjusted p values however (figure 5.14 B) and C)), these commonalities disappear; there are no commonly differentiated genes at an FDR-adjusted p value <0.1 and 0.05.

To elucidate these expressional changes further, the top 10 differentially expressed genes were then filtered and analysed.

5.4.2.4 Top 10 Differentially Expressed Genes in the Transition Zone

5.4.2.4.1 Glucoraphanin

Differential expression analysis demonstrates that consuming GFN causes the increased expression of several genes as discussed above. The top ten differentially expressed genes in participants consuming a GFN-containing intervention are shown below. Only the top four genes are significantly differentially expressed (an FDR-adjusted p value ≤ 0.1).

Table 5. 9 The top ten differentially expressed genes in the transition zone of the patients consuming a GFN-containing intervention.

ensemblID	Gene Name	log2Fold Change	padj	Description	Gene Biotype
ENSG00000170373	CST1	3.329	0.002	cystatin SN	protein_coding
ENSG00000272668	AL590560.3	-0.751	0.040	uncharacterized LOC107985216	long non-coding RNA
ENSG00000126733	DACH2	2.010	0.061	dachshund family transcription factor 2	protein_coding
ENSG00000120471	TP53AIP1	-0.009	0.061	tumor protein p53 regulated apoptosis inducing protein 1	protein_coding
ENSG00000183888	SRARP	2.344	0.105	steroid receptor associated and regulated protein	protein_coding
ENSG00000224331	AC019181.1	0.448	0.114	pseudogene similar to part of ribosomal protein L10	processed_pseudogene
ENSG00000233251	AC007743.1	-0.573	0.179	novel transcript, antisense to CCDC85A	long non-coding RNA
ENSG00000164283	ESM1	-1.032	0.179	endothelial cell specific molecule 1	protein_coding
ENSG00000287499	AL357139.2	1.957	0.179	novel transcript	long non-coding RNA
ENSG00000183833	CFAP91	-0.384	0.179	cilia and flagella associated protein 91	protein_coding

Table 5.9 demonstrates that GFN-intervention appears to be causing the differential expression of both coding and long non-coding RNA. This is an interesting finding, given recent evidence which suggests that non-coding RNA may play an important role in cancer development, and is discussed alongside other findings in more detail in section 5.5 'discussion'.

5.4.2.4.2 Alliin

The top ten differentially expressed genes in participants consuming an Alliin-containing intervention are shown in table 5.10. 145 genes in total are differentially expressed with an FDR-

adjusted p value ≤ 0.1, however, presented are the top 10 differentially expressed genes with the lowest adjusted p values.

Table 5. 10 The top ten differentially expressed genes in the transition zone of the patients consuming an Alliin-containing intervention.

ensemblID	Gene Name	log2Fold Change	padj	Description	Gene Biotype
ENSG00000109063	MYH3	1.566	0.004	myosin heavy chain 3	protein_coding
ENSG00000187122	SLIT1	1.141	0.004	slit guidance ligand 1	protein_coding
ENSG00000120729	MYOT	1.544	0.004	myotilin	protein_coding
ENSG00000114854	TNNC1	2.456	0.004	troponin C1, slow skeletal and cardiac type	protein_coding
ENSG00000173991	TCAP	2.577	0.004	titin-cap	protein_coding
ENSG00000184226	PCDH9	-0.423	0.005	protocadherin 9	protein_coding
ENSG00000159173	TNNI1	2.040	0.007	troponin I1, slow skeletal type	protein_coding
ENSG00000239474	KLHL41	1.757	0.007	kelch like family member 41	protein_coding
ENSG00000172399	MYOZ2	1.708	0.007	myozenin 2	protein_coding
ENSG00000235749	AL390860.1	1.563	0.009	novel transcript, antisense to OR13G1, OR6F1 and OR14A2	lncRNA

Table 5.10 does not appear to highlight any obvious patterns in the types of genes differentially expressed, other than that they are all protein-coding in nature. Myotilin encodes a cytoskeleton protein, and SLIT1 is involved in molecular guidance during cell migration during neural development. MYH3 has previously been identified as a potential 'hub gene', which may play an important role in the PTEN mutation pathway in PCa. Although not in the top ten, PTEN was also interestingly downregulated in response to an Alliin-containing intervention in the TZ (-0.163 padj 0.190).

5.4.2.5 Gene Set Enrichment Analysis

As previously discussed, GSEA using the Molecular Signatures Database (MSigDN) hallmark gene set was undertaken. GSEA was used in this comparison to ascertain whether functional biological pathways are influenced by GFN and/or Alliin interventions within the TZ.

All 42 of 42 gene sets in the hallmark gene set analysis returned an FDR-adjusted p value ≤ 0.05 in at least one compound in the TZ. A total of 14 gene sets were significant for both compounds in the TZ.

21 gene sets were significant in the GFN-containing intervention group only. 7 gene sets were significant in the GFN-containing intervention group only.

Table 5.11 below shows the gene sets which were significantly returned for both compounds in the TZ.

Table 5. 11 Gene set enrichment of the 14 significant gene sets (FDR-adjusted p value ≤ 0.05) that occurred in both treatment groups in the transition zone.

Msig Db Pathway	GFN-Containing Intervention		Alliin-Containing Intervention	
	NES	padj	NES	padj
ALLOGRAFT_REJECTION	2.412	<0.001	-3.030	<0.001
INTERFERON_GAMMA_RESPONSE	2.761	<0.001	-2.783	<0.001
IL6_JAK_STAT3_SIGNALING	2.226	<0.001	-2.467	<0.001
TNFA_SIGNALING_VIA_NFKB	2.180	<0.001	-2.397	<0.001
INTERFERON_ALPHA_RESPONSE	2.820	<0.001	-2.337	<0.001
ANDROGEN_RESPONSE	2.130	<0.001	1.970	<0.001
INFLAMMATORY_RESPONSE	1.877	<0.001	-2.570	<0.001
E2F_TARGETS	1.725	0.001	-2.219	<0.001
KRAS_SIGNALING_UP	1.616	0.003	-2.213	<0.001
COMPLEMENT	1.527	0.008	-2.535	<0.001
APOPTOSIS	1.792	<0.001	-1.858	0.001
IL2_STAT5_SIGNALING	1.840	<0.001	-1.808	0.002
G2M_CHECKPOINT	1.630	0.003	-1.662	0.003
CHOLESTEROL_HOMEOSTASIS	2.241	<0.001	1.634	0.007

[1]E2F, E2 Factor; G2M, G2-M DNA damage checkpoint; GFN, glucoraphanin; IL2, interleukin 2; IL6, interleukin 6; JAK, Janus Kinase; KRAS, V-Ki-Ras2 Kirsten Rat Sarcoma 2 Viral Oncogene Homolog; MSigDb, Molecular Signature Database; NES, normalized enrichment score; TNFA, tumour necrosis factor α; SIZE refers to the numbers of genes in the pathway. KRAS signalling UP refers to genes that are up regulated by KRAS signalling.

As was demonstrated in the PZ, all significantly returned gene sets in response to a GFN-containing intervention demonstrate upregulation (a positive normalised enrichment score), compared to an Alliin-containing intervention which caused the downregulation (a negative normalised enrichment score) of the same gene sets (with the exception of cholesterol homeostasis and androgen response). This again demonstrates that GFN and Alliin appear to be working in an opposing manner.

Table 5.12 below shows the gene sets which were significantly returned for a GFN-containing intervention in the TZ.

Table 5. 12 Gene set enrichment analysis of patients consuming a GFN-intervention in the transition zone. The 21 sets which returned a significant FDR-adjusted p value ≤ 0.05) in response to a GFN-containing intervention only are demonstrated.

Msig Db Pathway	GFN-Containing Intervention	
	NES	padj
UV_RESPONSE_UP	2.034	0.000
ESTROGEN_RESPONSE_EARLY	1.530	0.008
REACTIVE_OXYGEN_SPECIES_PATHWAY	1.896	0.000
P53_PATHWAY	1.861	0.000
DNA_REPAIR	2.059	0.000
FATTY_ACID_METABOLISM	1.955	0.000
HEME_METABOLISM	1.955	0.000
XENOBIOTIC_METABOLISM	1.635	0.003
PI3K_AKT_MTOR_SIGNALING	1.704	0.002
MYC_TARGETS_V1	2.630	0.000
ESTROGEN_RESPONSE_LATE	1.535	0.008
ADIPOGENESIS	1.547	0.007
BILE_ACID_METABOLISM	1.600	0.004
PROTEIN_SECRETION	2.022	0.000
GLYCOLYSIS	2.223	0.000
MTORC1_SIGNALING	2.532	0.000
PEROXISOME	1.735	0.001
MYC_TARGETS_V2	2.163	0.000
SPERMATOGENESIS	1.627	0.003
OXIDATIVE_PHOSPHORYLATION	2.400	0.000
UNFOLDED_PROTEIN_RESPONSE	1.937	0.000

[1]*GFN, glucoraphanin; MSigDb, Molecular Signature Database; MTORC1, mammalian target of rapamycin complex 1; MYC, myelocytomatosis; NES, normalized enrichment score; PI3K_AKT, Phosphoinositide 3-kinase_Protein kinase B; P53, tumour protein/suppressor p53; UV, ultraviolet. SIZE refers to the numbers of genes in the pathway. UV response UP refers to genes that are up regulated by UV radiation.*

21 gene sets were uniquely significantly returned in response to a GFN-containing intervention. As was also demonstrated in chapter 4, all returned sets demonstrate upregulation (a positive normalised enrichment score) in the TZ.

Table 5.13 below shows the gene sets which were significantly returned for an Alliin-containing intervention in the TZ.

Table 5. 13 Gene set enrichment analysis of patients consuming an Alliin-intervention in the transition zone. The 7 sets which returned a significant FDR-adjusted p value (≤ 0.05) in response to an Alliin-containing intervention only are demonstrated.

Msig Db Pathway	Alliin-Containing Intervention	
	NES	padj
MYOGENESIS	2.438	0.000
COAGULATION	-1.961	0.001
EPITHELIAL_MESENCHYMAL_TRANSITION	-1.716	0.003
NOTCH_SIGNALING	-1.603	0.007
APICAL_SURFACE	-1.559	0.010
ANGIOGENESIS	-1.538	0.011
KRAS_SIGNALING_DN	1.478	0.024

[1]GFN, glucoraphanin; MSigDb, Molecular Signature Database; NES, normalized enrichment score; SIZE refers to the numbers of genes in the pathway. KRAS signalling DN refers to genes that are down regulated by KRAS signalling.

5.5 Discussion

5.5.1 The Effect of Dietary Intervention in the Peripheral Zone

As demonstrated in chapter 3, SFN and the SFN metabolite SFN-NAC were detected in the PZ of the prostate to significantly higher levels than that of participants consuming a non-GFN containing intervention, which is likely due to reflux of these compounds which were significantly detected in the urine. In contrast, Alliin metabolites did not accumulate to significantly higher concentrations in the PZ of the prostate compared those consuming a non-Alliin containing intervention. It was therefore hypothesised that GFN would have a greater effect on the transcriptional signature of the PZ than Alliin.

Initial visual analysis of the data suggests that GFN samples appear to cluster together on PCA; a pattern which appeared to disappear when GFN is combined with Alliin, and vice versa. However, no interaction was demonstrated in the differential expression analysis to support this.

Differential expression analysis demonstrated that GFN did in fact have a greater impact on the PZ than Alliin, although modestly, causing 21 genes to be differentially expressed (FDR-adjusted P value <0.5), compared to 4 in the Alliin group. 2 of these differentially expressed genes remained significantly differentially expressed at FDR-adjusted P <0.01. Additionally, of the differentially expressed genes in the PZ, none were commonly expressed between the two different intervention types, even at p<0.5. The top four genes significantly differentially expressed (FDR-adjusted P value ≤ 0.1) in the GFN-containing intervention groups all demonstrate a positive log fold change (upregulation) and are all involved in immune regulation, in particular antigen binding via the variable region of immunoglobulins.

PCa, like several other cancers, develop multiple immune evasion mechanisms to enable them to escape the immune responses generated by the body (as well as those employed in immunotherapy) (438). These mechanisms include defective antigen presentation, defective T cell responses, and the development of an immunosuppressive microenvironment surrounding the tumour itself. Upregulation in genes relating to immune function as demonstrated in this study, may therefore provide a means of escaping development of tumour clones.

Interestingly, ENSG00000181847 encodes TIGIT (T cell immunoreceptor with immunoglobulin and immunoreceptor tyrosine-based inhibitory motif domain), which is emerging as a potential target in cancer immunotherapy and is upregulated in the PZ as a result of GFN treatment. TIGIT is a co-inhibitory receptor that is solely expressed on several classes of T cells and NK cells, and has received contrasting opinion regarding PCa. TIGIT is a member of the immunoglobulin superfamily of inhibitory receptors, which binds the poliovirus receptor (PVR) on tumour cells with high affinity to act as an immune checkpoint. Upon binding, TIGIT inhibits immune cell activation (downregulating the proliferation of both murine and human T cells), causing the increased secretion of IL-10 and decreased secretion of IL-12, thus suppressing T-cell activation by promoting the generation of mature immunoregulatory dendritic cells. TIGIT appears to have a complex role in cancer which is yet to be fully elucidated; TIGIT is expressed after the activation of T cells to mediate a cell-intrinsic inhibitory effect, compared to induction of TIGIT on NK cells which appears to inhibit cytotoxicity (439-441). Although the upregulation of this gene has previously demonstrated significance in both the development and progression of PCa, the subsequent increase in levels of IL-10 has been shown to have anti-tumourigenic and anti-angiogenic properties in both animal and *in vitro* models (442,

443). IL-10 appears to inhibit matrix metalloproteinase (MMP) 2 and 9 in PCa cell lines, reducing both tumour growth and tumour-cell angiogenesis thus preventing the tumour cells' ability to form microvasculature to enable metastasis (442).

The expressional changes associated with GFN treatment are also supported in the GSEA, which demonstrates that sets associated with immune regulation are impacted. In particular, the upregulation of IL-2 and TNFα signalling are demonstrated in those consuming a GFN-containing intervention, as well as known functional pathways associated with a potential reduction in carcinogenesis risk, such as apoptosis, DNA repair and reactive oxygen species response pathway. These findings are consistent with previous evidence that suggests that GFN-treatment may be capable of suppressing known oncogenic pathways (98).

The gene set 'IL-2 signalling' is significantly upregulated in the GFN-treated group only, and is an interesting observation. IL-2 is an essential cytokine and is noted to be a potential immune target for PCa. IL-2 is particularly well studied in relation to renal cell carcinoma, where it is widely utilised in immunotherapy for metastatic disease (444, 445). As previously discussed, prostate tumours accumulate T-regs, which inhibit THCs and deprive them of IL-2, whereas increased levels of IL-2 promote a pro-inflammatory M1 macrophage phenotype and thus a less favourable immune environment for PCa development and progression (434). Human trials have demonstrated that patients with metastatic hormone refractory PCa (HRPC) treated with zoledronate (a standard treatment) plus IL-2 for 12 months had a significantly higher survival rate than those treated with zoledronate monotherapy. In addition, of those who were still alive at 12-months, a longer progression-free period was demonstrated in the combination group (p<0.05), correlating well with immunologic response (as measured by circulating γδ T-cell levels) (446, 447). The observation that GFN treatment causes an upregulation in IL-2 signalling gene sets, provides encouraging evidence that GFN could potentially have a role as an adjuvant therapy to provide a similar immuno-modulatory effect as immune-based therapy for PCa progression.

The upregulation of the IFN-γ response gene set is also particularly interesting. IFN-γ is widely considered to play a central role in immune surveillance of cancer, by effecting both tumour and immune effector cells, and thus modifying the tumour microenvironment. IFN-γ enables tumour cells to become more susceptible to recognition and clearance by activated immune effector cells, enhances the known cytotoxic activity of NK and CTLs, and induces apoptotic cell death of cancer cells (448). In addition, secretion of IFN-γ by mesenchymal stromal cells appears to alter the tumour microenvironment by repolarising tumour-associated macrophages to the M1 inflammatory phenotype (as described in section 4.1 'introduction') (449). IFN-γ has been widely researched as a

potential gene therapy approach to PCa, given its ability to confer increased sensitivity to Fas-mediated PCa cell death (a 'death receptor' present on human PCa cells) (450), a 3-fold increase in apoptosis in PCa mouse xenografts (451), and its ability to reduce the affinity of PCa cells for bone matrix stroma, thus potentially reducing skeletal metastasis (452). Paradoxically however, evidence also suggests that treatment with IFN-γ may also alter cell-host immune system interactions, allowing tumours to escape immune surveillance, which would thus limit its clinical value (449, 453). Further clinical research into the effect of IFN-γ on early PCa and its progression are required to elucidate this link, and hence delineate the significance of GFN on this pathway.

The previously mentioned "hallmark" pathways known to be specifically upregulated in PCa such as fatty acid and cholesterol synthesis, were however, not shown to be significantly affected by a GFN-containing intervention in this GSEA.

In comparison to GFN, Alliin treatment appeared to have a very different effect on the PZ of the prostate. The finding that only one gene is significantly differentially expressed supports the hypothesis that given a lack of a significant Alliin or metabolite accumulation within the PZ tissue, and the low concentrations detected within the urine, there may not be a significant exposure of these compounds to the PZ via urinary reflux. The expression of the Mesothelin gene cannot be explained by PCa embryology or pathogenesis, as the prostate itself does not contain mesothelial cells nor can it produce the encoded protein mesothelin.

Interestingly however, GSEA reveals that Alliin does have a significant effect on multiple gene sets, but in an opposing manner to that of GFN. Unlike GFN, gene sets significantly enriched with Alliin treatment are almost all downregulated (as highlighted by a negative normalised enrichment score). Given the conflicting literature on the effect of Alliin at differing concentrations on upregulating or downregulating immuno-modulatory pathways however, this may not be surprising. More research is required to appreciate the complex relationship that Alliin may have on reducing the risk of PCa demonstrated in epidemiological studies.

As previously discussed, nrf-2 appears to be an important transcription factor involved in the anti-oxidant effects of both SFN and Alliin metabolites. Given the significant upregulation of the reactive oxygen species gene set associated with GFN treatment, known genes associated with nrf-2 induction were analysed. However, analysis of selected known nrf-2 target genes in this analysis did not reveal any significant differentially expressed genes, a finding which is in keeping with previous evidence (98). This may be due to the timing of the treatment given in this study. For example, cell studies suggest that the majority of direct nrf-2 targets are induced within 2-4 hours of treatment followed by a decrease in expression up to 24 hours (454, 455). Given that biopsy samples were

taken >24 hours following final consumption of the intervention, it may be that changes to these targets are no longer detectable. However, despite the absence of upregulation of Nrf-2 regulated genes, GSEA demonstrates an upregulation of pathways surrounding antioxidant response as a result of GFN-treatment.

5.5.2 The Effect of Dietary Intervention in the Transition Zone

As demonstrated in chapter 3, SFN was detected in the TZ of the prostate of patients consuming a GFN-containing intervention to significantly higher levels than a non-GFN containing intervention, which may be due to reflux of these compounds from the urine, or via the systemic circulation. In contrast to the PZ, the total concentration of Alliin metabolites detected in the TZ of the prostate of patients consuming an Alliin-containing intervention was significantly higher than those consuming a non-Alliin containing intervention. It was therefore hypothesised that in comparison to the PZ, Alliin would have a greater effect on the transcriptional profile in the TZ.

Surprisingly, differential expression analysis demonstrated that GFN caused the differential expression of more genes in the TZ compared to the PZ at FDR-adjusted $p < 0.5$ (302 genes compared to 21). However, only 2 genes remained significantly differentially expressed at $p < 0.01$. Alliin on the other hand, caused the differential expression of 4061 genes in the TZ (FDR-adjusted $p < 0.5$), 10 of which remained significantly expressed at $p < 0.01$). Alliin clearly has a greater impact on the expression of genes in the TZ compared to the PZ, and given the finding that Alliin metabolites accumulated in the TZ of the prostate, this fits with the above hypothesis. Interestingly, at FDR-adjusted $p < 0.5$, 106 of these genes were commonly expressed between the two intervention types, although all commonalities were lost at lower levels of significance.

Of the top 10 differentially expressed genes in the TZ in response to a GFN-intervention, only the top two were significantly differentially expressed to FDR-adjusted $p < 0.05$. These include CST1 – cystatin, which was upregulated, and a non-specified long non-coding RNA which demonstrated a negative log fold change (representing downregulation).

Cystatin (encoded by the CST gene) belongs to a class of protease inhibitors, and has 12 forms in human cells and tissue. Cystatin has multiple cellular functions, including inflammation, cell cycle, tumourigenesis and metastasis (456). In particular, cystatin appears to have an important role in cellular senescence – a process whereby irreversible cell cycle arrest occurs secondary to a variety of mechanisms in response to insult, that culminate in the activation of the p53 tumour suppressor

pathway (457). Cystatin is also able to participate in a variety of downstream signalling pathways such as AKT and IL-6 signalling pathways (458). The expression of cystatin appears to have a different role in cancers at different sites, with conflicting results; for example, cystatin has been implicated in the development of several cancers such as gastric (459), pancreatic (460) and colorectal (461), where it appears to be an independent prognostic factor. However, in oesophageal cancer, high cystatin expression appears to be an important survival factor following surgical intervention (462). Although the role of cystatin in PCa in unclear, overexpression of the cystatin CST6 has been shown to significantly inhibit tumour growth and the incidence of lung metastasis (463). Indeed, histone modifications leading to the downregulation and loss of the CST6 gene has been implicated in the progression of PCa, as well as other cancers (463-465). The role of cystatins in PCa warrants further investigation, as the ability of a GFN-containing intervention to upregulate this gene may convey a favourable advantage to PCa patients.

Another interesting observation is the downregulation of genes encoding long non-coding RNAs (LncRNAs). LncRNAs (which comprise the majority of the human genome) were previously considered 'junk' genes because of their lack of an open reading frame (ORF) and protein-coding ability. However, although their molecular mechanisms are unclear, recent studies have found that they play critical roles in human diseases and cancer development. The majority of lncRNAs that are associated with PCa are overexpressed in tumour tissues, and appear to exert oncogenic effects. For example, lncRNAs such as PCA3, GAS5, and HOTAIR are related to the occurrence and progression of PCa (466, 467), and aberrant expression of lncRNAs may promote PCa cell proliferation, invasion and migration. Evidence has demonstrated that between 257 and 407 lncRNAs are significantly differentially expressed in androgen-independent PC-3 and androgen-dependent LNCaP cells compared to a control PrEC cell type, and that SFN treatment is capable of downregulating many of these, even at low concentrations (5 μM) (468). In addition, one particular lncRNA (LINC01116) found to be significantly upregulated in PCa cell lines and was downregulated by SFN treatment, has been shown to promote cell proliferation in human cancer cell lines (468). The ability of GFN to downregulate lncRNAs in this analysis is therefore a significant finding, which goes further towards explaining a mechanistic hypothesis of SFNs anti-cancer properties in PCa. This finding warrants further investigation.

The GSEA for GFN in the TZ also highlights interesting observations. A GFN-containing intervention appears to have much the same effect on functional pathways in the TZ as was demonstrated in the PZ analysis. These pathways are upregulated and include known oncogenic pathways such as; apoptosis, inflammatory response, DNA repair, reactive oxygen species and the p53 pathways. Again, an upregulation of antioxidant response pathways appears to be occurring despite the

absence of upregulation of nrf-2 target genes. From this analysis it appears that GFN is acting upon a diverse range of potentially oncogenic pathways. Additionally, like the PZ analysis, GFN and Alliin appear to be working in opposing manners, as demonstrated by the opposing normalised enrichment scores in shared gene sets amongst the interventions.

Of the top 10 significantly differentially expressed genes in the TZ in response to an Alliin-containing intervention, none can be explicitly linked to a reduction in risk of PCa or other pathology. Myotilin encodes a cytoskeleton protein, and SLIT1 is involved in molecular guidance during cell migration during neural development. The differential expression of MYH3 is potentially an interesting finding. MYH3 (myosin heavy chain 3) is involved in embryonic skeletal muscle development, and has been identified as a potential 'hub gene' which may be important in the pathways of PTEN mutation in PCa (469). PTEN, a tumour suppressor whose expression is lost in approximately 70% of PCas (470, 471), is known to regulate cellular proliferation and modulate cell growth via both PI3K-AKT dependent and independent related pathways, and is documented to be the most commonly mutated gene in PCa (472). The underlying mechanisms of PTEN mutations have previously been analysed using RNA-sequencing methods, and following protein-protein interaction analysis, MYH3 has been identified as one of the top ten significant potential 'hub' genes. The role of this gene in PTEN mutation pathways and hence PCa is currently unknown, but warrants further investigation. PTEN interestingly was also differentially expressed (albeit modestly), in response to an Alliin-containing intervention in the TZ (-0.163 padj 0.190), however, the P13K-AKT signalling gene set, was not returned as significant in response to Alliin in the TZ (unlike in response to GFN in both zones).

Additionally, given the emerging interest in fibroblast growth factors (FGFs) and their receptors in PCa development (473), the finding of downregulation of multiple types of FGFs in response to Alliin treatment in the TZ is notable. The fibroblast growth factor (FGF) axis is required for normal prostate development and is well documented to be abnormally activated in PCa (473-475), resulting in the activation of multiple downstream pathways associated with PCa progression, including PIN and angiogenesis. As a result, there is increasing interest in blockade of these pathways as a therapeutic target (via FGF tyrosine kinase inhibitors, FGFR ligand 'traps' and monoclonal antibody treatment) (473, 474). The most significant FGF in the literature is FGF2 (a known regulator of angiogenesis), which was non- significantly downregulated in this analysis (log2foldchange -0.015 padj 0.527), compared to FGF7 (induced by androgens) - which has previously been demonstrated to be expressed in castrate-resistant tumours - which was significantly downregulated in this analysis (log2foldchange -0.485 padj 0.087).

The most striking observations in response to an Alliin-containing intervention in the TZ is the downregulation of gene sets which were previously shown (in chapter 4) to be upregulated in control samples in the TZ compared to the PZ. In chapter four, it was hypothesised that the finding of upregulated pathways in the TZ such as epithelial mesenchyme transition (EMT), could explain the propensity for BPH within this zone. In this chapter, it is notable that these pathways are indeed downregulated by an Alliin intervention. The most significant of these are epithelial mesenchyme transition (EMT) and angiogenesis, both of which were significantly downregulated (padj=0.003 and padj=0.011 respectively).

The pathogenic mechanisms underlying BPH development are complex, but EMT-associated markers have been detected to significantly higher levels in BPH tissue (476). In addition, there is accumulating evidence that the development and progression of BPH relies upon the upregulation of angiogenesis-related markers, which promotes prostatic cell proliferation as well as the inhibition of apoptosis. Angiogenesis is the physiological process of new vasculature growth from endothelial cell precursors, and is vital for multiple processes including wound healing and tissue development. Epithelial cells of the prostate however, appear to rely upon angiogenesis as a means of requiring adequate oxygen and nutrients from neighbouring vessels via passive diffusion (477-480). 5α-reductase inhibitors and α-adrenergic blockers remain the mainstay of the current pharmacological treatment for BPH treatment, which suppress prostate tissue growth via the inhibition of DHT or relax the smooth muscle of the prostate, respectively. However, both treatments come with significant side effects including orthostatic hypotension, and reduced erectile and ejaculatory function (481, 482). Interestingly however, Qianliening capsules (QC), a traditional Chinese formula that has been used clinically in China to treat BPH for many years, has demonstrated an ability *in vivo* to reduce prostate size via its effect on angiogenesis inhibition (483). In much the same way, Alliin supplementation could provide a potential candidate as an alternative treatment for BPH given its ability to downregulate both EMT and angiogenesis in the TZ, and warrants further investigation.

5.6 Conclusion

This chapter confirms that GFN and Alliin are both capable of altering the transcriptional profile of the prostate, but interestingly appear to act in opposing ways. The transcriptional effect of GFN on the prostate goes some way to support the evidence for its suppression of potentially oncogenic pathways. Interestingly however, Alliin has a significant effect on the transcriptional profile of the TZ, whereby pathways associated with BPH appear to be affected. The evidence presented in this

chapter demonstrates the complexities involved in attempting to reduce the beneficial effects of broccoli and/or garlic to a single compound, which may never fully elucidate the effects demonstrated in epidemiological studies. These results show that dietary bioactive compounds have multiple (and in this case often opposing) effects, and highlight that when these bioactives coexist in the same food, the picture becomes more complex.

Chapter Six

General Discussion

6.1 General Introduction

The work presented in this thesis has made a significant contribution to the current knowledge of the impact and biological activity of sulphur-containing dietary bioactives on the prostate, and how they may act to reduce the risk and/or progression of prostate PCa.

PCa is an increasingly diagnosed and treated problem; being the most commonly diagnosed form of non-cutaneous (internal) cancer in men, and the 2nd most common cause of cancer death in males in the UK, accounting for 14% of all male cancer deaths per year in the UK (9). It is estimated that more than half of all cancer diagnoses are preventable, by not smoking, reducing weight, increasing exercise and consuming a well-balanced diet enriched with fruit and vegetables (484). The increasing need for safe and tolerated therapeutic strategies in PCa is vital, given the long latent period of the disease in the case of patients following a program of active surveillance (485). Dietary intervention in such a cohort is an ideal way in which clinicians could advise and intervene to potentially reduce the risk of patients requiring more radical treatment in the future.

The cancer-preventative properties and effects linked to the consumption of cruciferous and alliaceous vegetables are strongly supported by epidemiological studies (86). However, whether these effects are isolated to the biological activity of the compounds, or their metabolites, is largely unknown. Additionally, whether these biologically active compounds effect the primary organ of interest via systemic or localised action, is questionable. Only by approaching these questions, is there the potential to mechanistically prove the effects of these compounds in reducing cancer risk, and explain how they may act to alter the transcriptional profile of the prostate.

The work presented in this thesis aimed to understand whether isolated sulphur-containing bioactive compounds derived from cruciferous and alliaceous vegetables are capable of accumulation within the prostate tissue, and whether this accumulation differs anatomically between the prostate zones. Additionally, this thesis aimed to determine whether the anatomical zones of the prostate possess individual transcriptional signatures, which may act to "prime" the PZ towards PCa over the TZ, given the differences in PCa incidence arising from this zone, and whether these signatures may be influenced by such dietary bioactive compounds.

This chapter discusses the novel findings obtained from the results of the 'Norfolk ADaPt' study, performed to meet the objectives of this thesis as follows:

- Carry out a randomised double-blinded factorial design dietary intervention study in men awaiting transperineal biopsy of the prostate for known or suspected prostate cancer.

- Assess whether dietary bioactive compounds from commercially available dietary supplements, or their metabolites, accumulate in the urine and prostate tissue.
- Assess whether the accumulation of dietary bioactive compounds from commercially available dietary supplements, or their metabolites, differs between the peripheral and transition zones of the prostate.
- Assess whether dietary bioactive compounds from commercially available dietary supplements, or their metabolites, alter the transcriptional environment of the prostate.

6.2 The Norfolk-ADaPt Study

The Norfolk-ADaPt study was a fully ethically approved study, conducted in compliance with local and national regulatory policies. The Norfolk-ADaPt study recruited patients who were on the waiting list for a transperineal biopsy (TPB) of the prostate. This included patients with a known diagnosis of PCa who were awaiting a routine biopsy as part of their active surveillance program, as well as patients who were awaiting a biopsy for a suspected PCa. Given the increasing demand for TPB in Norwich, this cohort provided an ideal opportunity for a short-term high-dose 'window of opportunity' study, and successfully allowed for the recruitment of 40 participants well within the 6-month time frame allocated. Block randomisation was undertaken to ensure equal distribution of recruited patients to each intervention combination, and allowed for the rolling recruitment and initiation of the interventions from the day of consent into the study. This study also accounted for known covariates such as baseline diet and GSTM1 genotype.

Despite the changes in central guidance and local policies during this period (as previously discussed in chapter 2), recruitment was highly successful, highlighting both the willingness of patients to engage with the research, and the dedicated hard-work of the study team. Recruitment into dietary intervention studies can be difficult (288), which often reflects the populations unwillingness to make alterations to their lifestyle; however, the ADaPt study (unlike previous dietary intervention studies at the QIB) utilised commercially available dietary supplements rather than requesting participants to eat alternative foods or change their usual diet, which may have aided with recruitment. Multiple participants recorded having little to no vegetable consumption in their daily diet and claimed that they would have been unwilling to participate had the intervention been a foodstuff rather than capsules. In addition, many participants took other daily medication each morning and reported that incorporating additional capsules into this routine was easier than altering their habitual diet, which therefore assisted with their daily compliance. The use of

commercially available dietary supplements which have previously been used in clinical trials, eliminated the risk of toxicity or side effects, as was confirmed by the lack of drop-outs secondary to this factor. The only drop-outs recorded were due to being offered an earlier biopsy date. One participant dropped out due to need for foreign travel, and was not replaced due to being a final participant in the study. 39 patients therefore completed the study in its entirety.

The 'Norfolk-ADaPt' study was a randomised double-blinded intervention study. Unlike previous dietary intervention studies undertaken at the QIB, the ADaPt study utilised a 2^2 factorial design rather than a traditional parallel design. This design maximised power comparisons, given the number of participants consuming an active intervention for comparison, and thus reduced the need for repeated measures from a small control cohort (486, 487). In addition to this, uniquely, participants were given an intervention daily for a pre-determined time, and ceased following the consumption of their intervention the day prior to their biopsy. This meant that all prostate samples were taken 24-36 hours following consumption of their last capsules. One further unique feature of this study was the use of biopsy tissue to analyse the transcriptional signature of the peripheral and transition zones of the prostate in control patients (those consuming only placebo capsules). Previous work analysing the difference in transcriptional signatures between the two prostatic zones has previously utilised biopsy samples taken from prostatectomy or cystoprostatectomy specimens (331-333, 362), in which changes in transcriptional pathways are likely to be significantly altered secondary to tissue ischaemic time (488).

The main limitation of the study was the lack of a baseline biopsy from each participant prior to commencing their interventions, thus not enabling paired sample analysis. This could be overcome in future studies by taking a study-specific single biopsy prior to commencing the study intervention, an approach which has been utilised in other 'window of opportunity' studies (489, 490). However, given the short intervention time, potential issues with increased risk of complications from additional biopsies, and potential to cause alterations to the transcriptional profile of the prostate secondary to the trauma/inflammation caused (491), this was not a plausible approach in this study. The short time-scale used in the ADaPt study may also be viewed as a limitation. For example, it is unknown whether the bioactive compounds used may take longer to elicit the transcriptional effects on the prostate tissue as demonstrated in previous studies (98, 492). However, to satisfy the primary outcome measure without delaying patients' biopsy procedures, a minimum 4-week intervention was deemed acceptable. Additionally, PCa cell studies have demonstrated that 'robust' changes in gene transcription and functional pathways (particularly those involved in cell cycle regulation and the phase 2 enzyme response), are demonstrated within 4-hours of treatment with SFN (455). Although it is difficult to compare and translate *in vitro* findings to *in vivo* research, the finding that

transcript alterations and the induction of phase 2 enzyme activity in the liver is upregulated within 4 hours in rats fed with 50 µmol oral SFN supports this finding further (493, 494), as well as directly in rat prostate following 5 days of treatment (495).

Further limitations come with the analysis of the Alliin metabolites. The volatility of these metabolites is well documented. Although an LCMS/MS method for the detection of four representative organosulphur compounds from garlic (alliin, S-allyl-L-cysteine, γ-glutamyl-S-allyl-L-cysteine, and allicin) has been described (496), the use of LCMS/MS to detect these compounds in prostate tissue is a unique feature of the study. For example, there is the possibility that further metabolites were present in the extracted samples which were not detectable using these methods. This is particularly relevant to the analysis of the urinary metabolites (which have previously been analysed using highly sensitive methods such as GC/MS) (299). This potential limitation could be overcome by undertaking patient catheterisation and sample collection at set intervals for the first 12 hours following capsule consumption on day 1 of the study, a well-documented method used in previous bioavailability studies, which may subsequently enable the detection of other highly volatile metabolites.

6.3 Metabolite accumulation in the prostate

The primary outcome of the Norfolk-ADaPt study was to determine whether dietary bioactive compounds in the form of dietary supplements were capable of accumulation within the prostate tissue. SFN or its metabolites have not previously been shown to accumulate in prostate tissue (133), unlike other tissues such as the breast (298), and synovium (497). More recently SFN has been detected to a very low concentration in prostate samples, although this was not deemed significant due to a very small sample size (n=3) (297).

The results of this thesis are the first to prove that SFN and metabolites are capable of accumulating within the prostate tissue, and to significantly higher concentrations in patients consuming myrosinase-activated GFN dietary supplements when compared to a placebo intervention. This finding significantly enhances our understanding of how these metabolites may be capable of exerting their bioactive effects, and potentially eliciting transcriptional effects on the prostate. This finding significantly helps to bridge the gaps in our understanding of the findings from epidemiological studies, by providing a potential mechanistic hypothesis. Given the known behaviour of ITC metabolites in urine, and the theory of urinary reflux primarily into the PZ, it was

postulated that accumulation may be secondary to this physiological mechanism. However, the finding that there was no difference between the concentrations of metabolites detected between the two zones, and moreover no association between the concentration of metabolites present in the urine and those detected in the prostate, disproves this. This surprising finding leads one to consider the systemic circulatory effects that these bioactive compounds may have. The finding that not all metabolites are excreted in the urine of patients consuming them (a consistent finding amongst ITC bioavailability studies), supports this, as the fate of the remaining metabolites is unaccounted for. Plasma metabolite samples were not analysed in this study, which is a factor that could be considered in future studies.

In additional to SFN metabolites, Alliin and its metabolites were also detected in the urine and prostate of participants consuming Alliin-containing dietary supplements. As previously discussed, the highly volatile nature of these products mean that Alliin derived metabolites have been detected in plasma and urine using highly sensitive gas chromatography-mass spectrometry/olfactometry (GC-MS/O) methods. In the ADaPt study however, using LCMS/MS methods, the water-soluble derivatives S-ally-L-cysteine (SAC) and N-acetyl-S-allyl-L-cysteine (NAC-SAC), were detected in the urine of participants consuming Alliin supplements. Moreover, the concentration of total Alliin and metabolites detected in urine was significantly higher in those consuming Alliin supplements compared to those who were not, which was largely driven by the excretion of NAC-SAC (a well-known urinary biomarker of Allium intake).

Despite previous evidence documenting plasma and urine detection of these metabolites, there is no evidence which supports the accumulation within the prostate tissue itself, despite it's known accumulation in rodent renal and prostate tissue. The ADaPt study is therefore, to the best of our knowledge, the first human intervention study to demonstrate the significant accumulation of Alliin metabolites in the human prostate using LCMS/MS or other methods. Compared to SFN metabolite accumulation however, Alliin metabolite accumulation was only deemed to be significant in the TZ of the prostate, which may be more likely secondary to systemic distribution rather than via urinary exposure.

The incorporation of plasma kinetics into this study would have potentially given a greater insight into the mechanisms in which the prostate may be exposed to Alliin-derived metabolites, and is an important factor to consider for future studies.

6.4 Transcriptomic analysis

The use of transcriptomics is vastly altering our understanding of the molecular complexities associated with PCa development and progression. It has been suggested that the diagnosis of PCa (based on histopathological analysis) is associated with significant levels of under detection error (498), including error of the Gleason scoring system which is estimated to be up to 39% (499). These significant error rates can be explained by the fact that more complex molecular processes which may perturb normal mechanisms such as methylation, overexpression of genes of benefit and silencing of genes of potential detriment, are likely to play a significant early role in PCa (and other cancers) tumourigenesis (500, 501). With the development of next-generation sequencing technologies, RNA sequencing has become a reproducible, accurate and sensitive way in which the cancer transcriptome of the prostate can be analysed, and is the dominant technology for gene expression measurement. In this way, transcriptomics can not only be utilised to determine the underlying mechanisms involved in tumourigenesis, but also in the development of PCa diagnosis and treatment (502, 503).

The transcriptional analysis of prostate samples in this thesis contributes significantly to our understanding of the mechanisms in which the prostate is potentially primed towards carcinogenesis, and how these pathways may be intercepted and altered via the consumption of sulphur-containing dietary bioactive compounds.

The transcriptional analysis of prostate samples collected from participants consuming a placebo intervention has allowed, for the first time, the transcriptional signature of the PZ and TZ to be analysed and compared from biopsy samples in patients with low-risk PCa on 'active surveillance' or under investigation for suspected PCa. The use of prostate biopsy tissue immediately submerged into RNA-stabilising solution, compared to subsequent tissue extraction from whole prostatectomy or cystoprostatectomy samples, avoids the risk of RNA degradation and genomic alterations associated with ischaemia (as discussed in chapter 4). The success of this method is confirmed by the finding that no prostate-specific ischaemic reference genes were upregulated in this analysis (395). The methods used therefore allowed for the most accurate and unperturbed analysis of the prostatic transcriptional signatures.

It is well documented that the PZ of the prostate is more likely to develop PCa, being the site of 70-80% all PCas (2). The evidence presented in this thesis demonstrates that the PZ may be 'primed' towards carcinogenesis compared to the TZ, due to a significantly higher expression of genes involved in PCa development. As previously demonstrated, this may be due to the propensity of the PZ to provide a more favourable environment for the growth and survival of cancer cells (by the upregulation of genes involved in fatty acid and cholesterol metabolism) (333), but also those

associated with hormonal pathways integral to the development and progression of PCa. Potentially the most significant finding of this analysis is that of AMACR overexpression in the PZ compared to the TZ. AMACR (alpha-methylacyl-CoAracemase) is a well characterised enzyme involved in peroxisomal beta-oxidation of dietary branched-chained fatty acids and is preferentially overexpressed in up to 80% of PCa diagnosed via prostate biopsy (504, 505). Meta-analysis have also demonstrated that AMACR expression significantly contributes to the risk of PCa (44). However, the finding that AMACR is preferentially expressed in the PZ compared to the TZ of the 'normal' prostate has not previously been described, and demonstrates potential zonal priming of the prostate on even an individual gene basis. This finding paves the way for future analysis of how the PZ is 'primed' for carcinogenesis and provides further evidence that AMACR is a significant molecular biomarker of PCa which could be targeted and manipulated to aid both PCa diagnostics and therapeutics (506).

By defining the transcriptional signature of the prostate from placebo samples initially, subsequent analysis of samples from participants consuming treatment interventions allowed direct comparisons to be made between individually expressed genes, as well as gene sets. Significantly, the results of this thesis demonstrate that not only are the dietary compounds GFN and Alliin and their metabolites capable of altering the transcriptional signature of the prostate, but to greater extents in the prostatic zone in which they demonstrated a significant tissue accumulation, i.e. GFN in the PZ and Alliin in the TZ. Whether this zonal accumulation is due to direct urinary reflux or systemic circulatory mechanisms, this finding confirms for the first time that the accumulation of these metabolites alters the transcriptional profile of the prostate following even a short-term high-dose exposure to these compounds.

The transcriptional alterations described in this thesis in response to the GFN-containing intervention are complex and highlight the difficulties of attempting to simplify and decipher an association demonstrated in epidemiological studies down to one individual compound. Nonetheless, the findings that GFN can alter the immune regulation of the PCa microenvironment is significant. As previously discussed, several cancers including PCa are able to escape immune responses via multiple immune evasion mechanisms such as the development of a tumour-immunosuppressive microenvironment, inhibition of antigen presentation and defective T cell responses (63, 64), factors which are demonstrated in this thesis to be influenced by the consumption of GFN. Conversely to GFN, Alliin caused the differential expression of more genes than GFN, and had the greatest impact on the transcriptional profile of the TZ compared to the PZ.

The differentiation between "metabolic" and "cytokine" genes is important for transcriptional analysis; regulatory enzymes and transporters involved in metabolic pathways exist in very low

concentrations, and hence altered gene expression even at low levels will significantly alter the abundance and activity of the enzyme or transporter. In comparison, the products of cytokine genes require larger gene expression changes in order to alter their protein products (37). It is likely that a combination of metabolic, cytokine and hormonal gene expression pathways are implicated in the development and progression of prostate cancer. This factor may explain the reason for relatively small changes in gene expression demonstrated at levels of low significance, and conversely, for the high numbers of low significance changes in gene expression causing vast changes in functional biological pathways demonstrated.

6.5 Future work

One surprising finding from the ADaPt study which is worthy of future research, is the evidence that Alliin appears to be capable of downregulating the transcriptional pathways associated with the development of BPH in the TZ. The ADaPt study was not designed to explore the effects of dietary supplements on non-cancerous pathology of the prostate, but given the high incidence of BPH in the population and the often-unacceptable side effects of current non-surgical treatment methods, Alliin supplementation is a potential candidate which is worthy of future research.

Another area pertinent to future work and our understanding of the impact of dietary metabolites and PCa is that of the prostatic microbiome. Microbiomes throughout the body are well documented – and well known to be impacted by factors such as diet and lifestyle. Given the new era of microbial discovery (due to the advent of high throughput molecular-based methods of identification and characterisation of complex microbial populations), the relationship between microbiological communities and pathogenesis can be explored. The prostate was traditionally thought to be a sterile gland; however, infective processes are known to affect the prostate, clinically resulting in acute prostatitis which may ultimately lead to chronic inflammatory processes. Chronic inflammation is well documented to be associated with the pathogeneses and progression of PCa (251, 507). Due to its topography, the prostate gland may be reached by members of the skin and gut microbiota, as well as via exposure via urine, which may be able or not to survive within the prostate microenvironment and outcompete other microbes. For example, prostatic inflammation induced by infections with uropathogenic *E. coli* and other pro-inflammatory species such as *P. Acnes* appear to induce morphological alterations (dysplasia) and hyperplasia via the decreased expression of the tumour suppressor NKX 3.1 (508). Additionally, modifications have been found in

the prostatic bacterial populations present in PCa samples which appear to enhance pro-inflammatory responses and alter the extracellular environment of the prostate (246, 509, 510).

Cavaretta *et. al.* provided the first evidence of a 'non-sterile' prostate, and indeed confirmed the presence of a local 'prostate-specific' microbiome which was specifically ascribable to histological tissue type. Tissue from non-tumoural, tumoural and peri-tumoural sites of the prostate from patients undergoing prostatectomy (with no history of previous urinary tract infection) has been analysed using ultra-deep pyrosequencing. *Actinobacteria* was found to be the dominant phylum in tissue from all sites, followed by *Firmicutes* and *Proteobacteria*. Interestingly, *Streptococcus* spp. was almost exclusively detected in non-tumour regions, suggesting that *Lactobacillales* form the normal prostatic microbiome and contribute to the balance of the physiological host extracellular environment (246). Similar findings were confirmed more recently using standard microarray analysis and pan-pathogen array (PathoChip) methods (247); 70% of bacteria detected in prostate tumour samples were gram negatives (Proteobacteria most predominant phylum – 55% of all). Others included Fermicutes (19%), Actinobacteria (11%), and Bacteroides (7%). More recently however, 16S ribosomal RNA sequencing of prostatic fluid has demonstrated that whilst the prostatic microbiome likely plays a beneficial role in maintaining the prostatic microenvironment, there is a potential pathophysiological correlation between the composition of the microbiome and PCa (511). Patients with PCa appear to have a reduced microbial density compared to those without PCa, suggesting that microbial diversity is vital in maintaining a healthy prostatic microenvironment.

The new developments in prostatic microbiome research may have important implications in the effect of dietary bioactive compounds on the prostate, particularly with regards to alterations following inflammatory processes, and is an area worthy of future work. It is well documented that certain compounds present in diet can indeed induce prostatic inflammation and aid in PCa development; polyunsaturated fats in the form of linoleic acid (LA) following metabolism are transformed into proinflammatory eicosanoids (prostaglandins and leukotrienes) leading to oxidative stress and inflammation, and heterocyclic amines (HCAs) from meat cooked at high temperatures appear to increase the risk of PIN and high grade PCa via similar mechanisms (512-517). Conversely therefore, it is plausible that dietary bioactive compounds which are capable of reducing or inhibiting inflammatory processes within the prostate may cause alterations in the prostatic microbiota, therefore reducing the risk of PCa pathogenesis and/or progression; a factor which has been previously been demonstrated with resveratrol (518). The immunomodulatory effects of GFN supplementation demonstrated in the transcriptomic analysis and gene expressional pathways in the ADaPt study may indeed act to modulate the prostate microbiota and reduce PCa

risk via this pathway. It may also be the case that members of the prostatic microbiome community are capable of aiding the metabolism of dietary bioactive compounds to their biologically active metabolites to reduce the risk of PCa incidence and progression (in much the same way as some members of the colonic microbiota are capable of producing myrosinase and aid in the metabolism of GFN compounds). The capability of sequencing 16S RNA extracted from biopsy samples from the ADaPt or other studies, could help to elucidate the potential relationship between dietary bioactive compounds, the prostate microbiota, and PCa in future analysis.

The overriding question however, is whether the results of the Norfolk ADaPt study and the work presented in this thesis justifies an interventional study with sulphur containing dietary compounds and a clinical outcome. The previously discussed ESCAPE trial demonstrated that sulphur containing dietary compounds are capable of suppressing the oncogenic pathways associated with the development of PCa in a dose-dependent manner (98), however, it was unknown whether this effect was due to a direct or indirect effect upon the prostate, given that accumulation within the prostate was up until that point, unproven. The SAP study further developed our knowledge by demonstrating that SMCSO, a related compound, is capable of accumulation within the prostate tissue (133). However, the results of the ADaPt study finally confirm that these transcriptional changes likely occur due to a direct accumulation and therefore direct effect of such compounds within the prostate tissue. The next logical step in further developing our understanding of the impact of these compounds on the development and progression of PCa, therefore lies in assessing the direct impact upon the clinical outcome of such patients. Of note, the ESCAPE study demonstrated a non-significant inverse correlation with consumption of cruciferous vegetable intake and WHO grade over the study period, and although not powered to assess a clinical outcome, the most significant inverse correlation was associated with consumption of SMCSO (98). This finding suggests that both GFN and Alliin/SACSO (due to its similar structure) may be capable of eliciting an impact at a clinical level, in a study powered specifically to assess such an endpoint.

With the changing in guidelines of patients undergoing a programme of active surveillance, and the development of new mpMRI reporting techniques, the presence of clinical progression/regression via mpMRI reporting is one potential marker (with or without PSA monitoring) which could be utilised in future studies to assess clinical outcome. Such a study has previously been commenced in Cambridge (the ESCAPE-ING trial, sponsored by the Quadram Institute Bioscience), but due to issues with recruitment, was terminated. Given the successful recruitment of the ADaPt study, and the increased availability of mpMRI due to guidance changes, this is a potentially plausible outcome

measure which could be utilised in a future trial to assess the clinical outcome of the consumption of sulphur-containing dietary compounds.

6.6 Conclusion

The ADaPt study was a highly successful, short-term high dose dietary-supplement intervention study. Uniquely to the ADaPt study, the recruitment of more patients and the use of a 2^2 factorial study design allowed for much greater statistical power. Given the changes to the diagnostic pathways of PCa, it may not however be plausible to utilise such a study design in the future.

The ADaPt study demonstrated, for the first time, that SFN and Alliin are capable of accumulating in the prostate tissue following a 4-week intervention of myrosinase-activated GFN and Alliin respectively. The detection of Alliin is particularly significant given the volatility of these metabolites and the ability to detect them using LCMS/MS methods. Furthermore, this thesis describes the unique transcriptional signature of the peripheral and transition zones, and demonstrates that dietary bioactive compounds are capable of altering the transcriptional profile of the prostate.

The findings presented in this thesis have significantly progressed our understanding of the way in which sulphur-containing dietary bioactives behave in the prostate, whilst drawing caution to the reductionist approach of attributing the putative cancer preventing abilities of plant foods to single compounds, and explain a possible link between the evidence derived from epidemiological studies and the pathogenesis of PCa.

References

1.   Reynard J, Brewster S, Biers S. Oxford Handbook of Urology, 3rd Ed, Oxford University Press, UK, 2013.

2.   McNeal JE, Redwine EA, Freiha FS, Stamey TA. Zonal distribution of prostatic adenocarcinoma. Correlation with histologic pattern and direction of spread. The American journal of surgical pathology. 1988;12(12):897-906.

3.   Butel R, Ball R. The distribution of BCG prostatitis: A clue for pathogenetic processes? 2018;78(15):1134-9.

4.   Fine SW, Reuter VE. Anatomy of the prostate revisited: implications for prostate biopsy and zonal origins of prostate cancer. 2012;60(1):142-52.

5.   Aaron L, Franco OE, Hayward SW. Review of Prostate Anatomy and Embryology and the Etiology of Benign Prostatic Hyperplasia. The Urologic clinics of North America. 2016;43(3):279-88.

6.   Huggins C, Neal W. Coagulation and liquefaction of semen. Proteolytic enzymes and citrate in prostatic fluid1942. 527-41 p.

7.   Balk SP, Ko YJ, Bubley GJ. Biology of prostate-specific antigen. Journal of clinical oncology : official journal of the American Society of Clinical Oncology. 2003;21(2):383-91.

8.   Lilja H. Structure, function, and regulation of the enzyme activity of prostate-specific antigen1993. 188-91 p.

9.   Cancer Research UK. Available online: http://www.cancerresearchuk.org/healthprofessional/cancer-statistics/statistics-by-cancer-type/prostate-cancer#heading-Zero (accessed 14 May 2019).

10.   3.Data were provided by ISD Scotland on request ASdcbfhhwioH-TCP.

11.   4.Data were provided by the Welsh Cancer Intelligence and Surveillance Unit HID, Public Health Wales on request, October 2017. Similar data can be found here: http://www.wcisu.wales.nhs.uk.

12.   5.Data were provided by the Northern Ireland Cancer Registry on request JSdcbfhhwqaur-cn.

13.   2. Data were provided by the Office for National Statistics on request JSdcbfhhwoguphcb.

14.   Ferlay J, Soerjomataram I, Dikshit R, Eser S, Mathers C, Rebelo M, et al. Cancer incidence and mortality worldwide: sources, methods and major patterns in GLOBOCAN 2012. International journal of cancer. 2015;136(5):E359-86.

15.   Bray F, Ferlay J, Soerjomataram I, Siegel RL, Torre LA, Jemal A. Global cancer statistics 2018: GLOBOCAN estimates of incidence and mortality worldwide for 36 cancers in 185 countries. CA: A Cancer Journal for Clinicians. 2018;68(6):394-424.

16.   Colli JL, Colli A. International comparisons of prostate cancer mortality rates with dietary practices and sunlight levels. Urologic oncology. 2006;24(3):184-94.

17.   Hsing AW, Tsao L, Devesa SS. International trends and patterns of prostate cancer incidence and mortality. International journal of cancer. 2000;85(1):60-7.

18.   Ambrosini GL, Fritschi L, de Klerk NH, Mackerras D, Leavy J. Dietary patterns identified using factor analysis and prostate cancer risk: a case control study in Western Australia. Annals of epidemiology. 2008;18(5):364-70.

19.   Wolk A. Diet, lifestyle and risk of prostate cancer. Acta oncologica (Stockholm, Sweden). 2005;44(3):277-81.

20.   Gandaglia G, Albers P, Abrahamsson P-A, Briganti A, Catto JWF, Chapple CR, et al. Structured Population-based Prostate-specific Antigen Screening for Prostate Cancer: The European Association of Urology Position in 2019. European urology. 2019;76(2):142-50.

21.   UK PC. The PSA test. wwwprostatecancerukorg/prostate-information/prostate-tests/psa-test. 2019.

22.   Thompson IM, Pauler DK, Goodman PJ, Tangen CM, Lucia MS, Parnes HL, et al. Prevalence of prostate cancer among men with a prostate-specific antigen level < or =4.0 ng per milliliter. N Engl J Med. 2004;350(22):2239-46.

23.   Ahmed HU, El-Shater Bosaily A, Brown LC, Gabe R, Kaplan R, Parmar MK, et al. Diagnostic accuracy of multi-parametric MRI and TRUS biopsy in prostate cancer (PROMIS): a paired validating confirmatory study. The Lancet. 2017;389(10071):815-22.

24.   Kasivisvanathan V, Rannikko AS, Borghi M, Panebianco V, Mynderse LA, Vaarala MH, et al. MRI-Targeted or Standard Biopsy for Prostate-Cancer Diagnosis. New England Journal of Medicine. 2018;378(19):1767-77.

25.   European Association of Urology Guidlines, Available at https://uroweb.org/guideline/prostate-cancer (accessed Jan 2021).

26.   National Institute for Health and Care Excellence (NICE) Guidelines. Available at https://www.nice.org.uk/guidance/ng131/chapter/Recommendations (accessed Jan 2021).

27.   Moore CM, Giganti F, Albertsen P, Allen C, Bangma C, Briganti A, et al. Reporting Magnetic Resonance Imaging in Men on Active Surveillance for Prostate Cancer: The PRECISE Recommendations-A Report of a European School of Oncology Task Force. European urology. 2017;71(4):648-55.

28.   (BAUS) TBAoUS. Prostate Procedures. 2019.

29.   Gleason DF, Mellinger GT. Prediction of prognosis for prostatic adenocarcinoma by combined histological grading and clinical staging. The Journal of urology. 1974;111(1):58-64.

30.   Epstein JI, Allsbrook WC, Jr., Amin MB, Egevad LL. The 2005 International Society of Urological Pathology (ISUP) Consensus Conference on Gleason Grading of Prostatic Carcinoma. The American journal of surgical pathology. 2005;29(9):1228-42.

31.   Epstein JI, Egevad L, Amin MB, Delahunt B, Srigley JR, Humphrey PA. The 2014 International Society of Urological Pathology (ISUP) Consensus Conference on Gleason Grading of Prostatic Carcinoma: Definition of Grading Patterns and Proposal for a New Grading System. The American journal of surgical pathology. 2016;40(2):244-52.

32.   Chen N, Zhou Q. The evolving Gleason grading system. Chinese journal of cancer research = Chung-kuo yen cheng yen chiu. 2016;28(1):58-64.

33.   Buyyounouski MK, Choyke PL, McKenney JK, Sartor O, Sandler HM, Amin MB, et al. Prostate cancer - major changes in the American Joint Committee on Cancer eighth edition cancer staging manual. CA Cancer J Clin. 2017;67(3):245-53.

34.   Akram M. Citric acid cycle and role of its intermediates in metabolism. Cell Biochem Biophys. 2014;68(3):475-8.

35.   Costello LC, Franklin RB. The intermediary metabolism of the prostate: a key to understanding the pathogenesis and progression of prostate malignancy. Oncology. 2000;59(4):269-82.

36.   Costello LC, Franklin RB. The clinical relevance of the metabolism of prostate cancer; zinc and tumor suppression: connecting the dots. Mol Cancer. 2006;5:17-.

37.   Costello LC, Franklin RB. A comprehensive review of the role of zinc in normal prostate function and metabolism; and its implications in prostate cancer. Arch Biochem Biophys. 2016;611:100-12.

38.   Burns JS, Manda G. Metabolic Pathways of the Warburg Effect in Health and Disease: Perspectives of Choice, Chain or Chance. International journal of molecular sciences. 2017;18(12):2755.

39.   Vander Heiden MG, Cantley LC, Thompson CB. Understanding the Warburg effect: the metabolic requirements of cell proliferation. Science. 2009;324(5930):1029-33.

40.   Jadvar H. FDG PET in Prostate Cancer. PET Clin. 2009;4(2):155-61.

41.   Bertilsson H, Tessem M-B, Flatberg A, Viset T, Gribbestad I, Angelsen A, et al. Changes in Gene Transcription Underlying the Aberrant Citrate and Choline Metabolism in Human Prostate Cancer Samples. Clinical Cancer Research. 2012;18(12):3261.

42.   Costello LC, Feng P, Milon B, Tan M, Franklin RB. Role of zinc in the pathogenesis and treatment of prostate cancer: critical issues to resolve. Prostate cancer and prostatic diseases. 2004;7(2):111-7.

43.   Costello LC, Franklin RB. Cytotoxic/tumor suppressor role of zinc for the treatment of cancer: an enigma and an opportunity. Expert Review of Anticancer Therapy. 2012;12(1):121-8.

44.   Jiang N, Zhu S, Chen J, Niu Y, Zhou L. A-methylacyl-CoA racemase (AMACR) and prostate-cancer risk: a meta-analysis of 4,385 participants. PloS one. 2013;8(10):e74386-e.

45.   GRAYHACK JT. Effect of Testosterone-Estradiol Administration on Citric Acid and Fructose Content of the Rat Prostate. Endocrinology. 1965;77(6):1068-74.

46.   Farnsworth WE. Testosterone stimulation of citric acid synthesis in the rat prostate. Biochimica et Biophysica Acta (BBA) - General Subjects. 1966;117(1):247-54.

47.   Grayhack J, Lebowitz J. Effect of prolactin on citric acid of lateral lobe of prostate of Sprague-Dawley rat. Invest Urol. 1967;5:87-94.

48.   Costello L, and, Franklin R. Testosterone and prolactin regulation of metabolic genes and citrate metabolism of prostate epithelial cells. Hormone and metabolic research= Hormon-und Stoffwechselforschung= Hormones et metabolisme. 2002;34(8):417.

49.   Schaffner CP. Prostatic cholesterol metabolism: regulation and alteration. Prog Clin Biol Res. 1981;75a:279-324.

50.   Swyer GIM. The Cholesterol Content of Normal and Enlarged Prostates. Cancer research. 1942;2(5):372.

51.   Olson RE. Discovery of the Lipoproteins, Their Role in Fat Transport and Their Significance as Risk Factors. The Journal of nutrition. 1998;128(2):439S-43S.

52.   Brown MS, Goldstein JL. A Receptor-Mediated Pathway for Cholesterol Homeostasis. Science. 1986;232(4746):34-47.

53.   Bloch K. The biological synthesis of cholesterol. 1965.

54.   Gill S, Stevenson J, Kristiana I, Brown AJ. Cholesterol-dependent degradation of squalene monooxygenase, a control point in cholesterol synthesis beyond HMG-CoA reductase. Cell metabolism. 2011;13(3):260-73.

55.   Brown MS, Goldstein JL. Cholesterol feedback: from Schoenheimer's bottle to Scap's MELADL. Journal of lipid research. 2009;50(Supplement):S15-S27.

56.   Brown AJ. CHOLESTEROL, STATINS AND CANCER. Clinical and Experimental Pharmacology and Physiology. 2007;34(3):135-41.

57.   Horton JD, Goldstein JL, Brown MS. SREBPs: activators of the complete program of cholesterol and fatty acid synthesis in the liver. J Clin Invest. 2002;109(9):1125-31.

58.   Horton JD, Shah NA, Warrington JA, Anderson NN, Park SW, Brown MS, et al. Combined analysis of oligonucleotide microarray data from transgenic and knockout mice identifies direct SREBP target genes. Proceedings of the National Academy of Sciences. 2003;100(21):12027-32.

59.   Su AI, Wiltshire T, Batalov S, Lapp H, Ching KA, Block D, et al. A gene atlas of the mouse and human protein-encoding transcriptomes. Proceedings of the National Academy of Sciences. 2004;101(16):6062-7.

60.   Tall AR, Costet P, Wang N. Regulation and mechanisms of macrophage cholesterol efflux. J Clin Invest. 2002;110(7):899-904.

61.   Zelcer N, Hong C, Boyadjian R, Tontonoz P. LXR regulates cholesterol uptake through Idol-dependent ubiquitination of the LDL receptor. Science. 2009;325(5936):100-4.

62.   Amemiya-Kudo M, Shimano H, Hasty AH, Yahagi N, Yoshikawa T, Matsuzaka T, et al. Transcriptional activities of nuclear SREBP-1a,-1c, and-2 to different target promoters of lipogenic and cholesterogenic genes. Journal of lipid research. 2002;43(8):1220-35.

63.   Beatty GL, Gladney WL. Immune escape mechanisms as a guide for cancer immunotherapy. Clinical cancer research : an official journal of the American Association for Cancer Research. 2015;21(4):687-92.

64.   Vitkin N, Nersesian S, Siemens DR, Koti M. The Tumor Immune Contexture of Prostate Cancer. Front Immunol. 2019;10:603.

65.   Lin D, Wang X, Choi SYC, Ci X, Dong X, Wang Y. Immune phenotypes of prostate cancer cells: Evidence of epithelial immune cell-like transition? Asian J Urol. 2016;3(4):195-202.

66.   Wu S-Q, Su H, Wang Y-H, Zhao X-K. Role of tumor-associated immune cells in prostate cancer: angel or devil? Asian J Androl. 2019;21(5):433-7.

67.   Ohue Y, Nishikawa H. Regulatory T (Treg) cells in cancer: Can Treg cells be a new therapeutic target? Cancer Sci. 2019;110(7):2080-9.

68.   Nardone V, Botta C, Caraglia M, Martino EC, Ambrosio MR, Carfagno T, et al. Tumor infiltrating T lymphocytes expressing FoxP3, CCR7 or PD-1 predict the outcome of prostate cancer patients subjected to salvage radiotherapy after biochemical relapse. Cancer Biol Ther. 2016;17(11):1213-20.

69.   Davidsson S, Andren O, Ohlson AL, Carlsson J, Andersson SO, Giunchi F, et al. FOXP3(+) regulatory T cells in normal prostate tissue, postatrophic hyperplasia, prostatic intraepithelial neoplasia, and tumor histological lesions in men with and without prostate cancer. Prostate. 2018;78(1):40-7.

70.   Takeuchi Y, Nishikawa H. Roles of regulatory T cells in cancer immunity. Int Immunol. 2016;28(8):401-9.

71.   Mohr A, Malhotra R, Mayer G, Gorochov G, Miyara M. Human FOXP3(+) T regulatory cell heterogeneity. Clin Transl Immunology. 2018;7(1):e1005.

72.   Takeya M, Komohara Y. Role of tumor-associated macrophages in human malignancies: friend or foe? Pathol Int. 2016;66(9):491-505.

73.   Lanciotti M, Masieri L, Raspollini MR, Minervini A, Mari A, Comito G, et al. The role of M1 and M2 macrophages in prostate cancer in relation to extracapsular tumor extension and biochemical recurrence after radical prostatectomy. Biomed Res Int. 2014;2014:486798.

74.   Chen PC, Cheng HC, Wang J, Wang SW, Tai HC, Lin CW, et al. Prostate cancer-derived CCN3 induces M2 macrophage infiltration and contributes to angiogenesis in prostate cancer microenvironment. Oncotarget. 2014;5(6):1595-608.

75.   Fridlender ZG, Sun J, Kim S, Kapoor V, Cheng G, Ling L, et al. Polarization of tumor-associated neutrophil phenotype by TGF-beta: "N1" versus "N2" TAN. Cancer cell. 2009;16(3):183-94.

76. Masucci MT, Minopoli M, Carriero MV. Tumor Associated Neutrophils. Their Role in Tumorigenesis, Metastasis, Prognosis and Therapy. Front Oncol. 2019;9:1146-.

77. Costanzo-Garvey DL, Keeley T, Case AJ, Watson GF, Alsamraae M, Yu Y, et al. Neutrophils are mediators of metastatic prostate cancer progression in bone. Cancer Immunology, Immunotherapy. 2020;69(6):1113-30.

78. Li H, Zhang Y, Glass A, Zellweger T, Gehan E, Bubendorf L, et al. Activation of signal transducer and activator of transcription-5 in prostate cancer predicts early recurrence. Clinical Cancer Research. 2005;11(16):5863-8.

79. Groth C, Hu X, Weber R, Fleming V, Altevogt P, Utikal J, et al. Immunosuppression mediated by myeloid-derived suppressor cells (MDSCs) during tumour progression. British journal of cancer. 2019;120(1):16-25.

80. Jachetti E, Cancila V, Rigoni A, Bongiovanni L, Cappetti B, Belmonte B, et al. Cross-Talk between Myeloid-Derived Suppressor Cells and Mast Cells Mediates Tumor-Specific Immunosuppression in Prostate Cancer. Cancer Immunology Research. 2018;6(5):552.

81. Ostrand-Rosenberg S, Sinha P, Beury DW, Clements VK. Cross-talk between myeloid-derived suppressor cells (MDSC), macrophages, and dendritic cells enhances tumor-induced immune suppression. Semin Cancer Biol. 2012;22(4):275-81.

82. Lopez-Bujanda Z, Drake CG. Myeloid-derived cells in prostate cancer progression: phenotype and prospective therapies. J Leukoc Biol. 2017;102(2):393-406.

83. Yin Y, Huang X, Lynn KD, Thorpe PE. Phosphatidylserine-targeting antibody induces M1 macrophage polarization and promotes myeloid-derived suppressor cell differentiation. Cancer Immunol Res. 2013;1(4):256-68.

84. Bou-Dargham MJ, Sha L, Sang Q-XA, Zhang J. Immune landscape of human prostate cancer: immune evasion mechanisms and biomarkers for personalized immunotherapy. BMC cancer. 2020;20(1):1-10.

85. Adamaki M, Zoumpourlis V. Immunotherapy as a Precision Medicine Tool for the Treatment of Prostate Cancer. Cancers (Basel). 2021;13(2):173.

86. Livingstone TL, Beasy G, Mills RD, Plumb J, Needs PW, Mithen R, et al. Plant Bioactives and the Prevention of Prostate Cancer: Evidence from Human Studies. Nutrients. 2019;11(9):2245.

87. Deneo-Pellegrini H, De Stefani E, Ronco A, Mendilaharsu M. Foods, nutrients and prostate cancer: a case-control study in Uruguay. British journal of cancer. 1999;80(3-4):591-7.

88. Augustsson K, Michaud DS, Rimm EB, Leitzmann MF, Stampfer MJ, Willett WC, et al. A prospective study of intake of fish and marine fatty acids and prostate cancer. Cancer epidemiology, biomarkers & prevention : a publication of the American Association for Cancer Research, cosponsored by the American Society of Preventive Oncology. 2003;12(1):64-7.

89. Capurso C, Vendemiale G. The Mediterranean Diet Reduces the Risk and Mortality of the Prostate Cancer: A Narrative Review. Frontiers in Nutrition. 2017;4(38).

90. Castello A, Boldo E, Amiano P, Castano-Vinyals G, Aragones N, Gomez-Acebo I, et al. Mediterranean Dietary Pattern is Associated with Low Risk of Aggressive Prostate Cancer: MCC-Spain Study. The Journal of urology. 2018;199(2):430-7.

91. Aghajanpour M, Nazer MR, Obeidavi Z, Akbari M, Ezati P, Kor NM. Functional foods and their role in cancer prevention and health promotion: a comprehensive review. American journal of cancer research. 2017;7(4):740-69.

92. W Watson G, M Beaver L, E Williams D, H Dashwood R, Ho E. Phytochemicals from cruciferous vegetables, epigenetics, and prostate cancer prevention. AAPS J. 2013;15(4):951-61.

93. Pratheeshkumar P, Son Y-O, Korangath P, Manu KA, Siveen KS. Phytochemicals in Cancer Prevention and Therapy. BioMed Research International. 2015;2015:2.

94. Salehi B, Fokou PVT, Yamthe LRT, Tali BT, Adetunji CO, Rahavian A, et al. Phytochemicals in Prostate Cancer: From Bioactive Molecules to Upcoming Therapeutic Agents. Nutrients. 2019;11(7):1483.

95. Iqbal J, Abbasi BA, Mahmood T, Kanwal S, Ali B, Shah SA, et al. Plant-derived anticancer agents: A green anticancer approach. Asian Pacific Journal of Tropical Biomedicine. 2017;7(12):1129-50.

96. Thomas R, Williams M, Sharma H, Chaudry A, Bellamy P. A double-blind, placebo-controlled randomised trial evaluating the effect of a polyphenol-rich whole food supplement on PSA progression in men with prostate cancer—the UK NCRN Pomi-T study. Prostate cancer and prostatic diseases. 2014;17:180.

97. Cooper CS, Eeles R, Wedge DC, Van Loo P, Gundem G, Alexandrov LB, et al. Analysis of the genetic phylogeny of multifocal prostate cancer identifies multiple independent clonal expansions in neoplastic and morphologically normal prostate tissue. Nature genetics. 2015;47(4):367-72.

98.   Traka MH, Melchini A, Coode-Bate J, Al Kadhi O, Saha S, Defernez M, et al. Transcriptional changes in prostate of men on active surveillance after a 12-mo glucoraphanin-rich broccoli intervention-results from the Effect of Sulforaphane on prostate CAncer PrEvention (ESCAPE) randomized controlled trial. Am J Clin Nutr. 2019;109(4):1133-44.

99.   Traka M. Health Benefits of Glucosinolates. 802016.

100.   Dinkova-Kostova A. Chemoprotection Against Cancer by Isothiocyanates: A Focus on the Animal Models and the Protective Mechanisms2012.

101.   Sturm C, Wagner AE. Brassica-Derived Plant Bioactives as Modulators of Chemopreventive and Inflammatory Signaling Pathways. Int J Mol Sci. 2017;18(9).

102.   Jaramillo MC, Zhang DD. The emerging role of the Nrf2-Keap1 signaling pathway in cancer. Genes & development. 2013;27(20):2179-91.

103.   Traka M, Mithen R. Glucosinolates, isothiocyanates and human health. Phytochemistry Reviews. 2009;8(1):269-82.

104.   Soundararajan P, Kim JS. Anti-Carcinogenic Glucosinolates in Cruciferous Vegetables and Their Antagonistic Effects on Prevention of Cancers. Molecules (Basel, Switzerland). 2018;23(11).

105.   Heiss E, Herhaus C, Klimo K, Bartsch H, Gerhauser C. Nuclear factor kappa B is a molecular target for sulforaphane-mediated anti-inflammatory mechanisms. J Biol Chem. 2001;276(34):32008-15.

106.   Singh SV, Warin R, Xiao D, Powolny AA, Stan SD, Arlotti JA, et al. Sulforaphane inhibits prostate carcinogenesis and pulmonary metastasis in TRAMP mice in association with increased cytotoxicity of natural killer cells. Cancer research. 2009;69(5):2117-25.

107.   Singh KB, Kim SH, Hahm ER, Pore SK, Jacobs BL, Singh SV. Prostate cancer chemoprevention by sulforaphane in a preclinical mouse model is associated with inhibition of fatty acid metabolism. Carcinogenesis. 2018;39(6):826-37.

108.   Ho E, Clarke JD, Dashwood RH. Dietary sulforaphane, a histone deacetylase inhibitor for cancer prevention. The Journal of nutrition. 2009;139(12):2393-6.

109.   Ferreira PMP, Rodrigues L, de Alencar Carnib LP, de Lima Sousa PV, Nolasco Lugo LM, Nunes NMF, et al. Cruciferous Vegetables as Antioxidative, Chemopreventive and Antineoplasic Functional Foods: Preclinical and Clinical Evidences of Sulforaphane Against Prostate Cancers. Curr Pharm Des. 2018;24(40):4779-93.

110.   Gibbs A, Schwartzman J, Deng V, Alumkal J. Sulforaphane destabilizes the androgen receptor in prostate cancer cells by inactivating histone deacetylase 6. Proc Natl Acad Sci U S A. 2009;106(39):16663-8.

111.   Beaver LM, Lhr CV, Clarke JD, Glasser ST, Watson GW, Wong CP, et al. Broccoli Sprouts Delay Prostate Cancer Formation and Decrease Prostate Cancer Severity with a Concurrent Decrease in HDAC3 Protein Expression in Transgenic Adenocarcinoma of the Mouse Prostate (TRAMP) Mice. Current developments in nutrition. 2018;2(3):nzy002.

112.   Zhou Y, Yang G, Tian H, Hu Y, Wu S, Geng Y, et al. Sulforaphane metabolites cause apoptosis via microtubule disruption in cancer. Endocr Relat Cancer. 2018;25(3):255-68.

113.   Liu B, Mao Q, Cao M, Xie L. Cruciferous vegetables intake and risk of prostate cancer: a meta-analysis. International journal of urology : official journal of the Japanese Urological Association. 2012;19(2):134-41.

114.   Richman EL, Carroll PR, Chan JM. Vegetable and fruit intake after diagnosis and risk of prostate cancer progression. International journal of cancer. 2012;131(1):201-10.

115.   Cohen JH, Kristal AR, Stanford JL. Fruit and vegetable intakes and prostate cancer risk. Journal of the National Cancer Institute. 2000;92(1):61-8.

116.   Jain MG, Hislop GT, Howe GR, Ghadirian P. Plant foods, antioxidants, and prostate cancer risk: findings from case-control studies in Canada. Nutrition and cancer. 1999;34(2):173-84.

117.   Kirsh VA, Peters U, Mayne ST, Subar AF, Chatterjee N, Johnson CC, et al. Prospective study of fruit and vegetable intake and risk of prostate cancer. Journal of the National Cancer Institute. 2007;99(15):1200-9.

118.   Richman EL, Carroll PR, Chan JM. Vegetable and fruit intake after diagnosis and risk of prostate cancer progression. International journal of cancer. 2012;131(1):201-10.

119.   Zhang Z, Garzotto M, Davis EW, 2nd, Mori M, Stoller WA, Farris PE, et al. Sulforaphane Bioavailability and Chemopreventive Activity in Men Presenting for Biopsy of the Prostate Gland: A Randomized Controlled Trial. Nutrition and cancer. 2019:1-14.

120.   Traka MH, Saha S, Huseby S, Kopriva S, Walley PG, Barker GC, et al. Genetic regulation of glucoraphanin accumulation in Beneforte broccoli. New Phytol. 2013;198(4):1085-95.

121.   Lawson LD, Wang ZJ. Allicin and Allicin-Derived Garlic Compounds Increase Breath Acetone through Allyl Methyl Sulfide: Use in Measuring Allicin Bioavailability. Journal of Agricultural and Food Chemistry. 2005;53(6):1974-83.

122.   Lawson LD, Hunsaker SM. Allicin Bioavailability and Bioequivalence from Garlic Supplements and Garlic Foods. Nutrients. 2018;10(7).

123.   Hanahan D, Weinberg RA. Hallmarks of cancer: the next generation. Cell. 2011;144(5):646-74.

124.   Arunkumar A, Vijayababu MR, Kanagaraj P, Balasubramanian K, Aruldhas MM, Arunakaran J. Growth suppressing effect of garlic compound diallyl disulfide on prostate cancer cell line (PC-3) in vitro. Biological & pharmaceutical bulletin. 2005;28(4):740-3.

125.   Herman-Antosiewicz A, Stan SD, Hahm ER, Xiao D, Singh SV. Activation of a novel ataxia-telangiectasia mutated and Rad3 related/checkpoint kinase 1-dependent prometaphase checkpoint in cancer cells by diallyl trisulfide, a promising cancer chemopreventive constituent of processed garlic. Molecular cancer therapeutics. 2007;6(4):1249-61.

126.   Shukla Y, Kalra N. Cancer chemoprevention with garlic and its constituents. Cancer letters. 2007;247(2):167-81.

127.   W. Wattenberg L. Inhibition of Carcinogenesis by minor Anutrient Constituents of the Diet1990. 173-83 p.

128.   Pinto J, Qiao C, Xing J, P. Suffoletto B, B. Schubert K, S. Rivlin R, et al. Alterations of prostate biomarker expression and testosterone utilization in human LNCaP prostatic carcinoma cells by garlic-derived S-allylmercaptocysteine2000. 304-14 p.

129.   Hsing AW, Chokkalingam AP, Gao Y-T, Madigan MP, Deng J, Gridley G, et al. Allium Vegetables and Risk of Prostate Cancer: A Population-Based Study. JNCI: Journal of the National Cancer Institute. 2002;94(21):1648-51.

130.   Zhou XF, Ding ZS, Liu NB. Allium vegetables and risk of prostate cancer: evidence from 132,192 subjects. Asian Pacific journal of cancer prevention : APJCP. 2013;14(7):4131-4.

131.   Setiawan VW, Yu G-P, Lu Q-Y, Lu M-L, Yu S-Z, Mu L, et al. Allium vegetables and stomach cancer risk in China. Asian Pacific journal of cancer prevention : APJCP. 2005;6(3):387-95.

132.   Edmands WMB, Gooderham NJ, Holmes E, Mitchell SC. S-Methyl-l-cysteine sulphoxide: the Cinderella phytochemical? Toxicology Research. 2013;2(1):11-22.

133.   Coode-Bate J ST, Melchini A, Saha S, Needs P, Dainty JR, Maicha J-B, Beasy G, Traka GH, Mills RD, Ball RY, Mithen RF* Accumulation of dietary S-methyl cysteine sulfoxide in human prostate tissue 2019:Awaiting publication. DOI: 10.1002/mnfr.201900461.

134.   Waring RH, Harris RM, Steventon GB, Mitchell SC. Degradation to sulphate of S-methyl-L-cysteine sulphoxide and S-carboxymethyl-L-cysteine sulphoxide in man. Drug metabolism and drug interactions. 2003;19(4):241-55.

135.   Cao DL, Ye DW, Dai B, Zhang HL, Shen YJ, Zhu Y, et al. Association of glutathione S-transferase T1 and M1 polymorphisms with prostate cancer susceptibility in populations of Asian descent: a meta-analysis. Oncotarget. 2015;6(34):35843-50.

136.   Gong M, Dong W, Shi Z, Xu Y, Ni W, An R. Genetic polymorphisms of GSTM1, GSTT1, and GSTP1 with prostate cancer risk: a meta-analysis of 57 studies. PloS one. 2012;7(11):e50587-e.

137.   Townsend DM, Tew KD. The role of glutathione-S-transferase in anti-cancer drug resistance. Oncogene. 2003;22(47):7369-75.

138.   Mo Z, Gao Y, Cao Y, Gao F, Jian L. An updating meta-analysis of the GSTM1, GSTT1, and GSTP1 polymorphisms and prostate cancer: a HuGE review. Prostate. 2009;69(6):662-88.

139.   Joseph MA, Moysich KB, Freudenheim JL, Shields PG, Bowman ED, Zhang Y, et al. Cruciferous vegetables, genetic polymorphisms in glutathione S-transferases M1 and T1, and prostate cancer risk. Nutrition and cancer. 2004;50(2):206-13.

140.   Zhang Y, Kolm RH, Mannervik B, Talalay P. Reversible conjugation of isothiocyanates with glutathione catalyzed by human glutathione transferases. Biochem Biophys Res Commun. 1995;206(2):748-55.

141.   Gasper AV, Al-Janobi A, Smith JA, Bacon JR, Fortun P, Atherton C, et al. Glutathione S-transferase M1 polymorphism and metabolism of sulforaphane from standard and high-glucosinolate broccoli. Am J Clin Nutr. 2005;82(6):1283-91.

142.   Steck SE, Gammon MD, Hebert JR, Wall DE, Zeisel SH. GSTM1, GSTT1, GSTP1, and GSTA1 polymorphisms and urinary isothiocyanate metabolites following broccoli consumption in humans. The Journal of nutrition. 2007;137(4):904-9.

143.   Wark PA, Grubben MJAL, Peters WHM, Nagengast FM, Kampman E, Kok FJ, et al. Habitual consumption of fruits and vegetables: associations with human rectal glutathione S -transferase. Carcinogenesis. 2004;25(11):2135-42.

144.   Lampe JW, Chen C, Li S, Prunty J, Grate MT, Meehan DE, et al. Modulation of Human Glutathione S-Transferases by Botanically Defined Vegetable Diets. Cancer Epidemiology Biomarkers &amp; Prevention. 2000;9(8):787.

145.   Hodges RE, Minich DM. Modulation of Metabolic Detoxification Pathways Using Foods and Food-Derived Components: A Scientific Review with Clinical Application. Journal of Nutrition and Metabolism. 2015;2015:760689.

146.   Hatono S, Jimenez A, Wargovich MJ. Chemopreventive effect of S-allylcysteine and its relationship to the detoxification enzyme glutathione S-transferase. Carcinogenesis. 1996;17(5):1041-4.

147.   Mangels AR, Holden JM, Beecher GR, Forman MR, Lanza E. Carotenoid content of fruits and vegetables: an evaluation of analytic data. Journal of the American Dietetic Association. 1993;93(3):284-96.

148.   Zechmeister L. Cis-trans Isomerization and Stereochemistry of Carotenoids and Diphenyl-polyenes. Chemical Reviews. 1944;34(2):267-344.

149.   Clinton SK. Lycopene: chemistry, biology, and implications for human health and disease. Nutrition reviews. 1998;56(2 Pt 1):35-51.

150.   Holzapfel NP, Holzapfel BM, Champ S, Feldthusen J, Clements J, Hutmacher DW. The potential role of lycopene for the prevention and therapy of prostate cancer: from molecular mechanisms to clinical evidence. International journal of molecular sciences. 2013;14(7):14620-46.

151.   Hart DJ, Scott KJ. Development and evaluation of an HPLC method for the analysis of carotenoids in foods, and the measurement of the carotenoid content of vegetables and fruits commonly consumed in the UK. Food Chemistry. 1995;54(1):101-11.

152.   Tonucci LH, Holden JM, Beecher GR, Khachik F, Davis CS, Mulokozi G. Carotenoid Content of Thermally Processed Tomato-Based Food Products. Journal of Agricultural and Food Chemistry. 1995;43(3):579-86.

153.   Story EN, Kopec RE, Schwartz SJ, Harris GK. An update on the health effects of tomato lycopene. Annu Rev Food Sci Technol. 2010;1:189-210.

154.   Rao AV, Ray MR, Rao LG. Lycopene. Advances in food and nutrition research. 2006;51:99-164.

155.   Sanadi RM DM, Ambulgekar JR and Khambatta X: Lycopene: It's Role in Health and Disease. Int J Pharm Sci Res. 3(12); 4578-4582. Lycopene: It's Role in Health and Disease

156.   Moran NE, Erdman JW, Jr., Clinton SK. Complex interactions between dietary and genetic factors impact lycopene metabolism and distribution. Arch Biochem Biophys. 2013;539(2):171-80.

157.   Kaplan LA, Lau JM, Stein EA. Carotenoid composition, concentrations, and relationships in various human organs. Clinical physiology and biochemistry. 1990;8(1):1-10.

158.   Durairajanayagam D, Agarwal A, Ong C, Prashast P. Lycopene and male infertility. Asian J Androl. 2014;16(3):420-5.

159.   Agarwal S, Rao AV. Tomato lycopene and its role in human health and chronic diseases. CMAJ : Canadian Medical Association journal = journal de l'Association medicale canadienne. 2000;163(6):739-44.

160.   Hwang ES, Bowen PE. Cell cycle arrest and induction of apoptosis by lycopene in LNCaP human prostate cancer cells. Journal of medicinal food. 2004;7(3):284-9.

161.   Ivanov NI, Cowell SP, Brown P, Rennie PS, Guns ES, Cox ME. Lycopene differentially induces quiescence and apoptosis in androgen-responsive and -independent prostate cancer cell lines. Clinical nutrition (Edinburgh, Scotland). 2007;26(2):252-63.

162.   Tang L, Jin T, Zeng X, Wang JS. Lycopene inhibits the growth of human androgen-independent prostate cancer cells in vitro and in BALB/c nude mice. The Journal of nutrition. 2005;135(2):287-90.

163.   Hantz HL, Young LF, Martin KR. Physiologically attainable concentrations of lycopene induce mitochondrial apoptosis in LNCaP human prostate cancer cells. Experimental biology and medicine (Maywood, NJ). 2005;230(3):171-9.

164.   Applegate CC, Rowles JL, 3rd, Erdman JW, Jr. Can Lycopene Impact the Androgen Axis in Prostate Cancer?: A Systematic Review of Cell Culture and Animal Studies. Nutrients. 2019;11(3).

165.   Rowles J, M Ranard K, Smith J, an R, Erdman Jr J. Increased dietary and circulating lycopene are associated with reduced prostate cancer risk: A systematic review and meta-analysis2017. 361 p.

166.   Wang Y, Cui R, Xiao Y, Fang J, Xu Q. Effect of Carotene and Lycopene on the Risk of Prostate Cancer: A Systematic Review and Dose-Response Meta-Analysis of Observational Studies. PloS one. 2015;10(9):e0137427-e.

167.   Van Hoang D, Pham NM, Lee AH, Tran DN, Binns CW. Dietary Carotenoid Intakes and Prostate Cancer Risk: A Case-Control Study from Vietnam. Nutrients. 2018;10(1):70.

168.   Key TJ, Appleby PN, Travis RC, Albanes D, Alberg AJ, Barricarte A, et al. Carotenoids, retinol, tocopherols, and prostate cancer risk: pooled analysis of 15 studies. The American journal of clinical nutrition. 2015;102(5):1142-57.

169.   Weaver CM, Miller JW. Challenges in conducting clinical nutrition research. Nutrition reviews. 2017;75(7):491-9.

170.   Giovannucci E, Rimm EB, Liu Y, Stampfer MJ, Willett WC. A prospective study of tomato products, lycopene, and prostate cancer risk. Journal of the National Cancer Institute. 2002;94(5):391-8.

171.   Kim HS, Bowen P, Chen L, Duncan C, Ghosh L, Sharifi R, et al. Effects of tomato sauce consumption on apoptotic cell death in prostate benign hyperplasia and carcinoma. Nutrition and cancer. 2003;47(1):40-7.

172.   Morgia G, Voce S, Palmieri F, Gentile M, Iapicca G, Giannantoni A, et al. Association between selenium and lycopene supplementation and incidence of prostate cancer: Results from the post-hoc analysis of the procomb trial. Phytomedicine : international journal of phytotherapy and phytopharmacology. 2017;34:1-5.

173.   Dybkowska E, Sadowska A, Swiderski F, Rakowska R, Wysocka K. The occurrence of resveratrol in foodstuffs and its potential for supporting cancer prevention and treatment. A review. Roczniki Panstwowego Zakladu Higieny. 2018;69(1):5-14.

174.   Fernandez-Marin M, Mateos R, Garcia-Parrilla M, Puertas B, Cantos-Villar E. Bioactive compounds in wine: Resveratrol, hydroxytyrosol and melatonin: A review2012. 797–813 p.

175.   Mikstacka R, Ignatowicz E. [Chemopreventive and chemotherapeutic effect of trans-resveratrol and its analogues in cancer]. Polski merkuriusz lekarski : organ Polskiego Towarzystwa Lekarskiego. 2010;28(168):496-500.

176.   Hurst WJ, Glinski JA, Miller KB, Apgar J, Davey MH, Stuart DA. Survey of the trans-resveratrol and trans-piceid content of cocoa-containing and chocolate products. J Agric Food Chem. 2008;56(18):8374-8.

177.   Patel KR, Brown VA, Jones DJ, Britton RG, Hemingway D, Miller AS, et al. Clinical pharmacology of resveratrol and its metabolites in colorectal cancer patients. Cancer research. 2010;70(19):7392-9.

178.   Singh CK, Ndiaye MA, Ahmad N. Resveratrol and cancer: Challenges for clinical translation. Biochim Biophys Acta. 2015;1852(6):1178-85.

179.   Almeida L, Vaz-da-Silva M, Falcao A, Soares E, Costa R, Loureiro AI, et al. Pharmacokinetic and safety profile of trans-resveratrol in a rising multiple-dose study in healthy volunteers. Molecular nutrition & food research. 2009;53 Suppl 1:S7-15.

180.   Ganapathy S, Chen Q, Singh KP, Shankar S, Srivastava RK. Resveratrol Enhances Antitumor Activity of TRAIL in Prostate Cancer Xenografts through Activation of FOXO Transcription Factor. PLOS ONE. 2011;5(12):e15627.

181.   Kumar A, Dhar S, Rimando AM, Lage JM, Lewin JR, Zhang X, et al. Epigenetic potential of resveratrol and analogs in preclinical models of prostate cancer. Ann N Y Acad Sci. 2015;1348(1):1-9.

182.   Kampa M, Hatzoglou A, Notas G, Damianaki A, Bakogeorgou E, Gemetzi C, et al. Wine antioxidant polyphenols inhibit the proliferation of human prostate cancer cell lines. Nutrition and cancer. 2000;37(2):223-33.

183.   Harper CE, Patel BB, Wang J, Arabshahi A, Eltoum IA, Lamartiniere CA. Resveratrol suppresses prostate cancer progression in transgenic mice. Carcinogenesis. 2007;28(9):1946-53.

184.   Jang YG, Go RE, Hwang KA, Choi KC. Resveratrol inhibits DHT-induced progression of prostate cancer cell line through interfering with the AR and CXCR4 pathway. J Steroid Biochem Mol Biol. 2019;192:105406.

185.   Benitez DA, Pozo-Guisado E, Clementi M, Castellón E, Fernandez-Salguero PM. Non-genomic action of resveratrol on androgen and oestrogen receptors in prostate cancer: modulation of the phosphoinositide 3-kinase pathway. British journal of cancer. 2007;96(10):1595-604.

186.   Zhao J, Stockwell T, Roemer A, Chikritzhs T. Is alcohol consumption a risk factor for prostate cancer? A systematic review and meta-analysis. BMC Cancer. 2016;16(1):845.

187.   Vartolomei MD, Kimura S, Ferro M, Foerster B, Abufaraj M, Briganti A, et al. The impact of moderate wine consumption on the risk of developing prostate cancer. Clin Epidemiol. 2018;10:431-44.

188.   Sutcliffe S, Giovannucci E, Leitzmann MF, Rimm EB, Stampfer MJ, Willett WC, et al. A prospective cohort study of red wine consumption and risk of prostate cancer. International journal of cancer. 2007;120(7):1529-35.

189.   Kjaer TN, Ornstrup MJ, Poulsen MM, Jorgensen JO, Hougaard DM, Cohen AS, et al. Resveratrol reduces the levels of circulating androgen precursors but has no effect on, testosterone, dihydrotestosterone, PSA levels or prostate volume. A 4-month randomised trial in middle-aged men. Prostate. 2015;75(12):1255-63.

190.   Yang CS, Wang H, Li GX, Yang Z, Guan F, Jin H. Cancer prevention by tea: Evidence from laboratory studies. Pharmacological research. 2011;64(2):113-22.

191.   Yang CS, Wang X, Lu G, Picinich SC. Cancer prevention by tea: animal studies, molecular mechanisms and human relevance. Nat Rev Cancer. 2009;9(6):429-39.

192.   Kumar NB, Dickinson SI, Schell MJ, Manley BJ, Poch MA, Pow-Sang J. Green tea extract for prevention of prostate cancer progression in patients on active surveillance. Oncotarget. 2018;9(102):37798-806.

193.   Chuu C-P, Chen R-Y, Kokontis JM, Hiipakka RA, Liao S. Suppression of androgen receptor signaling and prostate specific antigen expression by (-)-epigallocatechin-3-gallate in different progression stages of LNCaP prostate cancer cells. Cancer letters. 2009;275(1):86-92.

194.   Albrecht DS, Clubbs EA, Ferruzzi M, Bomser JA. Epigallocatechin-3-gallate (EGCG) inhibits PC-3 prostate cancer cell proliferation via MEK-independent ERK1/2 activation. Chemico-biological interactions. 2008;171(1):89-95.

195.   Rocha S, Generalov R, Pereira Mdo C, Peres I, Juzenas P, Coelho MA. Epigallocatechin gallate-loaded polysaccharide nanoparticles for prostate cancer chemoprevention. Nanomedicine (London, England). 2011;6(1):79-87.

196.   Johnson JJ, Bailey HH, Mukhtar H. Green tea polyphenols for prostate cancer chemoprevention: a translational perspective. Phytomedicine : international journal of phytotherapy and phytopharmacology. 2010;17(1):3-13.

197.   Guo Y, Zhi F, Chen P, Zhao K, Xiang H, Mao Q, et al. Green tea and the risk of prostate cancer: A systematic review and meta-analysis. Medicine (Baltimore). 2017;96(13):e6426-e.

198.   Lin YW, Hu ZH, Wang X, Mao QQ, Qin J, Zheng XY, et al. Tea consumption and prostate cancer: an updated meta-analysis. World J Surg Oncol. 2014;12:38.

199.   Fei X, Shen Y, Li X, Guo H. The association of tea consumption and the risk and progression of prostate cancer: a meta-analysis. Int J Clin Exp Med. 2014;7(11):3881-91.

200.   Jian L, Xie LP, Lee AH, Binns CW. Protective effect of green tea against prostate cancer: a case-control study in southeast China. International journal of cancer. 2004;108(1):130-5.

201.   Bettuzzi S, Brausi M, Rizzi F, Castagnetti G, Peracchia G, Corti A. Chemoprevention of human prostate cancer by oral administration of green tea catechins in volunteers with high-grade prostate intraepithelial neoplasia: a preliminary report from a one-year proof-of-principle study. Cancer research. 2006;66(2):1234-40.

202.   Kumar NB, Pow-Sang J, Egan KM, Spiess PE, Dickinson S, Salup R, et al. Randomized, Placebo-Controlled Trial of Green Tea Catechins for Prostate Cancer Prevention. Cancer Prev Res (Phila). 2015;8(10):879-87.

203.   Henning SM, Wang P, Said JW, Huang M, Grogan T, Elashoff D, et al. Randomized clinical trial of brewed green and black tea in men with prostate cancer prior to prostatectomy. Prostate. 2015;75(5):550-9.

204.   Hewlings SJ, Kalman DS. Curcumin: A Review of Its' Effects on Human Health. Foods. 2017;6(10):92.

205.   Pan MH, Huang TM, Lin JK. Biotransformation of curcumin through reduction and glucuronidation in mice. Drug metabolism and disposition: the biological fate of chemicals. 1999;27(4):486-94.

206.   Prasad S, Tyagi AK, Aggarwal BB. Recent developments in delivery, bioavailability, absorption and metabolism of curcumin: the golden pigment from golden spice. Cancer Res Treat. 2014;46(1):2-18.

207.   Shoba G, Joy D, Joseph T, Majeed M, Rajendran R, Srinivas PS. Influence of piperine on the pharmacokinetics of curcumin in animals and human volunteers. Planta medica. 1998;64(4):353-6.

208.   Yu XL, Jing T, Zhao H, Li PJ, Xu WH, Shang FF. Curcumin inhibits expression of inhibitor of DNA binding 1 in PC3 cells and xenografts. Asian Pacific journal of cancer prevention : APJCP. 2014;15(3):1465-70.

209.   Korang-Yeboah M, Patel D, Morton D, Sharma P, Gorantla Y, Joshi J, et al. Intra-tumoral delivery of functional ID4 protein via PCL/maltodextrin nano-particle inhibits prostate cancer growth. Oncotarget. 2016;7(42):68072-85.

210.   Khurana N, Sikka SC. Targeting Crosstalk between Nrf-2, NF-κB and Androgen Receptor Signaling in Prostate Cancer. Cancers (Basel). 2018;10(10):352.

211.   Li W, Su ZY, Guo Y, Zhang C, Wu R, Gao L, et al. Curcumin Derivative Epigenetically Reactivates Nrf2 Antioxidative Stress Signaling in Mouse Prostate Cancer TRAMP C1 Cells. Chem Res Toxicol. 2018;31(2):88-96.

212.   Nakamura K, Yasunaga Y, Segawa T, Ko D, Moul JW, Srivastava S, et al. Curcumin down-regulates AR gene expression and activation in prostate cancer cell lines. International journal of oncology. 2002;21(4):825-30.

213.   Shah S, Prasad S, Knudsen KE. Targeting pioneering factor and hormone receptor cooperative pathways to suppress tumor progression. Cancer research. 2012;72(5):1248-59.

214.   Choi YH, Han DH, Kim S-w, Kim M-J, Sung HH, Jeon HG, et al. A randomized, double-blind, placebo-controlled trial to evaluate the role of curcumin in prostate cancer patients with intermittent androgen deprivation. The Prostate. 2019;79(6):614-21.

215.   Hejazi J, Rastmanesh R, Taleban FA, Molana SH, Hejazi E, Ehtejab G, et al. Effect of Curcumin Supplementation During Radiotherapy on Oxidative Status of Patients with Prostate Cancer: A Double Blinded, Randomized, Placebo-Controlled Study. Nutrition and cancer. 2016;68(1):77-85.

216.   Selma MV, Beltran D, Luna MC, Romo-Vaquero M, Garcia-Villalba R, Mira A, et al. Isolation of Human Intestinal Bacteria Capable of Producing the Bioactive Metabolite Isourolithin A from Ellagic Acid. Front Microbiol. 2017;8:1521.

217.   Bassiri-Jahromi S. Punica granatum (Pomegranate) activity in health promotion and cancer prevention. Oncology reviews. 2018;12(1):345.

218.   Adaramoye O, Erguen B, Nitzsche B, Hopfner M, Jung K, Rabien A. Punicalagin, a polyphenol from pomegranate fruit, induces growth inhibition and apoptosis in human PC-3 and LNCaP cells. Chemico-biological interactions. 2017;274:100-6.

219.   Mohammed Saleem YI, Albassam H, Selim M. Urolithin A induces prostate cancer cell death in p53-dependent and in p53-independent manner. Eur J Nutr. 2019.

220.   Shi D, Gu W. Dual Roles of MDM2 in the Regulation of p53: Ubiquitination Dependent and Ubiquitination Independent Mechanisms of MDM2 Repression of p53 Activity. Genes Cancer. 2012;3(3-4):240-8.

221.   Deng Y, Li Y, Yang F, Zeng A, Yang S, Luo Y, et al. The extract from Punica granatum (pomegranate) peel induces apoptosis and impairs metastasis in prostate cancer cells. Biomed Pharmacother. 2017;93:976-84.

222.   Deng YL, Li YL, Zheng TT, Hu MX, Ye TH, Xie YM, et al. [The Extract from Punica Granatum (Pomegranate) Leaves Promotes Apoptosis and Impairs Metastasis in Prostate Cancer Cells]. Sichuan Da Xue Xue Bao Yi Xue Ban. 2018;49(1):8-12.

223.   Landete JM. Ellagitannins, ellagic acid and their derived metabolites: A review about source, metabolism, functions and health. Food research international. 2011;v. 44(no. 5):pp. 1150-60-2011 v.44 no.5.

224.   Paller CJ, Pantuck A, Carducci MA. A review of pomegranate in prostate cancer. Prostate cancer and prostatic diseases. 2017;20(3):265-70.

225.   Domingo-Domenech J, Mellado B, Ferrer B, Truan D, Codony-Servat J, Sauleda S, et al. Activation of nuclear factor-kappaB in human prostate carcinogenesis and association to biochemical relapse. British journal of cancer. 2005;93(11):1285-94.

226.   Fradet V, Lessard L, Begin LR, Karakiewicz P, Masson AM, Saad F. Nuclear factor-kappaB nuclear localization is predictive of biochemical recurrence in patients with positive margin prostate cancer. Clinical cancer research : an official journal of the American Association for Cancer Research. 2004;10(24):8460-4.

227.   Klein KA, Reiter RE, Redula J, Moradi H, Zhu XL, Brothman AR, et al. Progression of metastatic human prostate cancer to androgen independence in immunodeficient SCID mice. Nat Med. 1997;3(4):402-8.

228.   Rettig MB, Heber D, An J, Seeram NP, Rao JY, Liu H, et al. Pomegranate extract inhibits androgen-independent prostate cancer growth through a nuclear factor-kappaB-dependent mechanism. Molecular cancer therapeutics. 2008;7(9):2662-71.

229.   Wang Y, Zhang S, Iqbal S, Chen Z, Wang X, Wang YA, et al. Pomegranate extract inhibits the bone metastatic growth of human prostate cancer cells and enhances the in vivo efficacy of docetaxel chemotherapy. Prostate. 2013.

230.   Wang L, Martins-Green M. Pomegranate and its components as alternative treatment for prostate cancer. Int J Mol Sci. 2014;15(9):14949-66.

231.   Wang D, Ozen C, Abu-Reidah IM, Chigurupati S, Patra JK, Horbanczuk JO, et al. Vasculoprotective Effects of Pomegranate (Punica granatum L.). Frontiers in pharmacology. 2018;9:544.

232.   Pantuck AJ, Leppert JT, Zomorodian N, Aronson W, Hong J, Barnard RJ, et al. Phase II study of pomegranate juice for men with rising prostate-specific antigen following surgery or radiation for prostate cancer. Clinical cancer research : an official journal of the American Association for Cancer Research. 2006;12(13):4018-26.

233.   Paller CJ, Ye X, Wozniak PJ, Gillespie BK, Sieber PR, Greengold RH, et al. A randomized phase II study of pomegranate extract for men with rising PSA following initial therapy for localized prostate cancer. Prostate cancer and prostatic diseases. 2013;16(1):50-5.

234.   Stenner-Liewen F, Liewen H, Cathomas R, Renner C, Petrausch U, Sulser T, et al. Daily Pomegranate Intake Has No Impact on PSA Levels in Patients with Advanced Prostate Cancer - Results of a Phase IIb Randomized Controlled Trial. J Cancer. 2013;4(7):597-605.

235.   Freedland SJ, Carducci M, Kroeger N, Partin A, Rao JY, Jin Y, et al. A double-blind, randomized, neoadjuvant study of the tissue effects of POMx pills in men with prostate cancer before radical prostatectomy. Cancer Prev Res (Phila). 2013;6(10):1120-7.

236.   Sivapalan T, Melchini A, Saha S, Needs PW, Traka MH, Tapp H, et al. Bioavailability of Glucoraphanin and Sulforaphane from High-Glucoraphanin Broccoli. Molecular nutrition & food research. 2018;62(18):e1700911.

237.   Doble A, Walker MM, Harris JR, Taylor-Robinson D, Witherow RO. Intraprostatic antibody deposition in chronic abacterial prostatitis. Br J Urol. 1990;65(6):598-605.

238.   S Kirby R, Lowe D, I Bultitude M, E. D. Shuttleworth K. Intra-prostatic Urinary Reflux: an Aetiological Factor in Abacterial Prostatitis1983. 729-31 p.

239.   Balasar M, Doğan M, Kandemir A, Taskapu HH, Cicekci F, Toy H, et al. Investigation of granulomatous prostatitis incidence following intravesical BCG therapy. International journal of clinical and experimental medicine. 2014;7(6):1554-7.

240.   Terris MK, Macy M, Freiha FS. Transrectal Ultrasound Appearance of Prostatic Granulomas Secondary to Bacillus Calmette-Guerin Instillation. The Journal of urology. 1997;158(1):126-7.

241.   Blacklock NJ. Anatomical factors in prostatitis. Br J Urol. 1974;46(1):47-54.

242.   Nickel JC. Textbook of Prostatitis: Taylor and Francis; 1999.

243.   Fraser M, Sabelnykova VY, Yamaguchi TN, Heisler LE, Livingstone J, Huang V, et al. Genomic hallmarks of localized, non-indolent prostate cancer. Nature. 2017;541(7637):359-64.

244.   Abida W, Cyrta J, Heller G, Prandi D, Armenia J, Coleman I, et al. Genomic correlates of clinical outcome in advanced prostate cancer. Proc Natl Acad Sci U S A. 2019;116(23):11428-36.

245.   Quigley DA, Dang HX, Zhao SG, Lloyd P, Aggarwal R, Alumkal JJ, et al. Genomic Hallmarks and Structural Variation in Metastatic Prostate Cancer. Cell. 2018;174(3):758-69.e9.

246.   Cavarretta I, Ferrarese R, Cazzaniga W, Saita D, Lucianò R, Ceresola ER, et al. The Microbiome of the Prostate Tumor Microenvironment. European urology. 2017;72(4):625-31.

247.   Banerjee S, Alwine JC, Wei Z, Tian T, Shih N, Sperling C, et al. Microbiome signatures in prostate cancer. Carcinogenesis. 2019.

248.   Dennis LK, Lynch CF, Torner JC. Epidemiologic association between prostatitis and prostate cancer. Urology. 2002;60(1):78-83.

249.   Alfano M, Canducci F, Nebuloni M, Clementi M, Montorsi F, Salonia A. The interplay of extracellular matrix and microbiome in urothelial bladder cancer. Nature Reviews Urology. 2015;13:77.

250.   Simons BW, Durham NM, Bruno TC, Grosso JF, Schaeffer AJ, Ross AE, et al. A human prostatic bacterial isolate alters the prostatic microenvironment and accelerates prostate cancer progression. The Journal of pathology. 2015;235(3):478-89.

251.   Sfanos KS, De Marzo AM. Prostate cancer and inflammation: the evidence. Histopathology. 2012;60(1):199-215.

252.   Traka M, Mithen R. Glucosinolates, isothiocyanates and human health2009. 269-82 p.

253.   European Food Safety Authority (EFSA), available online at http://www.efsa.europa.eu/en/topics/topic/nutrition. Accessed August 2019.

254.   Lucey A, Heneghan C, Kiely ME. Guidance for the design and implementation of human dietary intervention studies for health claim submissions. Nutrition Bulletin. 2016;41(4):378-94.

255.   Sivapalan T, Melchini A, Saha S, Needs P, Traka M, Tapp H, et al. Bioavailability of Glucoraphanin and Sulforaphane From High-Glucoraphanin Broccoli. Molecular nutrition & food research. 2017;62.

256.   Pressman P, Clemens RA, Hayes AW. Bioavailability of micronutrients obtained from supplements and food: A survey and case study of the polyphenols. Toxicology Research and Application. 2017;1:2397847317696366.

257.   Mithen R, Faulkner K, Magrath R, Rose P, Williamson G, Marquez J. Development of isothiocyanate-enriched broccoli, and its enhanced ability to induce phase 2 detoxification enzymes in mammalian cells. Theor Appl Genet. 2003;106(4):727-34.

258.   Lentjes MAH. The balance between food and dietary supplements in the general population. Proc Nutr Soc. 2019;78(1):97-109.

259.   de Jong N, Ocké MC, Branderhorst HA, Friele R. Demographic and lifestyle characteristics of functional food consumers and dietary supplement users. Br J Nutr. 2003;89(2):273-81.

260.   Bailey RL, Gahche JJ, Miller PE, Thomas PR, Dwyer JT. Why US adults use dietary supplements. JAMA Intern Med. 2013;173(5):355-61.

261.   Public Health England Nutrition Science Team. Government Dietary Recommendations: Government recommendations for food energy and nutrients for males and females aged 1-18 years and 19+ years; 2016. 1–12. https://www.gov.uk/government/uploads/ system/uploads/attachment_data/file/618167/gover nment_dietary_recommendations.pdf [Accessed September 2020].

262.   Traka MH, Saha S, Huseby S, Kopriva S, Walley PG, Barker GC, et al. Genetic regulation of glucoraphanin accumulation in Beneforté broccoli. New Phytol. 2013;198(4):1085-95.

263.   Jack Coode-Bate1, Tharsini Sivapalan1, Antonietta Melchini1, Shikha Saha1, Paul Needs1, Jack R Dainty6, Maria H Traka1, Robert D Mills2, Richard Y Ball3, Richard F Mithen1* Accumulation of dietary S-methyl cysteine sulfoxide in human prostate tissue

264.   Agudo A, Slimani N, Ocké MC, Naska A, Miller AB, Kroke A, et al. Consumption of vegetables, fruit and other plant foods in the European Prospective Investigation into Cancer and Nutrition (EPIC) cohorts from 10 European countries. Public Health Nutrition. 2002;5(6b):1179-96.

265.   Shapiro TA, Fahey JW, Dinkova-Kostova AT, Holtzclaw WD, Stephenson KK, Wade KL, et al. Safety, tolerance, and metabolism of broccoli sprout glucosinolates and isothiocyanates: a clinical phase I study. Nutrition and cancer. 2006;55(1):53-62.

266.   Yagishita Y, Fahey JW, Dinkova-Kostova AT, Kensler TW. Broccoli or Sulforaphane: Is It the Source or Dose That Matters? Molecules (Basel, Switzerland). 2019;24(19):3593.

267.   Fahey JW, Wade KL, Stephenson KK, Panjwani AA, Liu H, Cornblatt G, et al. Bioavailability of Sulforaphane Following Ingestion of Glucoraphanin-Rich Broccoli Sprout and Seed Extracts with Active Myrosinase: A Pilot Study of the Effects of Proton Pump Inhibitor Administration. Nutrients. 2019;11(7).

268.   Atwell LL, Zhang Z, Mori M, Farris P, Vetto JT, Naik AM, et al. Sulforaphane Bioavailability and Chemopreventive Activity in Women Scheduled for Breast Biopsy. Cancer prevention research (Philadelphia, Pa). 2015;8(12):1184-91.

269.   Clarke JD, Hsu A, Riedl K, Bella D, Schwartz SJ, Stevens JF, et al. Bioavailability and inter-conversion of sulforaphane and erucin in human subjects consuming broccoli sprouts or broccoli supplement in a cross-over study design. Pharmacological research. 2011;64(5):456-63.

270.   Lawson LD. Garlic: A Review of Its Medicinal Effects and Indicated Active Compounds. Phytomedicines of Europe. ACS Symposium Series. 691: American Chemical Society; 1998. p. 176-209.

271.   Song K, Milner JA. The influence of heating on the anticancer properties of garlic. The Journal of nutrition. 2001;131(3s):1054s-7s.

272.   Cavagnaro PF, Camargo A, Galmarini CR, Simon PW. Effect of cooking on garlic (Allium sativum L.) antiplatelet activity and thiosulfinates content. J Agric Food Chem. 2007;55(4):1280-8.

273.   Song K, Milner JA. Heating garlic inhibits its ability to suppress 7, 12-dimethylbenz(a)anthracene-induced DNA adduct formation in rat mammary tissue. The Journal of nutrition. 1999;129(3):657-61.

274.   Bayan L, Koulivand PH, Gorji A. Garlic: a review of potential therapeutic effects. Avicenna J Phytomed. 2014;4(1):1-14.

275.   Staba EJ, Lash L, Staba JE. A commentary on the effects of garlic extraction and formulation on product composition. The Journal of nutrition. 2001;131(3s):1118s-9s.

276.   Dietary Supplements: Garlic. The United States Pharmacopeia. Rockville, MD: United States Pharmacopeial Convention, Inc.; 2005:2087-2092.

277.   Lawson LD, Wang ZJ. Low allicin release from garlic supplements: a major problem due to the sensitivities of alliinase activity. J Agric Food Chem. 2001;49(5):2592-9.

278.   Yamaguchi Y, Kumagai H. Characteristics, biosynthesis, decomposition, metabolism and functions of the garlic odour precursor, S-allyl-L-cysteine sulfoxide. Exp Ther Med. 2020;19(2):1528-35.

279.   Magrath R, Herron C, Giamoustaris A, Mithen R. The Inheritance of Aliphatic Glucosinolates in Brassica napus. Plant Breeding. 1993;111(1):55-72.

280.   Saha S, Hollands W, Teucher B, Needs PW, Narbad A, Ortori CA, et al. Isothiocyanate concentrations and interconversion of sulforaphane to erucin in human subjects after consumption of commercial frozen broccoli compared to fresh broccoli. Molecular nutrition & food research. 2012;56(12):1906-16.

281.   Sivapalan T, Melchini A, Coode-Bate J, Needs PW, Mithen RF, Saha S. An LC-MS/MS Method to Measure S-Methyl-l-Cysteine and S-Methyl-l-Cysteine Sulfoxide in Human Specimens Using Isotope Labelled Internal Standards. Molecules (Basel, Switzerland) [Internet]. 2019 2019/07//; 24(13). Available from: http://europepmc.org/abstract/MED/31269651

https://doi.org/10.3390/molecules24132427

https://europepmc.org/articles/PMC6651111

https://europepmc.org/articles/PMC6651111?pdf=render.

282.   Kensler TW, Chen JG, Egner PA, Fahey JW, Jacobson LP, Stephenson KK, et al. Effects of glucosinolate-rich broccoli sprouts on urinary levels of aflatoxin-DNA adducts and phenanthrene tetraols in a randomized clinical trial in He Zuo township, Qidong, People's Republic of China. Cancer epidemiology, biomarkers &

prevention : a publication of the American Association for Cancer Research, cosponsored by the American Society of Preventive Oncology. 2005;14(11 Pt 1):2605-13.

283. Zhu Q, Kakino K, Nogami C, Ohnuki K, Shimizu K. An LC-MS/MS-SRM Method for Simultaneous Quantification of Four Representative Organosulphur Compounds in Garlic Products. Food Analytical Methods. 2016;9(12):3378-84.

284. Thomson CA, Newton TR, Graver EJ, Jackson KA, Reid PM, Hartz VL, et al. Cruciferous vegetable intake questionnaire improves cruciferous vegetable intake estimates. Journal of the American Dietetic Association. 2007;107(4):631-43.

285. United States Deparment of Agriculture Food Composition Databases (USDA). Available online: https://ndb.nal.usda.gov/ndb/ (accessed 14 June 2019).

286. Kasivisvanathan V, Rannikko AS, Borghi M, Panebianco V, Mynderse LA, Vaarala MH, et al. MRI-Targeted or Standard Biopsy for Prostate-Cancer Diagnosis. N Engl J Med. 2018;378(19):1767-77.

287. National Institute for Health and Care Excellence (NICE) Guidance 2019. Accessed 23.09.2020 https://www.nice.org.uk/guidance/NG131.

288. Forster SE, Jones L, Saxton JM, Flower DJ, Foulds G, Powers HJ, et al. Recruiting older people to a randomised controlled dietary intervention trial - how hard can it be? BMC Medical Research Methodology. 2010;10(1):17.

289. Wood AM, White IR, Thompson SG. Are missing outcome data adequately handled? A review of published randomized controlled trials in major medical journals. Clin Trials. 2004;1(4):368-76.

290. Bell ML, Kenward MG, Fairclough DL, Horton NJ. Differential dropout and bias in randomised controlled trials: when it matters and when it may not. BMJ. 2013;346:e8668-e.

291. Shapiro TA, Fahey JW, Wade KL, Stephenson KK, Talalay P. Chemoprotective Glucosinolates and Isothiocyanates of Broccoli Sprouts. Metabolism and Excretion in Humans. 2001;10(5):501-8.

292. Barba FJ, Nikmaram N, Roohinejad S, Khelfa A, Zhu Z, Koubaa M. Bioavailability of Glucosinolates and Their Breakdown Products: Impact of Processing. Frontiers in nutrition. 2016;3:24-.

293. Clarke JD, Hsu A, Riedl K, Bella D, Schwartz SJ, Stevens JF, et al. Bioavailability and inter-conversion of sulforaphane and erucin in human subjects consuming broccoli sprouts or broccoli supplement in a cross-over study design. Pharmacological research. 2011;64(5):456-63.

294. Gasper AV, Al-janobi A, Smith JA, Bacon JR, Fortun P, Atherton C, et al. Glutathione S-transferase M1 polymorphism and metabolism of sulforaphane from standard and high-glucosinolate broccoli. The American Journal of Clinical Nutrition. 2005;82(6):1283-91.

295. Saha S, Hollands W, Teucher B, Needs PW, Narbad A, Ortori CA, et al. Isothiocyanate concentrations and interconversion of sulforaphane to erucin in human subjects after consumption of commercial frozen broccoli compared to fresh broccoli. Molecular nutrition & food research. 2012;56(12):1906-16.

296. Conaway CC, Getahun SM, Liebes LL, Pusateri DJ, Topham DK, Botero-Omary M, et al. Disposition of glucosinolates and sulforaphane in humans after ingestion of steamed and fresh broccoli. Nutrition and cancer. 2000;38(2):168-78.

297. Zhang Z, Garzotto M, Davis EW, Mori M, Stoller WA, Farris PE, et al. Sulforaphane Bioavailability and Chemopreventive Activity in Men Presenting for Biopsy of the Prostate Gland: A Randomized Controlled Trial. Nutrition and cancer. 2020;72(1):74-87.

298. Cornblatt BS, Ye L, Dinkova-Kostova AT, Erb M, Fahey JW, Singh NK, et al. Preclinical and clinical evaluation of sulforaphane for chemoprevention in the breast. Carcinogenesis. 2007;28(7):1485-90.

299. Scheffler L, Sauermann Y, Heinlein A, Sharapa C, Buettner A. Detection of Volatile Metabolites Derived from Garlic (Allium sativum) in Human Urine. Metabolites. 2016;6(4):43.

300. Germain E, Auger J, Ginies C, Siess MH, Teyssier C. In vivo metabolism of diallyl disulphide in the rat: identification of two new metabolites. Xenobiotica. 2002;32(12):1127-38.

301. Bergman EN. Energy contributions of volatile fatty acids from the gastrointestinal tract in various species. Physiol Rev. 1990;70(2):567-90.

302. Verhagen H, Hageman GJ, Rauma AL, Versluis-de Haan G, van Herwijnen MH, de Groot J, et al. Biomonitoring the intake of garlic via urinary excretion of allyl mercapturic acid. Br J Nutr. 2001;86 Suppl 1:S111-4.

303. Praticò G, Gao Q, Manach C, Dragsted LO. Biomarkers of food intake for Allium vegetables. Genes & nutrition. 2018;13:34-.

304. Amagase H, Petesch BL, Matsuura H, Kasuga S, Itakura Y. Intake of Garlic and Its Bioactive Components. The Journal of nutrition. 2001;131(3):955S-62S.

305.   Budoff MJ, Takasu J, Flores FR, Niihara Y, Lu B, Lau BH, et al. Inhibiting progression of coronary calcification using Aged Garlic Extract in patients receiving statin therapy: a preliminary study. Prev Med. 2004;39(5):985-91.

306.   Jandke J, Spiteller G. Unusual conjugates in biological profiles originating from consumption of onions and garlic. J Chromatogr. 1987;421(1):1-8.

307.   Cope K, Seifried H, Seifried R, Milner J, Kris-Etherton P, Harrison EH. A gas chromatography-mass spectrometry method for the quantitation of N-nitrosoproline and N-acetyl-S-allylcysteine in human urine: application to a study of the effects of garlic consumption on nitrosation. Anal Biochem. 2009;394(2):243-8.

308.   de Rooij BM, Boogaard PJ, Rijksen DA, Commandeur JN, Vermeulen NP. Urinary excretion of N-acetyl-S-allyl-L-cysteine upon garlic consumption by human volunteers. Arch Toxicol. 1996;70(10):635-9.

309.   Scheffler L, Sauermann Y, Heinlein A, Sharapa C, Buettner A. Detection of Volatile Metabolites Derived from Garlic (Allium sativum) in Human Urine. Metabolites. 2016;6(4).

310.   Rosen RT, Hiserodt RD, Fukuda EK, Ruiz RJ, Zhou Z, Lech J, et al. Determination of allicin, S-allylcysteine and volatile metabolites of garlic in breath, plasma or simulated gastric fluids. The Journal of nutrition. 2001;131(3s):968s-71s.

311.   Kolm RH, Danielson UH, Zhang Y, Talalay P, Mannervik B. Isothiocyanates as substrates for human glutathione transferases: structure-activity studies. Biochem J. 1995;311 (Pt 2)(Pt 2):453-9.

312.   Seow A, Shi CY, Chung FL, Jiao D, Hankin JH, Lee HP, et al. Urinary total isothiocyanate (ITC) in a population-based sample of middle-aged and older Chinese in Singapore: relationship with dietary total ITC and glutathione S-transferase M1/T1/P1 genotypes. Cancer epidemiology, biomarkers & prevention : a publication of the American Association for Cancer Research, cosponsored by the American Society of Preventive Oncology. 1998;7(9):775-81.

313.   Narbad A, Rossiter JT. Gut Glucosinolate Metabolism and Isothiocyanate Production. Molecular nutrition & food research. 2018;62(18):e1700991-e.

314.   Bilhim T, Tinto HR, Fernandes L, Martins Pisco J. Radiological anatomy of prostatic arteries. Tech Vasc Interv Radiol. 2012;15(4):276-85.

315.   Lampe JW, Chen C, Li S, Prunty J, Grate MT, Meehan DE, et al. Modulation of Human Glutathione S-Transferases by Botanically Defined Vegetable Diets. Cancer Epidemiology Biomarkers & Prevention. 2000;9(8):787-93.

316.   McNeal JE. Normal histology of the prostate. The American journal of surgical pathology. 1988;12(8):619-33.

317.   Lee JJ, Thomas IC, Nolley R, Ferrari M, Brooks JD, Leppert JT. Biologic differences between peripheral and transition zone prostate cancer. The Prostate. 2015;75(2):183-90.

318.   King CR, Ferrari M, Brooks JD. Prognostic significance of prostate cancer originating from the transition zone. Urologic oncology. 2009;27(6):592-7.

319.   Elgamal A-AA, Van Poppel HP, Van de Voorde WM, Van Dorpe JA, Oyen RH, Baert LV. Impalpable invisible stage T1c prostate cancer: characteristics and clinical relevance in 100 radical prostatectomy specimens-a different view. The Journal of urology. 1997;157(1):244-50.

320.   Noguchi M, Stamey TA, NEAL JEM, Yemoto CE. An analysis of 148 consecutive transition zone cancers: clinical and histological characteristics. The Journal of urology. 2000;163(6):1751-5.

321.   Sakai I, HARADA KI, Kurahashi T, Yamanaka K, Hara I, Miyake H. Analysis of differences in clinicopathological features between prostate cancers located in the transition and peripheral zones. International journal of urology. 2006;13(4):368-72.

322.   Stamey TA, McNeal JE, Yemoto CM, Sigal BM, Johnstone IM. Biological determinants of cancer progression in men with prostate cancer. Jama. 1999;281(15):1395-400.

323.   Knoedler JJ, Karnes RJ, Thompson RH, Rangel LJ, Bergstralh EJ, Boorjian SA. The association of tumor volume with mortality following radical prostatectomy. Prostate cancer and prostatic diseases. 2014;17(2):144-8.

324.   Finley DS, Pantuck AJ, Belldegrun AS. Tumor biology and prognostic factors in renal cell carcinoma. Oncologist. 2011;16 Suppl 2(Suppl 2):4-13.

325.   Erbersdobler A, Fritz H, Schnöger S, Graefen M, Hammerer P, Huland H, et al. Tumour grade, proliferation, apoptosis, microvessel density, p53, and bcl-2 in prostate cancers: differences between tumours located in the transition zone and in the peripheral zone. European urology. 2002;41(1):40-6.

326.   Grignon DJ, Sakr WA. Zonal origin of prostatic adenocarcinoma: are there biologic differences between transition zone and peripheral zone adenocarcinomas of the prostate gland? J Cell Biochem Suppl. 1994;19:267-9.

327.   Lavery HJ, Droller MJ. Do Gleason patterns 3 and 4 prostate cancer represent separate disease states? The Journal of urology. 2012;188(5):1667-75.

328.   Carlsson J, Helenius G, Karlsson MG, Andrén O, Klinga-Levan K, Olsson B. Differences in microRNA expression during tumor development in the transition and peripheral zones of the prostate. BMC Cancer. 2013;13(1):362.

329.   Lexander H, Franzén B, Hirschberg D, Becker S, Hellström M, Bergman T, et al. Differential protein expression in anatomical zones of the prostate. Proteomics. 2005;5(10):2570-6.

330.   Laczkó I, Hudson DL, Freeman A, Feneley MR, Masters JR. Comparison of the zones of the human prostate with the seminal vesicle: Morphology, immunohistochemistry, and cell kinetics. The Prostate. 2005;62(3):260-6.

331.   Noel EE, Ragavan N, Walsh MJ, James SY, Matanhelia SS, Nicholson CM, et al. Differential gene expression in the peripheral zone compared to the transition zone of the human prostate gland. Prostate cancer and prostatic diseases. 2008;11(2):173-80.

332.   van der Heul-Nieuwenhuijsen L, Hendriksen PJ, van der Kwast TH, Jenster G. Gene expression profiling of the human prostate zones. BJU Int. 2006;98(4):886-97.

333.   Al Kadhi O, Traka MH, Melchini A, Troncoso-Rey P, Jurkowski W, Defernez M, et al. Increased transcriptional and metabolic capacity for lipid metabolism in the peripheral zone of the prostate may underpin its increased susceptibility to cancer. Oncotarget. 2017;8(49):84902-16.

334.   Cussenot O, Azzouzi AR, Nicolaiew N, Fromont G, Mangin P, Cormier L, et al. Combination of polymorphisms from genes related to estrogen metabolism and risk of prostate cancers: the hidden face of estrogens. Journal of clinical oncology : official journal of the American Society of Clinical Oncology. 2007;25(24):3596-602.

335.   John K, Ragavan N, Pratt MM, Singh PB, Al-Buheissi S, Matanhelia SS, et al. Quantification of phase I/II metabolizing enzyme gene expression and polycyclic aromatic hydrocarbon-DNA adduct levels in human prostate. Prostate. 2009;69(5):505-19.

336.   Ragavan N, Hewitt R, Cooper LJ, Ashton KM, Hindley AC, Nicholson CM, et al. CYP1B1 expression in prostate is higher in the peripheral than in the transition zone. Cancer letters. 2004;215(1):69-78.

337.   Pertea M, Kim D, Pertea GM, Leek JT, Salzberg SL. Transcript-level expression analysis of RNA-seq experiments with HISAT, StringTie and Ballgown. Nat Protoc. 2016;11(9):1650-67.

338.   Norwich Bioscience Institute's Computing Intrastructure for Science (CiS). Available at http://cis.nbi.ac.uk/.

339.   https://github.com/FelixKrueger/TrimGalore.

340.   Felix Krueger, Babraham Institute, Trim galore v0.5.0. Available at https://github.com/FelixKrueger/TrimGalore.

341.   Kim D, Langmead B, Salzberg SL. HISAT: a fast spliced aligner with low memory requirements. Nat Methods. 2015;12(4):357-60.

342.   Human assembly and gene annotation, available at http://www.ensembl.org/Homo_sapiens/Info/Annotation.

343.   Li H, Durbin R. Fast and accurate short read alignment with Burrows-Wheeler transform. Bioinformatics (Oxford, England). 2009;25(14):1754-60.

344.   Pertea G, Pertea M. GFF Utilities: GffRead and GffCompare [version 2; peer review: 3 approved]. F1000Research. 2020;9(304).

345.   Love MI, Huber W, Anders S. Moderated estimation of fold change and dispersion for RNA-seq data with DESeq2. Genome Biology. 2014;15(12):550.

346.   Zhu A, Ibrahim JG, Love MI. Heavy-tailed prior distributions for sequence count data: removing the noise and preserving large differences. bioRxiv. 2018:303255.

347.   Plaisier SB, Taschereau R, Wong JA, Graeber TG. Rank–rank hypergeometric overlap: identification of statistically significant overlap between gene-expression signatures. Nucleic Acids Research. 2010;38(17):e169-e.

348.   Zhang JS, Gong A, Gomero W, Young CY. ZNF185, a LIM-domain protein, is a candidate tumor suppressor in prostate cancer and functions in focal adhesion pathway. Cancer research. 2004;64(7 Supplement):619.

349.   Cassandri M, Smirnov A, Novelli F, Pitolli C, Agostini M, Malewicz M, et al. Zinc-finger proteins in health and disease. Cell Death Discovery. 2017;3(1):17071.

350.   Zhang JS, Gong A, Young CYF. ZNF185, an actin–cytoskeleton-associated growth inhibitory LIM protein in prostate cancer. Oncogene. 2007;26(1):111-22.

351.   Vanaja DK, Cheville JC, Iturria SJ, Young CY. Transcriptional silencing of zinc finger protein 185 identified by expression profiling is associated with prostate cancer progression. Cancer research. 2003;63(14):3877-82.

352.   Jung Y-S, Park J-I. Wnt signaling in cancer: therapeutic targeting of Wnt signaling beyond β-catenin and the destruction complex. Experimental & Molecular Medicine. 2020;52(2):183-91.

353.   Ying Y, Tao Q. Epigenetic disruption of the WNT/ß-catenin signaling pathway in human cancers. Epigenetics. 2009;4(5):307-12.

354.   Pohl S, Scott R, Arfuso F, Perumal V, Dharmarajan A. Secreted frizzled-related protein 4 and its implications in cancer and apoptosis. Tumor Biology. 2015;36(1):143-52.

355.   Luo JH, Yu YP, Cieply K, Lin F, Deflavia P, Dhir R, et al. Gene expression analysis of prostate cancers. Molecular Carcinogenesis: Published in cooperation with the University of Texas MD Anderson Cancer Center. 2002;33(1):25-35.

356.   Wissmann C, Wild PJ, Kaiser S, Roepcke S, Stoehr R, Woenckhaus M, et al. WIF1, a component of the Wnt pathway, is down-regulated in prostate, breast, lung, and bladder cancer. The Journal of Pathology: A Journal of the Pathological Society of Great Britain and Ireland. 2003;201(2):204-12.

357.   Mortensen MM, Høyer S, Lynnerup A-S, Ørntoft TF, Sørensen KD, Borre M, et al. Expression profiling of prostate cancer tissue delineates genes associated with recurrence after prostatectomy. Scientific reports. 2015;5(1):1-11.

358.   Sandsmark E, Andersen MK, Bofin AM, Bertilsson H, Drabløs F, Bathen TF, et al. SFRP4 gene expression is increased in aggressive prostate cancer. Scientific Reports. 2017;7(1):14276.

359.   Horvath LG, Henshall SM, Kench JG, Saunders DN, Lee C-S, Golovsky D, et al. Membranous expression of secreted frizzled-related protein 4 predicts for good prognosis in localized prostate cancer and inhibits PC3 cellular proliferation in vitro. Clinical cancer research. 2004;10(2):615-25.

360.   Horvath LG, Lelliott JE, Kench JG, Lee CS, Williams ED, Saunders DN, et al. Secreted frizzled-related protein 4 inhibits proliferation and metastatic potential in prostate cancer. The Prostate. 2007;67(10):1081-90.

361.   He B, Lee AY, Dadfarmay S, You L, Xu Z, Reguart N, et al. Secreted frizzled-related protein 4 is silenced by hypermethylation and induces apoptosis in beta-catenin-deficient human mesothelioma cells. Cancer research. 2005;65(3):743-8.

362.   Shaikhibrahim Z, Lindstrot A, Ellinger J, Rogenhofer S, Buettner R, Wernert N. Genes differentially expressed in the peripheral zone compared to the transitional zone of the normal human prostate and their potential regulation by ETS factors. Molecular medicine reports. 2012;5(1):32-6.

363.   Wu Z, Wang T, Fang M, Huang W, Sun Z, Xiao J, et al. MFAP5 promotes tumor progression and bone metastasis by regulating ERK/MMP signaling pathways in breast cancer. Biochem Biophys Res Commun. 2018;498(3):495-501.

364.   Navab R, Strumpf D, Bandarchi B, Zhu C-Q, Pintilie M, Ramnarine VR, et al. Prognostic gene-expression signature of carcinoma-associated fibroblasts in non-small cell lung cancer. Proceedings of the National Academy of Sciences. 2011;108(17):7160-5.

365.   López-Casas PP, López-Fernández LA. Gene-expression profiling in pancreatic cancer. Expert review of molecular diagnostics. 2010;10(5):591-601.

366.   Leung CS, Yeung T-L, Yip K-P, Pradeep S, Balasubramanian L, Liu J, et al. Calcium-dependent FAK/CREB/TNNC1 signalling mediates the effect of stromal MFAP5 on ovarian cancer metastatic potential. Nature communications. 2014;5(1):1-15.

367.   Dakhova O, Ozen M, Creighton CJ, Li R, Ayala G, Rowley D, et al. Global gene expression analysis of reactive stroma in prostate cancer. Clinical cancer research. 2009;15(12):3979-89.

368.   Pascal LE, Goo YA, Vêncio RZ, Page LS, Chambers AA, Liebeskind ES, et al. Gene expression down-regulation in CD90+ prostate tumor-associated stromal cells involves potential organ-specific genes. BMC cancer. 2009;9(1):1-12.

369.   Orr B, Riddick A, Stewart G, Anderson R, Franco O, Hayward S, et al. Identification of stromally expressed molecules in the prostate by tag-profiling of cancer-associated fibroblasts, normal fibroblasts and fetal prostate. Oncogene. 2012;31(9):1130-42.

370.   Rochette A, Boufaied N, Scarlata E, Hamel L, Brimo F, Whitaker HC, et al. Asporin is a stromally expressed marker associated with prostate cancer progression. British journal of cancer. 2017;116(6):775-84.

371.   Jiang Z, Woda BA, Rock KL, Xu Y, Savas L, Khan A, et al. P504S: a new molecular marker for the detection of prostate carcinoma. The American journal of surgical pathology. 2001;25(11):1397-404.

372.   Luo J, Zha S, Gage WR, Dunn TA, Hicks JL, Bennett CJ, et al. α-Methylacyl-CoA Racemase. A New Molecular Marker for Prostate Cancer. 2002;62(8):2220-6.

373.   Zhou M, Chinnaiyan AM, Kleer CG, Lucas PC, Rubin MA. Alpha-Methylacyl-CoA racemase: a novel tumor marker over-expressed in several human cancers and their precursor lesions. The American journal of surgical pathology. 2002;26(7):926-31.

374.   Rubin MA, Zhou M, Dhanasekaran SM, Varambally S, Barrette TR, Sanda MG, et al. α-Methylacyl coenzyme A racemase as a tissue biomarker for prostate cancer. Jama. 2002;287(13):1662-70.

375.   Leav I, McNeal JE, Ho SM, Jiang Z. Alpha-methylacyl-CoA racemase (P504S) expression in evolving carcinomas within benign prostatic hyperplasia and in cancers of the transition zone. Hum Pathol. 2003;34(3):228-33.

376.   Sinnott JA, Rider JR, Carlsson J, Gerke T, Tyekucheva S, Penney KL, et al. Molecular differences in transition zone and peripheral zone prostate tumors. Carcinogenesis. 2015;36(6):632-8.

377.   David CJ, Massagué J. Contextual determinants of TGFβ action in development, immunity and cancer. Nature reviews Molecular cell biology. 2018;19(7):419-35.

378.   Bobinac D, Marić I, Zoričić S, Španjol J, Đorđević G, Mustać E, et al. Expression of bone morphogenetic proteins in human metastatic prostate and breast cancer. Croatian medical journal. 2005;46(3).

379.   Spanjol J, Djordjević G, Markić D, Klarić M, Fuckar D, Bobinac D. Role of bone morphogenetic proteins in human prostate cancer pathogenesis and development of bone metastases: immunohistochemical study. Coll Antropol. 2010;34 Suppl 2:119-25.

380.   Dermer GB. Basal cell proliferation in benign prostatic hyperplasia. Cancer. 1978;41(5):1857-62.

381.   Luo J, Dunn T, Ewing C, Sauvageot J, Chen Y, Trent J, et al. Gene expression signature of benign prostatic hyperplasia revealed by cDNA microarray analysis. Prostate. 2002;51(3):189-200.

382.   Love HD, Booton SE, Boone BE, Breyer JP, Koyama T, Revelo MP, et al. Androgen Regulated Genes in Human Prostate Xenografts in Mice: Relation to BPH and Prostate Cancer. PLOS ONE. 2009;4(12):e8384.

383.   Watanabe TK, Katagiri T, Suzuki M, Shimizu F, Fujiwara T, Kanemoto N, et al. Cloning and characterization of two novel human cDNAs (NELL1 and NELL2) encoding proteins with six EGF-like repeats. Genomics. 1996;38(3):273-6.

384.   Kim H, Ha CM, Choi J, Choi EJ, Jeon J, Kim C, et al. Ontogeny and the possible function of a novel epidermal growth factor-like repeat domain-containing protein, NELL2, in the rat brain. Journal of neurochemistry. 2002;83(6):1389-400.

385.   Nakamura R, Oyama T, Tajiri R, Mizokami A, Namiki M, Nakamoto M, et al. Expression and regulatory effects on cancer cell behavior of NELL1 and NELL2 in human renal cell carcinoma. Cancer Sci. 2015;106(5):656-64.

386.   DiLella AG, Toner TJ, Austin CP, Connolly BM. Identification of Genes Differentially Expressed in Benign Prostatic Hyperplasia. Journal of Histochemistry & Cytochemistry. 2001;49(5):669-70.

387.   Okada H, Danoff TM, Kalluri R, Neilson EG. Early role of Fsp1 in epithelial-mesenchymal transformation. American Journal of Physiology-Renal Physiology. 1997;273(4):F563-F74.

388.   Strutz F, Okada H, Lo CW, Danoff T, Carone RL, Tomaszewski JE, et al. Identification and characterization of a fibroblast marker: FSP1. The Journal of cell biology. 1995;130(2):393-405.

389.   Iwano M, Plieth D, Danoff TM, Xue C, Okada H, Neilson EG. Evidence that fibroblasts derive from epithelium during tissue fibrosis. J Clin Invest. 2002;110(3):341-50.

390.   Shapiro E, Becich MJ, Hartanto V, Lepor H. The relative proportion of stromal and epithelial hyperplasia is related to the development of symptomatic benign prostate hyperplasia. The Journal of urology. 1992;147(5):1293-7.

391.   Zhao H, Ramos CF, Brooks JD, Peehl DM. Distinctive gene expression of prostatic stromal cells cultured from diseased versus normal tissues. Journal of Cellular Physiology. 2007;210(1):111-21.

392.   Cunha GR, Hayward SW, Wang Y. Role of stroma in carcinogenesis of the prostate. Differentiation: REVIEW. 2002;70(9-10):473-85.

393.   Gupta GP, Massagué J. Cancer metastasis: building a framework. Cell. 2006;127(4):679-95.

394.   Saleem M, Adhami VM, Ahmad N, Gupta S, Mukhtar H. Prognostic Significance of Metastasis-Associated Protein S100A4 (Mts1) in Prostate Cancer Progression and Chemoprevention Regimens in an Autochthonous Mouse Model. Clinical Cancer Research. 2005;11(1):147.

395.   Dash A, Maine IP, Varambally S, Shen R, Chinnaiyan AM, Rubin MA. Changes in differential gene expression because of warm ischemia time of radical prostatectomy specimens. Am J Pathol. 2002;161(5):1743-8.

396.   Hai T, Hartman MG. The molecular biology and nomenclature of the activating transcription factor/cAMP responsive element binding family of transcription factors: activating transcription factor proteins and homeostasis. Gene. 2001;273(1):1-11.

397.   Ohvo-Rekilä H, Ramstedt B, Leppimäki P, Peter Slotte J. Cholesterol interactions with phospholipids in membranes. Progress in Lipid Research. 2002;41(1):66-97.

398.   Simons K, Ikonen E. Functional rafts in cell membranes. Nature. 1997;387(6633):569-72.

399.   Zhuang L, Lin J, Lu ML, Solomon KR, Freeman MR. Cholesterol-rich Lipid Rafts Mediate Akt-regulated Survival in Prostate Cancer Cells. Cancer research. 2002;62(8):2227.

400.   Llaverias G, Danilo C, Wang Y, Witkiewicz AK, Daumer K, Lisanti MP, et al. A Western-Type Diet Accelerates Tumor Progression in an Autochthonous Mouse Model of Prostate Cancer. The American Journal of Pathology. 2010;177(6):3180-91.

401.   Heinlein CA, Chang C. Androgen receptor in prostate cancer. Endocrine reviews. 2004;25(2):276-308.

402.   Krycer JR, Brown AJ. Cross-talk between the Androgen Receptor and the Liver X Receptor implications for cholesterol homeostasis. Journal of Biological Chemistry. 2011;286(23):20637-47.

403.   Sadi MV, Walsh PC, Barrack ER. Immunohistochemical study of androgen receptors in metastatic prostate cancer. Comparison of receptor content and response to hormonal therapy. Cancer. 1991;67(12):3057-64.

404.   Chodak GW, Kranc DM, Puy LA, Takeda H, Johnson K, Chang C. Nuclear localization of androgen receptor in heterogeneous samples of normal, hyperplastic and neoplastic human prostate. The Journal of urology. 1992;147(3 Pt 2):798-803.

405.   Ruizeveld de Winter JA, Janssen PJ, Sleddens HM, Verleun-Mooijman MC, Trapman J, Brinkmann AO, et al. Androgen receptor status in localized and locally progressive hormone refractory human prostate cancer. Am J Pathol. 1994;144(4):735-46.

406.   Krycer JR, Brown AJ. Cross-talk between the Androgen Receptor and the Liver X Receptor: IMPLICATIONS FOR CHOLESTEROL HOMEOSTASIS. Journal of Biological Chemistry. 2011;286(23):20637-47.

407.   Ho SM, Tang WY, Belmonte de Frausto J, Prins GS. Developmental exposure to estradiol and bisphenol A increases susceptibility to prostate carcinogenesis and epigenetically regulates phosphodiesterase type 4 variant 4. Cancer research. 2006;66(11):5624-32.

408.   Prins GS, Ho SM. Early-life estrogens and prostate cancer in an animal model. J Dev Orig Health Dis. 2010;1(6):365-70.

409.   Yegnasubramanian S, Kowalski J, Gonzalgo ML, Zahurak M, Piantadosi S, Walsh PC, et al. Hypermethylation of CpG islands in primary and metastatic human prostate cancer. Cancer research. 2004;64(6):1975-86.

410.   Enokida H, Shiina H, Urakami S, Igawa M, Ogishima T, Li LC, et al. Multigene methylation analysis for detection and staging of prostate cancer. Clinical cancer research : an official journal of the American Association for Cancer Research. 2005;11(18):6582-8.

411.   Esteller M. Aberrant DNA methylation as a cancer-inducing mechanism. Annu Rev Pharmacol Toxicol. 2005;45:629-56.

412.   Jacobson EM, Hugo ER, Tuttle TR, Papoian R, Ben-Jonathan N. Unexploited therapies in breast and prostate cancer: blockade of the prolactin receptor. Trends Endocrinol Metab. 2010;21(11):691-8.

413.   Fernandez I, Touraine P, Goffin V. Prolactin and human tumourogenesis. J Neuroendocrinol. 2010;22(7):771-7.

414.   Gilleran JP, Putz O, DeJong M, DeJong S, Birch L, Pu Y, et al. The role of prolactin in the prostatic inflammatory response to neonatal estrogen. Endocrinology. 2003;144(5):2046-54.

415.   Van Coppenolle F, Slomianny C, Carpentier F, Le Bourhis X, Ahidouch A, Croix D, et al. Effects of hyperprolactinemia on rat prostate growth: evidence of androgeno-dependence. Am J Physiol Endocrinol Metab. 2001;280(1):E120-9.

416.   Ahonen TJ, Härkönen PL, Laine J, Rui H, Martikainen PM, Nevalainen MT. Prolactin is a survival factor for androgen-deprived rat dorsal and lateral prostate epithelium in organ culture. Endocrinology. 1999;140(11):5412-21.

417.   Rohr HP, Bartsch G. Human benign prostatic hyperplasia: A stromal disease? New perspectives by quantitative morphology. Urology. 1980;16(6):625-33.

418.   Novara G, Galfano A, Berto RB, Ficarra V, Navarrete RV, Artibani W. Inflammation, Apoptosis, and BPH: What is the Evidence? European Urology Supplements. 2006;5(4):401-9.

419.   Kalluri R, Weinberg RA. The basics of epithelial-mesenchymal transition. J Clin Invest. 2009;119(6):1420-8.

420.   Alonso-Magdalena P, Brössner C, Reiner A, Cheng G, Sugiyama N, Warner M, et al. A role for epithelial-mesenchymal transition in the etiology of benign prostatic hyperplasia. Proceedings of the National Academy of Sciences. 2009;106(8):2859.

421.   He F, Ru X, Wen T. NRF2, a Transcription Factor for Stress Response and Beyond. International journal of molecular sciences. 2020;21(13):4777.

422.   Hayes JD, Dinkova-Kostova AT. The Nrf2 regulatory network provides an interface between redox and intermediary metabolism. Trends Biochem Sci. 2014;39(4):199-218.

423.   Tebay LE, Robertson H, Durant ST, Vitale SR, Penning TM, Dinkova-Kostova AT, et al. Mechanisms of activation of the transcription factor Nrf2 by redox stressors, nutrient cues, and energy status and the pathways through which it attenuates degenerative disease. Free Radic Biol Med. 2015;88(Pt B):108-46.

424.   Maria H Traka1 AM, Jack Coode-Bate1,2, Omar Al Kadhi1,2. Transcriptional changes in prostate of men on active surveillance following a

12-month glucoraphanin-rich broccoli intervention – results from the ESCAPE

randomized controlled trial. AJCN - accepted for publication. 2018.

425.   Seligson DB, Horvath S, Shi T, Yu H, Tze S, Grunstein M, et al. Global histone modification patterns predict risk of prostate cancer recurrence. Nature. 2005;435(7046):1262-6.

426.   Sterner DE, Berger SL. Acetylation of histones and transcription-related factors. Microbiol Mol Biol Rev. 2000;64(2):435-59.

427.   Kuo MH, Allis CD. Roles of histone acetyltransferases and deacetylases in gene regulation. Bioessays. 1998;20(8):615-26.

428.   Wade PA. Transcriptional control at regulatory checkpoints by histone deacetylases: molecular connections between cancer and chromatin. Hum Mol Genet. 2001;10(7):693-8.

429.   Dokmanovic M, Marks PA. Prospects: histone deacetylase inhibitors. J Cell Biochem. 2005;96(2):293-304.

430.   Nian H, Delage B, Pinto JT, Dashwood RH. Allyl mercaptan, a garlic-derived organosulphur compound, inhibits histone deacetylase and enhances Sp3 binding on the P21WAF1 promoter. Carcinogenesis. 2008;29(9):1816-24.

431.   Arreola R, Quintero-Fabián S, López-Roa RI, Flores-Gutiérrez EO, Reyes-Grajeda JP, Carrera-Quintanar L, et al. Immunomodulation and anti-inflammatory effects of garlic compounds. J Immunol Res. 2015;2015:401630-.

432.   Kyo E, Uda N, Kasuga S, Itakura Y. Immunomodulatory effects of aged garlic extract. The Journal of nutrition. 2001;131(3s):1075s-9s.

433.   Schäfer G, Kaschula CH. The immunomodulation and anti-inflammatory effects of garlic organosulphur compounds in cancer chemoprevention. Anticancer Agents Med Chem. 2014;14(2):233-40.

434.   Doersch KM, Moses KA, Zimmer WE. Synergistic immunologic targets for the treatment of prostate cancer. Experimental biology and medicine (Maywood, NJ). 2016;241(17):1900-10.

435.   Lamm DL, Riggs DR. Enhanced immunocompetence by garlic: role in bladder cancer and other malignancies. The Journal of nutrition. 2001;131(3s):1067s-70s.

436.   Kyo E, Uda N, Suzuki A, Kakimoto M, Ushijima M, Kasuga S, et al. Immunomodulation and antitumor activities of Aged Garlic Extract. Phytomedicine : international journal of phytotherapy and phytopharmacology. 1998;5(4):259-67.

437.   Witten DM. Classification and clustering of sequencing data using a Poisson model. Ann Appl Stat. 2011;5(4):2493-518.

438.   Thakur A, Vaishampayan U, Lum LG. Immunotherapy and immune evasion in prostate cancer. Cancers (Basel). 2013;5(2):569-90.

439.   Pende D, Castriconi R, Romagnani P, Spaggiari GM, Marcenaro S, Dondero A, et al. Expression of the DNAM-1 ligands, Nectin-2 (CD112) and poliovirus receptor (CD155), on dendritic cells: relevance for natural killer-dendritic cell interaction. Blood. 2006;107(5):2030-6.

440.   Joller N, Hafler JP, Brynedal B, Kassam N, Spoerl S, Levin SD, et al. Cutting edge: TIGIT has T cell-intrinsic inhibitory functions. J Immunol. 2011;186(3):1338-42.

441.   Whelan S, Ophir E, Kotturi MF, Levy O, Ganguly S, Leung L, et al. PVRIG and PVRL2 Are Induced in Cancer and Inhibit CD8(+) T-cell Function. Cancer Immunol Res. 2019;7(2):257-68.

442.   Shao N, Xu B, Mi Yy, Hua Lx. IL-10 polymorphisms and prostate cancer risk: a meta-analysis. Prostate cancer and prostatic diseases. 2011;14(2):129-35.

443.   Stearns ME, Rhim J, Wang M. Interleukin 10 (IL-10) Inhibition of Primary Human Prostate Cell-induced Angiogenesis. Clinical Cancer Research. 1999;5(1):189.

444.   Klapper JA, Downey SG, Smith FO, Yang JC, Hughes MS, Kammula US, et al. High-dose interleukin-2 for the treatment of metastatic renal cell carcinoma : a retrospective analysis of response and survival in patients

treated in the surgery branch at the National Cancer Institute between 1986 and 2006. Cancer. 2008;113(2):293-301.

445.   Jiang T, Zhou C, Ren S. Role of IL-2 in cancer immunotherapy. Oncoimmunology. 2016;5(6):e1163462-e.

446.   Dieli F, Vermijlen D, Fulfaro F, Caccamo N, Meraviglia S, Cicero G, et al. Targeting human {gamma}delta} T cells with zoledronate and interleukin-2 for immunotherapy of hormone-refractory prostate cancer. Cancer research. 2007;67(15):7450-7.

447.   Risk M, Corman JM. The role of immunotherapy in prostate cancer: an overview of current approaches in development. Rev Urol. 2009;11(1):16-27.

448.   Castro F, Cardoso AP, Gonçalves RM, Serre K, Oliveira MJ. Interferon-Gamma at the Crossroads of Tumor Immune Surveillance or Evasion. Front Immunol. 2018;9:847-.

449.   Zaidi MR. The Interferon-Gamma Paradox in Cancer. Journal of Interferon & Cytokine Research. 2018;39(1):30-8.

450.   Selleck WA, Canfield SE, Hassen WA, Meseck M, Kuzmin AI, Eisensmith RC, et al. IFN-gamma sensitization of prostate cancer cells to Fas-mediated death: a gene therapy approach. Mol Ther. 2003;7(2):185-92.

451.   Selleck WA, Canfield SE, Hassen WA, Meseck M, Kuzmin AI, Eisensmith RC, et al. IFN-γ sensitization of prostate cancer cells to fas-mediated death: a gene therapy approach. Molecular Therapy. 2003;7(2):185-92.

452.   Sokoloff MH, Tso CL, Kaboo R, Taneja S, Pang S, deKernion JB, et al. In vitro modulation of tumor progression-associated properties of hormone refractory prostate carcinoma cell lines by cytokines. Cancer. 1996;77(9):1862-72.

453.   Hastie C. Interferon gamma, a possible therapeutic approach for late-stage prostate cancer? Anticancer Res. 2008;28(5b):2843-9.

454.   Huang Y, Li W, Su Z-y, Kong A-NT. The complexity of the Nrf2 pathway: beyond the antioxidant response. J Nutr Biochem. 2015;26(12):1401-13.

455.   Bhamre S, Sahoo D, Tibshirani R, Dill DL, Brooks JD. Temporal changes in gene expression induced by sulforaphane in human prostate cancer cells. The Prostate. 2009;69(2):181-90.

456.   Jiang J, Liu H-L, Tao L, Lin X-Y, Yang Y-D, Tan S-W, et al. Let-7d inhibits colorectal cancer cell proliferation through the CST1/p65 pathway. International journal of oncology. 2018;53(2):781-90.

457.   Keppler D, Zhang J, Bihani T, Lin AW. Novel expression of CST1 as candidate senescence marker. J Gerontol A Biol Sci Med Sci. 2011;66(7):723-31.

458.   Liu Y, Yao J. Research progress of cystatin SN in cancer. Onco Targets Ther. 2019;12:3411-9.

459.   Choi EH, Kim JT, Kim JH, Kim SY, Song EY, Kim JW, et al. Upregulation of the cysteine protease inhibitor, cystatin SN, contributes to cell proliferation and cathepsin inhibition in gastric cancer. Clin Chim Acta. 2009;406(1-2):45-51.

460.   Jiang J, Liu HL, Liu ZH, Tan SW, Wu B. Identification of cystatin SN as a novel biomarker for pancreatic cancer. Tumour biology : the journal of the International Society for Oncodevelopmental Biology and Medicine. 2015;36(5):3903-10.

461.   Yoneda K, Iida H, Endo H, Hosono K, Akiyama T, Takahashi H, et al. Identification of Cystatin SN as a novel tumor marker for colorectal cancer. International journal of oncology. 2009;35(1):33-40.

462.   Chen YF, Ma G, Cao X, Luo RZ, He LR, He JH, et al. Overexpression of cystatin SN positively affects survival of patients with surgically resected esophageal squamous cell carcinoma. BMC Surg. 2013;13:15.

463.   Pulukuri SM, Gorantla B, Knost JA, Rao JS. Frequent loss of cystatin E/M expression implicated in the progression of prostate cancer. Oncogene. 2009;28(31):2829-38.

464.   Ai L, Kim WJ, Kim TY, Fields CR, Massoll NA, Robertson KD, et al. Epigenetic silencing of the tumor suppressor cystatin M occurs during breast cancer progression. Cancer research. 2006;66(16):7899-909.

465.   Schagdarsurengin U, Pfeifer GP, Dammann R. Frequent epigenetic inactivation of cystatin M in breast carcinoma. Oncogene. 2007;26(21):3089-94.

466.   Xu Y-H, Deng J-L, Wang G, Zhu Y-S. Long non-coding RNAs in prostate cancer: Functional roles and clinical implications. Cancer letters. 2019;464:37-55.

467.   Aird J, Baird A-M, Lim MCJ, McDermott R, Finn SP, Gray SG. Carcinogenesis in prostate cancer: The role of long non-coding RNAs. Non-coding RNA Research. 2018;3(1):29-38.

468.   Beaver LM, Kuintzle R, Buchanan A, Wiley MW, Glasser ST, Wong CP, et al. Long noncoding RNAs and sulforaphane: a target for chemoprevention and suppression of prostate cancer. J Nutr Biochem. 2017;42:72-83.

469.   Sun J, Li S, Wang F, Fan C, Wang J. Identification of key pathways and genes in PTEN mutation prostate cancer by bioinformatics analysis. BMC Medical Genetics. 2019;20(1):191.

470. Wang S, Gao J, Lei Q, Rozengurt N, Pritchard C, Jiao J, et al. Prostate-specific deletion of the murine Pten tumor suppressor gene leads to metastatic prostate cancer. Cancer cell. 2003;4(3):209-21.

471. Robinson D, Van Allen EM, Wu Y-M, Schultz N, Lonigro RJ, Mosquera J-M, et al. Integrative clinical genomics of advanced prostate cancer. Cell. 2015;161(5):1215-28.

472. Maehama T, Taylor GS, Dixon JE. PTEN and Myotubularin: Novel Phosphoinositide Phosphatases. Annual Review of Biochemistry. 2001;70(1):247-79.

473. Corn PG, Wang F, McKeehan WL, Navone N. Targeting fibroblast growth factor pathways in prostate cancer. Clinical cancer research : an official journal of the American Association for Cancer Research. 2013;19(21):5856-66.

474. Daniele G, Corral J, Molife LR, De Bono JS. FGF receptor inhibitors: role in cancer therapy. Current oncology reports. 2012;14(2):111-9.

475. Beenken A, Mohammadi M. The FGF family: biology, pathophysiology and therapy. Nature reviews Drug discovery. 2009;8(3):235-53.

476. Lu T, Lin W-J, Izumi K, Wang X, Xu D, Fang L-Y, et al. Targeting Androgen Receptor to Suppress Macrophage-induced EMT and Benign Prostatic Hyperplasia (BPH) Development. Molecular Endocrinology. 2012;26(10):1707-15.

477. Folkman J. Is tissue mass regulated by vascular endothelial cells? Prostate as the first evidence. Endocrinology. 1998;139(2):441-2.

478. Soulitzis N, Karyotis I, Delakas D, Spandidos DA. Expression analysis of peptide growth factors VEGF, FGF2, TGFB1, EGF and IGF1 in prostate cancer and benign prostatic hyperplasia. International journal of oncology. 2006;29(2):305-14.

479. Ren J, Huan Y, Wang H, Chang YJ, Zhao HT, Ge YL, et al. Dynamic contrast-enhanced MRI of benign prostatic hyperplasia and prostatic carcinoma: correlation with angiogenesis. Clin Radiol. 2008;63(2):153-9.

480. Lucia MS, Lambert JR. Growth factors in benign prostatic hyperplasia: basic science implications. Curr Urol Rep. 2008;9(4):272-8.

481. Roehrborn CG, Nuckolls JG, Wei JT, Steers W. The benign prostatic hyperplasia registry and patient survey: study design, methods and patient baseline characteristics. BJU Int. 2007;100(4):813-9.

482. Stojanović N, Ignjatović I, Djenić N, Bogdanović D. Adverse Effects of Pharmacological Therapy of Benign Prostatic Hyperplasia on Sexual Function in Men. Srp Arh Celok Lek. 2015;143(5-6):284-9.

483. Lin J, Zhou J, Xu W, Hong Z, Peng J. Qianliening capsule inhibits benign prostatic hyperplasia angiogenesis via the HIF-1α signaling pathway. Exp Ther Med. 2014;8(1):118-24.

484. World Health Organisation (WHO), International Agency for Research on Cancer. Available online: https://www.iarc.fr/ (accessed 06 Sept 2018).

485. Choyke PL, Loeb S. Active Surveillance of Prostate Cancer. Oncology (Williston Park). 2017;31(1):67-70.

486. Baker TB, Smith SS, Bolt DM, Loh W-Y, Mermelstein R, Fiore MC, et al. Implementing Clinical Research Using Factorial Designs: A Primer. Behav Ther. 2017;48(4):567-80.

487. The SAGE Encyclopedia of Communication Research Methods. 2017.

488. Erickson HS, Josephson JW, Vira M, Albert PS, Gillespie JW, Rodriguez-Canales J, et al. Influence of hypoxia induced by minimally invasive prostatectomy on gene expression: implications for biomarker analysis. Am J Transl Res. 2010;2(3):210-22.

489. Schmitz S, Duhoux F, Machiels J. Window of opportunity studies: Do they fulfil our expectations? Cancer treatment reviews. 2016;43:50-7.

490. Arnaout A, Robertson S, Kuchuk I, Simos D, Pond GR, Addison CL, et al. Evaluating the feasibility of performing window of opportunity trials in breast cancer. Int J Surg Oncol. 2015;2015:785793.

491. Loeb S, Vellekoop A, Ahmed HU, Catto J, Emberton M, Nam R, et al. Systematic Review of Complications of Prostate Biopsy. European urology. 2013;64(6):876-92.

492. Swift J, Coruzzi GM. A matter of time - How transient transcription factor interactions create dynamic gene regulatory networks. Biochim Biophys Acta Gene Regul Mech. 2017;1860(1):75-83.

493. Hu R, Hebbar V, Kim BR, Chen C, Winnik B, Buckley B, et al. In vivo pharmacokinetics and regulation of gene expression profiles by isothiocyanate sulforaphane in the rat. J Pharmacol Exp Ther. 2004;310(1):263-71.

494. Hu R, Xu C, Shen G, Jain MR, Khor TO, Gopalkrishnan A, et al. Gene expression profiles induced by cancer chemopreventive isothiocyanate sulforaphane in the liver of C57BL/6J mice and C57BL/6J/Nrf2 (-/-) mice. Cancer letters. 2006;243(2):170-92.

495. Jones SB, Brooks JD. Modest induction of phase 2 enzyme activity in the F-344 rat prostate. BMC Cancer. 2006;6:62.

496.   Zhu Q, Kakino K, Nogami C, Ohnuki K, Shimizu K. An LC-MS/MS-SRM Method for Simultaneous Quantification of Four Representative Organosulphur Compounds in Garlic Products. Food Analytical Methods. 2016;9.

497.   Davidson R, Gardner S, Jupp O, Bullough A, Butters S, Watts L, et al. Isothiocyanates are detected in human synovial fluid following broccoli consumption and can affect the tissues of the knee joint. Scientific Reports. 2017;7(1):3398.

498.   Graif T, Loeb S, Roehl KA, Gashti SN, Griffin C, Yu X, et al. Under diagnosis and over diagnosis of prostate cancer. The Journal of urology. 2007;178(1):88-92.

499.   Goodman M, Ward KC, Osunkoya AO, Datta MW, Luthringer D, Young AN, et al. Frequency and determinants of disagreement and error in Gleason scores: a population-based study of prostate cancer. The Prostate. 2012;72(13):1389-98.

500.   Nikas JB, Nikas EG. Genome-wide DNA methylation model for the diagnosis of prostate cancer. ACS omega. 2019;4(12):14895-901.

501.   van Veldhoven K, Polidoro S, Baglietto L, Severi G, Sacerdote C, Panico S, et al. Epigenome-wide association study reveals decreased average methylation levels years before breast cancer diagnosis. Clinical epigenetics. 2015;7(1):1-12.

502.   Byron SA, Van Keuren-Jensen KR, Engelthaler DM, Carpten JD, Craig DW. Translating RNA sequencing into clinical diagnostics: opportunities and challenges. Nature Reviews Genetics. 2016;17(5):257-71.

503.   Nikas JB, Mitanis NT, Nikas EG. Whole Exome and Transcriptome RNA-Sequencing Model for the Diagnosis of Prostate Cancer. ACS omega. 2019;5(1):481-6.

504.   Kunju LP, Chinnaiyan AM, Shah RB. Comparison of monoclonal antibody (P504S) and polyclonal antibody to alpha methylacyl-CoA racemase (AMACR) in the work-up of prostate cancer. Histopathology. 2005;47(6):587-96.

505.   Zhou M, Aydin H, Kanane H, Epstein JI. How often does alpha-methylacyl-CoA-racemase contribute to resolving an atypical diagnosis on prostate needle biopsy beyond that provided by basal cell markers? The American journal of surgical pathology. 2004;28(2):239-43.

506.   Lin P-Y, Cheng K-L, McGuffin-Cawley JD, Shieu F-S, Samia AC, Gupta S, et al. Detection of Alpha-Methylacyl-CoA Racemase (AMACR), a Biomarker of Prostate Cancer, in Patient Blood Samples Using a Nanoparticle Electrochemical Biosensor. Biosensors (Basel). 2012;2(4):377-87.

507.   Taverna G, Pedretti E, Di Caro G, Borroni EM, Marchesi F, Grizzi F. Inflammation and prostate cancer: friends or foe? Inflammation Research. 2015;64(5):275-86.

508.   Shinohara DB, Vaghasia AM, Yu SH, Mak TN, Brüggemann H, Nelson WG, et al. A mouse model of chronic prostatic inflammation using a human prostate cancer-derived isolate of Propionibacterium acnes. Prostate. 2013;73(9):1007-15.

509.   Cohen RJ, Shannon BA, McNEAL JE, Shannon T, Garrett KL. Propionibacterium acnes associated with inflammation in radical prostatectomy specimens: a possible link to cancer evolution? The Journal of urology. 2005;173(6):1969-74.

510.   Shinohara DB, Vaghasia AM, Yu SH, Mak TN, Brüggemann H, Nelson WG, et al. A mouse model of chronic prostatic inflammation using a human prostate cancer-derived isolate of Propionibacterium acnes. The Prostate. 2013;73(9):1007-15.

511.   Ma X, Chi C, Fan L, Dong B, Shao X, Xie S, et al. The Microbiome of Prostate Fluid Is Associated With Prostate Cancer. Frontiers in Microbiology. 2019;10(1664).

512.   Nelson WG, DeWeese TL, DeMarzo AM. The diet, prostate inflammation, and the development of prostate cancer. Cancer Metastasis Rev. 2002;21(1):3-16.

513.   Schut HA, Snyderwine EG. DNA adducts of heterocyclic amine food mutagens: implications for mutagenesis and carcinogenesis. Carcinogenesis. 1999;20(3):353-68.

514.   Rodriguez C, McCullough ML, Mondul AM, Jacobs EJ, Chao A, Patel AV, et al. Meat consumption among Black and White men and risk of prostate cancer in the Cancer Prevention Study II Nutrition Cohort. Cancer epidemiology, biomarkers & prevention : a publication of the American Association for Cancer Research, cosponsored by the American Society of Preventive Oncology. 2006;15(2):211-6.

515.   Sinha R, Park Y, Graubard BI, Leitzmann MF, Hollenbeck A, Schatzkin A, et al. Meat and meat-related compounds and risk of prostate cancer in a large prospective cohort study in the United States. Am J Epidemiol. 2009;170(9):1165-77.

516.   James MJ, Gibson RA, Cleland LG. Dietary polyunsaturated fatty acids and inflammatory mediator production. Am J Clin Nutr. 2000;71(1 Suppl):343s-8s.

517.   Neuhouser ML, Barnett MJ, Kristal AR, Ambrosone CB, King I, Thornquist M, et al. (n-6) PUFA increase and dairy foods decrease prostate cancer risk in heavy smokers. The Journal of nutrition. 2007;137(7):1821-7.

518. He Y, Zeng H, Yu Y, Zhang J, Zeng X, Gong F, et al. Resveratrol improved the progression of chronic prostatitis via the downregulation of c-kit/SCF by activating Sirt1. Journal of agricultural and food chemistry. 2017;65(28):5668-73.